



Characterisation and Spatial Variability
of the Magnetic and Electrical Resistivity
Geophysical Properties of the Soils of
Counties Kildare and Wicklow,
Eastern Ireland.

Samar Alduraibi

Supervisor: Doctor Paul Gibson

Thesis submitted for the degree of Ph.D.

Faculty of Social Science

Department of Geography

Maynooth University

May 2018

CONTENTS

ABSTRACT.....	XIV
ACKNOWLEDGMENTS.....	XV

CHAPTER 1 INTRODUCTION

1.1 Introduction	1
1.2 Geographical characteristics of the study area	2
1.3 Aims and Objectives and Research Question	7
1.4 Layout of the thesis	8

CHAPTER 2 Theoretical Concepts and Research Methodology

2.1 Introduction	10
2.2 Magnetic methodology and theoretical concepts.....	10
2.2.1 Introduction	10
2.2.2 Magnetic domains	12
2.2.3 Remanent Magnetism	13
2.2.4 Field collection procedures for magnetic data.....	13
2.2.5 Laboratory measurement of mass specific susceptibility.....	20
2.2.6 Frequency dependent magnetic susceptibility	24
2.2.7 Magnetic susceptibility of fractional data	25
2.2.8 Laboratory measurement of variation of volume susceptibility with temperature	28
2.2.9 Collection of data for remanent magnetism measurements	31
2.2.10 Laboratory measurement of remanent magnetism.....	33
2.3 Resistivity methodology and theoretical concepts.....	37
2.3.1 Introduction.....	37
2.3.2 Factors which control the resistivity/conductivity of a soil.....	38
2.3.3 Resistivity of lithologies, unconsolidated sediments and soils.....	45

2.3.4 Collection of resistivity data in the field.....	46
2.3.5 Forward modelling of resistivity data.....	56
2.3.6 Inverse modelling of apparent resistivity data.....	62
2.3.7 Azimuthal resistivity.....	67
2.3.8 Time lapse ERT.....	68
2.4 Summary	68

CHAPTER 3

Literature Review of the Study Area

3.1 Introduction.....	70
3.2 Geological Evolution of the study area	70
3.3 Glaciations in Ireland	75
3.4 Glacial processes and landforms in the study area	78
3.5 Soil formation in Ireland	81
3.6 Soils of the study area	86
3.7 Geophysical Applications in Environmental Field	90
3.7.1 Introduction	90
3.7.2 Magnetic susceptibility applications	92
3.7.3 Electrical Resistivity Methods	94
3.8 Geophysical Research in Ireland	96
3.9 Magnetic characteristics of Irish rocks.....	99
3.10 Magnetic characteristics of soils.....	104
3.11 Summary.....	106

CHAPTER 4

MAGNETIC AND ELECTRICAL RESISTIVITY RESULTS FOR COUNTY KILDARE

4.1 Introduction.....	108
4.2 Particle size distribution and clastic characteristics of County Kildare soils...109	
4.3 Statistical characteristics of the bulk magnetic parameters of the Kildare soils.....	113

4.4 Spatial variability of the bulk magnetic parameters of the Kildare soils.....	118
4.5 K-T data analysis.....	125
4.6 Measurement of remanent magnetic declination and inclination angles.....	129
4.7 Statistical characteristics of the magnetic parameters of individual Kildare soils.....	133
4.8 Characteristics of the magnetic parameters of grain size fractions for individual and bulk Kildare soils.....	136
4.8.1 Statistical characteristics.....	136
4.8.2 Spatial variation for individual fractional sizes.....	138
4.8.3 Variation of χ_{lf} and $\chi_{fd}\%$ with particle size.....	142
4.9 Resistivity data for Co. Kildare.....	145
4.10 Summary.....	151

CHAPTER 5
MAGNETIC AND ELECTRICAL RESISTIVITY RESULTS
FOR COUNTY WICKLOW

5.1 Introduction.....	153
5.2 Particle size distribution and clastic characteristics of County Wicklow soils.....	154
5.3 Statistical characteristics of the magnetic parameters of the Wicklow soils....	157
5.4 Spatial variability of the bulk magnetic parameters of the Wicklow soils.....	161
5.5 K-T data analysis.....	170
5.6 Statistical characteristics of the magnetic parameters of individual Wicklow soils.....	172
5.7 Characteristics of the magnetic parameters of grain size fractions for individual and bulk Wicklow soils.....	176
5.7.1 Statistical characteristics.....	176
5.7.2 Spatial variation for individual fractional sizes.....	177
5.7.3 Particle size distribution of χ_{lf} and $\chi_{fd}\%$ for main Wicklow soils...	179
5.8 Resistivity results for Co. Wicklow sites.....	185
5.9 Summary.....	188

CHAPTER 6

Analysis and Discussion of Results

6.1 Introduction.....	191
6.2 Spatial variation of the magnetic susceptibility, frequency dependent susceptibility and volume susceptibility of the study area.....	191
6.3 Characteristics of the magnetic properties of the soils of the study area.....	196
6.4 Assessment of correlation between magnetic susceptibility and frequency dependent susceptibility for the soils of the study area.....	199
6.5 Electrical resistivity properties of the soils of the study area.....	205
6.5.1 Introduction.....	205
6.5.2 Time lapse resistivity results.....	205
6.5.3 Analysis of resistivity sites in the study area.....	212
6.6 Principal Component Multivariate Analysis of GIS database.....	217
6.7 What are the biogeoscientific processes that result in different magnetic and electrical properties of soil?.....	223
6.8 Summary.....	230

CHAPTER 7

Summary and Conclusions

7.1 Introduction.....	233
7.2 Research objectives fulfilment.....	233
7.3 Research aims fulfilment.....	238
7.4 Research question.....	243
7.5 Limitations of the current research.....	244
 REFERENCES.....	 248

List of Figures

Figure 1.1: Study area of Counties Kildare (green) and Wicklow (blue).....	3
Figure 1.2: Geographical location of sites mentioned in the thesis.....	6
Figure 2.1: Sample sites in Counties Kildare and Wicklow where soil samples were collected for magnetic susceptibility measurements.....	14
Figure 2.2: Sampling procedure for the collection of soil samples and for collecting volume susceptibility data.....	16
Figure 2.3: Fall-off in volume magnetic susceptibility values with distance from surface.....	18
Figure 2.4: Soil preparation procedure to ensure representative samples are analysed.....	23
Figure 2.5: Magnetic susceptibility values for grain size fractions for soils K8 and K11.....	27
Figure 2.6: Variation of magnetic susceptibility with temperature for magnetic minerals.....	29
Figure 2.7: (a) Typical heating and (b)cooling K-T curves for soils in study area...31	
Figure 2.8: Lower hemisphere equal area plots of inclination and declination.....	35
Figure 2.9: Seasonal variation in (a) temperature and (b) precipitation for the study area.....	44
Figure 2.10: Standard resistivity arrays used in ERT.....	48
Figure 2.11: Construction of apparent resistivity pseudosection.....	49
Figure 2.12: Sensitivity sections for different resistivity arrays.....	50
Figure 2.13: Resistivity pseudosections for Wenner, Wenner-Schlumberger and Dipole-Dipole arrays.....	52
Figure 2.14: ImagerPro pseudosections for Wenner-Schlumberger and Dipole-Dipole arrays used in collection of data.....	53
Figure 2.15: Effect of changing electrode spacing: top: 0.5m; bottom: 1m.....	55
Figure 2.16: Simple model created with RES2DMOD.....	57

Figure 2.17: Apparent resistivity Wenner-Schlumberger and Dipole-Dipole pseudosections for two horizontal layers model.....	58
Figure 2.18: Apparent resistivity Wenner-Schlumberger and Dipole-Dipole pseudosections for three horizontal layers model.....	59
Figure 2.19: Apparent resistivity Wenner-Schlumberger and Dipole-Dipole pseudosections for a two vertical contacts model.....	60
Figure 2.20: Apparent resistivity Wenner-Schlumberger and Dipole-Dipole pseudosections for a surface channel model.....	61
Figure 2.21: Apparent resistivity Wenner-Schlumberger and Dipole-Dipole pseudosections for a deep channel model.....	62
Figure 2.22: Inverse modelling of pseudosections shown in Figure 2.13.....	63
Figure 2.23: Inversion of Dipole-Dipole three layers model pseudosection.....	64
Figure 2.24: Inversion of Wenner-Schlumberger and Dipole-Dipole deep channel model pseudosections.....	65
Figure 2.25: Inversion of two vertical contacts model pseudosections.....	66
Figure 2.26: Comparison of (a) variation in average apparent resistivity and (b) average modelled resistivity values for E-W and N-S lines.....	67
Figure 3.1: Simplified geological map of study area. KI: Kildare Inlier.....	72
Figure 3.2: Expansion and decay of ice sheet and main landforms produced during the late Midlandian glaciation.....	77
Figure 3.3: Glacial movement across study area.....	80
Figure 3.4: Geochemical maps showing cadmium, iron, mercury, lithium concentrations in study area.....	89
Figure 3.5: Magnetic traverse in Co. Wicklow.....	97
Figure 3.6: Magnetic susceptibility ranges for different lithologies and superficial deposits.....	102

Figure 4.1: The geographical locations of the soil types and sites where data were collected.....	110
Figure 4.2: Histogram plot of (a) all χ_{lf} and (b) detail of χ_{lf} from 0-20.....	114
Figure 4.3: Histogram of (a) $\chi_{fd}\%$ and (b) volume susceptibility k	115
Figure 4.4: (a) Plot of χ_{lf} and $\chi_{fd}\%$ and (b) between χ_{lf} and K.....	118
Figure 4.5: Magnetic susceptibility map of Kildare in which blue shows areas $<10 \times 10^{-8} \text{ m}^3\text{kg}^{-1}$ and red shows areas $>10 \times 10^{-8} \text{ m}^3\text{kg}^{-1}$	121
Figure 4.6: Magnetic susceptibility map of Kildare (χ_{lf})	122
Figure 4.7: $\chi_{fd}\%$ map of Kildare.....	123
Figure 4.8: Magnetic susceptibility map of Kildare (K).....	124
Figure 4.9: Relative standard deviation (χ_{lf}) of Kildare.....	125
Figure 4.10: Typical K-T graphs for Kildare	126
Figure 4.11: Sample Stereoplots.....	132
Figure 4.12: Spatial maps of Kildare showing variation in susceptibility for (a) $>2000\mu\text{m}$ and (b) $<63\mu\text{m}$ fractions.....	139
Figure 4.13: Spatial maps of Kildare showing variation in $\chi_{fd}\%$ for (a) $>2000\mu\text{m}$ and (b) $<63\mu\text{m}$ fractions.....	141
Figure 4.14: Typical χ_{lf} and $\chi_{fd}\%$ histograms for the Kildare Soils	143
Figure 4.15: Average (a) χ_{lf} and (b) $\chi_{fd}\%$ for Kildare.....	145
Figure 4.16: Resistivity model for site K81.....	147
Figure 4.17: Resistivity model for site K189.....	148
Figure 4.18: Resistivity model for site K89.....	149
Figure 4.19: Average resistivity model for (a) K81, (b) K189 and (c) K89.....	150

Figure 5.1: The geographical locations of magnetic and resistivity sites.....	155
Figure 5.2: Histogram plot of (a) χ_{lf} , (b) $\chi_{fd}\%$ and (c) volume susceptibility (K).....	158
Figure 5.3: Correlation between (a) χ_{lf} and $\chi_{fd}\%$ and (b) between χ_{lf} and K.....	161
Figure 5.4: Magnetic susceptibility threshold map of Wicklow.....	164
Figure 5.5: Magnetic susceptibility map of Wicklow (χ_{lf})	165
Figure 5.6: Magnetic susceptibility map of high values in Wicklow (χ_{lf})	166
Figure 5.7: Magnetic susceptibility map of Wicklow (K).....	167
Figure 5.8: $\chi_{fd}\%$ map of Wicklow.....	168
Figure 5.9: Relative standard deviation map (χ_{lf}) of Wicklow.....	169
Figure 5.10: Typical Wicklow K-T heating curves.....	171
Figure 5.11: Correlation between (a) 2000-900 μm and 900-600 μm fractions and (b) 125-63 μm and <63 μm for all Wicklow soils.....	178
Figure 5.12: Average susceptibility for the main Wicklow soil types.....	181
Figure 5.13: Average $\chi_{fd}\%$ for the main Wicklow soil types.....	183
Figure 5.14: 2D resistivity model for site W79.....	186
Figure 5.15: 2D resistivity model for site W210.....	187
Figure 5.16: Average resistivity model for (a) W79 and (b) W210.....	188
Figure 6.1: Spatial variability for low frequency magnetic susceptibility.....	193
Figure 6.2: Spatial variability for frequency dependent susceptibility.....	194
Figure 6.3: Spatial variability of volume susceptibility.....	195
Figure 6.4: Plot of $\Delta\chi$ and χ_{lf} for (a) Kildare and (b) Wicklow data.....	202
Figure 6.5: Plot of χ_{lf} against $\Delta\chi$ for all the study area soils.....	203
Figure 6.6: (a) Plot of $\chi_{fd}\%$ against χ_{lf} for the study area. (b) Similar plot for Welsh topsoils and for (c) Chinese loess.....	204
Figure 6.7: Temperature and precipitation changes during time lapse experiment.....	206

Figure 6.8: RES2DINV modelled resistivity profiles from near the surface and 2m depth for one year.....	207
Figure 6.9: Time lapse image for site K1 for (a) January-April and (b) April-July periods in resistivity ratio format.....	209
Figure 6.10: Time lapse image for site K1 for July-October and October-December periods in resistivity ratio format.....	210
Figure 6.11: Time lapse image and the separate April and June models.....	211
Figure 6.12: Spatial variation of modeled average resistivity for topmost soil layer (50 cm)	217
Figure 6.13: Plot of (a) χ_{lf} data against average modelled resistivity data and (b) $\chi_{fd}\%$ against average modelled resistivity for layer1.....	220
Figure 6.14: Principal components map of study area in which PC1 is projected in red, PC2 in green and PC3 in blue light.....	222
Figure 6.15: Plot of average χ_{lf} data against average modelled resistivity data for layer 1 for soil types listed in Table 6.6.....	230

List of Plates

Plate 1.1: Sample soils taken from a small area in County Wicklow.....	2
Plate 1.2: Thematic Mapper false colour satellite image of Co. Kildare.....	4
Plate 1.3: Thematic Mapper false colour satellite image of Co. Wicklow.....	5
Plate 2.1: Use of MS2D Bartington loop detector to obtain volume magnetic susceptibility data.....	16
Plate 2.2: (Top) Bartington MS2B and (bottom) MS2W sensors.....	23
Plate 2.3: Collection of samples for remanent magnetism studies.....	32
Plate 2.4: Molspin magnetometer for remanent magnetism.....	33
Plate 2.5: Collection of resistivity data using multicore cable.....	47
Plate 3.1: Photograph of Wicklow granite.....	74
Plate 3.2: (Upper) sub-horizontal near site K92 and (Lower) folded Carboniferous limestone near site K1.....	75
Plate 3.3: Thick sand deposits near site K227.....	78
Plate 3.4: (a) U-shaped valley and (b) Scalp meltwater channel in Co. Wicklow....	79
Plate 3.5: Pleistocene till deposits near site K1.....	81
Plate 3.6: Fluvioglacial deposits at Blessington, Kildare-Wicklow border.....	81
Plate 3.7: Peat deposits in west Kildare. Section is 4m high.....	85
Plate 3.8: Hill of Allen basalts in study area.....	101
Plate 3.9: Formation of iron oxide in shales near site K1.....	103

List of Tables

Table 2.1: MS2D loop probe correction factor.....	19
Table 2.2: Statistics based on susceptibility values for two hypothetical sites H1 and H2.....	20
Table 2.3 Variation in mass specific magnetic susceptibility for subsamples A, B, C, D for typical sites from Kildare and Wicklow.....	22
Table 2.4: Fractional sizes for 7 sieves employed in thesis.....	26
Table 2.5: TC and TN values.....	29
Table 2.6: Declination and inclination results for 2 sites, S1 and S2.....	35
Table 2.7: Temperature correction factors.....	43
Table 2.8: Typical measured resistivity values in Ireland.....	46
Table 2.9: Electrodes employed in Wenner-Schlumberger and Dipole-Dipole arrays.....	54
Table 4.1: Kildare sites by soil type.....	111
Table 4.2: Average percentage of sample in each size fraction for Kildare soils...112	
Table 4.3: Statistics for the bulk Kildare soils.....	116
Table 4.4: Statistical data for main Kildare soils.....	134
Table 4.5: Individual fractional statistics for Kildare soils (excluding peat).....	136
Table 5.1: Soil groups in County Wicklow.....	156
Table 5.2: Statistics for the bulk Wicklow soils.....	157
Table 5.3: Statistical data for ADPDM soils.....	173
Table 5.4: Statistical data for ADWDM soils.....	174
Table 5.5: Statistical data for ASWDM soils.....	174
Table 5.6: Statistical data for BSWDM soils (exc. W103).....	175

Table 5.7: Statistical data for ASP soils (exc. W167).....	175
Table 5.8: Individual fractional statistics for all Wicklow soils.....	176
Table 5.9: Average χ_{lf} , $\chi_{fd}\%$ and K for Wicklow soils.....	189
Table 6.1: Statistical characteristics of the study area.....	196
Table 6.2: Soil type characterisation based on χ_{lf} and $\chi_{fd}\%$	197
Table 6.3: Hypothetical variation of $\Delta\chi$ with $\chi_{fd}\%$	200
Table 6.4: Minimum and maximum model resistivity values for Kildare and Wicklow soils.....	213
Table 6.5: Average minimum and maximum model resistivity values.....	215
Table: 6.6: Magnetic and resistivity characteristics of study area soils.....	224

Supplementary Data on CD

CD contains thesis.docx

Folder 1 **Particle Size** which contains file:

File 4.1s.docx - Particle size distribution of sample of Kildare.

Folder 2 **K-T data** which contains files:

File 4.2s.docx - K-T graphs for Kildare.

File 5.1s.docx - K-T graphs for Wicklow.

Folder 3 **Stereoplots** which contains file:

File 4.3s.docx - stereoplots.

Folder 4 **Histograms** which contains files:

File 4.4s.docx - Typical χ_{lf} and $\chi_{fd}\%$ histograms for the Kildare soils.

File 5.2s.docx - Typical χ_{lf} and $\chi_{fd}\%$ histograms for the Wicklow soils.

Folder 5 **Resistivity Data** which contains files:

File 4.5s.docx - Resistivity model for Kildare.

File 5.3s.docx - Resistivity model for Wicklow.

ABSTRACT

The magnetic characteristics (low and high frequency mass specific magnetic susceptibility [χ], volume susceptibility [K] and K-T data) and electrical resistivity characteristics were obtained for the soils of Co. Kildare and Co. Wicklow, eastern Ireland (an area of 3688 km²). Spatially, the magnetic susceptibility shows a general pattern of values increasing from the northwest to the southeast over a two orders of magnitude range. A northeast trending broad zone of high resistivity with values 1-2 orders of magnitude higher than background corresponds spatially with the Wicklow Mountains.

Analysis of a 17 variable GIS database shows that χ_{lf} has a high positive correlation with soil iron content and weaker positive ones with copper, lithium, tin, lead, mercury and uranium and a weak negative correlation with nickel and zinc. There is a high positive correlation between χ_{lf} and frequency dependent susceptibility ($\chi_{fd}\%$). The correlation between χ_{lf} and resistivity, between $\chi_{fd}\%$ and resistivity and between χ_{lf} and topography is statistically virtually zero. The correlation between χ_{lf} and geology and glacial sediments is very weak (0.08). There is however, a good correlation between χ_{lf} and soils. A strong positive correlation exists between resistivity and topography and soils. Correlation between resistivity and geology and glacial sediments is close to zero. The magnetic properties of the soils in the study area depend greatly on the formation of superparamagnetic (SP) secondary ferrimagnetic minerals (almost exclusively magnetite). 80% of the study area soils are characterised by a high degree of secondary enrichment. For 89% of the acquired magnetic data, the greater the amount of SP grains, the higher the susceptibility. A well drained soil environment which undergoes fluctuating reducing and oxidising conditions facilitates the formation of SP grains and in this study was best achieved by Acid Deep Well Drained Mineral (ADWDM) and Acid Shallow Well Drained Mineral (ASWDM) soils (highest χ_{lf} and $\chi_{fd}\%$ values). Poorly drained soils have a low χ_{lf} and a low $\chi_{fd}\%$. A small percentage of soils have a high χ_{lf} but a low $\chi_{fd}\%$. Such frequency independent soils tend to have an anthropogenic origin and are located around Avoca, a site of former industrial activity. Using averaged values at the soil type level, a strong positive correlation between magnetic susceptibility and resistivity values for the topmost soil layer was determined.

ACKNOWLEDGEMENTS

I would like to express my sincere gratitude to my supervisor Dr. Paul Gibson for the continuous support of my Ph.D. study and related research, for his patience, motivation, and immense knowledge. His guidance helped me in all the time of research and writing of this thesis. I could not have imagined having a better supervisor for my Ph.D. study.

I would like to thank the following university staff especially: Michael Bolger for his unfailing support. Many thanks to all farmers for allowing me collect samples from their fields.

I will never have been able to thank my parents, sisters, Ameerah and Malak, brother in law, and my husband. They have provided me through moral and emotional support in my life. I am also grateful to my other family members and friends who have supported me along the way.

In conclusion, I recognize that this research would not have been possible without the financial assistance of The Custodian of The Two Holy Mosques' Overseas Scholarship Program from Kingdom of Saudi Arabia.

CHAPTER 1

INTRODUCTION

1.1 Introduction

The types of soil that develop in any area depend to a large extent on:

- The nature/density of the overlying vegetation,
- The character of the underlying non-organic material such as rock type,
- The topographic expression,
- The climate under which the soil develops,
- The nature of the processes that occur within it such as oxidation and reduction,
- Human influence,
- Time.

The situation in Ireland is further complicated because of the large variation in the nature and thickness of the underlying glacial sediments and because the detailed distribution of these sediments is often not known. In some areas, well-drained, thick layered gravels were deposited whereas in others, poorly drained till and clays may predominate. Even small changes in relief may alter the type of soil that develops. The soils in Ireland also developed under changing climatic and vegetational regimes. At the end of the last glacial period, 10,000 years ago, the Irish Midlands were initially a vegetationless, poorly drained region, which later developed bogs and a deciduous forest cover (Mitchell and Ryan, 2001). However, today a large proportion of the soils are developing under a grassland cover whose chemical composition has been artificially altered by the addition of fertiliser. Leaching and other chemical and physical processes often result in the development of soil horizons where a section shows layers with different physical and/or chemical characteristics. This zonation may be employed in identifying various soil types, podzols; for example, are soils which have a pronounced leached upper horizon. Organic soils (of the soil order: histosols) have a very high organic content and are associated with raised bog and blanket peat deposits. In poorly drained water logged areas, the oxidised form of iron (ferric) may be chemically reduced to the ferrous form resulting in a grey-blue gley.

Soils are generally classified based on physical and chemical properties such as texture, structure and colour, Plate 1.1. However, soils also possess geophysical characteristics such as resistivity or magnetic susceptibility which are usually totally ignored often because they are poorly understood. These geophysical properties and their spatial variability can provide valuable information on, for example, palaeoenvironmental evolution, palaeodating, effects of pollution and may be employed as proxies for sedimentological, biological, geochemical and mineralogical processes (Gautam et al., 2004; Samouelian et al., 2005). Virtually nothing is known about the variability of soil geophysical signatures in Ireland and the proposed research will be the first regional in-depth study.



Plate 1.1: Sample soils taken from a small area in County Wicklow.
Note colour variation.

1.2 Geographical characteristics of the study area

The study area for this research encompasses Counties Kildare and Wicklow in eastern Ireland (areas of 1688 km² and 2000 km² respectively), Figure 1.1. These regions have been chosen for a number of reasons. The available soil maps of Kildare and Wicklow show that a range of soils are present in these counties which will allow for detailed correlation with geophysical parameters. A range of lithologies of various ages are

contained within the study area: Precambrian greywackes, slates, Caledonian granite, Carboniferous limestone and shales and Quaternary sediments. The relief varies from sea level to over 900m.

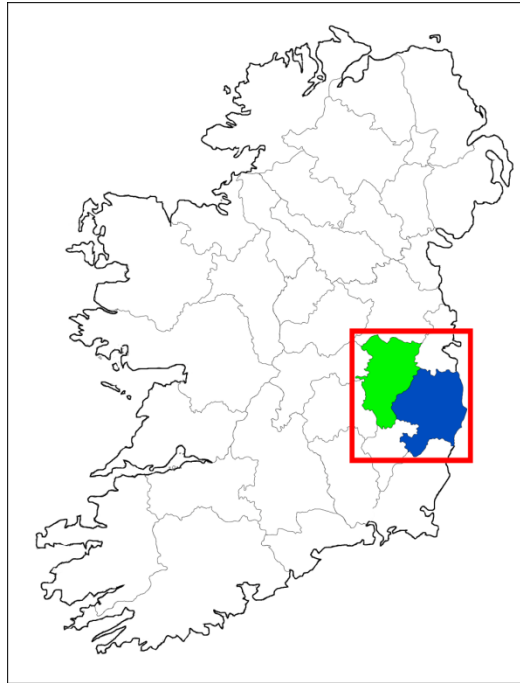


Figure 1.1: Study area of Counties Kildare (green) and Wicklow (blue).

The land-use in the study area can be determined from the Kildare and Wicklow Landsat 5 Thematic Mapper satellite images. These have been created by projecting Thematic Mapper bands 4 (0.76-0.90 μm), 5 (0.63-0.69 μm) and 3 (0.63-0.69 μm) in red, green and blue respectively) Plates 1.2 and 1.3. This band combination (one red and two infrared bands) as well as reducing atmospheric scattering, produces a wide range of spectral signatures for the vegetation types in the study area.

County Kildare is an agricultural county with a few small towns shown in dark blue. The satellite image is dominated by an orange-red signature which represents healthy green vegetation, mainly pasture in the north and east. Small isolated dark-red-brown areas in the scene are forests. Fallow fields (those with bare soil) are shown in regular pale blue colours, of which there is a particular large concentration in the southwest. It is used extensively for rearing beef cattle. Northwest Kildare is characterised by large regular

areas shown in green where peat is harvested commercially (see Plate 3.7 for ground view).

Topographically, Kildare is a relatively low lying flat county with over 60% of it being below 100m O.D. though in the south the land is undulating in places. Elevations in the northwest, are in the 60-120m range. North of Kildare town, a series of small hills (Dunmurry Hill, Grange Hill) reach heights of 234m. Eastern Kildare is substantially higher than the rest of the county. Elevations are 150-349m and this region represents the foothills of the Wicklow Mountains.

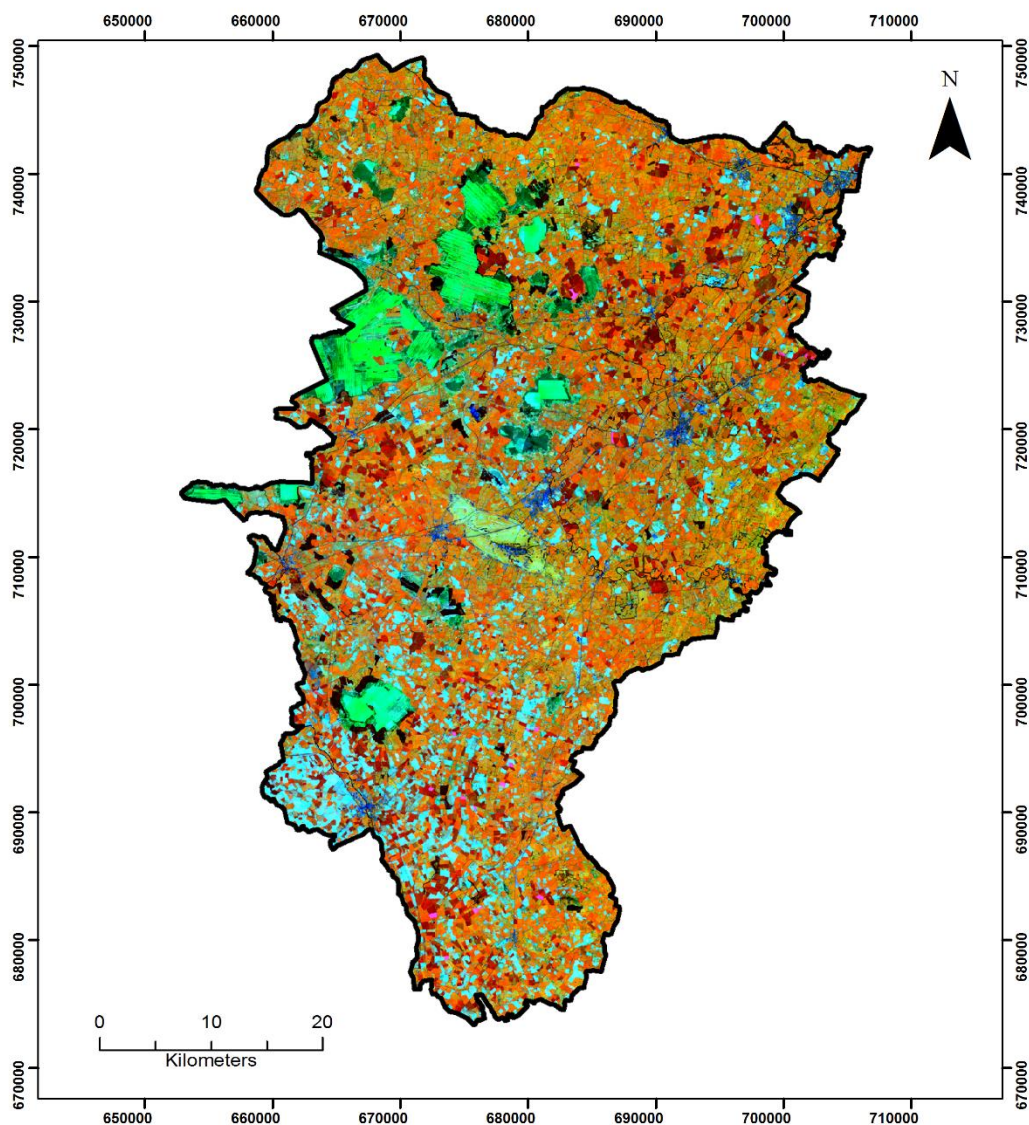


Plate 1.2: Thematic Mapper false colour satellite image of Co. Kildare.

The Wicklow Mountains dominate Wicklow County and are characterised by scrub, heather and blanket bog with an associated green signature on the false colour satellite image, Plate 1.3. Coniferous plantations in the same area are shown in red/brown. Lake Blessington is in the northwest. 12% of the county (mainly in the east) is used for cereals, mostly wheat and barley. Sheep and cattle are raised on the remaining pasture fields.

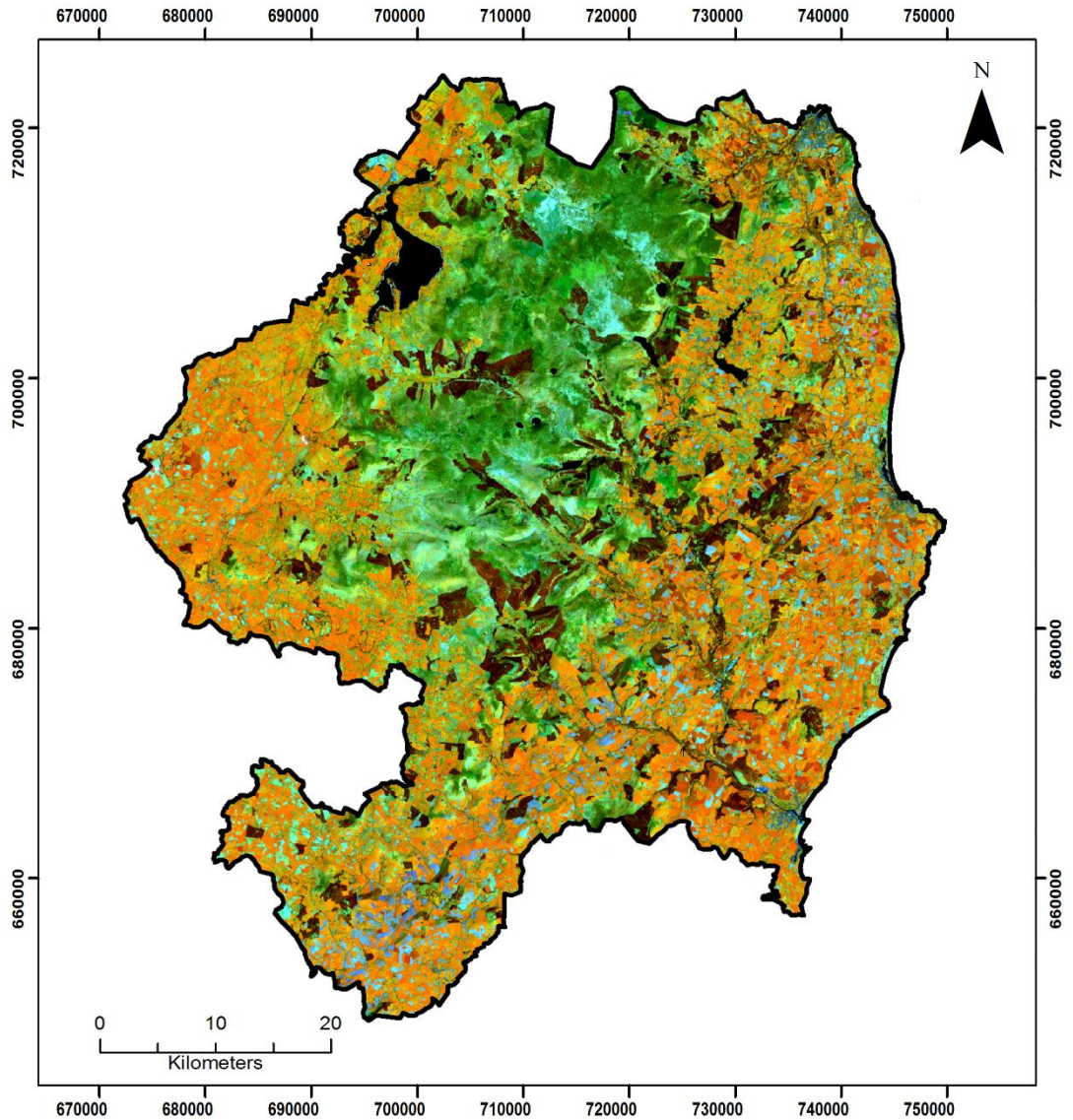


Plate 1.3: Thematic Mapper false colour satellite image of Co. Wicklow.

Topographic variation is significantly greater in Wicklow than in Kildare, with some parts of the county being at sea level and the highest point being Lugnaquilla (925m). The mountains are typically 450-650m in height). The River Liffey is the most important river in the study area, Figure 1.2. It rises in the Wicklow Mountains and flows west. Originally it flowed to the River Barrow at Monasterevin, but a glacial moraine diverted it to flow north-westwards.

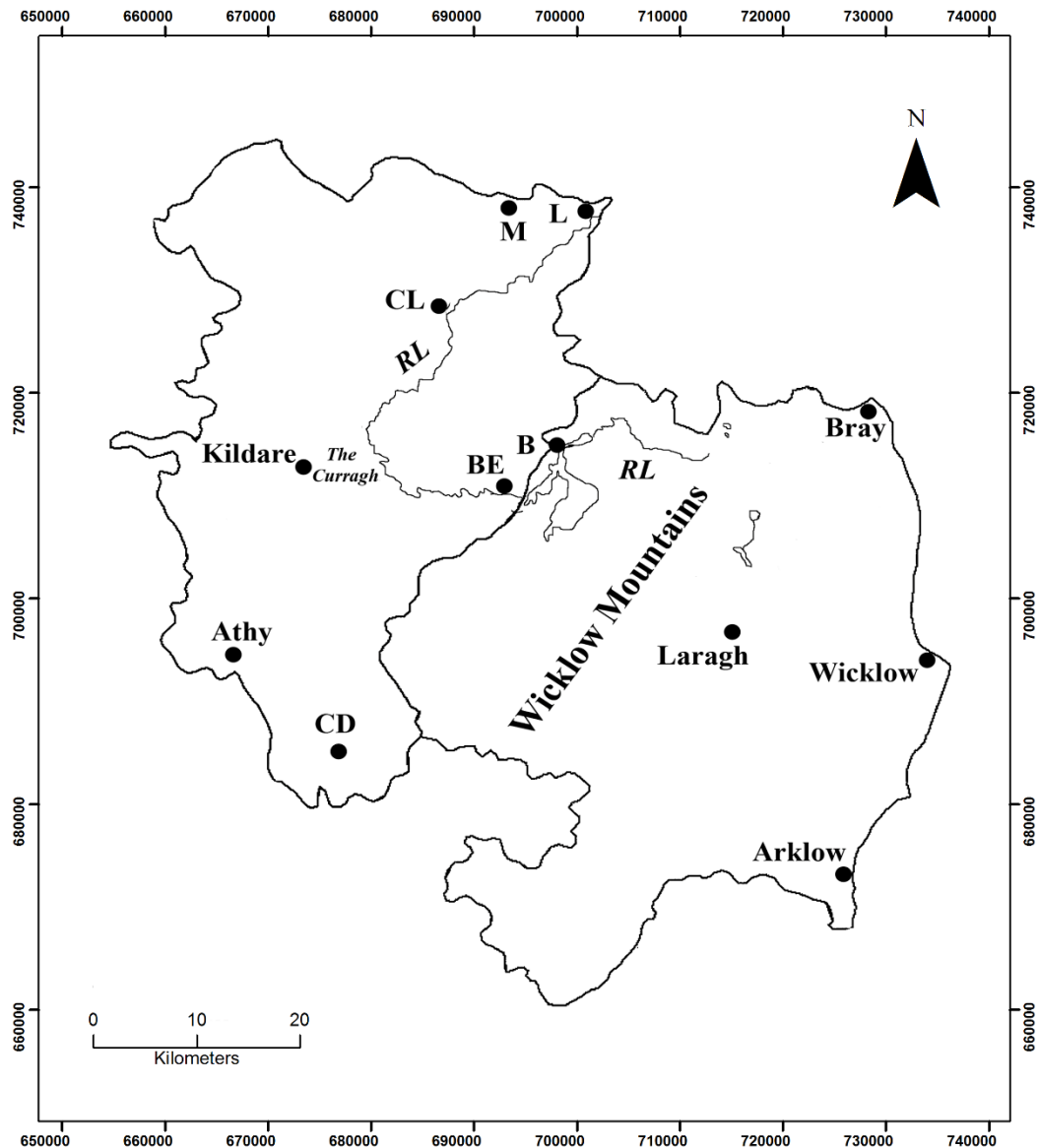


Figure 1.2: Geographical location of sites mentioned in the thesis. Arklow, Athy, B: Blessington, BE: Ballymore Eustace, Bray, CD: Castledermott, CL: Clane, Kildare, L: Leixlip, Laragh, M: Maynooth, RL: River Liffey, Wicklow.

The co-ordinate system used throughout this thesis is the Irish Transverse Mercator (ITM). From a geographical perspective, the centre of the study area has a latitude co-ordinate of 53 degrees 3 minutes and 9.467 seconds north and a longitude co-ordinate of 6 degrees 31 minutes and 58.254 seconds west. All parts of the study area are within 0.8 degrees of these co-ordinates.

1.3 Aims and Objectives and Research Question

There are 6 research aims to the thesis:

Aim 1: To determine if Irish soil types in Counties Kildare and Wicklow have characteristic magnetic or electrical resistivity geophysical properties.

Aim 2: To produce the first spatially referenced county scale maps of volume magnetic susceptibility (K), mass specific magnetic susceptibility (χ) and percentage frequency dependent susceptibility ($\chi_{fd}\%$) in Ireland.

Aim 3: To determine the magnetic mineralogy and magnetic domain format of the soils of Counties Kildare and Wicklow.

Aim 4: Ascertain if different fractional size ranges carry the same or different magnetic signals.

Aim 5: Within the scientific literature (for different parts of the world) various claims have been made regarding the correlation between mass specific magnetic susceptibility and percentage frequency dependent susceptibility (χ and $\chi_{fd}\%$). The existence or otherwise of such correlations for soils within the study area will be evaluated.

Aim 6: Construct and analyse a Geographic Information System (GIS) database for the study area.

In order to achieve these aims, a number of objectives have to be achieved:

Objective 1: Collection of samples from a sufficiently large number of spatially referenced sites for analysis in the laboratory of mass specific magnetic susceptibility at high and low frequency and percentage frequency dependent susceptibility.

Objective 2: Measurement of volume magnetic susceptibility in the field at spatially referenced sites.

Objective 3: Production of representative soil samples and measurement of their low and high frequency magnetic susceptibility.

Objective 4: Fractional analysis of representative soil samples and the measurement of low and high frequency magnetic susceptibility for individual fractions.

Objective 5: Collection and analysis of K-T data to determine Curie temperatures for magnetic minerals in the soils of the research area and determine the magnetic mineralogy and magnetic domain format.

Objective 6: Collection and analysis of oriented soil samples for laboratory remanent magnetism, inclination and declination measurement.

Objective 7: Formulation of and forward modelling of subsurface resistivity models.

Objective 8: Acquisition of 2D apparent resistivity pseudosection data using different array types at a representative number of sites and inverse modelling of the results.

Objective 9: Determine electrical homogeneity of subsurface soil at a representative number of sites by employing azimuthal resistivity surveying.

Objective 10: Determine the annual temporal degree of resistivity change using time-lapse electrical resistivity imaging at a selected site.

The research question to be answered by this study is: Based upon an extensive study of a variety of soil types, what are the biogeoscientific processes that result in different magnetic and electrical properties of soil?

1.4 Layout of the thesis

Following the introduction to the thesis (current chapter), Chapters 2 and 3 represent the literature review which is split over two chapters with the latter concentrating mainly (but not exclusively) on the study area and Ireland and the former on techniques and their relevant research literature.

The geophysical techniques employed in this thesis are:

Magnetic methods

- Low frequency mass specific magnetic susceptibility.
- High frequency mass specific magnetic susceptibility.

- Volume magnetic susceptibility.
- Variation of volume magnetic susceptibility with temperature.
- Remanent magnetism, inclination and declination.

Resistivity methods

- 2D Electrical Resistivity Tomography (ERT): Wenner-Schlumberger format and inverse modeling.
- 2D Electrical Resistivity Tomography: Dipole-Dipole format and inverse modeling
- 2D Forward modeling.
- Azimuthal 2D ERT.
- Time-lapse 2D ERT.

The methodological approach to the collection of such geophysical data, the relevant research literature and theoretical concepts are discussed in Chapter 2.

Chapter 3 is divided into two main sections, the first of which deals with relevant physical aspects of the research region such as geological evolution; glacial processes, soil formation and soils. The second section considers geophysical research appropriate to this thesis and environmental geophysical research in Ireland. Chapters 4 and 5 present the main results for Kildare and Wicklow respectively. These include particle size distribution analysis, magnetic susceptibility measurements, the results of K-T analysis, remanent magnetism results and inverse modelling of resistivity data. A vast amount of data were collected and analysed for this thesis and most are shown digitally in a supplementary CD rather than in hardcopy format.

A discussion of the results for both Wicklow and Kildare is to be found in Chapter 6. A summary chapter is provided in Chapter 7. The thesis concludes with a References section.

CHAPTER 2

Theoretical Concepts and Research Methodology

2.1 Introduction

The chapter commences with a discussion on the theoretical concepts underlying magnetic properties of substances, most specifically the concept of magnetic susceptibility, magnetic domains, types of magnetic behaviour and remanent magnetism. These sections are followed by ones relating to magnetic susceptibility which explain the procedures used to collect representative samples and the laboratory analyses performed on the soils. These include a discussion on frequency dependent magnetic susceptibility, fractional analyses and measurements of the variation of volume susceptibility with temperature. A discussion on the collection of samples for remanent magnetism analysis and their processing follows.

The chapter concludes with sections relating to the second major geophysical technique employed in this research: electrical resistivity. The theoretical principles are initially considered and followed by a section on factors which control the resistivity/conductivity of a soil and a discussion of the resistivity of typical Irish rocks/sediments and the important parameters in a resistivity survey. Forward and inverse modeling is discussed in some detail. The chapter concludes with brief discussions on azimuth and time-lapse resistivity. The literature relevant to both magnetism and resistivity is cited and discussed in the appropriate sections.

2.2 Magnetic methodology and theoretical concepts

2.2.1 Introduction

Most people are aware that some substances, especially those containing iron, are considered magnetic. However, the situation is much more complex. A pyrite crystal, for example, is about 47% iron yet it possesses an extremely weak magnetism, whereas magnetite is 72% iron and is about 2000 times more magnetic than pyrite. Ultimately,

magnetism is an atomic level process caused by the interaction of electrons spinning about their own axis and their orbital movement around the nucleus (Maher, 2007).

Magnetic behaviour and Susceptibility

When a substance is placed in a magnetic field H , a magnetisation J_i will be induced such that:

$$J_i = KH$$

Units of magnetisation and magnetic field are Amp m^{-1} . K (Kappa) is the volume magnetic susceptibility of the substance and is dimensionless in the S.I. system. It is also possible to determine the mass specific magnetic susceptibility χ (Chi) which equals K/ρ (where ρ is the density in kgm^{-3}). The units of χ are m^3kg^{-1} , though in this thesis, units of $10^{-8} \text{ m}^3\text{kg}^{-1}$ are employed. How the substance interacts with the induced magnetic field determines the type of magnetic behaviour of which Dearing (1999a) considers five main types:

- diamagnetism - weakest
- paramagnetism
- canted antiferromagnetism
- ferrimagnetism
- ferromagnetism - strongest

When a diamagnetic material is placed in a magnetic field, the induced magnetism is very small and is in the opposite direction to the applied magnetic field, hence the magnetic susceptibility is negative. Natural substances such as quartz, kaolinite, calcite and feldspar are diamagnetic as are some man-made substances, such as plastic (Potter, 2005). Vegetation/organic matter is also diamagnetic as is water which has a magnetic susceptibility of $-0.9 \times 10^{-8} \text{ m}^3\text{kg}^{-1}$.

Paramagnetic minerals, such as olivine, pyroxene, pyrite and biotite are associated with a weak positive magnetism, typically $1-10 \times 10^{-8} \text{ m}^3\text{kg}^{-1}$. The strongest positive susceptibility is produced by ferromagnetic substances such as iron, nickel or chromium.

Even, with small induced fields, the magnetic moments all align (parallel coupling) with the induced field direction (Thompson and Oldfield, 1986). Susceptibility values of $20,000,000 \times 10^{-8} \text{ m}^3\text{kg}^{-1}$ may result; however, in the context of this thesis and most environmental research, ferromagnetic minerals are a source of contamination. One sample collected for this research gave a magnetic susceptibility two orders of magnitude greater than the others. Visual examination showed that it contained a small bit of iron. Ferrimagnetic behaviour results from antiparallel coupling of unequal moments producing a strong positive susceptibility. Magnetite, titanomagnetite, maghemite and pyrrhotite are the most important ferrimagnetic minerals with the former having susceptibility of around $50,000\text{-}110,000 \times 10^{-8} \text{ m}^3\text{kg}^{-1}$ (Maher, 2007). Spin canting resulting from imperfect antiparallel moment coupling can yield a moderate positive susceptibility (Thompson and Oldfield, 1986). Haematite exhibits such canted antiferromagnetism and has susceptibility of $27\text{-}100 \times 10^{-8} \text{ m}^3\text{kg}^{-1}$. The susceptibility of a sample will depend on the relative proportions of which type of magnetic mineral are present, though even a small percentage of a ferrimagnetic mineral may dominate the magnetic signal. In theory, the presence of diamagnetic minerals will reduce susceptibility, but their effects are so small (except for example in organic matter or limestone) their effect may be neglected (Hrouda, 2011).

2.2.2 Magnetic domains

A magnetic domain is a small region within a crystal in which the magnetic moments are parallel (Smith, 1999). The direction differs for adjacent domains when the crystal is demagnetised. The susceptibility of magnetite varies with grain size (Dearing, 1994). When the grains are large ($>$ than about $2\mu\text{m}$), then a number of domains can form and they exhibit multidomain (MD) behaviour whereas in smaller grains (c. $0.03\text{-}0.07\mu\text{m}$) only a stable single domain (SD) can form. Intermediate to these are the pseudosingle (PSD) domain grains. MD grains have a lower magnetic stability and susceptibility (Maher, 1986). In extremely small crystals ($<0.03\mu\text{m}$), the susceptibility is high but unstable. These superparamagnetic (SP) crystals are important and are discussed further in section 2.2.6.

2.2.3 Remanent Magnetism

When a magnetic field is removed from a diamagnetic or paramagnetic mineral, the induced magnetisation disappears. However, ferrimagnetic and ferromagnetic minerals possess a ‘remanent’ magnetism which persists. This remanent magnetism property is employed in palaeomagnetic studies of rocks and sediments (Gaigalas et al., 2002; Koc and Pagac, 1973; Sprowl and Banerjee, 1985). As a magma cools through its Curie temperature, its magnetic domains align themselves with the Earth’s magnetic field. There are three components important to remanent magnetism, the intensity of the magnetic field, its declination and its inclination. The magnetic flux density for the study area today is c. 49000 nT. The declination is the angle that the vector points, measured from north, and the inclination angle is the angle the magnetic field vector makes with the horizontal. For eastern Ireland today, the declination is approximately 356 degrees as magnetic north is 4 degrees west of true north and the inclination is 68 degrees. The Tertiary (c. 60 million years ago) basalts in NE Ireland have a declination of 185 degrees and an inclination of -54 degrees (Wilson, 1959, 1970). This shows that the basalts formed during a magnetic field reversal and that Ireland lay further south than now. Within the study area, the Ordovician andesites of the Kildare Inlier have been palaeomagnetically sampled and the results have been interpreted as indicating a later Permian remagnetisation, similar to the Carboniferous limestone (Morris and Robinson, 1971).

2.2.4 Field collection procedures for magnetic data

In all, 300 samples in Co. Kildare and 250 samples in Co. Wicklow were collected for magnetic susceptibility measurements in the laboratory, Figure 2.1. Such data can be collected in a regular grid format (Magiera et al., 2006) or using irregularly spaced data (Gautam et al., 2004; Gibbs-Egar et al., 1999; Moreno, et al., 2003). The latter approach was adopted for this research for a number of reasons.

- If a regular grid approach was adopted and two adjacent sites have a large difference in magnetic values, it would not have been possible to determine more

precisely was there a gradual change or an abrupt one and where it was located. However, with the ‘irregular grid’ approach, additional sites could be included to help reconcile this issue.

- The most important magnetic area in Co. Kildare is the Kildare Inlier as the lithologies it contains may be the source of magnetic grains in the soils. Hence the concentration of sample sites was increased in this region.
- It was important that sample sites be located on a wide range of soil types and in the case of the major soils that a number of samples be taken in different geographic areas. This was best achieved using irregularly spaced data.

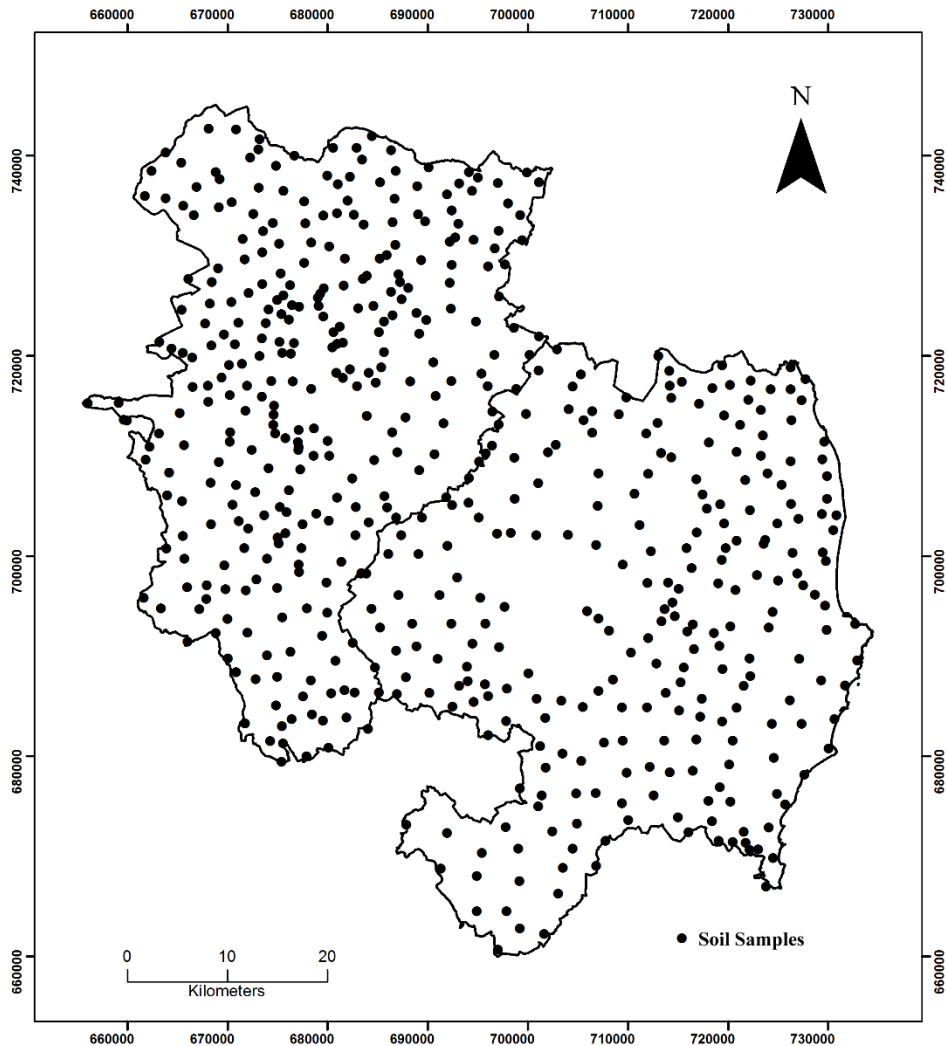


Figure 2.1: Sample sites in Counties Kildare and Wicklow where soil samples were collected for magnetic susceptibility measurements.

The data were then interpolated into a regular grid using SURFER software and input into an ArcMap Geographical Information System which contained other georeferenced datasets such as satellite data and a soil map.

Most of the sample sites in County Kildare were taken in pasture fields which represent over 80% of the county. Peat forms about 12% and the rest of the data were collected in cultivated fields. The upland areas of Wicklow tend to be poorly cultivated consisting of scrub, heather and peat with cultivated/pasture fields confined to lower elevations. Two aspects of the data collection approach were particularly important, i.e. that the sample be as natural as possible (no contamination) and that it be representative of the site. Magnetic susceptibility values taken near road verges often show elevated values due to contamination from vehicular traffic (Hoffman et al., 1999). To minimize this effect, sites were chosen, where possible, on minor roads with low traffic. Most fields were separated from the road by a high thick hedge which further reduced contamination and data were collected about 30m from the road in a location devoid of any obvious interference.

Rather than collect soil from a single point source, a 7m sided triangle was constructed at each site for whose centre, the Irish Grid co-ordinates were acquired using a Trimble GPS system, Figure 2.2. A shallow (top 10-15cm) soil sample was taken from each of the three corners of the triangle using a non-magnetic trowel and put into a labelled sealed sample bag. The total (wet) weight of soil collected at each site was typically 1.2-1.4 kg and was returned to the laboratory for mass specific susceptibility measurements. In addition to the soils samples, 20 volume susceptibility in situ measurements were taken at each of the sites shown in Figure 2.1. A Shapiro-Wilk test was performed on the 20 volume susceptibility data to ascertain if they conformed statistically to a normal distribution (Seaby et al., 2007). This test returns a parameter W which is the squared correlation coefficient between the data and their corresponding normal scores. If $W = 1$ then there is a perfect fit to a normal distribution. The data were in the $W = 0.94-0.98$ range and the QED STATISTICS software typically reported that ‘the distribution of the variable does not deviate significantly from a normal distribution (Shapiro-Wilk test, $W = 0.982708$, $n = 20$, $P = >0.05$)’. The equipment used to collect these data in the field

was the Bartington MS2 meter in conjunction with the MS2D loop probe, Plate 2.1. This measures the volume magnetic susceptibility, which is given the symbol: K .

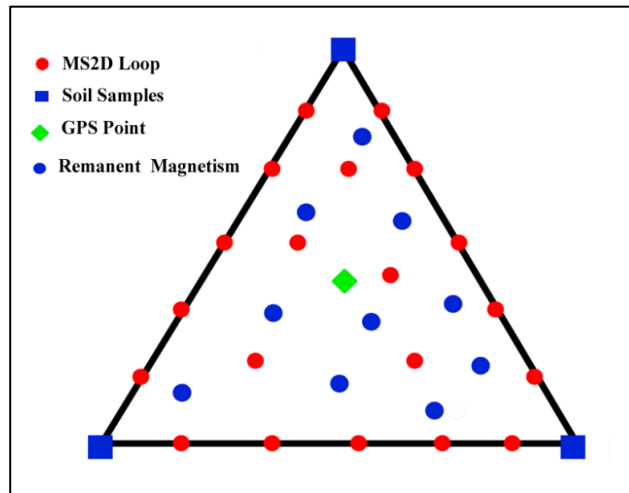


Figure 2.2: Sampling procedure for the collection of soil samples and for collecting volume susceptibility data.



Plate 2.1: Use of MS2D Bartington loop detector to obtain volume magnetic susceptibility data. The MS2 measuring system is based on equation 2.1 (Bartington Instruments, 1994):

$$\mu_0 K = \mu - \mu_0$$

equation 2.1

where μ is the permeability of the sample, μ_0 is the permeability of free space (units are NA^{-2}) and K is the volume magnetic susceptibility. K is calculated once the permeabilities are measured (Bartington Instruments, 1994).

The Bartington sensor works on the basis of induction and contains a high thermal stability oscillator. Power is supplied to the oscillator which generates a low intensity (c. 80 A/m) alternating magnetic field. The frequency of oscillation is determined by μ_0 when an air measurement is taken. If a measurement is taken with a specimen present, the value μ determines the oscillation frequency. By appropriate calibration, the oscillation frequencies can be converted into magnetic susceptibility values (Evans and Heller, 2003).

The MS2D loop is 18.58 cm in diameter and operates at a frequency of 0.958 kHz and has a sensitivity of 2×10^{-6} S.I. The loop is pressed against the ground surface and a reading obtained. Data were collected for this thesis using the toggle switch facility. Initially the loop is held up in the air and zeroed. The toggle switch was then turned to 'measure' and 5 readings were taken, still with the probe off the ground to determine that no drift was occurring as may happen in high magnetic gradients or if the instrument's temperature had not stabilised. Only then was a reading taken with the probe pushed firmly into the ground. The readings were allowed to stabilise and the measurement noted. Five readings were taken from equalled spaced stations along each of the three sides of the triangle (and zeroed after each side was completed) and five readings within the triangle, Figure 2.2. Bartington Instruments (1994) report that the depth of investigation of the instrument is approximately equal to its diameter (18.5 cm). Leconanet et al. (1999) in a series of experiments, conclude that the loop sensor can be used to map the spatial extent of different soils but that 95% of its response is within the top 8 cm of the surface. The instrument senses an integrated volume of 4300 cm^3 (Gautam et al., 2004). There is a rapid fall off in signal as distance from the surface is increased. Dearing (1994) reports that if the probe is used on a surface with a 5mm thick (non-magnetic) leaf litter, the susceptibility value measured is only 75% of its true value.

An experiment was conducted in which the susceptibility was measured at different distances (0 mm direct contact), Table 2.1 and Figure 2.3.

The experiment showed an exponential decrease in values with distance. For example, with a 12mm thick layer, the measured value is slightly over half (51.6%) the true value. This effect needs to be taken into account when doing inter-sites comparisons because over 80% of the readings were obtained in pasture and different sites will have different grass cover thicknesses. Two sites may have a measured susceptibility value of 56×10^{-5} (S.I.) but if the grass cover in site 1 is 6 mm its true value is 80×10^{-5} (S.I.) and the true value for site 2 is 126×10^{-5} (S.I.) if its grass cover is 15mm thick. It was not feasible to measure the thickness of grass at each site (when compressed by the ring probe) or remove the grass cover from each site for each measurement (see section on limitations of the research, Chapter 7. However, at each site, two measurements were taken with the grass present and with it removed. The first such reading for Site K51, for example, had a susceptibility value of 35×10^{-5} (S.I.) with grass and 46×10^{-5} (S.I.) without it (correction factor of 1.31) and the second reading had a susceptibility value of 29×10^{-5} (S.I.) with grass and 33×10^{-5} (S.I.) without it (correction factor of 1.14). An average correction factor of 1.22 was employed for Site K51.

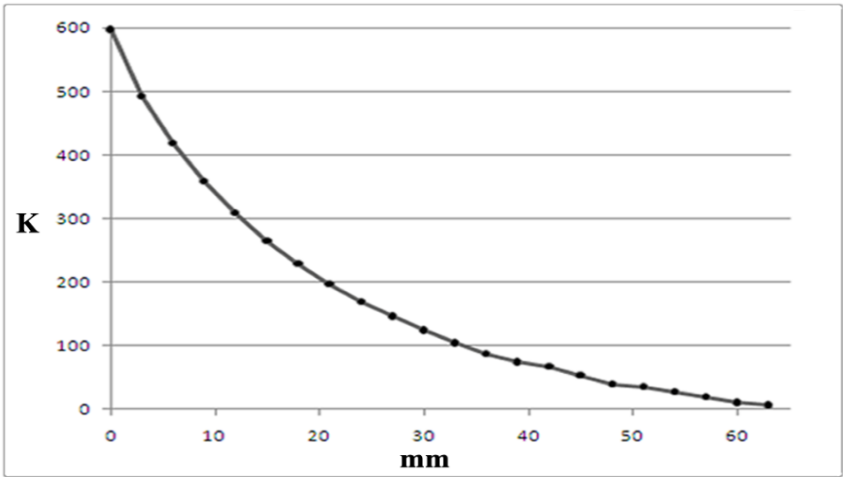


Figure 2.3: Fall-off in volume magnetic susceptibility values with distance from surface. Vertical scale $\times 10^{-5}$ (S. I.).

mm	K value	%	Correction Factor
----	---------	---	-------------------

0	597	100	1
3	492	82.4	1.21
6	418	70	1.43
9	359	60.1	1.66
12	308	51.6	1.94
15	265	44.4	2.25
18	229	38.4	2.61
21	197	33	3
24	169	28.3	3.53
27	146	24.5	4.1
30	124	20.8	4.8
33	104	17.4	5.74
36	87	14.6	6.86
39	74	12.4	8.1
42	67	11.2	8.9
45	53	8.9	11.3
48	39	6.5	15.3
51	35	5.9	17.1
54	27	4.5	22.1
57	19	3.2	31.4
60	10	1.7	59.7
63	6	1	99.5

Table 2.1: MS2D loop probe correction factor.

The standard deviation for the 20 volume susceptibility readings was acquired as well as the mean value. If all measurements were identical, then the standard deviation would be 0. Such a situation would imply that the site is very stable, that the magnetic mineral forming processes are constant and that disturbance is at a minimum. However, it is not possible to map the variation of standard deviation and simply conclude that lower values indicate sites where conditions are more stable. Consider the susceptibility values for two hypothetical sites H1 and H2, Table 2.2. Values for Site H2 are simply an order of magnitude higher than for Site H1. However, relative values and distribution are similar for both sites: the highest value is 10.5 times the lowest value; the second lowest value is 50% higher than the smallest one, etc. However, because the susceptibility values are

so much higher for Site H2 than Site H1, the calculated standard deviation is 10 times higher. Volume susceptibility collected for this thesis ranged over two orders of magnitude. For this thesis, the percentage relative standard deviation (%RSD), used extensively in analytical chemistry, was employed. This yields the absolute value of the coefficient of variation and is calculated by dividing the standard deviation by the mean and multiplying the result by 100. A lower %RSD value means that there is less variability at the site. Sites H1 and H2 which have a similar distribution pattern, have the same %RSD. Maps showing the variation in %RSD are in Chapters 4 and 5.

Site	H1	H2
Values	2	20
	3	30
	4	40
	-	-
	-	-
	-	-
	19	190
	20	200
	21	210
Mean	11.50	115
Standard deviation	5.92	59.16
Relative standard deviation %	51.44	51.44

Table 2.2: Statistics based on susceptibility values for two hypothetical sites H1 and H2.

2.2.5 Laboratory measurement of mass specific susceptibility

The large soil sample collected in the field was dried at ambient room temperature as heating could have caused new magnetic mineral to form. It was important that the samples analysed were representative of the site, i.e. have the sample proportion of coarse, medium and fine grained proportions as the soil. However, if the soil was stored in a beaker, the fine material would move towards the bottom. The sample was initially poured through a funnel which produced a cone of sediment with approximate evenly

spread equal amounts of coarse, medium and fine grained material around it, Figure 2.4, (Open University, 1997). This cone was subdivided into 4 quarters, which were individually thoroughly mixed on a flat surface and four samples from A, B, C, D quarters were packed into standard 10 cm³ pots and weighed. Because the specimens used with the MS2B sensor is weighed, it is possible to calculate the mass specific magnetic susceptibility which has units of m³kg⁻¹.

Soil samples were measuring using Multisus software in conjunction with a Bartington MS2 system with an MS2B sensor, Plate 2.2. All measurements were initially taken at the low frequency setting (0.46 kHz) on the 0.1 sensitivity range. This takes considerably longer than the 1.0 range (11 seconds as opposed to 1) but is more accurate for samples with a weak magnetic susceptibility.

The same procedure was followed for all samples. The equipment was turned on 15 minutes prior to measurements being taken to let the operating temperature stabilise. At the beginning and end of each measuring session, a calibrated sample was measured to ensure consistency. Throughout the duration of this research, the values obtained for the calibration sample did not vary by more than 1.5%. The weight of an empty pot and its mass specific susceptibility is input into the program before sample A is measured. To further minimize instrument drift an initial ‘air reading’ is taken without the sample, then the pot with the soil sample is lowered into the MS2B sensor and its susceptibility measured, then a second ‘air’ reading is obtained. The corrected susceptibility reading is thus:

$$\text{Sample reading} - ((\text{first air reading} + \text{second air reading})/2)$$

Samples B, C and D are treated similarly and the magnetic susceptibility value allocated to each site (bulk data) is the average of the 4 readings. The magnetic susceptibility value acquired is the low frequency one and in this thesis is given the symbol: χ_{lf} . The procedure is repeated at a high frequency (4.6 kHz) and high frequency susceptibility is obtained (given the symbol: χ_{hf}). These values are used to calculate the frequency dependent magnetic susceptibility.

It is possible to measure to a precision of $0.1 \times 10^{-8} \text{ m}^3\text{kg}^{-1}$. If a sample has a mass specific magnetic susceptibility of greater than $10 \times 10^{-8} \text{ m}^3\text{kg}^{-1}$ then it generally indicates that it contains ferrimagnetic minerals such as magnetite (Dearing, 1999b). Maher et al. (2002) report that this susceptibility would be possible with a magnetite concentration of 0.04%. As a typical soil sample weighed 15g, this equates to the presence of 0.006g of magnetite. Table 2.3 provides an example of typical results for six sites encompassing a range of susceptibilities and as can be seen the susceptibility values are consistent for each subsample.

Kildare	<i>χ/f</i>		Wicklow	<i>χ/f</i>
K1-A	107.8		W196-A	88.9
k1-B	111.7		W196-B	79.5
K1-C	129.6		W196-C	89.1
K1-D	118.8		W196-D	85.7
K2-A	5.9		W204-A	572
K2-B	8.4		W204-B	509.4
K2-C	6.5		W204-C	520.6
K2-D	5.7		W204-D	542.2
K111-A	107.2		W246-A	4.6
K111-B	104.1		W246-B	4
K111-C	109.7		W246-C	4.4
K111-D	108.1		W246-D	4.1

Table 2.3: Variation in mass specific magnetic susceptibility for subsamples A, B, C, D for typical sites K1, K2 and K111 from Kildare and sites W196, W204, W246 from Wicklow. Units are $\times 10^{-8} \text{ m}^3\text{kg}^{-1}$.

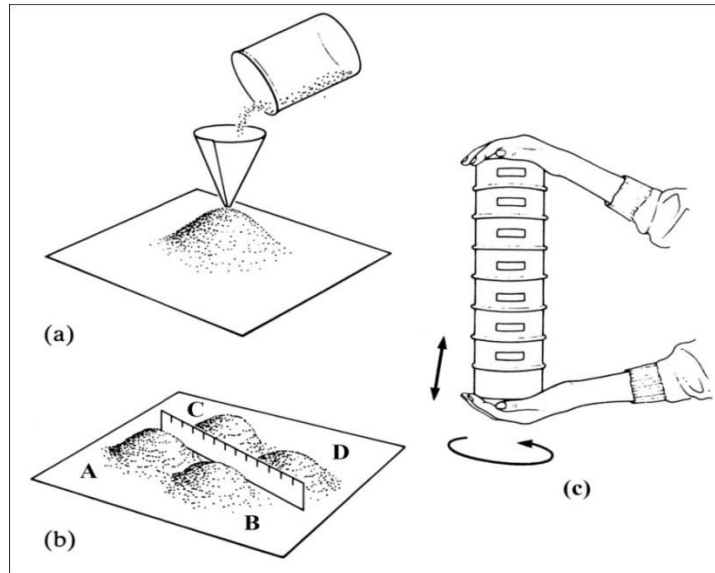


Figure 2.4: Soil preparation procedure to ensure representative samples are analysed, modified after Open University (1997).

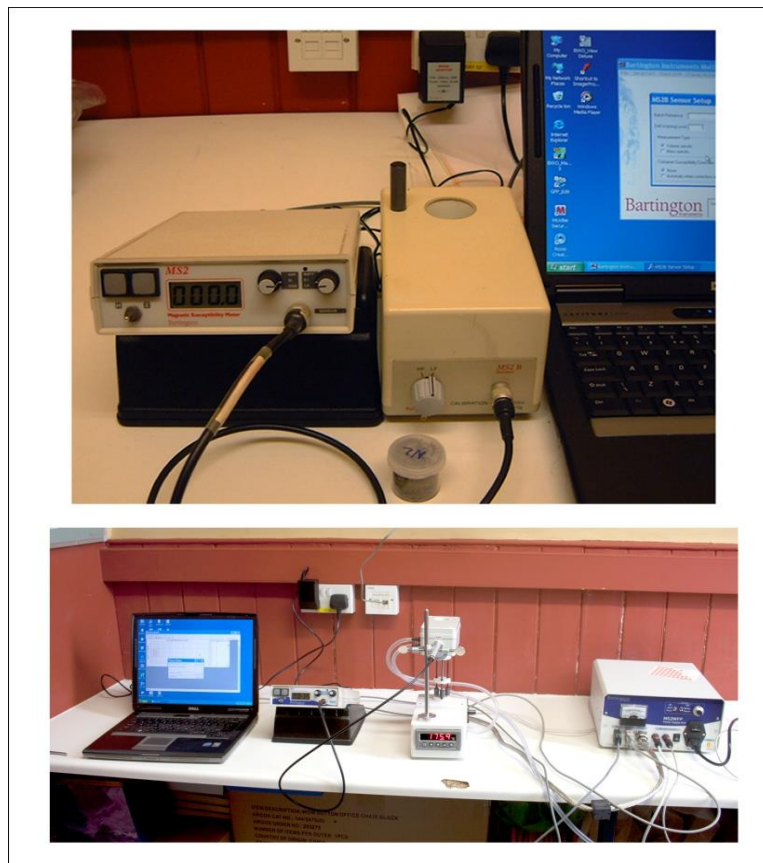


Plate 2.2: (Top) Bartington MS2B and (bottom) MS2W sensors.

2.2.6 Frequency dependent magnetic susceptibility

The Bartington MS2B sensor allows a further level of information about a sample to be determined. Consider a situation in which two samples are measured and they both yield an χ_{lf} value of $20 \times 10^{-8} \text{ m}^3\text{kg}^{-1}$. Using χ_{lf} alone, the samples cannot be differentiated. The standard operating frequency for the MS2B sensor is 0.46 kHz but it is also possible to obtain the measurements at 4.6 kHz, an order of magnitude difference. If the sample is composed of multidomain (MD) grains then the susceptibility measured at the low frequency (χ_{lf}) will be the same as that obtained at the higher frequency (χ_{hf}). However, if the sample contains superparamagnetic (SP) grains which are $<0.03 \mu\text{m}$ in size then the susceptibility obtained at the higher frequency will be slightly lower. Dearing (1999b) has provided an explanation for this phenomenon. The SP grains are so small that they lose their induced magnetism virtually instantaneously once the current is removed because of thermal agitation. At the higher frequency the boundary between superparamagnetic grains and single domains (SD) shifts to a smaller size, thus SP grains near the boundary act as SD grains which have a lower susceptibility (Dearing et al., 1996a; Eyre, 1997; Maher, 1988). This characteristic allows the percentage frequency dependent susceptibility ($\chi_{fd}\%$) to be measured which is given as:

$$\chi_{fd}\% = 100 \times (\chi_{lf} - \chi_{hf}) / \chi_{lf}$$

equation 2.2

where χ_{hf} and χ_{lf} are the mass specific susceptibility values obtained at the high and low frequency respectively. $\chi_{fd}\%$ values range from 0 to 15%. An $\chi_{fd}\%$ of 2% indicates the sample contains about 10% SP grains and a 10% $\chi_{fd}\%$ indicates about 75% SP grains (Dearing, 1999b). There is no simple relationship between susceptibility values (χ_{lf}) and percentage frequency dependent susceptibility ($\chi_{fd}\%$) but many authors record a positive correlation. Huo et al. (2010) reported positive correlations between χ_{lf} and $\chi_{fd}\%$ for both palaeosols and loess at Dali with the loess always having a lower $\chi_{fd}\%$ than the palaeosols. A similar positive correlation was found in Iran between χ_{lf} and $\chi_{fd}\%$ (Mokhtari et al., 2011). Dearing et al. (1996a) report that the most strongly magnetic soils in England are rich in SP ferrimagnetic minerals. However, Lu and Bai (2008)

found an inverse correlation between χ_{lf} and $\chi_{fd}\%$ for urban soils in Hangzhou city, China and Lu et al., (2008) found an inverse relationship for basaltic soils. In an investigation of soils from Panama, Hawaii and Ghana, van Dam et al. (2004) concluded there was no correlation between magnetic susceptibility and frequency dependence.

2.2.7 Magnetic susceptibility of fractional data

The discussion above shows that if magnetic susceptibility values are similar then $\chi_{fd}\%$ values may allow differentiation. However, what if the two samples both yield an χ_{lf} value of $20 \times 10^{-8} \text{ m}^3\text{kg}^{-1}$ and a similar $\chi_{fd}\%$ value? Each soil sample is composed of a range of grain sizes and the underlying assumption up to now is that all grain sizes contribute equally to the bulk susceptibility. Whilst this situation may pertain in some instances, it may not always be the case. In a study of soils from Russia, the magnetic susceptibility was seen to decrease with an increase in grain size (Semenov and Pakhotnova (1998). This inverse relationship was also reported for Pleistocene deposits in Nepal (Gautam et al., 2004). A similar pattern is reported for Lough Catherine, in northern Ireland (Snowball and Thompson, 1990) whereas Booth et al. (2008) concluded ‘the significant relationships between mineral magnetic and particle size properties observed in other environmental settings are not replicated in the data presented here for soils from the Isle of Man’. These findings i.e. little variation in susceptibility with grain size, were supported by work on inter-drumlin lake sediments from northern Ireland (Hirons and Thompson, 1986).

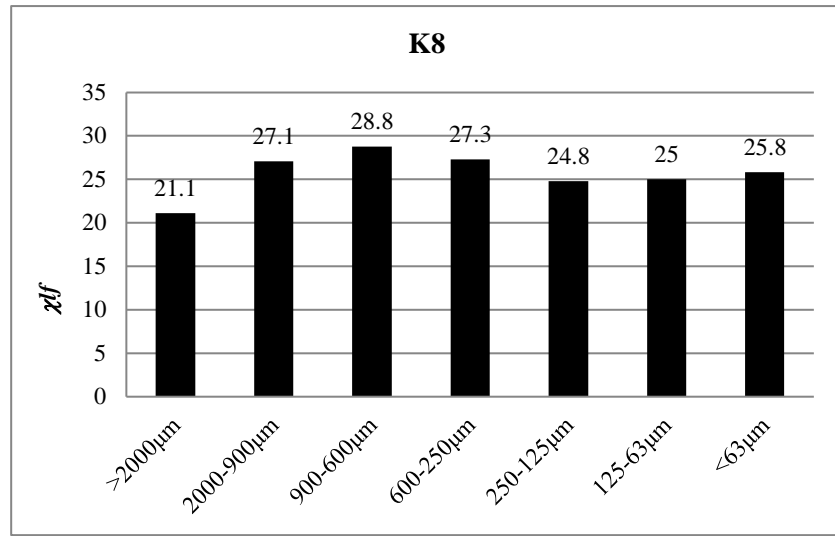
However, in a study of turbidites from Lake Baikal, the coarse fraction ($K= 120 \times 10^{-5}$) was significantly more magnetic than the fine grained material ($K= 15 \times 10^{-5}$). On the other hand, a study of brown earths from Aberdeenshire, found that soils with a grain size of around $200\mu\text{m}$ were significantly more magnetic than soils with higher ($500\text{-}1000\mu\text{m}$) or lower ($20\text{-}150\mu\text{m}$) grain sizes (Mullins, 1977). The above discussion clearly shows any correlation of magnetic susceptibility and grain size is site specific. In addition, the $\chi_{fd}\%$ values for the separate fractions can also be determined resulting in a very high level of detail. The soils in the study area were sieved into 7 standard fractions, Table 2.4, (Greensmith, 1978):

Sieve Number	Grain Size (μm)	Qualitative Grain Size Description
1	>2000	Granules and small pebble size
2	<2000 >900	Very Coarse sand grade
3	<900 >600	Coarse sand grade
4	<600 >250	Medium sand grade
5	<250 >125	Fine sand grade
6	<125 >63	Very fine sand grade
7	< 63	Silt/Clay grade

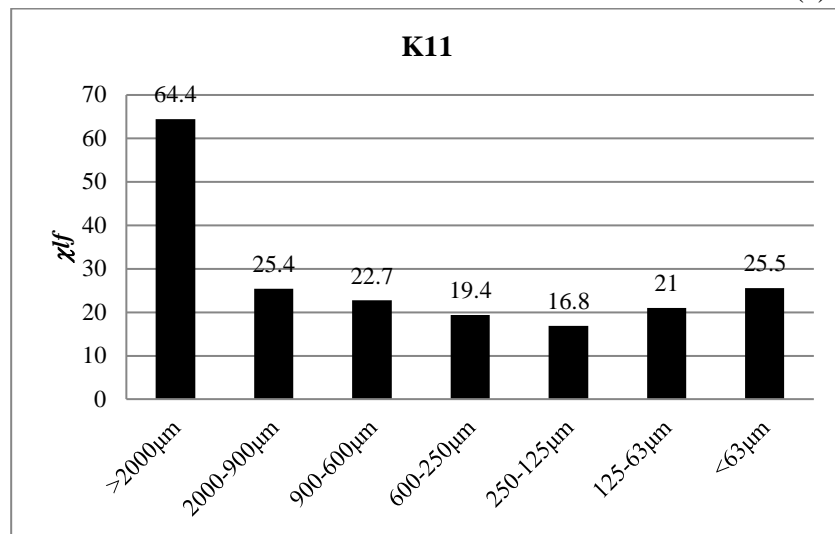
Table 2.4: Fractional sizes for 7 sieves employed in thesis.

Sieve 1 for most of the study area represents small pebbles which have not yet been disaggregated, though some large clasts of quartz were also noted. For each sample, the lithology of the pebbles was ascertained and their size and shape noted. The presence of a specific rock type which was not the same at the site lithology was also recorded at a number of locations. Sieve 7 represented the smallest fraction (silt/clay grade) whereas sieves 2-6 represent a range of sand grade sizes.

The inclusion of particle size susceptibility data in this research means a large amount of detailed information can be extracted from the data, see Chapters 4 and 5 for further discussion. A simple example is given in Figure 2.5 which shows the χ/f value for individual fractions for 2 soils from Kildare (K8 and K11).



(a)



(b)

Figure 2.5: Magnetic susceptibility values for grain size fractions for Soils (a) K8 and (b) K11.

Both soils have a reasonably similar bulk susceptibility values ($25.5 \times 10^{-8} \text{ m}^3\text{kg}^{-1}$ for K8 and $18.6 \times 10^{-8} \text{ m}^3\text{kg}^{-1}$ for K11) but in soil K8, each of the fractions contribute approximately equally to the bulk susceptibility whereas in K11 the $>2000\mu\text{m}$ fraction carries a very strong magnetic signal which could not be determined from the bulk data. Other samples show a similar pattern to K11 but the highest susceptibility is carried by the smallest grain size, not the highest one. As well as the magnetic properties for each fraction being determined, the percentage of each fraction was also obtained. Although the $>2000\mu\text{m}$ fraction for K11 is very high ($64.4 \times 10^{-8} \text{ m}^3\text{kg}^{-1}$), this fraction only forms

5.5% of the sample. Thompson and Oldfield (1986) report that secondary magnetic minerals are most often single domain size and associated with the clay fraction whereas primary magnetic minerals tend to be found in sand and coarse silt size fraction.

2.2.8 Laboratory measurement of variation of volume susceptibility with temperature

All magnetic susceptibility measurements discussed so far have been taken at ambient temperature. However, it is known that susceptibility can vary with temperature (Egli, 2009; Vahle and Konty, 2005; Zhang et al., 2010) and that this variation can provide information on domain state and mineralogy. The Bartington K-T system employs the MS2W sensor which was used in conjunction with the MS2 meter to acquire these data, Plate 2.2. The equipment could be used at very low temperatures using liquid nitrogen (-200°C to room temperature) or using the MS2WF furnace to obtain data in the range 20°C - 800°C. Only the latter mode was employed for this study. Data were taken using the 0.1 MS2 scale at 5°C intervals using a 'heating ramp' of 10°C/minute. Once the maximum temperature of 800°C was reached, the furnace was removed and the specimen cooled naturally during which measurements were again made at 5°C intervals. The samples each weighed c. 2.5g at the start of this process and loss on ignition was around 15%. The entire cycle took approximately 4 hours and the data were processed using Geolabsoft software.

As a sample is heated, the extra thermal energy begins to destabilise the magnetic domains. For paramagnetic grains the susceptibility decreases exponentially, Figure 2.6. Other minerals such as magnetite (ferrimagnetic) or haematite (canted antiferromagnetic) have approximately constant susceptibility values until the Curie (T_C) or Neel (T_N) temperature is reached. The Curie temperature is the temperature at which ferromagnetic or ferrimagnetic material become paramagnetic. The Neel temperature is the temperature at which antiferromagnetic material become paramagnetic. T_C and T_N values for some magnetic minerals are given in Table 2.5.

Mineral	T _C	T _N
Magnetite (Fe ₃ O ₄)	580	
Maghemite (γFe ₂ O ₃)	600	
Haemitite (αFe ₂ O ₃)		675
Monoclinic pyrrhotite (Fe ₇ S ₈)	325	
Hexagonal pyrrhotite (Fe ₇ S ₈)	270	
Greigite (Fe ₃ S ₄)	330	
Jacobsite (MnFe ₂ O ₄)	300	
Trevorite (NiFe ₂ O ₄)	585	
Troilite (FeS)	305	

Table 2.5: T_C and T_N values, source:
http://www.irm.umn.edu/hg2m/hg2m_b/hg2m_b.html

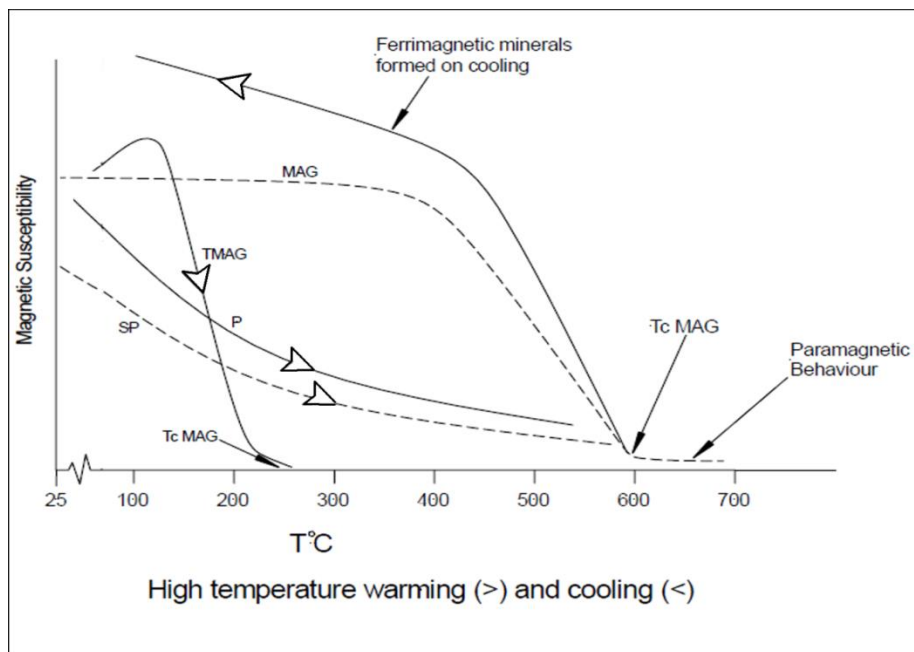


Figure 2.6: Variation of magnetic susceptibility with temperature for magnetic minerals, modified after Dearing (1999b).

Figure 2.7a shows the susceptibility changes in a 20-800°C heating cycle for bulk sample K21. Three points must be borne in mind when interpreting such graphs.

- Firstly, the Curie temperatures given in Table 2.5 and reported in the literature are often theoretical values for ‘perfect’ samples whereas real life magnetic grains will be of variable shapes, sizes, purity and magnetisms.
- Secondly, a typical soil sample may contain a range of minerals in different proportions each with different susceptibilities and different Curie temperatures. The resultant graph will to a large extent be due to a combination of all inputs. As such, this is particularly useful as subtle differences in soil magnetic components may be detected.
- Thirdly, as samples are heated, they may become unstable and be altered to another mineral with a different susceptibility. For example, maghemite is converted to haematite at temperatures greater than 300-350°C producing a decrease in susceptibility (Lowrie, 1997), lepidocrocite is altered to maghemite at 250-350°C (gain in susceptibility) and Li and Zhang (2005) reported that pyrite which is paramagnetic and has a low susceptibility can be converted to magnetite or pyrrhotite by heating.

For Figure 2.7a, susceptibility values remain approximately constant at 52×10^{-5} (S.I.) to 200°C and then rise to 62×10^{-5} (S.I.) at 270°C as some new mineral growth occurs. At higher temperatures there is a relatively rapid decrease in susceptibility initially, possibly due to alteration of maghemite to haematite, followed by an abrupt rise at 460°C. This peak, which occurs just before susceptibility drops to zero, is known as a Hopkinson peak after its first description in the scientific literature (Hopkinson, 1889). It is caused by the unblocking of SD grains and their conversion to superparamagnetic ones (Dunlop, 1995, Mahmood and Bsoul, 2012). The Curie temperature for the sample shown in Figure 2.7a is 585°C which from Table 2.5 shows it is magnetite. Both the cooling curve and the heating curves are shown in Figure 2.7b. In general, the cooling curve can have significantly higher susceptibility values than the heating curve, be approximately the same, or be much lower (Maher, 2007) - the former is typical of the study area. The new minerals which start to grow from about 580°C are very magnetic and are probably

magnetite. The maximum cooling susceptibility is approximately 8 times the maximum heating susceptibility and occurs at 250°C. The broad nature of the slope suggests a range of grain sizes were produced on cooling. Values decrease by about 12% at temperatures less than 250°C.

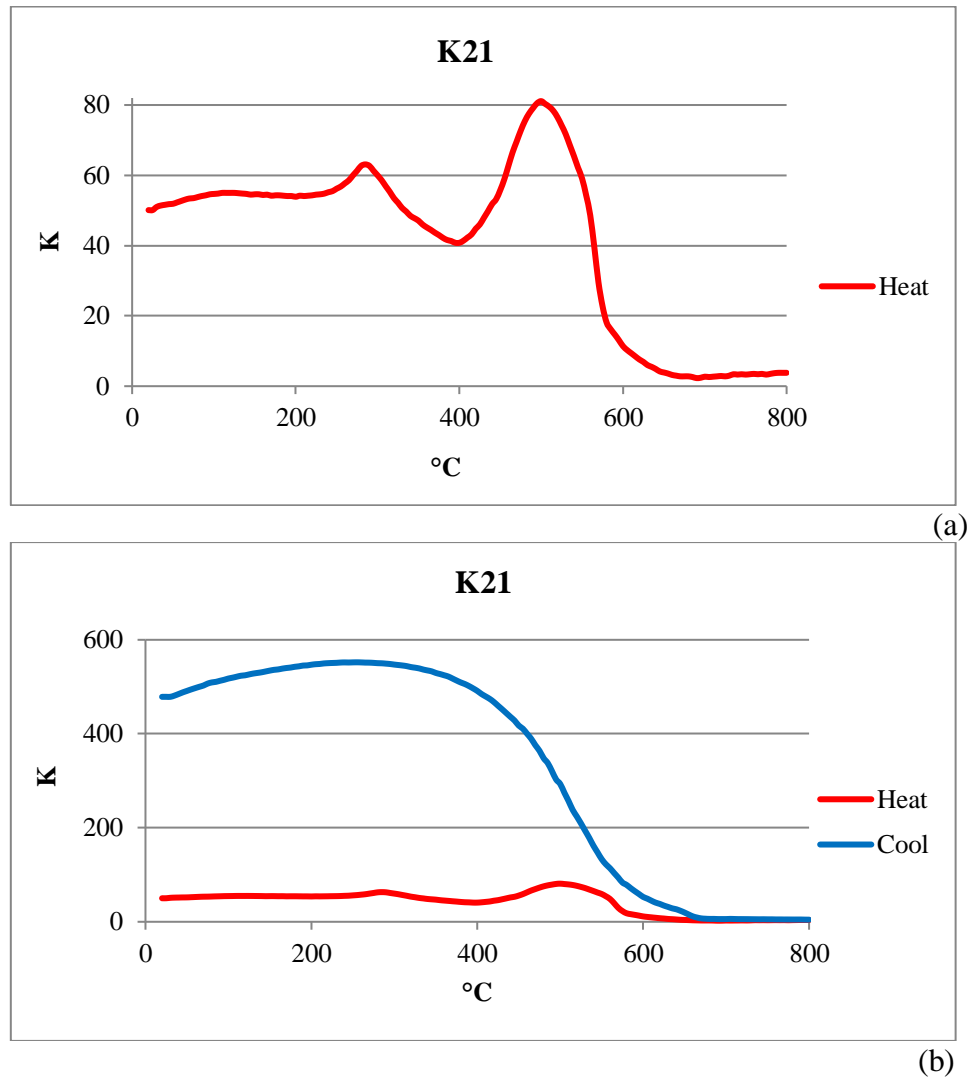


Figure 2.7: (a) Typical heating and (b) cooling K-T curves for soils in study area.

2.2.9 Collection of data for remanent magnetism measurements

Two important considerations have to be borne in mind when collecting data for remanent magnetism measurements: the samples should be extracted from the ground with as little disturbance as possible and the in situ orientation of the sample must be obtained before it is removed to the laboratory. In order to minimise the disturbance, an

aluminium (non-magnetic) tube with a rectangular cross-section was inserted into the ground to a depth of about 10-15 cm, Plate 2.3. In theory the tube should be orientated exactly north-south and be in an exactly vertical position. These conditions were rarely met, thus dip and strike measurements were taken in order to apply later corrections. A Suunto surveying compass was used to obtain the orientation which was usually within 10 degrees of geographic north. The compass could be read to an accuracy of 2 degrees and proximity to the ground did not affect the reading. The deviation from the vertical was obtained using a digital Pro 360 protractor to an accuracy of 0.1 degrees. For the current magnetic epoch, magnetic north is 4 degrees west of true north for east Ireland (study area) and the appropriate conversions were made for compass bearings. The specimen tube was then removed from the ground and a plunger was used to gently transfer the sample to its measurement box, a non-magnetic cube with approximate dimensions $5 \times 5 \times 5$ cm.



Plate 2.3: Collection of samples for remanent magnetism studies.

2.2.10 Laboratory measurement of remanent magnetism

The remanent magnetism parameters (intensity, declination and inclination) were measured using a Molspin spinner magnetometer, Plate 2.4. This apparatus works by electromagnetic induction. The cube of soil is placed into the Molspin in a predetermined orientation and spun about a vertical axis. This produces an oscillating magnetic field which induces a voltage in the detector which is amplified. The amplitude and phase of the signal depends on the remanent magnetism vector.



Plate 2.4: Molspin magnetometer for remanent magnetism measurement.

This procedure is repeated with the sample in a second orientation, hence the oscillating magnetic field is different and different results are obtained. For this research, 6 set orientations were applied to each sample and the results stored automatically in the computer controlled spinner magnetometer software interface. The remanent magnetism vector's intensity declination and inclination were calculated from these results (Borradaile and Geneviciene, 2007).

Ten sample boxes were obtained at each of a number of sites and the intensity, declination and inclination were measured and the results combined to yield an average orientation for the site and statistical information on the dispersion of data. Simple 'linear' statistics are not applicable to remanent magnetism vectors as they are three dimensional features. For example, the average of 358 and 2 is 180. However, the average of a declination of 358° and a declination of 2° is zero (or 360° which is equivalent). Fisher statistics are the 3D equivalent to 'linear' statistics and were employed in this research (Fisher, 1993; Fisher et al., 1987). Further details on the mathematical formulae used in Fisher statistics can be obtained from Mardia and Jupp, (1999).

Table 2.6 shows in tabular form, the declination and inclination results for two test sites S1 and S2. The data are displayed on lower hemisphere equal area Schmidt plots using the software PMagTools created by Mark Hounslow of the University of Lancaster, Figure 2.8. The data for Site S1 is grouped in a small area whereas there is a large scatter for Site S2 data. Both sites have fairly similar Fisher mean directions. Alpha (95%) values show the cone of confidence which indicates that with 95% probability the true mean lies within the indicated radius about the mean. S1 has a cone of confidence angular radius of 4.2° which is significantly lower than Alpha (95%) for site S2 (28°). Various 'dispersion' parameters can be employed in the analysis of the data. The concentration factor 'k' is much higher for site S1 than site S2, indicating the former has a lower scatter.

Site S1		Site S2	
Declination	Inclination	Declination	Inclination
343	71	5	70
333	73	300	65
346	66	280	26
1	72	355	60
5	71	190	52
345	68	307	73
1	78	90	46
350	67	187	25
2	69	43	67
355	70	17	76

Table 2.6: Declination and inclination results for 2 sites, S1 and S2.

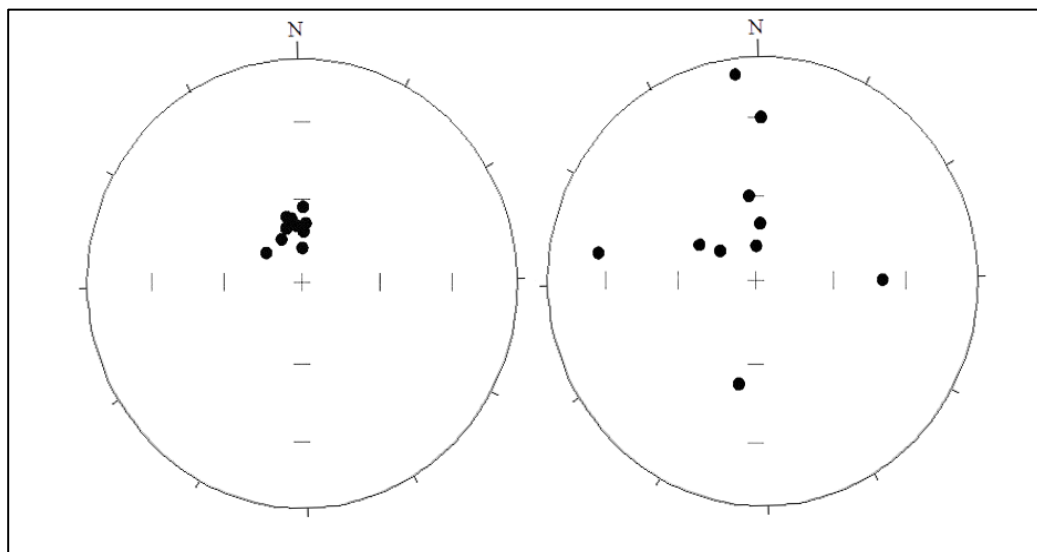


Figure 2.8: Lower hemisphere equal area plots of inclination and declination for soils. S1 on left, S2 on right.

Site S1

Fisher Mean Direction: Declination= 349.2°, Inclination= 70.8°, Alpha(95%)= 4.2°, $k = 135.43$, $R = 9.9335$, $R\text{-bar} = 0.9934$, Spherical Variance= 0.0066, csd (37%)= 6.96°, csd (5%)= 12.03°, Rayleigh Test: Uniformity rejected at 99% probability, Fisher Model: fit acceptable (95% probability).

Site S2

Fisher Mean Direction: Declination= 340.8°, Inclination= 67.3°, Alpha (95%)= 28.0°, $k = 3.94$, $R = 7.7183$, $R\text{-bar} = 0.7718$, Spherical Variance= 0.2282, csd (37%)= 40.78°, csd (5%)= 70.49°, Rayleigh Test: Uniformity rejected at 99% probability, Fisher Model: fit not acceptable (rejected at 95% probability).

R is known as the resultant length, and R-bar the mean resultant length (i.e. R divided by number of samples) and both are measures of dispersion with larger values indicating less dispersion. R can range from 0 to number of samples and R-bar ranges from 0 to 1. Again, Site S1 is seen to be more compact than S2. The angular equivalent of the variance for a normal distribution is known as the spherical variance and is equal to $1 - R\text{-bar}$. This is virtually 0 for Site S1. CSD is the circular standard deviation and is the spherical analogue of the standard deviation for a normal distribution, and is expressed in degrees. It is quoted in two forms CSD (37%), and CSD (5%) which are the radius of the cones which contains 63% and 95% of the data respectively. Again, it indicates how scattered the data are for Site 2. Finally, two general tests are conducted: a uniformity test which indicates the likelihood that the dataset is drawn from a uniform distribution and the suitability of the data being described by a Fisher distribution (Hounslow, 2006). Both sites have the uniformity rejected at 99% probability, it is appropriate to describe Site 1 as a Fisher distribution but not Site S2.

Whilst remanent magnetism data have the capability to provide very useful discriminating information about the soils in the study area, there is one fundamental condition that must be met in order for the information to have any value. The measured magnetic parameters (remanent magnetism vector intensity inclination and declination) must be as a result of natural processes in the soil and human disturbance/interference on

the results should be non-existent or at the least minimal. The degree to which this condition is met is discussed in Chapter 4.

2.3 Resistivity methodology and theoretical concepts

2.3.1 Introduction

If an electrical current (I) measured in Amperes is passed through a uniform cube of cross-sectional area A (m^2) and length L (m), the voltage drop in volts (V) across the cube is given by Ohm's Law which states that $V = RI$ where R is the constant of proportionality called the resistance, measured in Ohms (Reynolds, 2011). Because R is proportional to A and inversely proportional to L , it is possible to write:

$$\rho = R \frac{A}{L}$$

equation 2.3

where ρ is the resistivity measured in Ohm-m. The inverse of resistivity is conductivity. When collecting resistivity data in the field, 4 electrodes are employed, two of which are current electrodes (c1, source); (c2, sink) and two potential electrodes, p1 and p2, across which the potential difference is measured. It is possible to show that resistivity ρ is given by equation 2.4 where r_1 is the distance between c1 and p1, r_2 is the distance between p1 and c2, r_3 is the distance between c1 and p2 and r_4 is the distance between p2 and c2 (Gibson and George, 2013).

$$\rho = \frac{2\pi\Delta v}{I} \left[\frac{1}{\frac{1}{r_1} - \frac{1}{r_2} - \frac{1}{r_3} + \frac{1}{r_4}} \right]$$

equation 2.4

Equation 2.4 applies to a homogeneous subsurface. However, the subsurface is non-homogeneous, thus the equation allows ρ_a , the apparent resistivity, to be determined. To obtain the true resistivity, the data are modelled, see section 2.3.6.

2.3.2 Factors which control the resistivity/conductivity of a soil

A typical soil consists of particles and voids which may be air filled, wholly or partially water filled or even cement filled. The resistivity/conductivity of a soil depends on characteristics of the soil particles such as mineralogy or grain size, characteristics of the voids such as connectivity, size and electrical resistivity of any fluid present (Samouelian et al., 2005). Other factors such as porosity, compaction, temperature and evapotranspiration are also important. For example, in a study of compacted clay, Abu-Hassanein et al. (1996) report that 'lower electrical resistivity is attained with higher compacted effort because the electrical resistance has decreased in the pores and along the solid surfaces'. Dry soils, in which the voids are air filled have high resistivities but when water filled, a liquid phase pathway can exist and resistivity may be much lower. A negative correlation generally exists between resistivity and water content but it is non-linear (Liangfu and Bingua, 2012). McCarter (1984) reports that at low moisture contents, resistivity decreases rapidly with increasing moisture content but that the rate of decrease reduces considerably at moisture contents in excess of 15%, and to a minimum for moisture content in excess of 20%.

The electrical properties of the pore fluid are important in determining resistivity. Pure water has a relatively high resistivity; c. 10^6 Ohm-m, but the water within the pores is natural water with a much lower resistivity, 1-1000 Ohm-m (Musset and Khan, 2000). Natural water contain dissolved salts and conductivity is greater in such instances.

A soil with a high porosity has the potential to hold more water than a low porosity one. Gibb et al. (1984) report that a soil will have a low porosity if sorting is poor (small grains fill in spaces between large ones), if packing is close and if the grains are rounded as they tend to pack more closely. They also record that clays like illite or montmorillonite which are platy pack tighter than kaolinite and thus in general, have a lower porosity. The porosity and permeability are important characteristics of a soil or sediment layer. In general, the literature shows that gravel, coarse sand and fine sand have a porosity range of about 0.23-0.46. The porosity for finer grained sediments overlap with this range but tends to be higher: silty clay 0.2-0.64, soft organic clay 0.66, inorganic clay 0.39-0.59. It should be borne in mind that porosity is likely to be site

specific as physical conditions, such as for example, compaction pressure can vary. Regarding permeability, the British Geological Survey has produced a report on permeability indices (Lewis et al. 2006). Sand has a hydraulic conductivity of 10^{-1} - 5×10^2 m/day while clay is much lower 5×10^{-7} - 10^{-3} . However, again there may be site variations. They state that montmorillonite clay is up to 2 orders of magnitude less permeable than kaolinite clay, thus depending on the type of clay at a site, different permeabilities may be obtained.

Electrical conductance can take place through a number of pathways: a liquid phase pathway via dissolved solids in the soil water occupying the large pores; a solid-liquid phase pathway via exchangeable cations associated with clay minerals and a solid pathway via soil particles that are in direct and continuous contact with one another (Corwin and Leach, 2005). Corwin and Leach (2005) have produced a wide ranging paper detailing the usefulness of apparent conductivity measurements in agricultural settings, especially in GPS precision situations, the range of techniques that can be employed to measure conductivity and its usefulness in determining (at the scale of individual fields) the variability of some soil properties. Following a theoretical section, the authors discuss the techniques that can be employed to determine soil conductivity, namely electrical resistivity, time domain reflectometry or electromagnetic induction. Their Table 1 provides an excellent summary of the parameters that have been measured: salinity, water content, texture, bulk density, cation exchange capacity, leaching, ground water recharge or soil drainage class and the authors of the relevant research papers. Other anthropogenic field activities such as compaction, irrigation or drainage patterns can also be determined.

Various authors have investigated controls on electrical conductivity, especially the importance of clay minerals. Revil et al. (1998) report that the interpretation of electrical conductivity is more complicated when there is a clay component present. Clays have a charge deficit and the counterions needed to balance this deficit are located on what has been termed 'the electrical double layer', which forms at the clay mineral/pore water interface. In a laboratory experiment using 4 soil cores, (clay content 6-29%), Rhoades et al. (1976) developed an equation for the relationships between soil conductivity (EC_a),

water content (Θ), the conductivity of soil water (EC_w) and relevant soil properties. The relevant equation is

$$EC_a = (\text{transmission coefficient}) \times \Theta \times EC_w + \text{surfaceconductivity}$$

equation 2.5

The transmission coefficient take into account decreases in the mobility of the ions near the solid-liquid and liquid-gas interfaces.

Rinaldi and Cuestas (2002) in a series of laboratory experiments on Argentinean loess, investigated the relationship between electrical conductivity and parameters such as frequency, degree of saturation, temperature, soil density, electrolyte type and concentration. They showed that, at a frequency of $> 10,000$ Hz, that electrical conductivity of the electrolyte remains constant. The conductivity for the loess sediment is frequency independent at values >3000 Hz. An almost positive linear relationship exists between conductivity and conductivity of the electrolyte whereas a non-linear positive one exists between degree of saturation and conductivity. Conductivity was found to increase with temperature by about 2% per $^{\circ}\text{C}$ for each degree of temperature increase with respect to a standard 18°C (see later discussion on temperature). They outline how hydraulic conductivity and electrical conductivity depend on different variables. Porosity and degree of saturation are both very important parameters and are positively correlated with hydraulic conductivity and electrical conductivity. However, the authors show that as grain size increases, so does hydraulic conductivity but electrical conductivity decreases. Size gradation has the opposite effect, as it increases, hydraulic conductivity decreases but electrical conductivity rises.

Waxman and Smits, (1968) produced an important paper detailing their results of laboratory based experiments on electrical conductivities on oil bearing shaly sands in which their samples encompassed a wide range of cation exchange capacities. Cores 1-17 were 90-100% kaolinite and cores 21-27 contained 80-100% montmorillonite. The authors constructed a model which led to an equation (now known as the Waxman-Smits equation) which related the electrical conductivity of a shaly sand that was water saturated to the cation exchange capacity per unit pore volume of the rock and to the

water conductivity. They further explored cases where both oil and water were present. Revil et al. (1998) also developed a model to explain the electrical conductivity in shaly sands which took account of clay composition and content, ionic composition of the pore water and electrical double layer and temperature. Bulk conductivity in the interconnected pore spaces and the surface conductivity at the grain-water interface are both important in determining the electrical conductivity of a saturated sand-clay mixture. They tested their model using high salinity data from Waxman and Smits (1968) against the Waxman-Smits model and concluded that their model led to ‘an improvement in the ability to predict laboratory electrical conductivity measurements’.

Although, soil moisture forms only a very small part (0.05%) of the global hydrological cycle, it makes a contribution to precipitation distribution and is important in the global energy balance. Thus, its measurement and vertical and lateral variation is of major significance (Robinson et al., 2008). Spatially, soil moisture (θ) is controlled by soil texture, layering, vegetation and depth to water table and in turn it controls rainfall-runoff response and soil geochemistry and physical properties. Robinson et al. (2008) provide an extensive review of the techniques that can be employed to map soil water content especially at the watershed scale. The standard approach to obtaining volumetric water content is by oven drying a soil sample at 105°C. Of particular relevance to the present study is the measurement of geophysical parameters using such methods as ground penetrating radar (GPR), electromagnetic induction or direct current resistivity.

The relative permittivity of the subsurface can be related to soil moisture and as GPR data can be collected quickly, large areas can be investigated often using the common midpoint method. The signal obtained by an electromagnetic instrument depends on the conductivity of the subsurface which is related to soil moisture. However, Robinson et al. (2008) report ‘the major difficulty with this method is interpreting the signal and the causes of the response’. The direct current resistivity approach is discussed extensively later in this chapter. Passive and active remote sensing techniques can be used to determine subsurface properties. Measurements in the thermal infrared can be used to determine soil surface temperature whilst radar, an active system which can collect data

with different polarizations can be employed to measure backscattering coefficients which can be used to determine soil moisture (Robinson et al., 2008).

An important empirical relationship called Archie's Law was developed for non-clay bearing rocks (Archie, 1942) which related the effective rock resistivity (ρ) and pore resistivity (ρ_{ω}). It can be expressed thus:

$$\rho = a\phi^{-m}S^{-n}\rho_{\omega}$$

equation 2.6

where s is the volume fraction of pores with water, (ϕ) is the porosity and a , m and n are constants. Typically, a is in the range 0.5-2.5, n is circa 2 and m , which depends on cementation, is 1.3-2.5. The formation factor (F) is the ratio of effective rock resistivity (ρ) / pore resistivity (ρ_{ω}).

The resistivity data collected for this thesis were obtained mainly during 2014 and 2015. Data were obtained during colder conditions or in hotter conditions. However, as temperature increases, conductivity increases because viscosity of fluid decreases causing ion mobility to increase. As conductivity is the inverse of resistivity, the measured resistivity would be expected to be lower than it would be if it was measured at a lower temperature. In order to compare data collected at different time of the year (i.e. different temperature conditions), the temperature effect has to be removed. The methodology proposed by Keller and Frischknecht (1966) was employed to correct the measured data to a standard temperature. Equation 2.7 (below) is a modified version of the one used by Keller and Frischknecht (1966).

$$\rho_{10} = \rho_T \times (1 + \alpha(T - 10))$$

equation 2.7

ρ_T is the measured resistivity, T is the temperature, α is an empirical coefficient derived by Brunet et al. (2010). It has a value of 0.025, i.e. the resistivity changes by 2.5% for every degree Celsius. ρ_{10} is the resistivity at the standard temperature of 10°C employed throughout this research. The average temperature from Figure 2.9 is 10.36°C. The 30

year (1981-2010) average temperature for Dublin airport is 9.8°C. Pellicer et al. (2012) in resistivity studies in Offaly also employed 10°C as the standard.

Temperature °C	Correction Factor
2	0.8
4	0.85
65	0.9
8	0.95
10	1
12	1.05
14	1.1
16	1.15
18	1.2
20	1.25
22	1.3
24	1.35

Table 2.7: Temperature correction factors.

Table 2.7 shows the correction factors for the temperatures that occurred during the research. When $T > 10$, the correction factor is > 1 because the measured resistivity is too low and has to be increased. The temperatures employed in the above calculations was the average obtained from two Met Eireann synoptic weather stations, Casement Airport on the Kildare-Dublin border near Leixlip and Oak Park near Carlow, 3 km south of Kildare. No such data were available for County Wicklow. The 2 selected stations are those closest to the study area and encompass its north-south extent. The temperature employed was the temperature of the soil at a depth of 10 cm, roughly the same depth at which magnetic susceptibility samples were acquired. Figure 2.9 shows that temperature varies gradually from a minimum of c. 4°C to a maximum of 19°C whereas the precipitation in the same period is much more variable. It consists of 3 major rainfall peaks, February 2014, August 2014 and November 2014. The lowest monthly rainfall, September 2014, occurs shortly before the highest one. When resistivity data were collected precipitation was abnormally high (Murphy personal communication).

Temperature decreases with elevation at a rate of about 6.5°C for every 1000m of elevation and this was taken into account where some of the sites in Wicklow were at a significantly greater height than the synoptic weather stations. From the above discussion, it might seem that during the summer that resistivity would be lower because

of higher temperatures. However, the process of evapotranspiration needs to be considered. Evapotranspiration involves the removal of soil moisture by evaporation and transpiration in plants and depends on humidity, wind speed and most importantly temperature. Thus, in the warm summer, moisture is removed from the soil and consequently the overall effect is to have an increase in resistivity during the warm summer months. This is discussed further in Chapter 6.

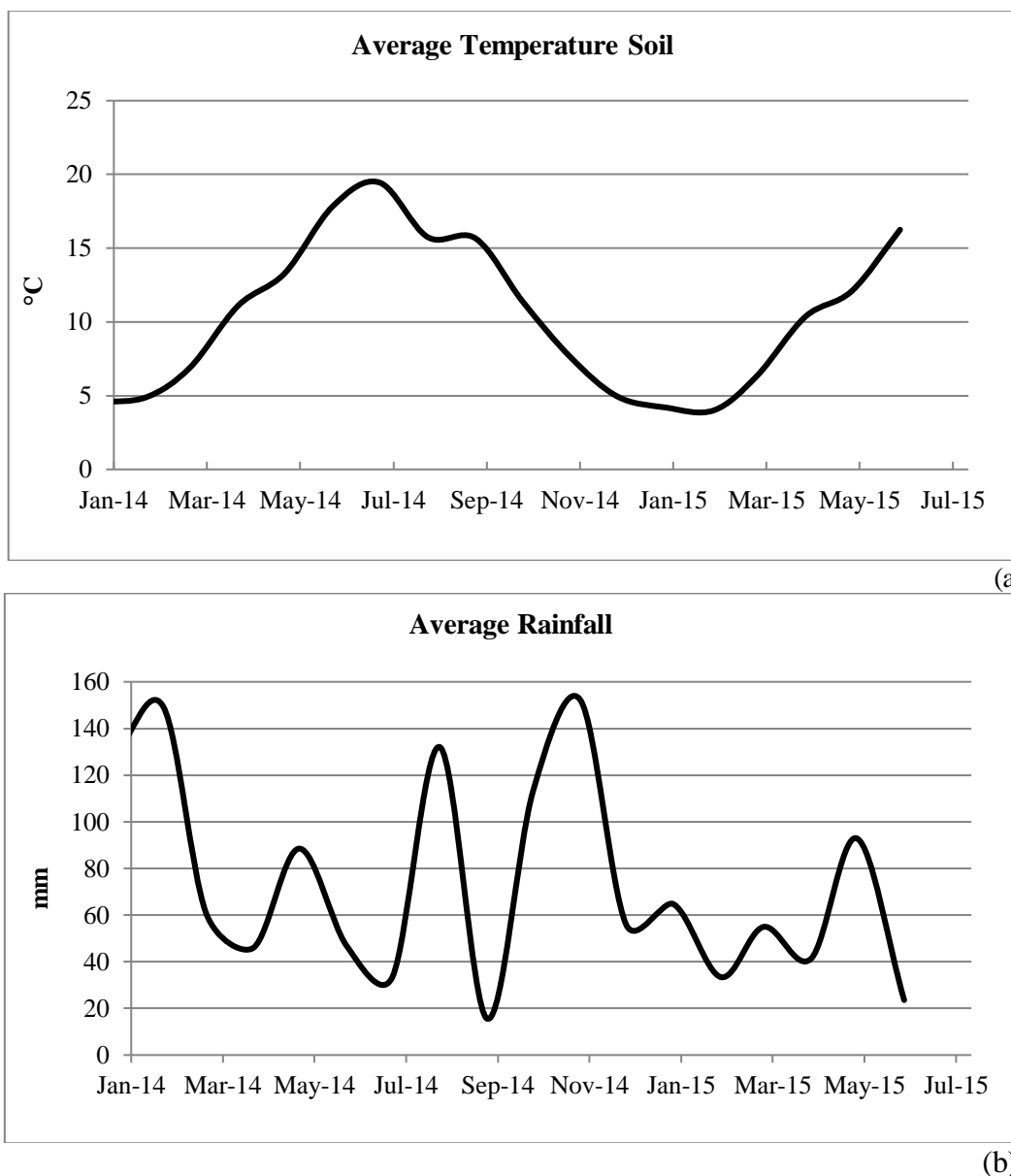


Figure 2.9: Seasonal variation in (a) temperature and (b) precipitation for the study area.

2.3.3 Resistivity of lithologies, unconsolidated sediments and soils

The resistivity values given in the literature range over many orders of magnitude for the same material. Reynolds (2011) for example gives a resistivity of 100 to 250×10^6 Ohm-m for marble whilst Robinson and Coruh (1988) list limestone with a range of 50 to 10×10^6 Ohm-m. Such high values are seldom realised in real situations. Limestone is the commonest rock type in Ireland and many resistivity lines have been taken over it and the vast bulk were mainly three orders of magnitude lower than the highest given in the literature (Gibson, personal communication and fieldwork). The reason why such ranges exist is because of the physical condition of the material. A hard compact limestone with no fractures will have a considerably higher resistivity than one with an extensive fracture system which is water filled. Table 2.8 lists typical resistivity values that were actually measured in Ireland (often within the study area) and within which the present research should be considered. Most of these data were obtained from relevant research theses and from personal communication (with Calaco-Casado, George, Gibson and Pellicer). It is very important that Irish values be employed rather than simply using data from the literature. Reynolds (2011), for example gives a 30-225 Ohm-m range for sand and gravel which is considerably less than that found in Ireland, see Table 2.8.

The importance of water in determining electrical resistivity is obvious from Table 2.8. The greater the degree of saturation, the lower the resistivity is. Gibson (2012) presented the results of an experiment which showed that the addition of water from a point source could reduce the resistivity to 45-55% of its original value to a depth of 70 cm and lateral spread of 1.85m within an hour. Contaminated soils (i.e. contains saltwater or domestic waste), yield very low values of c. 15 Ohm-m. The electrical values for bedrock vary by about an order of magnitude. Carboniferous limestone a few kilometres west of the study area has high resistivity values (c. 6000 Ohm-m), contains very few fractures and is employed in cement production because of its good quality. This is a comparatively high value within an Irish context. However, around Site K1, values for the limestone are considerably lower (c. 800-1000 Ohm-m) and more variable. This is probably due to the effects of folding during the Variscan Orogeny. The limestone around site K1 has been folded and fractured and contains layers of friable shale whereas in the west, the limestone is unfolded and contains very few shale layers. The metamorphic rocks found in Wicklow extend north to Killiney where resistivity values c. 600-1000 Ohm-m were

recorded (Gibson et al., 2012) and Devonian sandstone on Clare Island has a resistivity of c. 600 Ohm-m (Coxon et al., 2013).

Type of sediment	Resistivity Values Ohm-m
Soil/Peat saturated	10-40
Soil/Peat wet	50-200
Soil/Peat contaminated	5-20
Soil peat dry	150-500
Silt/Clay	50-200
Diamicton	500-700
Sand and gravel, well drained	1000-2000
Sand and gravel, poorly drained	750-1000
Bedrock	600-6000

Table 2.8: Typical measured resistivity values in Ireland.

2.3.4 Collection of resistivity data in the field

Although it is possible to use only 4 electrodes in a resistivity survey, which would then have to be continually moved, the vast majority of such surveys are undertaken with a line of electrodes connected by a multi-core cable (e.g. Baines et al., 2002; Zhou et al., 2002). Electrical Resistivity Tomography (ERT) involves the collection of electrical data using these electrodes in sequence to build up a pseudosection which displays the variation in apparent resistivity in 2D or 3D (Loke, 2001). The term RESTOM is equivalent to ERT (van Schoor, 2002). For this study, an Allied Associates Geophysical Ltd Tigre32 resistivity meter with 32 equally spaced electrodes was employed (Allied Associates, 2000), Plate 2.5. There are two main considerations which have to be borne in mind when designing an electrical resistivity survey: Array type and Electrode spacing.



Plate 2.5: Collection of resistivity data using multicore cable.

Array type

Ideally the resistivity data for this research would be collected in 3D format, however, it was only possible to collect 2D resistivity data. This limitation is discussed in Chapter 7. An assumption in 2D resistivity is that if one detects a subsurface body in, for example, a N-S line, that the body extends in an E-W direction to infinity. It is possible to configure 4 electrodes into a large number of current and potential arrays; however, such an approach would entail the calculation of a large number of geometric factors. Instead, over time a number of standard array formats were developed, three of the commonest of which are shown in Figure 2.10. The Wenner (alpha) array has equally spaced electrodes with the order $c_1-p_1-p_2-c_2$. The order is the same for the Schlumberger array but the c_1-p_1 distance is a multiple of the p_1-p_2 spacing. The Dipole-Dipole array is in

the order c2-c1-p1-p2 with the c2-c1 and p1-p2 separations being equal and c1-p1 being a multiple of it. The geometric factor is easily calculated and for the

- Wenner array is $2\pi a$.
- Schlumberger array is $\pi n(n+1)a$.
- Dipole-Dipole array is $\pi n(n+1)(n+2)a$.

where 'a' is the dipole length and 'n' the dipole separation factor (Loke, 2001).

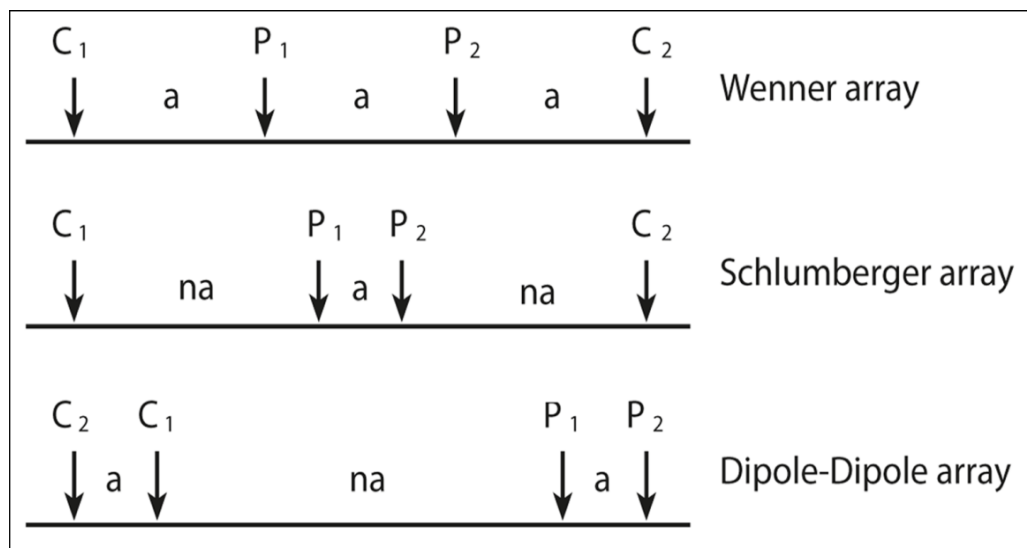


Figure 2.10: Standard resistivity arrays used in ERT.

Figure 2.11 illustrates how a resistivity pseudosection is constructed for a Wenner array (Loke, 2014). A computer program is used to create a parameter file which determines which electrode combinations to employ. The first reading uses electrodes 1, 2, 3, 4 for c1-p1-p2-c2 with a spacing of 'a', then electrodes 2,3,4,5 etc. until the n=1 level is filled in. The procedure is repeated for spacing 2a starting with electrodes 1, 3, 5, 7 and continues to level n= 2 is completed. Note, as the spacing increases the number of data points decrease, data point 56 uses electrodes 1, 7, 13, 19 for c1-p1-p2-c2. It is obvious that if a number of arrays are employed, they each have disadvantages and advantages.

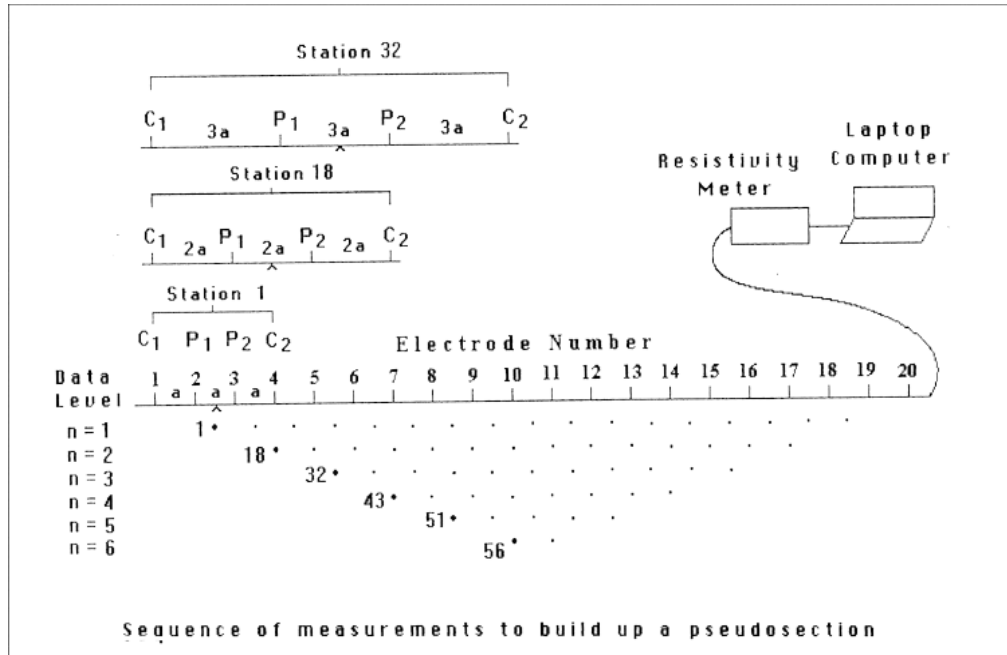


Figure 2.11: Construction of apparent resistivity pseudosection after Loke (2014).

A Wenner array has a very good signal strength (because of the low geometric factor) but for a given number of electrodes collects the fewest data points and has very poor horizontal coverage as the number of data points collected at each level drops off quickly with depth. One of the most commonly employed arrays is the hybrid Wenner-Schlumberger one which combines the advantages of both. This array has better coverage than the Wenner and is sensitive to horizontal (low 'n') and vertical features (high 'n' values) and has a larger median depth of investigation than the Wenner (Loke, 2001). The 2D sensitivity sections for the Wenner, Wenner-Schlumberger and Dipole-Dipole arrays for n= 3 are given in Figure 2.12. Mathematically, they are determined from the Frechet derivative (McGillivray and Oldenburg 1990). These show the degree to which a subsurface change in resistivity affects the measured potential with greatest effect shown in blue or red (Loke, 2001). The negative values (shown in blue) mean that if there is a high resistivity body (higher than background) in this region it will produce a low measured apparent resistivity value. The Dipole-Dipole array is good for mapping vertical structures, see Figure 2.25 (Loke, 2012). See Okpoli (2013) for further discussion on sensitivity functions of different array types.

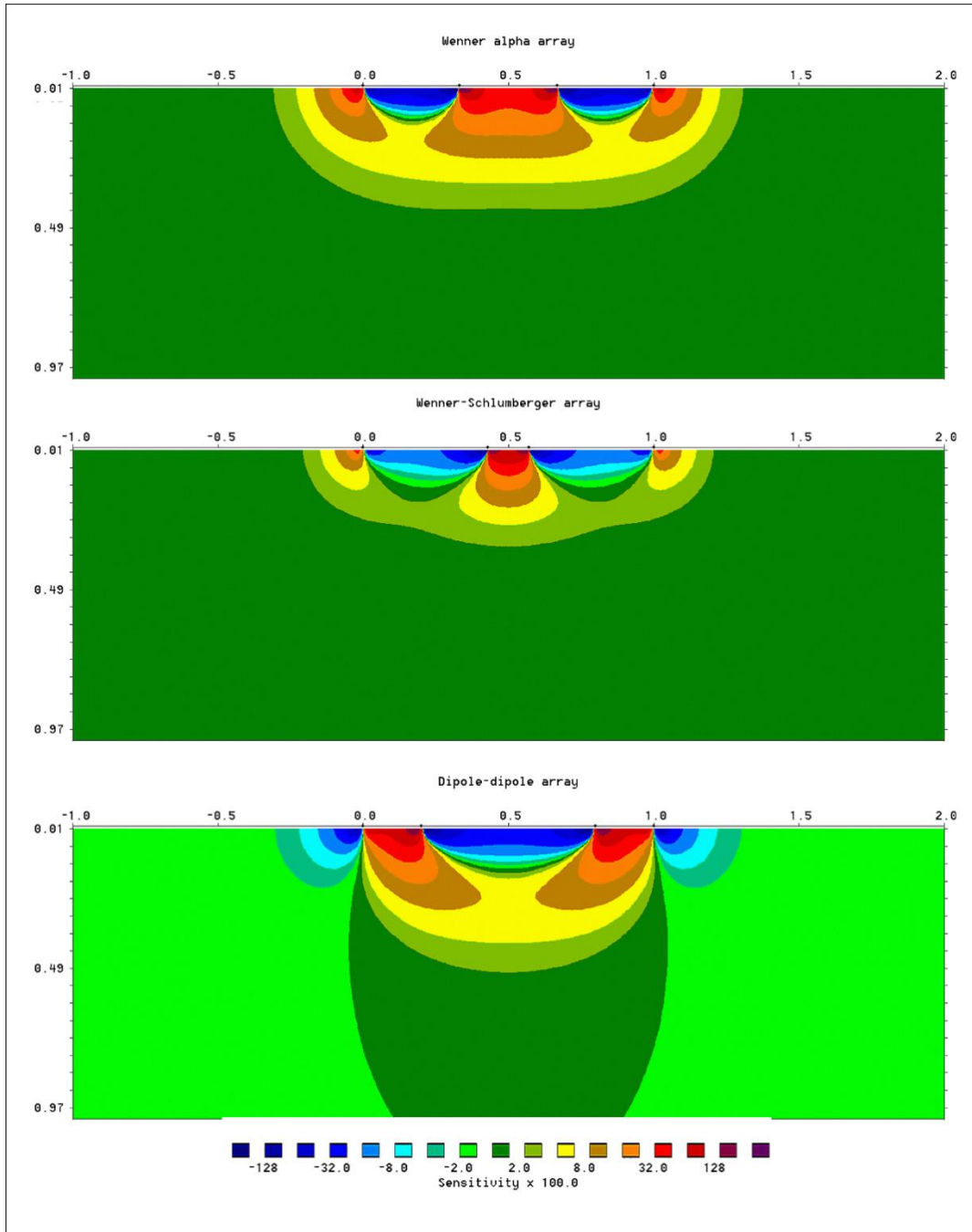


Figure 2.12: Sensitivity sections for different resistivity arrays.

The pseudosections for Wenner, Wenner-Schlumberger and Dipole-Dipole arrays for the same line are given in Figure 2.13. The Wenner and Wenner-Schlumberger pseudosections are fairly similar, though the latter has a markedly increased depth of

investigation, which is also greater than the Dipole-Dipole array which has a far better lateral coverage. Both the Wenner-Schlumberger (Pellicer et al., 2012; Ravindran and Prabhu, 2012; Tonkov, 2008) and Dipole-Dipole (Ahmed and Carpenter, 2003; Ogungbe et al., 2010; Zaidi et al., 2012) arrays are used widely in research. Consequently, for this research, data were always collected using both arrays within one hour of each other. This allowed the advantages of both type to be exploited and provided a useful check. It should also be remembered that Figure 2.13 shows apparent resistivity and pseudo depths and the pseudosections for different arrays are often markedly different (see Figure 2.20 for example).

Figure 2.14 shows the pseudosection data blocks collected for the Wenner-Schlumberger and Dipole-Dipole arrays using ImagerPro2006 software and Table 2.9 gives the electrodes used. In all, 234 data points were collected in Dipole-Dipole format and 198 in Wenner-Schlumberger format. The apparent resistivity values were calculated using the geometric factors given earlier. The 'a' value for Wenner-Schlumberger level 1 is 1m (p1-p2 distance) with an 'n' value of 0.5 $((c1-p1)/(p1-p2))$. Level 2 has an 'n' value of 1 down to an 'n' value of 5.5 for level 11. The electrodes employed for the Dipole-Dipole array were different as was the geometric factor and 'n' and 'a' values. For level 1, 'a' was equal to p1-p2 separation (1.5m) and 'n' $(c1-p1)/p1-p2$, 0.33. The 'n' value for level 2 was 0.66 and for level 12 was 4.

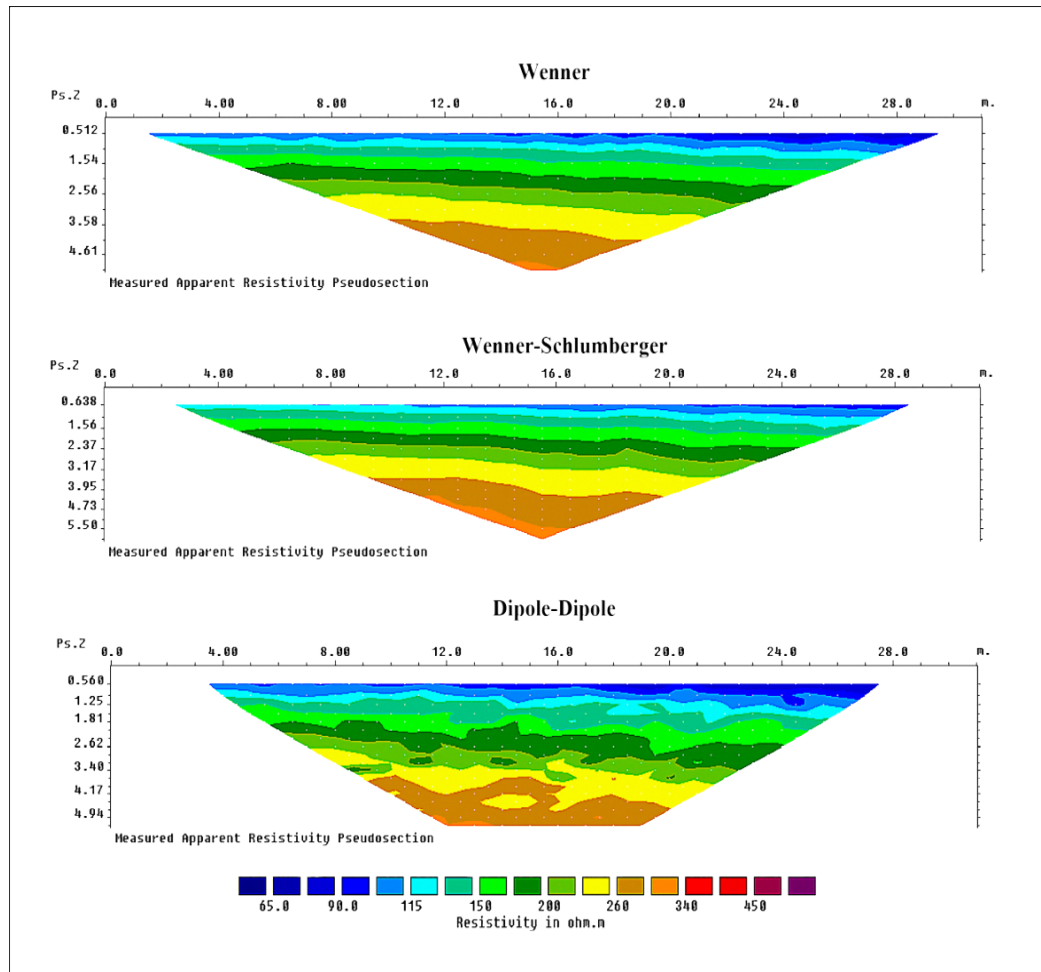


Figure 2.13: Resistivity pseudosections for Wenner, Wenner-Schlumberger and Dipole-Dipole arrays.

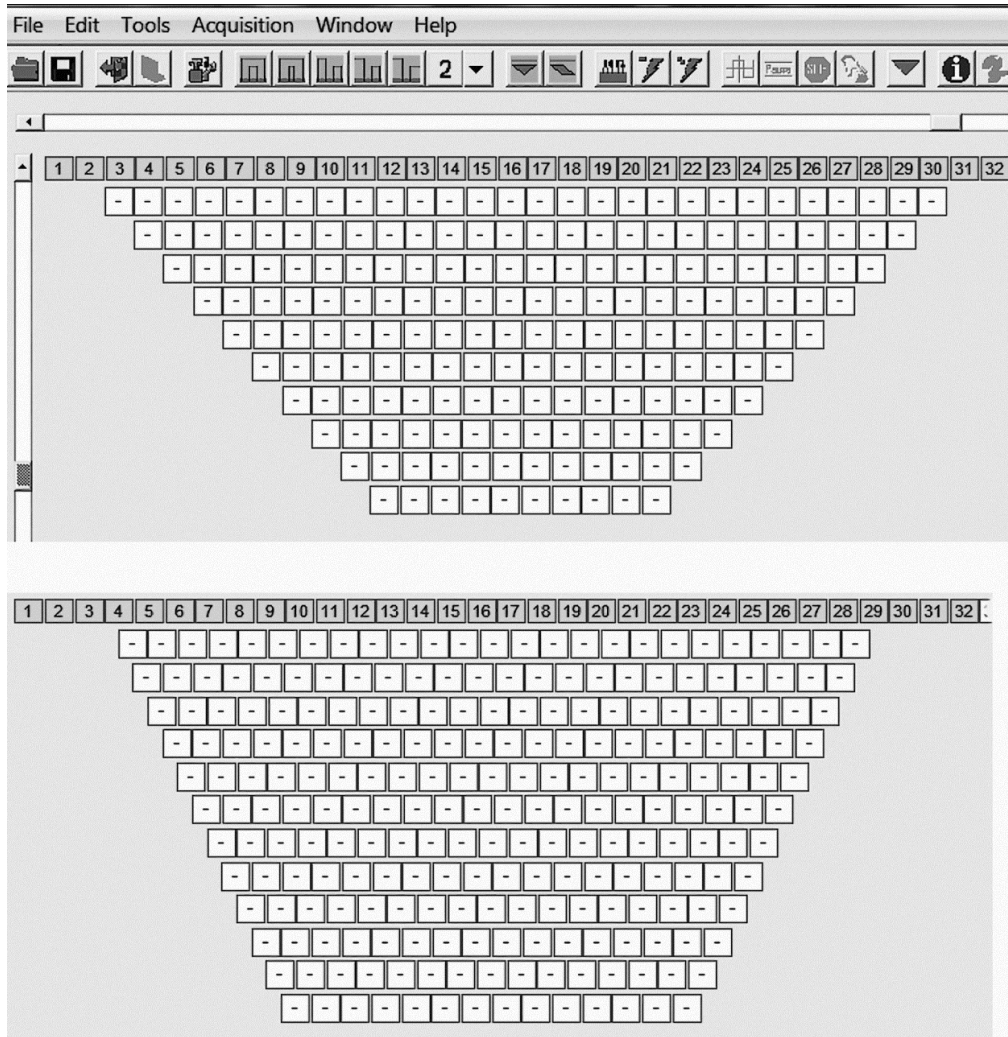


Figure 2.14: ImagerPro pseudosections for Wenner-Schlumberger and Dipole-Dipole arrays used in collection of data.

Electrode spacing

In a multi-core ERT survey, the electrodes are equally spaced, but the operator can decide on the distance between them. Doubling the electrode spacing double the depth of investigation for any particular array, but as the same amount of data is acquired, irrespective of the spacing, less detail is obtained. An electrode spacing of 1m gives a depth of investigation of about 4m. A study of the available literature and field observations showed that apart from peat, the soil thickness in the study area is much less than 4m. An electrode spacing of 0.5m was employed for this research which

provided good detailed measurements throughout the soil profile to a depth of c. 2m. The difference between using a 0.5m and 1m spacing is illustrated in Figure 2.15. Considerably more variation in resistivity is apparent with the smaller spacing at depths less than 2m. The larger 1m spacing averages out the subtle changes and represents the upper 2m as a relatively uniform blue colour.

Wenner-Schlumberger					Dipole-Dipole			
C1	P1	P2	C2	level 1	C1	P1	P2	C2
1	2	4	5		4	5	8	1
2	3	5	6		5	6	9	2
-----					-----			
28	29	31	32		28	29	32	25
C1	P1	P2	C2	level 2	C1	P1	P2	C2
1	3	5	7		4	6	9	1
2	4	6	8		5	7	10	2
-----					-----			
26	28	30	32		27	29	32	24
.....							
C1	P1	P2	C2	level 11 (WS)/12 (DD)	C1	P1	P2	C2
1	12	14	25		4	16	19	1
2	13	15	26		5	17	20	2
-----					-----			
8	19	21	32		17	29	32	14

Table 2.9: Electrodes employed in Wenner-Schlumberger and Dipole-Dipole arrays.

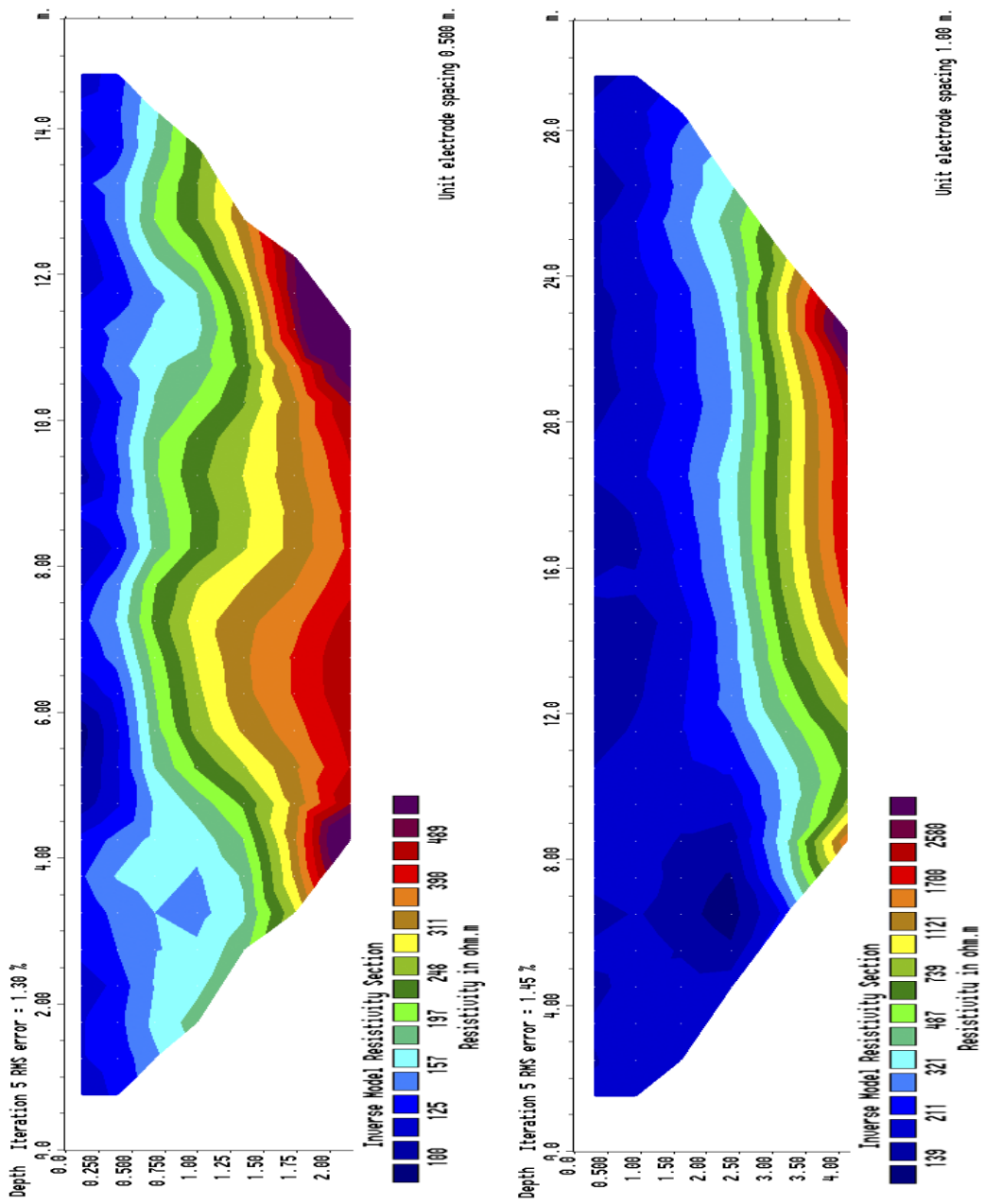


Figure 2.15: Effect of changing electrode spacing: top: 0.5m; bottom: 1m.

Other considerations for ERT surveys

A number of other factors have to be borne in mind when conducting an ERT survey. Data were collected some distance from any electricity pylons. Many fields contained electric fences which were earthed to the ground. These were disconnected before the survey commenced. ImagerPro2006 software was employed to set some of the important parameters in a resistivity survey. The software was fully integrated with Allied Associates Tigre 32 Resistivity System. Before the collection of any data, the contact resistance for each electrode was tested. To ensure good earth contact, the value had to be less than 2000 Ohms (Allied Associates, 2000). During the very dry summer of 2014 when data were being collected, some electrodes (especially those where sand and gravel were near the surface) yielded higher values. These were then drenched with salt water and retested to ensure that a good contact was established. The average resistance for this project was in the range 800-1350 Ohms. The input current for level 1 was 0.5mA which was increased to 10mA for the highest level (12) because of the much longer current path. The average of 3 readings were stored and a percentage error of 5% was used.

2.3.5 Forward modelling of resistivity data

The data collected during a resistivity survey is the apparent resistivity in the form of a pseudosection. However, this may bear little relationship to the subsurface structures which formed it. It is possible to create relatively simple subsurface models and from these, determine the apparent resistivity pseudosection they would produce. This provides some insight into the real pseudosections that are found in the field. This approach was adopted by Kilner et al. (2005) and Pellicer (2010). This forward modelling was undertaken for this research using RES2DMOD software from Geotomo Software. This program uses a finite difference or finite-element method in which the subsurface is broken up into a rectangular mesh of 4 horizontal nodes per unit electrode spacing (Loke, 2002). Thus with an electrode spacing of 0.5m, resistivity values could be allocated every 12.5 cm. A simple subsurface model is illustrated in Figure 2.16 which consists of 3 layers with different resistivity (shown as 0, 1, 2) in vertical contact with each other. Up to 16 different resistivity values can be used.

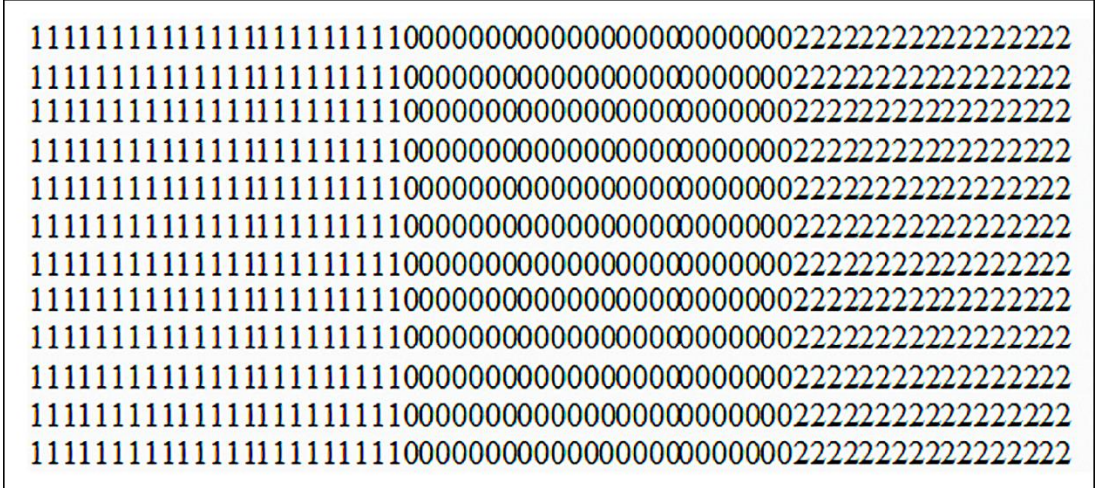


Figure 2.16: Simple model created with RES2DMOD.

Five different models were constructed:

- Two horizontal layer models.
- Three horizontal layer models.
- Two fault models.
- Surface channel model.
- Deep channel model.

Various permutations of each model were created and tested but are not shown here. For example, the effects of different resistivity contrasts and layer thicknesses were determined. In the three-horizontal layer model, the effects of changing the order of resistivity from top to bottom (high medium low; low high low; low high medium) was examined. The apparent resistivity Wenner-Schlumberger and Dipole-Dipole pseudosections for two horizontal layers model with upper layer at 100 Ohm-m and the lower at 800 Ohm-m are very similar, with the former model having a greater range, Figure 2.17. Decreasing the resistivity range of the two layers to 100-450 Ohm-m yields the same image with a lower upper limit. Similarly, increasing the thickness of the upper low resistivity layer, only alters the lower apparent resistivity slightly but decreases the upper value from 392 Ohm-m to 275 Ohm-m for Wenner-Schlumberger and from 287 Ohm-m to 172 Ohm-m for Dipole-Dipole. In three layers horizontal model, in which the

middle layer has a smaller resistivity than the layer above or below, RES2DMOD pseudosection shows the existence of 3 layers, Figure 2.18. Note though that whereas in the theoretical model, the top layer has a lower resistivity than the bottom one, in the Dipole-Dipole pseudosection, the top layer has a higher apparent resistivity than the bottom one. However, if the resistivity values for the layers decrease downwards, the resultant pseudosection is very similar to the two layers pseudosections shown in Figure 2.17.

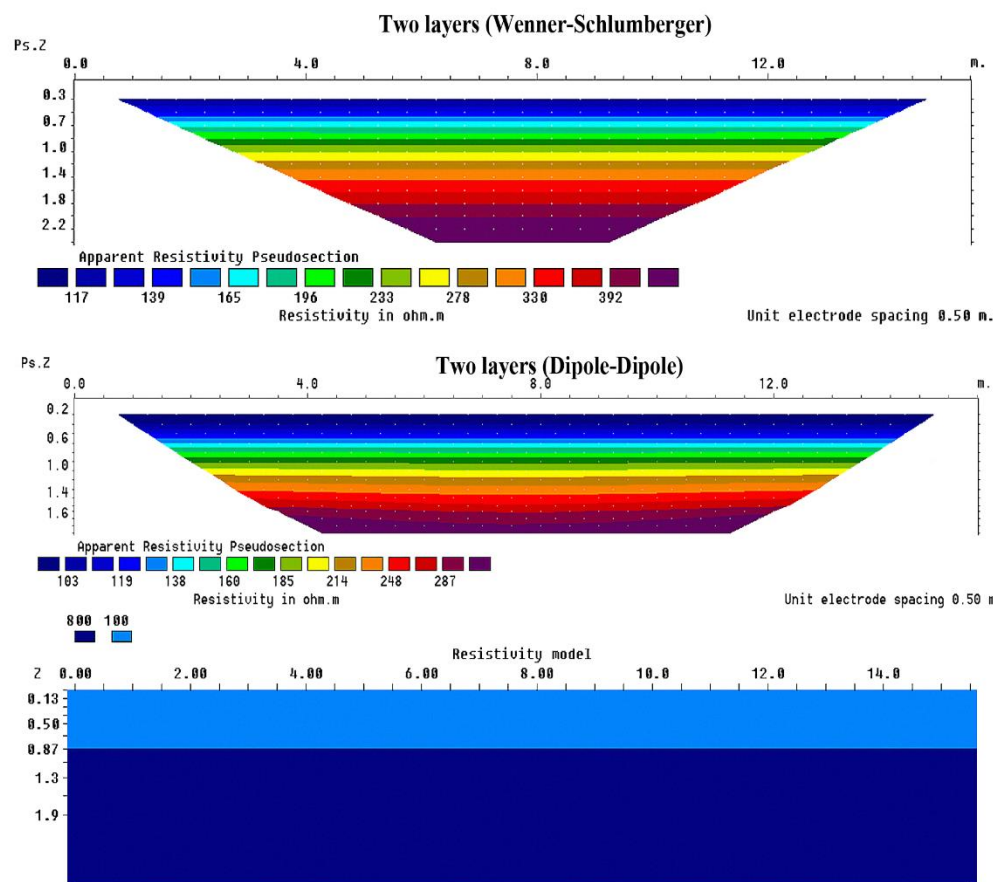


Figure 2.17: Apparent resistivity Wenner-Schlumberger and Dipole-Dipole pseudosections for two horizontal layers model.

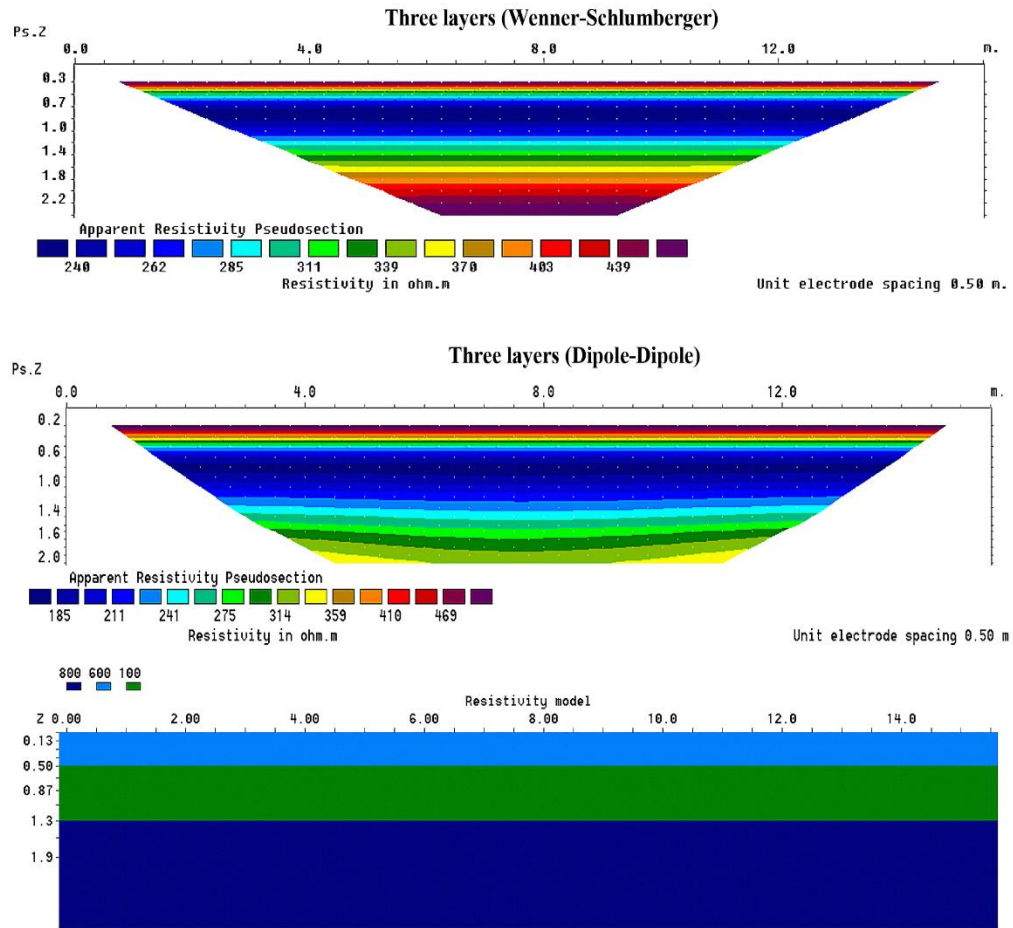


Figure 2.18: Apparent resistivity Wenner-Schlumberger and Dipole-Dipole pseudosections for three horizontal layers model.

The apparent resistivity pseudosections for two vertical contacts are very different, the Wenner-Schlumberger one is not dissimilar to the model but the Dipole-Dipole array provides no evidence of vertical structures, Figure 2.19. Shallow and deep channel models are illustrated in Figures 2.20 and 2.21 respectively. Both array types indicate the presence of the shallow channel, whereas the location of the deep channel would be difficult to determine in the Dipole-Dipole arrangement.

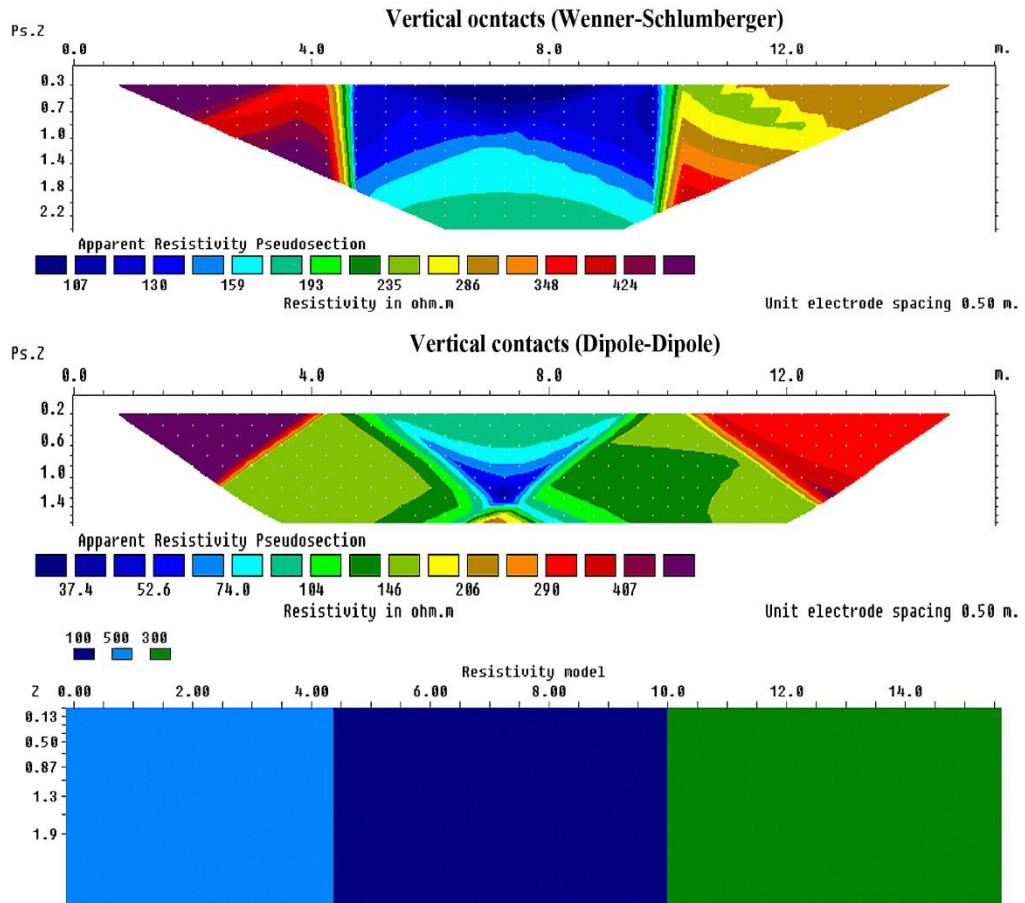


Figure 2.19: Apparent resistivity Wenner-Schlumberger and Dipole-Dipole pseudosections for a two vertical contacts model.

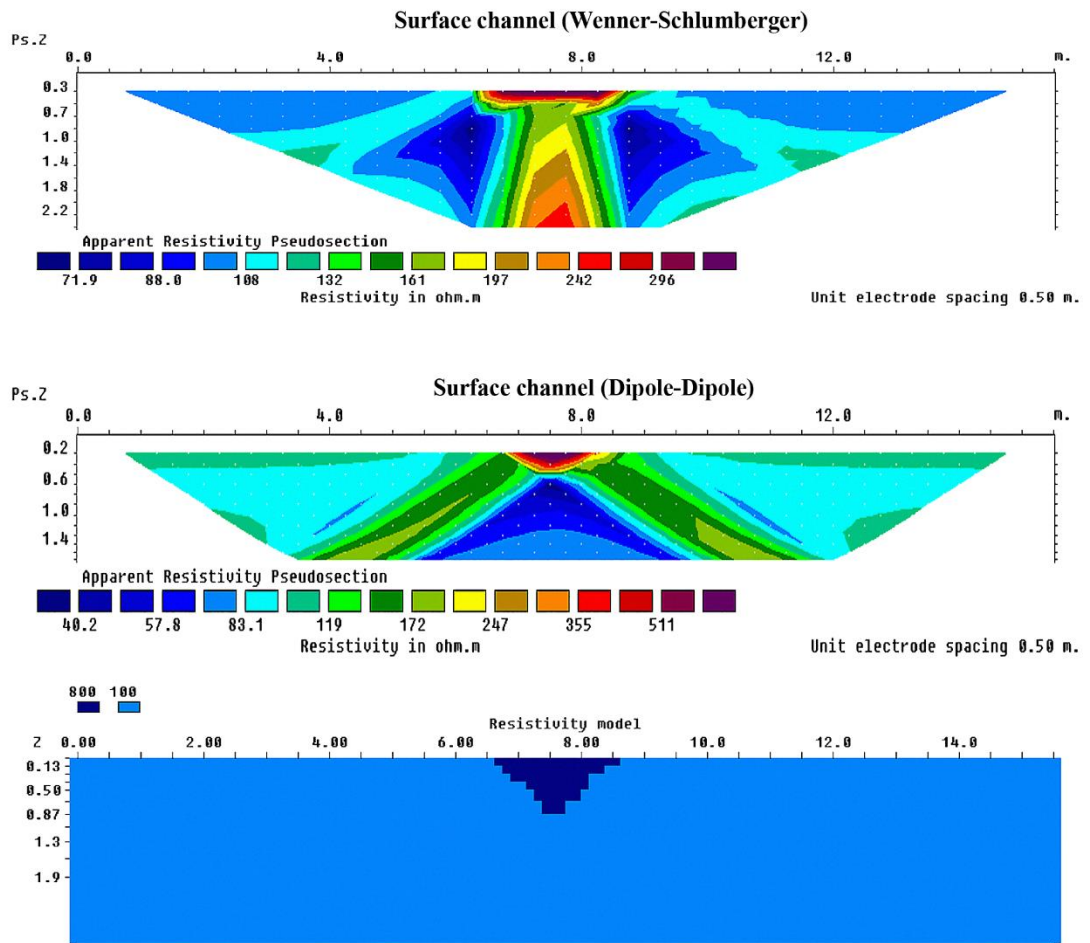


Figure 2.20: Apparent resistivity Wenner-Schlumberger and Dipole-Dipole pseudosections for a surface channel model.

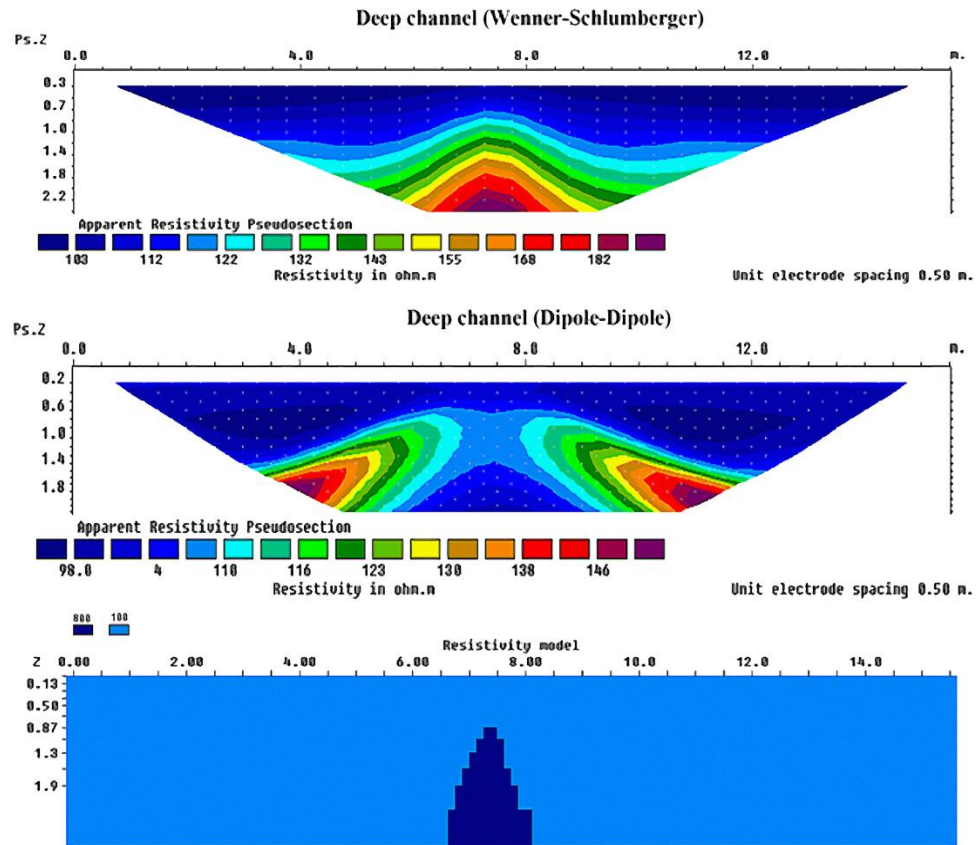


Figure 2.21: Apparent resistivity Wenner-Schlumberger and Dipole-Dipole pseudosections for a deep channel model.

2.3.6 Inverse modelling of apparent resistivity data

Whilst a resistivity pseudosection may give an indication of the nature of the subsurface, some seem totally strange (see Dipole-Dipole arrays in previous section). In order to obtain the true resistivity and true depths from a pseudosection, the data need to be inverted. The inversion program employed in this research is RES2DINV from Geotomo Software which is commonly used throughout the world (Baharuddin et al., 2009; Barker, 1997; Gibson and George, 2006; Jinmin et al., 2013; Karavul et al., 2010). This program initially breaks the subsurface down into a number of blocks, each of which is assigned a resistivity value. The median depth of investigation for layer 1 is 0.5 times the electrode spacing and the block thickness is increased by 10% for each successive layer to account for increasingly poorer resolution with depth (Loke, 2012). The purpose of the software is to produce a calculated pseudosection that is very similar to the

measured pseudosection which it attempts to do using a smoothness least-square Gauss-Newton or quasi-Newton method (Loke, 2001; Loke and Barker, 1995, 1996).

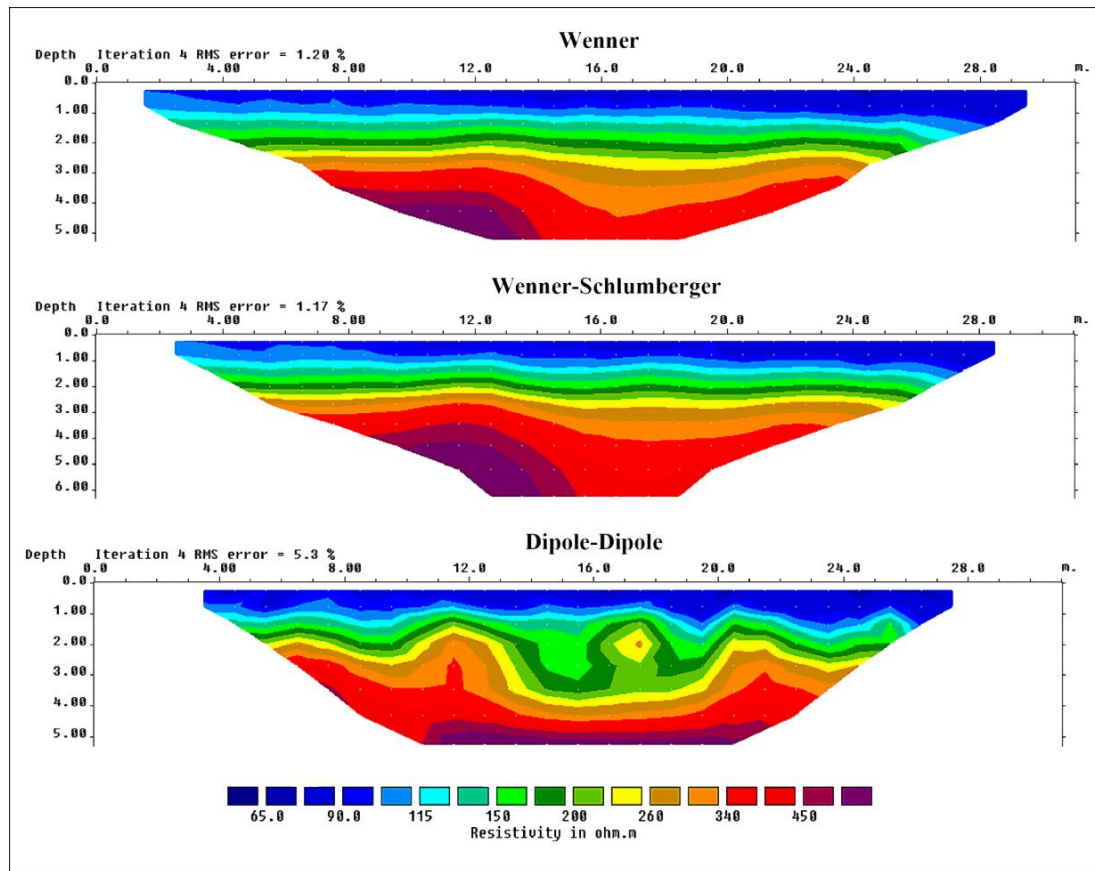


Figure 2.22: Inverse modelling of pseudosections shown in Figure 2.13.

The program goes through a number of iterations (5 are usually sufficient) in which the block resistivity is progressively altered to converge the measured and calculated apparent resistivity. A measure of the difference is given by the RMS error which is usually less than 3%. All resistivity data were inverted using the same program parameters in order to ensure consistency between them and so the inversion results could be compared. The inverse models for the Wenner, Wenner-Schlumberger and Dipole-Dipole pseudosections (Figure 2.13) are given in Figure 2.22. All models show a low resistivity surface layer, c. 70 Ohm-m overlying high resistivity layers. The Dipole-Dipole model has greater variability but its RMS error is relatively high.

Any modelling program can yield artefacts or may not result in a true representation of the subsurface. To determine any potential limitations of RES2DINV, the apparent resistivity pseudosections discussed in section 2.3.5 were inverted in order to ascertain how closely they resembled the original models. The Dipole-Dipole inversion model of a low resistivity zone sandwiched between two higher resistivity ones is a good representation in terms of values and depths of the RES2DMOD model, Figure 2.23.

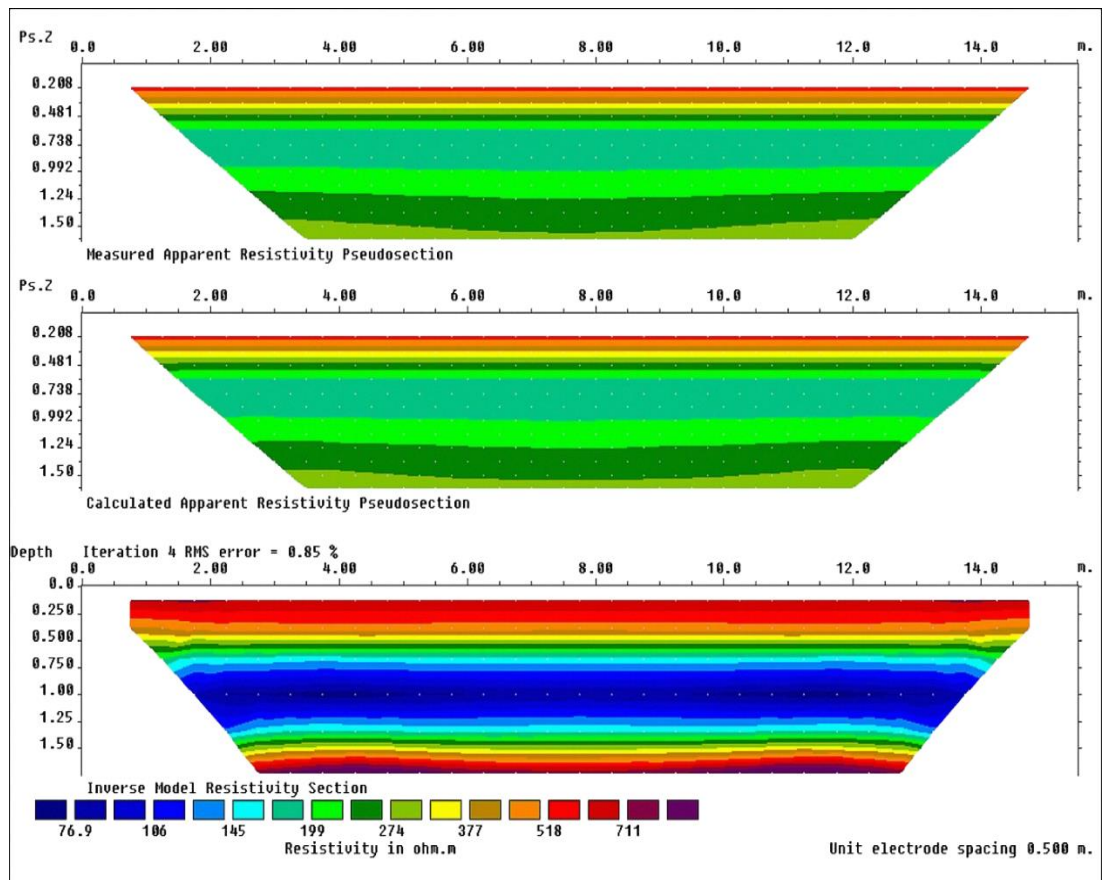


Figure 2.23: Inversion of Dipole-Dipole three layers model pseudosection.

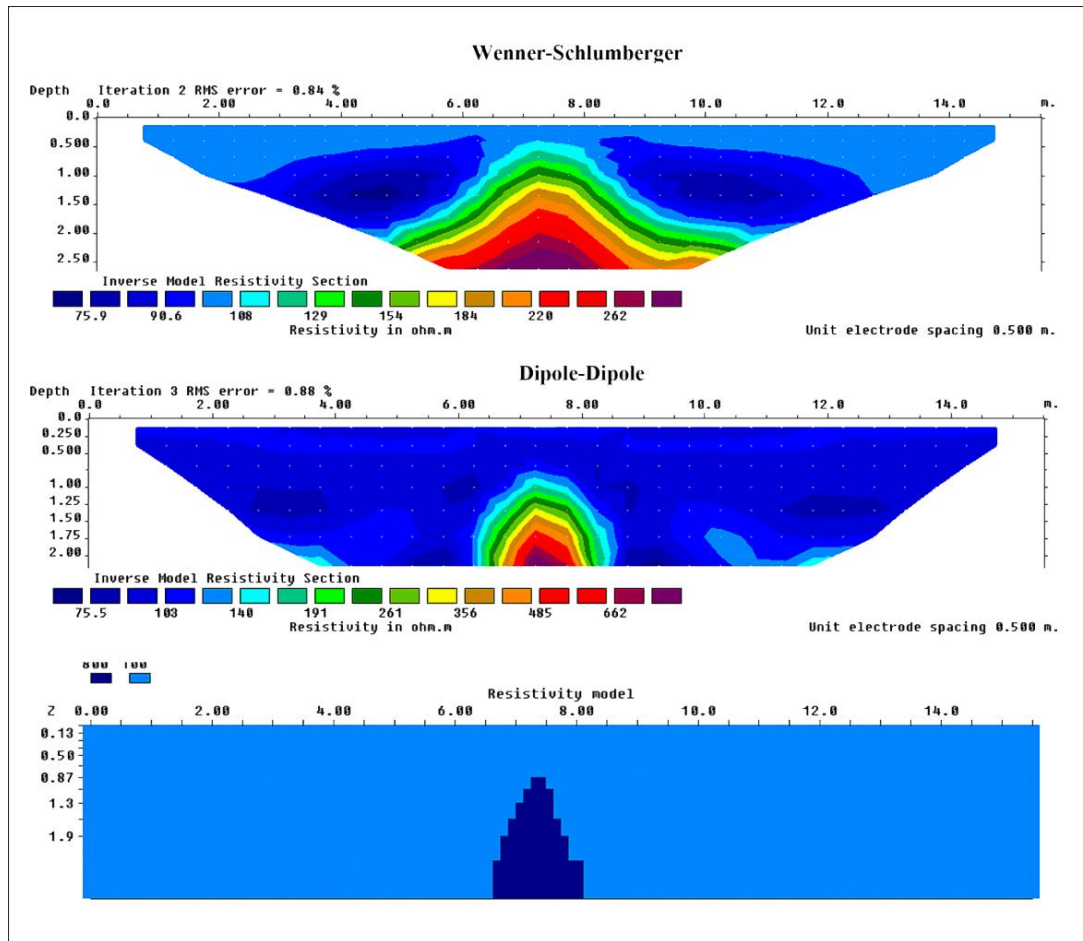


Figure 2.24: Inversion of Wenner-Schlumberger and Dipole-Dipole deep channel model pseudosections.

Both the Dipole-Dipole and Wenner-Schlumberger array inverse models produced equally good representations of the surface channel but the buried channel was much better defined on the Dipole-Dipole model, Figure 2.24. Regarding the horizontal layer models, in the author's opinion, the inversion of Dipole-Dipole array data yielded a better fit to the models than the Wenner-Schlumberger array. This was most manifest in the allocation of a model resistivity to the lower high resistivity layer. In the original models this had a resistivity of 800 Ohm-m (see Figure 2.18) but the Wenner-Schlumberger inversion model values tended to be higher (c 1500 Ohm-m) compared to the Dipole-Dipole model values.

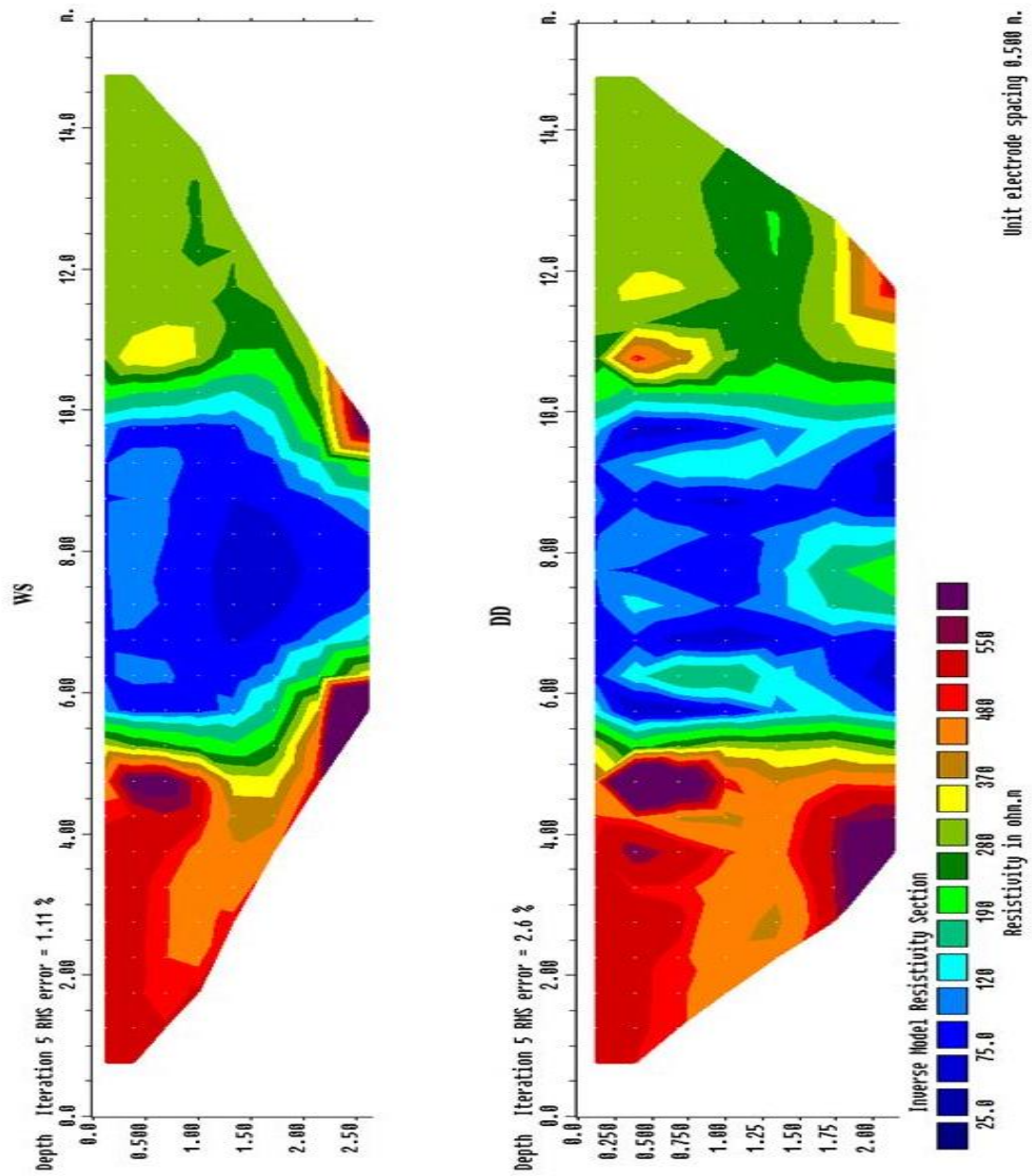


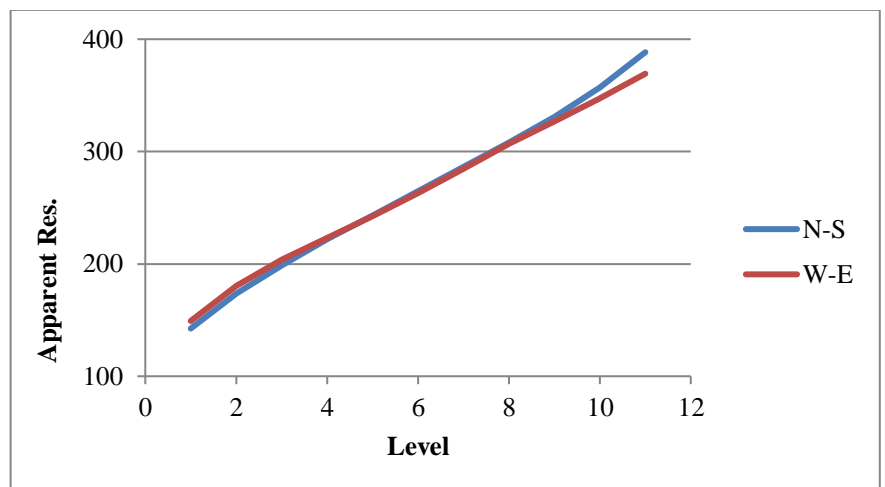
Figure 2.25: Inversion of two vertical contacts model pseudosections.
 WS: Wenner-Schlumberger, DD: Dipole-Dipole.

The apparent resistivity for the two fault models (Figure 2.19) was also inverted using RED2DINV, Figure 2.25. Both array types approximately displayed the correct

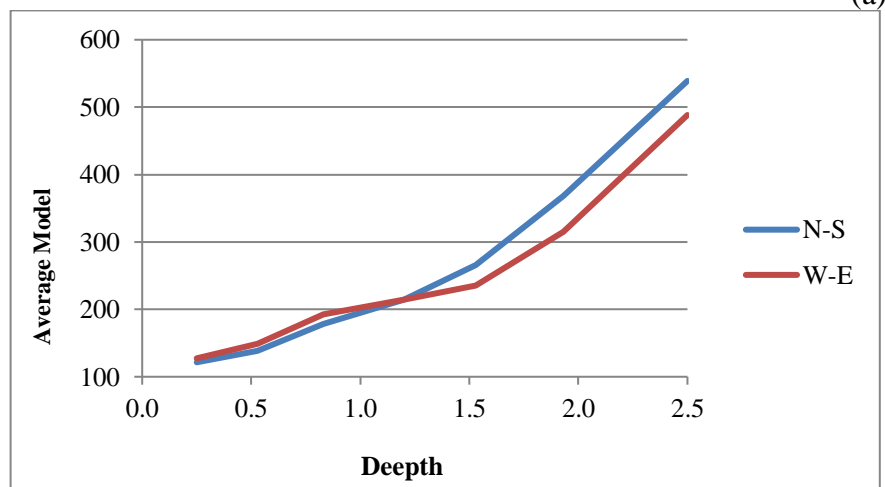
resistivity values (500, 100, and 300 Ohm-m) but the Dipole-Dipole was superior in the definition of the vertical contacts.

2.3.7 Azimuthal resistivity

If the subsurface is composed of layers of a constant thickness each of which has a constant resistivity, then the same apparent resistivity pseudosection would be obtained irrespective of the orientation of the array. However, in reality, layers dip is vary in thickness and resistivity. By taking data about a central point but with different orientations the degree of homogeneity can be determined. Such an azimuthal approach has particular application in geology (Busby, 2000; Watson and Barker, 1999). For this research, at each site where resistivity data were collected, 2 north-south arrays were deployed (Wenner-Schlumberger and Dipole-Dipole) followed by 2 west-east lines.



(a)



(b)

Figure 2.26: Comparison of (a) variation in average apparent resistivity and (b) average modelled resistivity values for E-W and N-S lines.

Figure 2.26a shows how the average apparent resistivity varies for levels 1-12 for a W-E (red) and N-S (blue) Wenner-Schlumberger array. In this instance, both datasets are very similar indicating a good degree of homogeneity in this locality. After modelling with RES2DINV, the resistivity to a depth of around 1.25m is similar in a W-E (red) and N-S (blue) direction. For both lines, resistivity increases gradually from about 125 to 215 Ohm-m. At greater depths the resistivity values increase at a greater rate and are about 10% higher for the N-S line, Figure 2.26b.

2.3.8 Time lapse ERT

Ideally all resistivity data for this thesis would have been collected in one day to eliminate variability in weather, a clearly impossible task, and the actual collection period extended over many years. Time lapse ERT involves collecting data for the same line at several fixed time intervals (Gibson, 2003, 2005, Gibson and Pellicer, 2012). It has particular uses in mapping temporal changes in the subsurface such as monitoring the movement of contaminant plumes (Barker and Moore, 1998; Gibson, 2003, 2007). Pellicer and Gibson (2012) collected resistivity data at monthly intervals during 2006 to investigate Quaternary sediments in central Ireland and Bonsall (2014) employed time lapse resistance surveys to determine the best month to undertake an archaeological geophysical survey in Ireland in order to ensure a good contrast with the background. Time lapse Wenner-Schlumberger and Dipole-Dipole resistivity data were collected at one monthly intervals for 12 months, commencing January 2015 at Site K1 in order to assess the natural variability in resistivity over a long time period.

2.4 Summary

The methodological approach employed for the collection of data and the theoretical concepts underpinning the two techniques employed in this research (magnetism and electrical resistivity) were considered in this chapter. Soil samples were collected from 300 sites in County Kildare and from 250 in County Wicklow, their susceptibilities

measured at two frequencies (0.46 kHz and 4.6 kHz) and percentage frequency dependent susceptibility ($\chi_{fd}\%$) calculated. Volume susceptibility field data were also collected at the 550 sites. The sites were chosen to give a good geographical spread and to include representative samples from each of the main soils in the study area. The bulk samples were later sieved, separated into 7 size fractions and the magnetic measurements were repeated for each individual fraction. This approach provided an extra level of magnetic discrimination for the soils.

The Bartington K-T system was used to obtain magnetic susceptibility data at 5°C intervals in the range 20°C-800°C for 200 sites. The graphical outputs, combined with a knowledge of mineral Curie temperatures, provided information on magnetic mineralogical content of the soils and the alteration processes that occurred. 300 oriented soil samples were taken for remanent magnetism measurements.

Electrical resistivity data were collected at 57 of the sites, at which magnetic susceptibility was also measured. Data were collected in 2D format using a Tigre 32 instrument with 32 electrodes spaced at equal intervals of 0.5m. Two array formats were employed: Wenner-Schlumberger and Dipole-Dipole. Data were obtained in both N-S and W-E orientations in order to determine azimuthal variability. A long-term experiment was conducted at Site K1 over one year period in order to determine natural temporal resistivity variability.

A number of 'standardisation corrections' were required in order to ensure comparative analyses were correct. The variable thickness of grass at the sites, which would have caused errors in the measurement of volume magnetic susceptibility, was accounted for as was the errors introduced into the collection of data for remanent magnetisation when the collection tube was not oriented correctly. Electrical resistivity data, which were collected throughout the year were standardized to a temperature of 10°C. The important parameters which control the resistivity/conductivity of soils were discussed.

CHAPTER 3

Literature Review of the Study Area

3.1 Introduction

Literature relevant to the thesis is discussed in this chapter within two main categories (physical landscape and geophysics) under several separate headings. Sections 3.2 to 3.6 deal with the physical characteristics of the study area which are relevant to the current research. This commences with a discussion on the geological evolution of the study area and a detailed description of the lithologies that are located there. Weathering of these rock types may, to a greater or lesser extent, be a source of magnetic grains in the region and control to some extent the topographic variation which may indirectly affect magnetic susceptibility. Various publications of the Geological Survey of Ireland as well as reviewed academic literature are relevant to this section: (Bruck, 1970; Bruck and O'Connor, 1977; Bruck and Reeves, 1983; McConnell and Philcox, 1994; Reeves, 1997; Sleeman et al., 2004). This is followed by a discussion on glaciation in Ireland and the glacial processes and landforms in the study area as an understanding of these may help in understanding any observed magnetic patterns. The soils of the research area are considered in the following section. The soils in County Kildare have been mapped in some detail during a national soil survey, but there is considerably less information available on Wicklow soils which did not receive the same attention. The second part of Chapter 3 deals with the geophysical techniques, specific to this research, their uses and applications in a regional/global context, to illustrate that the correct approach is being followed here. This is followed with a section on geophysical research in Ireland in order to put this research in context. The chapter concludes with sections on the magnetic characteristics of Irish soils and rocks.

3.2 Geological Evolution of the study area

An examination of the simplified geological map of Counties Kildare and Wicklow shows that the rocks are not randomly arranged but there is a distinct zonation, Figure 3.1. Carboniferous limestone occurs exclusively in the west and units such as the Kildare Inlier (KI); Caledonian Granite and the Silurian greywackes exhibit a pronounced NE-

SW trend. A large proportion of the rocks within the study area formed as a consequence of the Caledonian Orogeny, the most important geological event to affect Ireland (Williams and Harper, 2003). Approximately 750 million years ago (Ma), the supercontinent Rodinia fragmented to form Laurentia (North America and northern Europe and included NW Ireland) and Gondwana, (South America, Africa, India and Australia). Further fragmentation of Gondwana produced Avalonia which included SE Ireland (Sleeman et al., 2004). The ocean between Laurentia and Avalonia, called the Iapetus Ocean, at its maximum was around 2000 km wide and from c. 500 Ma began to close. The collision of the two plates, which brought NW and SE Ireland together, produced massive deformation, extensive igneous activity and metamorphism.

The oldest rocks within the study area are Cambrian in age, c. 520 Ma. These are the Bray Group which includes the Bray Head Formation and the Devil's Glen Formation (McConnell and Philcox, 1994). They are mainly composed of greywackes, and slates, and to a lesser extent quartzites (Holland, 2001). The latter form the distinctive conical Great Sugar Loaf Mountain. The greywackes (composed of muddy sands) were deposited by turbidity currents which were probably triggered by earthquakes. The Iapetus Ocean began to close in the early Ordovician (c. 500 Ma) as a subduction zone formed over a convergent plate margin. The rocks formed at this time are best represented by the Maulin Formation, which consists of fine-grained metasediments, mainly siltstones and shales. South of Wicklow town, the upper Ordovician is best represented by the Duncannon Group - mainly shales and slates (Graham, 2001a). As subduction proceeded, the high temperatures produced by the subducting plate resulted in minor volcanic activity in Wicklow, mainly andesite and dolerite.

The Silurian (c. 420Ma) rocks form the western border of Wicklow and the eastern border of Kildare. The region is represented by the Kilcullen Group (which includes the Tipperkevin Slate Quarries and Glen Ding Formations). It is similar to the Ordovician rocks and is dominated by greywackes, shales and slates (Bruck, 1970).

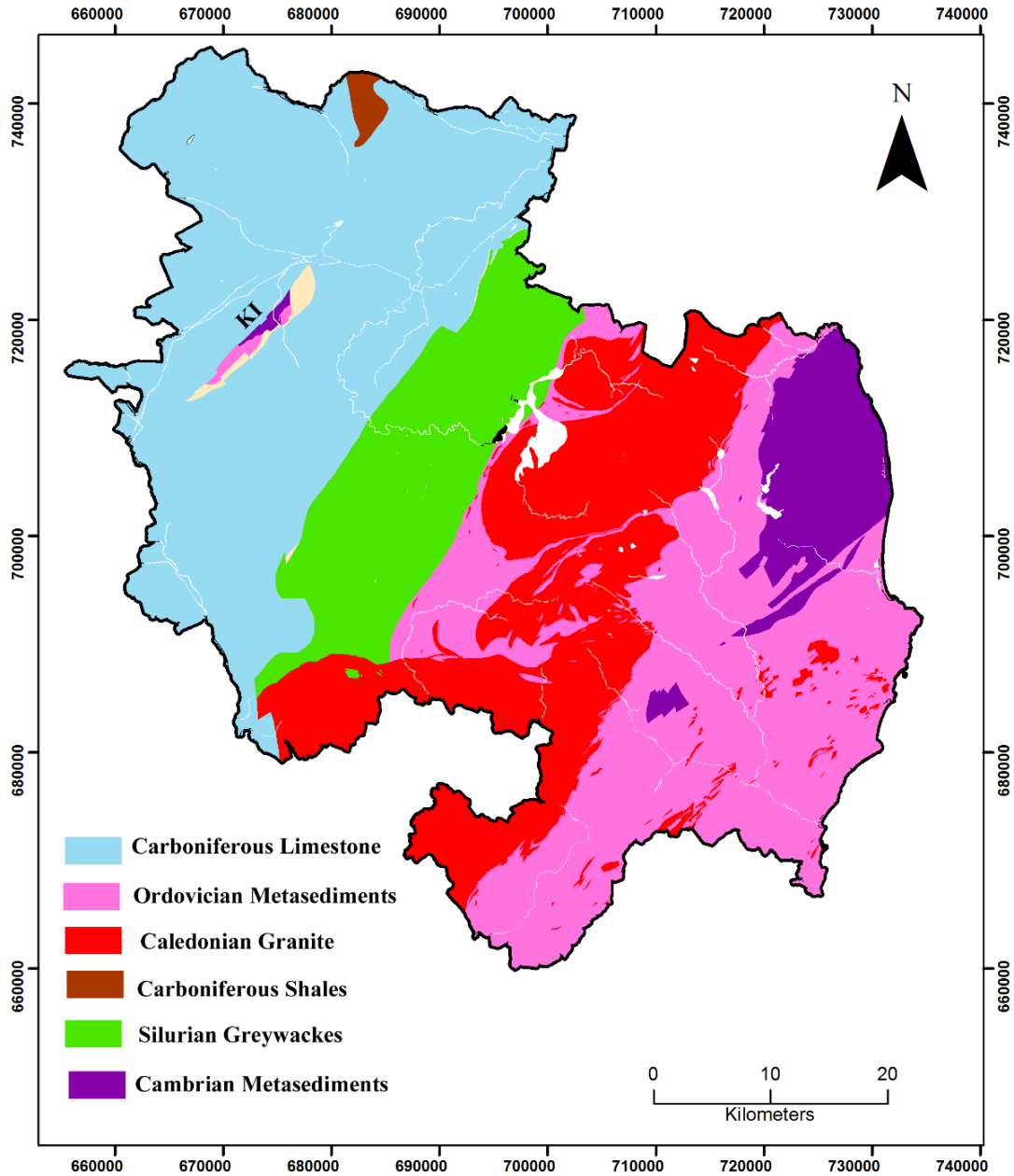


Figure 3.1: Simplified geological map of study area. KI: Kildare Inlier.

The core of the Leinster Mountains is formed of Caledonian Granite which was emplaced c. 405 Ma ago (O'Connor and Bruck, 1978). Five units have been identified though only

three are within the research area: Upper Liffey Valley Unit, Northern Unit and the Lugnquillia Unit (Brindley, 1973). These have been further divided, for example the Lugnquillia Unit is formed of 5 granitic varieties (Bruck and Reeves, 1983).

Although the granites today outcrop as a mountainous upland area with elevations greater than 600m above sea level, they were not formed in this geomorphological setting. Granite is an igneous mass of magma which cools at depth, possibly up to 3-5 km below the surface as evidenced by its coarse crystal size (Plate 3.1). The presence of granitic clasts in Devonian rocks shows that it was unroofed by about 350 Ma. However, a thin schist roof indicates it could not have remained exposed since then. It has been postulated that late Tertiary uplift elevated the region to its present position and removed younger protective rocks (Davies and Stephens, 1978).

The Kildare Inlier (KI, Figure 3.1) is an 11 km long, 1 km wide zone of older rocks surrounded by younger limestones. The rocks are resistant and are represented in the landscape as a series of hills: Grange Hill, Dunmurry Hill, Chair of Kildare and the Hill of Allen). Early work was carried out in this area by duNoyer et al. (1858). The region is composed of Ordovician and Silurian metasedimentary rocks and more importantly for the purposes of this research associated basaltic and andesitic rocks which could be an important source of magnetic grains.



Plate 3.1: Photograph of Wicklow granite.

There is little evidence of geological activity within the research area immediately after the Caledonian Orogeny. Ireland lay near the southern edge of a large continental mass at a high elevation where it underwent erosion and deposition. Old Red Sandstone (conglomerate, sandstones and siltstones) is exposed near the Kildare Inlier but the outcrop is very small. The palaeoenvironment of Ireland changed during the Carboniferous (c. 345 Ma ago) when a warm shallow sea inundated Ireland from the south (Williams and Harper, 2003). Initially, Dinantian rocks, composed of the Tournaisian and Visean Series were formed (Sevastopulo and Wyse Jackson, 2001). In the main, these consisted of limestones formed in different environments (shelf, reef, basin). In the later Upper Carboniferous, there was a greater carbon input into the ocean resulting in the presence of black shales, mostly in the north Kildare area. The sediments deposited during the Carboniferous were sub-horizontal. However, tectonic activity to the south of Ireland resulted in the layers being folded into anticlines and synclines (Plate 3.2) during what is known as the Hercynian/Variscan Orogeny (Graham, 2001b). Later rocks were either not deposited or have been eroded away and the next significant event to have affected the study area was the glaciation during the Quaternary.



Plate 3.2: (Upper) sub-horizontal near site K92 and (Lower) folded Carboniferous limestone near site K1.

3.3 Glaciations in Ireland

Evidence from oceanic cores has shown that the earth began to cool about 35 million years (Ma) ago (Wilson et al., 2000). This cooling process was most extreme during the Pleistocene epoch of the Quaternary period which is composed of the Pleistocene (2.6 MA – 10,000 years ago) and the Holocene (last 10,000 years). Based on the analysis of glacial sediments in the Irish landscape, two main glacial periods (i.e. times when there was extensive glacial ice on the land as opposed to cold tundra conditions) have been recognised: an older Munsterian and a younger Midlandian. The former is dated c. 300,000-130,000 years ago and the latter 120,000-10,000 years ago (Coxon, 2001). Within a European context, the Midlandian correlated with the Weichselian stage

(Oxygen Isotope Stage 2-5d) and the Munsterian with the Saalian stage (Oxygen Isotope Stage 6-8), (Mitchell et al., 1973). The effects of the later Midlandian glaciation are extensive throughout Ireland, especially within the study area and all further discussion relates to the Midlandian glaciation.

McCabe (2008) has produced an evolutionary age-constrained model for the expansion and decay of the Midlandian ice sheet which is similar to earlier work (Charlesworth, 1928, Flint, 1930). Around 28,000 years ago ice began to form in the upland areas of Donegal and Connemara. As temperatures decreased, by 27,000 years ago, a lowland ice axis formed running from Galway (southwest) to Lough Neagh (northeast), from which glaciers moved southwards across Ireland. The southernmost limit of the ice was reached about 22,000 years ago – the last glacial maximum (LGM). The ice margin lay to the south of Ireland and mountainous areas such as Kerry and Wicklow had their own smaller ice centres (Figure 3.2). Ice began to retreat and during a major standstill phase, the South Ireland End Moraine formed. Continued retreat was interrupted by a later standstill phase during which the Galtrim moraine and the midland esker system was produced and a re-advance around 17,000 years ago during which the Irish drumlins were created. By about 14,500 years ago, Ireland was much warmer but then became much cooler. During this short-lived Younger Dryas period some small corrie glaciers formed in upland regions before all glacial activity ceased, around 10,500 years ago.

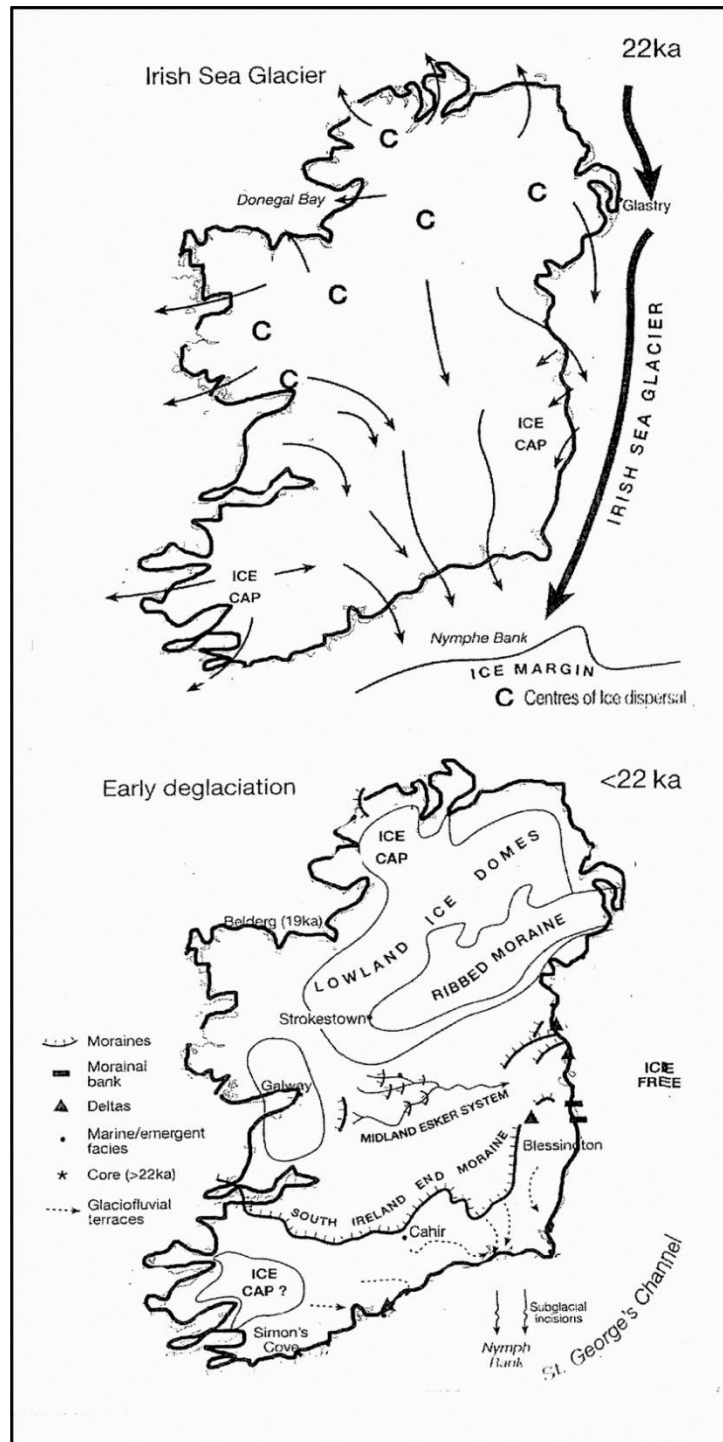


Figure 3.2: Expansion and decay of ice sheet and main landforms produced during the late Midlandian glaciation after McCabe (2008).

3.4 Glacial processes and landforms in the study area

The landscape of the study area has been extensively modified by Midlandian glacial processes in different ways. Wicklow is an upland region and is generally characterised by erosional landforms with little deposition (Farrington, 1934, 1944) whereas Kildare is a flat lowland region of glacial deposition. The Curragh of Kildare is formed of glaciolacustrine, fluviglacial and glacial sediments up to 60m thick (Hammond et al., 1987). Adjacent to the most westerly site investigated in Co. Kildare (site K227), thick fine grained sand deposits are found within a kame environment (Plate 3.3).



Plate 3.3: Thick sand deposits near site K227.

Midland Irish ice moved across Kildare in a general southeast direction. It tried to override the Wicklow Mountains but encountered small ice cap glaciers moving down from the upland mountainous corries where they formed (Figure 3.3). At the same time, the Irish Sea glacier was moving south and inland where it also encountered Wicklow mountain glaciers. The Wicklow Mountains are characterised by both U-shaped valleys

(Plate 3.4a) and a large number of corries such as Lough Bray or Lough Nahanagan. As the ice began to melt, the vast volume of water produced, which carried enormous amounts of sediment, cut their way through solid rock producing meltwater channels such as the Glen of the Downs or the Scalp, Plate 3.4b. These are concentrated east and west of the Wicklow Mountains.



Plate 3.4: (a) U-shaped valley and (b) Scalp meltwater channel in Co. Wicklow.

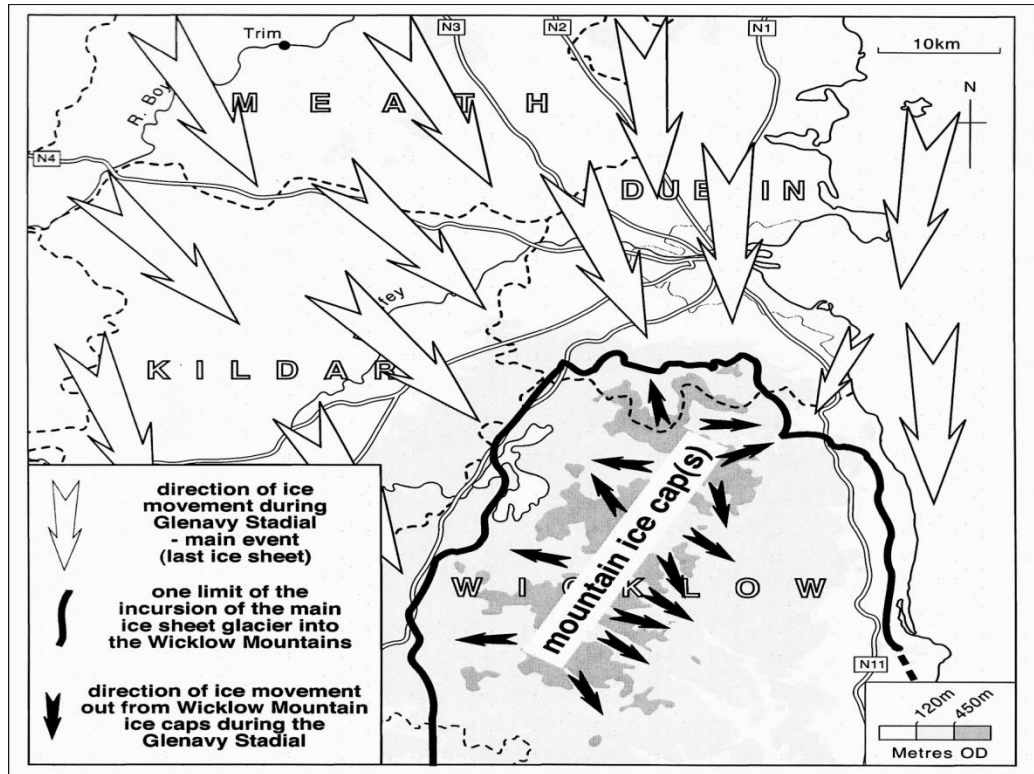


Figure 3.3: Glacial movement across study area (Coxon et al., 2012).

The character of sediments deposited directly from glaciers as they move (till) is completely different from fluvio-glacial sediments formed as a result of ice melting. As glaciers move they collect vast amounts of sediment which they extrude from their sole and plaster onto the underlying surface. Till is unstructured and unlayered and is composed of angular rock fragments of all grain sizes, Plate 3.5. This is the commonest glacial deposit in the study area and is found throughout Kildare. Fluvio-glacial deposits are generally well sorted into distinct layers of different grain sizes. In the early stages of deglaciation, a lake formed on the Kildare/Wicklow border. This is known as glacial Lake Blessington and was 24 km long, 7 km wide and 100m deep (Farrington, 1957) making it the largest Pleistocene glacial feature in the study area. The lake was surrounded by thick (>60m) deltaic fluvio-glacial sediments with well defined layers, Plate 3.6. The glacial sediments will influence the types of soils in the study area as they greatly control the resultant drainage properties. Coarse fluvio-glacial sediments facilitate good drainage which is poorer on tills and very poor on clays.



Plate 3.5: Pleistocene till deposits near site K1. (2m wide)



Plate 3.6: Fluvioglacial deposits at Blessington,
Kildare-Wicklow border.

3.5 Soil formation in Ireland

Soil formation is a complex procedure and the soils in Ireland began to develop at the beginning of the Holocene, approximately 10,000 years ago (Mitchell and Ryan, 2001). The last glacial activity ceased c. 10,500 years ago leaving a landscape of water filled

depressions and vast amounts of till, sand, gravel and clay. The increased temperatures led to the re-colonisation of the land by vegetation which decomposed to form a humus component to the newly developed soil. The increased temperatures combined with the free water facilitated chemical reactions which promoted soil production. Orme (1970) states that there were six parameters which control soil production by influencing weathering rates, composition and chemical gains and losses. The parameters are:

- Nature of the parent material.
- Climate.
- Living organisms.
- Topography/relief.
- Time.
- Human influences.

There is a degree of correlation between these parameters. Some rock types are extremely resistant and can form steep upland areas whereas others erode easily and have a rolling lowland topography. The human influences tend to be minimal on steep mountainous regions and greatest in flat lowland areas.

The parent material is the solid rock or the superficial glacial sediments derived from it. Different rocks contain different minerals which when they decompose release different elements into the soil profile. Basalt contains olivine which breaks down easily to release iron into the soil which would not occur for a pure limestone which contains no iron. In Site K1, for example, a large piece of chert was left in the $>2000\mu\text{m}$ sieve. This is an extremely hard form of microcrystalline quartz which breaks down very slowly to release the element Si into the soil. However, rotted granite was found for some Wicklow sites in the $>2000\mu\text{m}$ sieve. The feldspars are decomposing easily to clay minerals and along with the abundant muscovite mica, is releasing, silicon, calcium and potassium into the soil.

Two aspects of climate are important in soil formation: precipitation and temperature (Nevill, 1963). Soils evolve into separate layers because of leaching which require the downward movement of rainwater and chemical reaction progress quicker the higher the

temperature. Soil organisms include plants and bacteria, the former provide organic matter to the soil and the latter control how it is broken down and at what rate. As soils age and mature, they will in general undergo a greater degree of leaching than a younger one and will have better developed horizons. Rainfall runoff on steep slopes tends to be greater than on shallow slopes and consequently less rain infiltrates through the soil. Erosion rates tend to be greater on steep slopes and also on long slopes. This can result in the preferential movement of fine material from the top of a slope to the bottom. It may also lead to a change in the measured magnetic susceptibility of soils as (a) sometimes the finest grain fraction carries the highest magnetic signal and (b) removal and translocation of the magnetically enhanced topsoil may occur. Anthropogenic input into soils has the capacity to change their character. The addition of lime will change the natural chemical balance and drainage schemes, which were widespread in some parts of Ireland, can also have a major effect on soil evolution.

Soils have evolved mainly through the interaction of leaching and gleyisation (gleisation) processes (Gardiner and Radford, 1980). The end result of these two processes is often a distinctive soil profile formed of layers separated by horizons which is often characteristic of a particular soil group. 10 Great Soil Groups have been identified for Ireland based on development of horizons, chemical composition, layering, drainage, texture, organic content, colour and maturity (Gardiner and Radford, 1980). The soils groups are:

- Podzols.
- Brown podzols.
- Brown earths.
- Grey brown podzols.
- Blanket peat.
- Gleys.
- Basin Peats.
- Rendzinas.
- Regosols.
- Lithosols.

As water trickles through the top layer of soil, it transports soluble bases such as sodium and calcium downwards where they may be reprecipitated. In the process, the upper layer becomes more acidic. Fine clays may also be removed from the upper layer. The uppermost A layer is often the most depleted especially in extreme leaching condition when iron and aluminium may also be removed. This A layer may be below an O (organic) layer and can be subdivided (A1, A2 ...) dependent on colour, textural or chemical differences. The A2 layer is always more bleached than the A1 layer which can contain darker organic material. The underlying B layer contains fewer organisms but higher iron and aluminium levels. The C horizon indicates the junction of the soil with the underlying rock or glacial deposits. When a soil is water logged, movement of water downwards is seriously retarded. Reduction can occur in such situations resulting in a grey/dark blue 'heavy' soil. They are mineral soils formed under anaerobic conditions. This process is called gleyisation. Gleys, in the main, are poor water logged soils. When all the iron has not been reduced, they often have a brown mottled effect (Holden, 2005).

Podzols are intensely leached poor soils with sharply defined horizons and a thin A1 and thicker A2 layer. The brown podzols and grey brown podzols have undergone less leaching and the 'grey' characteristic of the latter is due to a strong calcareous parent input and as such are well represented in Co. Kildare. Brown earths are well drained and show a weak layering profile and as such have not undergone much leaching. Grey brown podzols and brown earth soils have a wide range of agricultural uses (Holden, 2008).

Peat, whether of the blanket or basin peat (raised bog and fen bog) variety is a common feature in some parts of the Irish landscape, Plate 3.7. Originally peat covered approximately 16% of the land (about 1.3 million hectares) with blanket bog making up about 75% of the total (Hammond, 1981). Peat has been exploited as fuel in Ireland for millennia and as a result only 20% of blanket bog remains and only 8% of raised bog has not been affected by anthropogenic activity (Gibson, 2007a).



Plate 3.7: Peat deposits in west Kildare. Section is 4m high.

Peat began to form soon after the beginning of the Holocene, approximately 10,000 years ago. Raised peat bogs evolved differently from blanket bogs, the latter require rainfall amounts to be greater than 1.25m per annum whereas raised bogs develop in much drier conditions, c. 0.75-1.0m. Thus, within the study area, blanket bog – a term first employed by Tansley (1939) – is confined to the Wicklow mountains and raised bogs are found in the Kildare lowlands which conditions are drier. Water filled depressions and lakes became quickly colonised by plants whose dead remains sank to the bottom. However, full decomposition did not occur and over time this material was compressed into fen peat. Nutrients came from alkaline groundwater because of the extensive limestone rock. However, an increasing thickness of fen peat prevented the plants roots reaching the water table and slightly acidic nutrient poor rainwater were taken up. New plants, such as sphagnum moss, which could thrive in such conditions flourished, and accumulated on the lake floors to form bog peat (Gibson, 2007a). The capillary action of the plants

drew up moisture, thus the bog grew upwards into a domed shaped producing a raised bog. The raised bogs in western Kildare are typically 4-7m thick. Raised bogs were probably developing by about 7500 years ago when Ireland became wetter (Mitchell and Ryan, 2001) but there is some evidence to indicate that blanket bog may have developed later in some locations (Smith et al., 1971). Blanket bog tends to be shallower, have less sphagnum species and less layering than raised bogs.

The last three Great Soil Groups do not occur to any great extent in the study area. Rendzinas are thin (50 cm) and possess a dark surface layer. Lithosols are very immature, stony soils and occur on scree whereas regosols often contain no B layer.

3.6 Soils of the study area

A national soil survey of Ireland took place in the period 1959-1985, however not all the counties were mapped at a scale of 1:126720. Most midland counties were covered, Offaly, Laois, Carlow as well as Wexford, Clare and Waterford whereas others such as Kerry, Louth and Monaghan were not completed. For the research area considered here, County Kildare was mapped whereas Wicklow was not (Dally and Fealy, 2005). Therefore, there is more secondary information, to soil series level, for the former county. An Foras Taluntais (1970) recorded 19 Soil Series and 6 Soil Complexes in Co. Kildare, though 73% of the area is made up of only 8 of them.

The Grey Brown podzol Great Soil Group in County Kildare is formed of seven soils series namely: Elton [59]; Fontstown [120]; Donaghcumper [119]; Grange [121]; Kellistown [89]; Kennycourt [122] and Mortarstown [90]. Note, numbers in square brackets are codes assigned to soils by An Foras Taluntais (1970). These soil series combined account for 46.2% of land surface of Kildare with most of this belonging to the Elton Series (20.42%) and the Fontstown Series (16.89%). The former is found throughout most of the county, though larger areas are located in central Kildare and it is absent in the south. This is in contrast to the Fontstown Series which is virtually absent in the north but occurs widely in the southwest around Athy. The Elton Series is found on flat slightly undulating terrain, at elevations less than 150m and its main parent material is limestone till. The northern part tends to have slightly more clay than the

eastern regions, probably reflecting an input from Upper Carboniferous shales. The Fontstown Series is quite similar, though is often significantly thinner (38-46 cm) than the Elton Series (63-127 cm) and is less loamy.

Four complex soils Allenwood [127], Athy [117]; Finnelly [132] and the Straffan Complex [133] form about 23% of Kildare's soil with the Straffan Complex being most important (13.4%) followed by the Athy Complex (6.6%). The former is found almost exclusively in the north-eastern part of the county with the largest outcrop west of Maynooth. The Athy Complex tends to occur as a number of small outcrops in east central Kildare, at elevations of c. 50m though near the eastern boundary with Wicklow it can be found at elevations of up to 275m and has as its parent material mainly fluvioglacial sands and gravels. The complexes comprise a mixture of soil types. The Athy Complex is made up of 4 soil types with grey brown podzols (60%) and brown earths (30%) being most important. This contrasts greatly with the Straffan Complex formed of 6 soil types, 5 of which are gleys (90%). However, the Straffan Series which forms 65% of it has had its drainage improved greatly by artificial drainage.

The Gley Group is formed of 6 series: Dunnstown [126]; Garristown [127]; Kilpatrick [128]; Mylerstown [129]; Newtown [111] and Sayerswood [130] and forms approx. 12% of the surface, mostly made up of the Dunnstown (5.4%) and Mylerstown Series (3%). The former is mostly located in the north-western part of the county and a smaller area near Naas whereas the latter is mainly east of Athy. Dunnstown Series is often associated with low lying areas near the Elton Series. It tends to be thinner (0.75-1.5m) than the Kilpatrick Series (1-1.5m). Raised bog peats are formed of the Allen Series [1b]; Clonsast Complex [1c] and Boora Complex [1d] and make up about 12% of Kildare with smaller areas of fen peat Pollardstown Series [1e] and of reclaimed peat Banagher Series [1f]. Most of the peat occurs as large tracts in the northwest with smaller areas east of Monasterevin. It varies in depth from 3-8m. Over 90% by weight is water, the rest is organic vegetable matter. Substantial amounts of wood, including entire trees are found enclosed in the peat. The Brown Earth Group (Hughstown Series [123]), the Podzol Group (Cupidstownhill Series [124] and the Regosol Group (Liffey Series [125]) represent very small areas.

One other countywide source of soil data exists for Kildare - the georeferenced soil maps of the Environmental Protection Agency of Ireland (EPA) website – see Fealy et al. (2009) (<http://gis.epa.ie/GetData/Download>).

The 5 main soils are termed:

- Alluvium (abbreviated to ALLUV).
- Deep Well Drained Mineral soil (abbreviated to DWDM).
- Deep Poorly Drained Mineral soil (abbreviated to DPDM).
- Shallow Poorly Drained Mineral soil (abbreviated to SWDM).
- Peat.

The EPA recognise 22 different soils in Co. Wicklow but most of the area consists of 1 of 6 types. Unlike Kildare, where most of the soils (except peat) are basic, the Wicklow soils are mainly acidic.

- ADPDM: Acid Deep Poorly Drained Mineral soil.
- ASWDM: Acid Shallow Well Drained Mineral soil.
- ADWDM: Acid Deep Well Drained Mineral soil.
- BSWDM: Basic Shallow Well Drained Mineral soil.
- ASP: Acid Shallow partially Podzolic.
- BP: Blanket Peat.

Blanket peat occupies the highest ground in Wicklow and is aligned along the mountain axis. It occurs mainly above 700m and covers an area of 12% (232 Km²). The peat is surrounded by acid shallow partially podzolic soil (ASP) with some development of peat. It is found at lower elevations (400m). It has an area of c. 19% of county (374 Km²). Acid deep - ADWDM and Shallow - ASWDM- well-drained soil is generally found below 300m. The deeper soil is more common west of the mountain axis. It forms 49 % of Wicklow (964 Km²). Acid deep poorly drained soil (ADPDM) is found along the coast. The parent material here is till dumped by the Irish Sea glacier. It forms c. 8 % (155 Km²). Basic shallow well drained soil (BSWDM) is found mainly along the border with Kildare, reflecting a calcareous input from the west as glaciers transported limestone. It forms 3% of the county (62 Km²).

The trace element concentration for 40 elements has been mapped for Ireland (Fay et al., 2007). This survey covered 36 sites in Kildare and 34 in Wicklow and the results for 4 elements (cadmium, iron, lithium and mercury) are shown here, Figure 3.4. The soil samples were taken from a depth of 10 cm, approximately the same depth as the magnetic susceptibility samples were acquired for this research. In the examples shown, distinct spatial variations can be seen. The older rocks in the study area (Wicklow) have relatively low cadmium levels, with the highest in the northern half of Kildare. The spatial distribution is very similar to the calcium levels and is related to facies within the Carboniferous limestone.

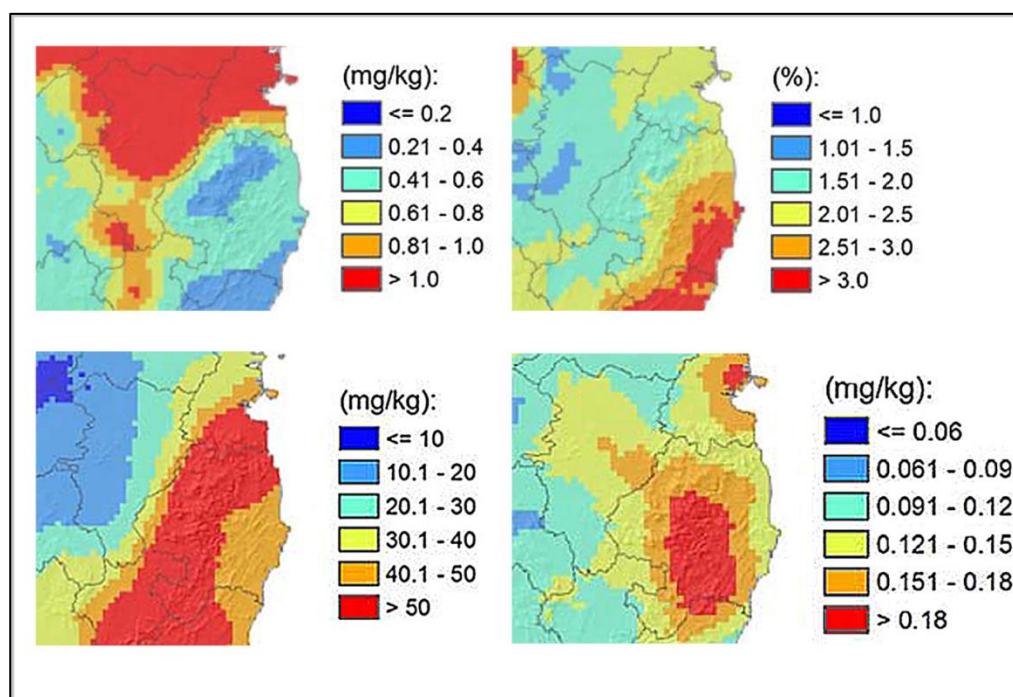


Figure 3.4 Geochemical maps showing (clockwise from top left) cadmium, iron, mercury and lithium concentrations in study area, modified after Fay et al., (2007).

The highest concentrations of iron are located in southeast Wicklow, and the lowest in Kildare. The former area includes the mineralised Avoca region and its associated volcanic rocks which are rich in iron. The highest concentrations of mercury in Ireland are located in a small area of central Dublin, due to anthropogenic effects and a large area concentrated in central Wicklow. The latter is believed to be as a result of historic

mining in the 17-19th centuries. However, in absolute terms, the values are low. Lithium levels show a pronounced eastward increase. It is an alkali metal like sodium, potassium and rubidium which occurs in acidic igneous rock like granite which is present in central Wicklow.

3.7 Geophysical Applications in Environmental Field

3.7.1 Introduction

Discounting magnetic investigations in the 17th and 18th centuries, some of the earliest geophysical experiments in the world took place on Killiney Beach, approximately 5 km north of the study area. In 1845, Robert Mallet constructed a basic seismometer to measure the speed of seismic waves which he generated artificially by detonating gunpowder. Early geophysical studies were, in general focused on the large scale, such as mapping the Earth's magnetic field, determining global variations in gravity or the nature of the Earth's internal structure (Lillie, 1999). Geophysics development in the early 20th century continued to be large-scale as exploration companies used various techniques to map ore bodies or locate major hydrocarbon sources. Lawyer et al. (2001) and Sweet (1978) provide an excellent history of this development.

The work in this thesis is much more detailed and is concerned with the top few metres of the surface, thus some techniques, such as gravity or VLF are not applicable. Two geophysical techniques were employed during this research: Magnetic methods and Resistivity methods. Other geophysical approaches could have been employed. Near surface conductivity (quad-phase) and magnetic susceptibility (in-phase) can be obtained using instruments like the Geonics EM38 in which radiation is input into the ground by a transmitter coil (loop) to generate a primary electromagnetic field and the secondary electromagnetic field arising from induced currents in the ground is measured at a receiver coil. Terms such as HLEM (horizontal loop electromagnetic) system or Slingram method are also used to describe such instruments. There are types of magnetic measurements, other than those used in this research which can be used. If a soil sample is subjected to a strong increasing magnetic field, it acquires an isothermal remanent

magnetisation (IRM). The maximum value is called the saturation isothermal remanent magnetisation (sIRM) and this varies with magnetic mineralogy and grain size.

Ground penetrating radar (GPR) is ideal for detailed work and relies on differences in relative permeability due to variations in grain size, sediment type, water content and porosity. Huisman et al. (2003) provide a good review of how GPR can be employed to map spatial and temporal variations of water in the vadose zone. An important parameter in ground penetrating radar is the frequency of the antennae, the higher the frequency, the more the detail but the less the penetration. The resistivity sections imaged 2m depth and such a depth would be required for the radar. Based on work at Maynooth university and experience gained at Minerex, such ground penetrating radar should be collected at 5cm intervals using 400-500 MHz antennae. Induced polarization (IP) is a technique similar to resistivity (some equipment, such as IRIS Syscal, collect data in either format) and can be used to obtain data in the time domain or frequency domain. In the former, the chargeability (M) is obtained and in the latter, apparent resistivity at low and high frequency is acquired. Kibaru (2002) in a series of laboratory experiments on 43 soils showed that the IP response was dependent on the amount of water and cation exchange capacity in the soils which he directly related to clay minerals.

Soils, sediments and rocks can contain small concentrations (parts per million) of radioactive minerals which decay to more stable elements. For example, ^{238}U (uranium) decays to ^{206}Pb (lead). During the decay process, alpha and beta particles and gamma radiation are emitted which can be measured by ground based or airborne detectors. Tellus is a geo-environmental mapping project which provides data on soils, waters and rocks across Ireland and integrates these with existing data (Hodgson and Ture, 2016). It has 2 main components: ground based geochemical soil and water surveys and airborne surveys. The airborne surveys employed a frequency-domain electromagnetic system which operated at four frequencies, (0.9, 3, 11.9 and 24.5 KHz) with a transmitter-receiver coil separation of 21.4m. Magnetic data are collected using two Geometrics optically pumped caesium magnetometers and a 256 channel gamma-ray spectrometer was employed to collect radiometric data on potassium, uranium and thorium. The output data is georeferenced to Irish Transverse Mercator coordinates which were also

employed in this thesis. At time of writing only the northern part of the study area has been investigated.

Magnetic and resistivity methods were chosen because of the availability of equipment and their expected usefulness to fulfill the aims and objectives of this research given in Chapter 1. The use of a range of techniques, each of which depends on a different subsurface parameter, will allow a better geophysical classification of the soils of the study area. Literature relevant to each of these two methods is considered separately below and is followed by a discussion of the literature with particular relevance to Ireland.

3.7.2 Magnetic susceptibility applications

Magnetism is undoubtedly the oldest geophysical technique and it has been studied for well over 1000 years. A large array of magnetic measurements can be made, either in the field or in laboratory based studies. Magnetic susceptibility has been used for many years in a large number of disciplines, ranging from archaeology in the USA (Dalan, 2008) and to aid petrophysical appraisals in hydrocarbon sites (Potter, 2005). Anthropogenic activity can yield significant pollution. Traffic produces large amounts of magnetic dust from corrosion, catalytic converters and brakes thus roads are often associated with elevated magnetic susceptibility values. Gautam et al. (2004) took traverses across roads in Kathmandu and showed volume susceptibility values of $240 - 850 \times 10^{-5}$ (S. I.) adjacent to roads whereas the background values were in the range $3 - 35 \times 10^{-5}$ (S. I.). Magnetic studies on the take up of pollution by leaves in Rome show the least effects in parks and greatest effects nears roads and railways (Moreno et al., 2003). In Tuebingen, Germany, background volume susceptibility was $10 - 20 \times 10^{-5}$ (S. I.) and up to 250×10^{-5} (S. I.) adjacent to the road (Hoffmann et al., 1999). Also in Germany, high volume magnetic susceptibility was associated with the polluted Steyreggerwald locality near Linz (Boyko et al., 2004).

Industrial activity has the capacity to produce significant pollution. Fly ash released from coal fired power stations is often associated with iron oxide phases and with what are

often termed 'heavy metals' such as zinc, cadmium, lead, nickel and cobalt (Lu et al., 2009). The scale produced from steel production in Austria which contained chromium, zinc and lead, was easily mapped from the Mur River sediments using magnetic susceptibility, with typical values of 200×10^{-5} (S. I.) (Scholger, 1998). Peat bog sites close to Post Second World War industrialisation in Poland yielded mass specific susceptibilities of up to $350 \times 10^{-8} \text{ m}^3\text{kg}^{-1}$ whereas those far away from such areas have a maximum value of $10 \times 10^{-8} \text{ m}^3\text{kg}^{-1}$ (Strzyszez and Magiera, 2001). An extensive study in central Europe showed that the highest susceptibility values were located in Silesia (SW Poland), northern Moravia and Bohemia (Czech Republic) and east Saxony (Germany) and were associated with industrial centers and coal burning power station (Magiera et al., 2006). This association has been recorded in England and Wales (Blundell et al., 2009), China (Lu and Bai, 2006 and Yang et al., 2009), Greece (Botsou et al., 2011) and elsewhere (Dong et al., 2014; Durza, 1999; El Baghdadi, 2012 and Evans and Heller, 2003).

During the Quaternary period (last 2 million years), thick windblown fine-grained loess sediments were deposited in north central China near Lanzhou. During glacial stages, the deposition rate was fast and burial was rapid. However, during interglacial stages, deposition rate was slow, vegetation thrived and weathering was much more intense, leading to the formation of palaeosols (Maher, 2009). Magnetic susceptibility measurements of these loess/palaeosol sequences demonstrates clear differences with the palaeosols consistently having higher susceptibilities (Maher, 1998) and that a positive correlation exists between magnetic content and annual rainfall (Maher et al. 2002). Kukla et al. (1988) demonstrated the correlation between magnetic susceptibility values for the Chinese loess and oxygen isotope stages which are used in dating glacial interglacial stages.

Various authors have employed magnetic methods in order to study some aspect of the landscape. This has usually entailed measurements being made on soils or sediments from rivers or lakes. Various types of erosion studies have employed magnetism as part of the research. Hatfield and Maher (2009) used 'magnetic fingerprinting' to determine the erosion sources of sediment inputs into Bassenthwaite Lake in England whilst

Landgraf and Royall (2006) used soil magnetism to map soil redistribution in Alabama. The volume magnetic susceptibility for cores from Lake Geneva was used to determine sediment accumulation rates (Loizeau et al., 2003) and a similar approach in Lake Baikal identified sedimentation patterns (Lees et al., 1998). Magnetic susceptibility of cores was also a major component of an erosion characteristics study of Lough Frisa, Scotland (Appleby et al., 1985). The magnetic susceptibility values reported in this study were extremely high, most likely because the lough is surrounded by highly magnetic basalts.

3.7.3 Electrical Resistivity Methods

Significant early developments in active electrical resistivity surveying (in which an electrical current was input into the ground) were made in 1915 by Wenner (1915) and in the 1920s by Conrad and Marcel Schlumberger in France who formed the Societe de Prospection Electrique in 1926. This early work was aimed at deep structures in the search for hydrocarbons. The equipment was quite basic and surveys labour intensive. However, enhanced technology and improvements in computer processing means, that today, resistivity surveys are relatively easy to conduct and are used extensively in shallow environmental work. A large proportion of electrical resistivity surveys reported in the current research literature are 2D ones. 1D resistivity work is rarely carried out today and 3D surveys are more complex and difficult to conduct. Only 2D surveys were undertaken for this thesis and the methodology employed and theoretical concepts underpinning them were discussed in Chapter 2.

Electrical Resistivity Tomography (ERT) has proved itself particularly useful in a range of fields. In an engineering context it is particularly suited to investigating landfill sites (Fenning and Williams, 1997). Leachate from domestic waste has a very low resistivity value, c. 15 Ohm-m, thus potential leaks, contaminant plumes or the sites of illegible dumps may be determined (Barker, 1997; Chambers et al., 2006; DeCarlo, 2013; Grellier, 2007; Lemke et al., 1997). Cave systems and collapse features if air-filled are often associated with high resistivity values and have been mapped with ERT (van Schoor, 2002; Zhou et al., 2002). Buried well drained sands and gravels also have high

resistivity values. This knowledge was used to locate economic gravel deposits in Iowa. The gravels had a resistivity of 300-1500 Ohm-m, much greater than the other non-gravel sediments, 30-40 Ohm-m, (Beresnev et al., 2002). Baines et al. (2002) mapped a number of small (c. 6m deep) and large (c. 58m thick) channels in Canada, most of which had resistivity an order of magnitude greater than the background. On the other hand, the presence of water, especially saline water yields much lower resistivity.

Samouelian et al. (2005) have produced a review paper regarding electrical resistivity and soil science and conclude that resistivity ‘can be considered as a proxy for the spatial and temporal variability of many other soil properties (i.e. structure, water content or fluid composition)’. A significant amount of electrical resistivity research has been conducted in France. Resistivity was found to produce accurate results in the determination of the percentage of rock fragments in stony soils in the Beauce region (Tetegan et al., 2012) and the structural heterogeneity of the soil tilled layer was mapped at the Somme (Seger et al., 2009). A characteristic of soils, discussed earlier is that of the soil profile, which over time, forms into layers. This layering can be determined using electrical resistivity methods (Tabbagh et al., 2000). The most important area of soil research is concentrated on soil water content/composition. This may be important for water balance, pollution or hydraulic studies (French et al., 2002; Kemna et al., 2002; Zhou et al., 2001). Many conventional methods involve in situ measurements. However, this approach disturbs the subsurface and may nullify the results. ERT was employed in Italy to determine that cover-cropped olive orchards were more efficient at storing rainwater than tilled soils (Celano et al., 2011). Soil water deficits, important parameters in predicting hillslope runoff and river floods, were analysed in the Cevennes region of France (Brunet et al., 2010) and Cousin et al. (2009) created areal resistivity maps to determine field scale soil hydraulics.

3.8 Geophysical Research in Ireland

Many third level institutions in Ireland have some form of geophysical activity but most are unrelated to the research conducted for this thesis. A lot of the work carried out by

the Dublin Institute of Advanced Studies, the Geophysics Group from University College Dublin and the Geophysics Research Group from the University of Ulster is unrelated to Ireland. It concentrates on deep structural and lithospheric studies, wave propagation, earthquake modeling and numerical and theoretical analysis. The Applied Geophysics Unit in University College Galway is no longer in operation though currently marine geophysical research is carried out at this institution.

Most of the environmental geophysics in Ireland is carried out at the Environmental Geophysics Unit of the National University of Ireland, Maynooth, though shallow level ground penetrating radar research is carried out at Queen's University Belfast (Ruffell and McKinley, 2008). A range of research Masters and doctoral theses with a major geophysical component (mostly magnetic and/or electrical resistivity) have been written. These include ones concentrating on:

Geology: (Conway, 1993; Devilly, 1995; Gibson, 1991; Morris, 1970; Mulhall 2000).

Archaeology: (Bonsall, 2014; Byrne, 1995; 2005; Corcoran, 2007; Creevey, 2005; Jennings, 2008; Madden, 1999; O'Reilly, 2005; O'Rourke, 2008, Shinnors, 2007).

Glacial sediments: (Breen, 2003; Calaco-Casado, 2006; Callaghan, 2002; Doughan, 2004; Pellicer, 2010; Reilly, 2003; Smyth, 1994).

Environment: (Gleeson, 2003; Murphy, 2002; O'Connor, 2000; Ormsby, 2002).

The theses produced by Conway (1993) and Devilly (1995) are particularly relevant to the present study. The study area of Conway was the Wicklow Mountains and his magnetic traverses showed that rocks with different magnetic properties exist in the region, Figure 3.5. Devilly (1995) took a number of magnetic traverses over the Kildare Inlier and once again the magnetic pattern indicates these rocks are considerably more magnetic than the surroundings, indicating that the Kildare Inlier may be important source of magnetic minerals which could be dispersed over the non-magnetic limestone of County Kildare by glacial movement.

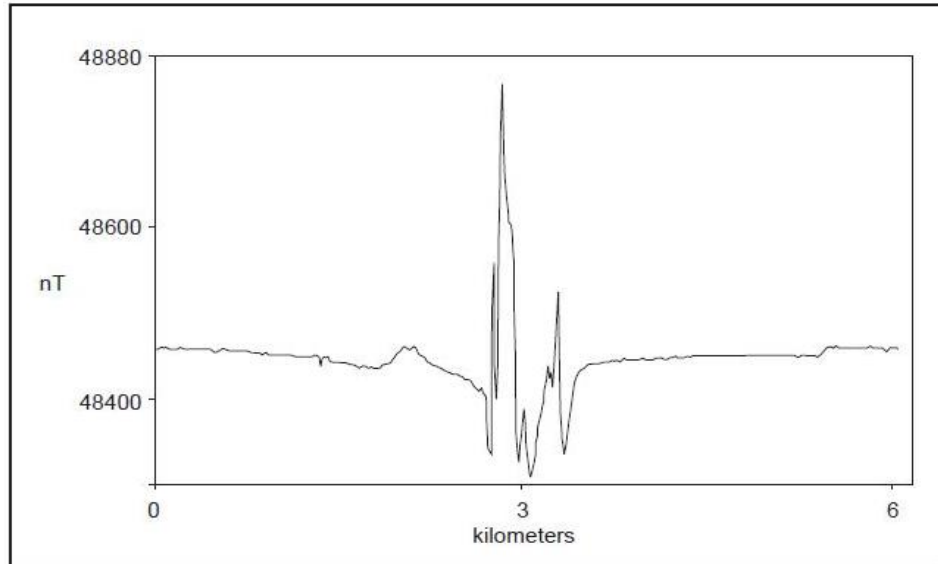


Figure 3.5: Magnetic traverse in Co. Wicklow showing a major anomaly at 3 km. Units nT are nanoTesla (after Conway 1993).

Magnetic investigations in Ireland first started in the late 1950s (Aitken, 1959). Remanent magnetism studies have been undertaken by Morris (1972), Morris and Robinson (1971) and Wilson (1959, 1970). Some magnetic work was undertaken by the Geological Survey over the Corvock granite in Co. Mayo (Inamdar and Kelly, 1980). The magnetic patterns acquired over most of the lithologies within Ireland have been investigated extensively (Gibson, 1993, 2004; Gibson and Lyle, 1993a, 1993b; Gibson et al., 1996a, 1996b, 2004, Lyle and Gibson, 1994).

Magnetic susceptibility measurements form an important component of this research but for Ireland, very little has been published in the scientific literature. Gibson et al. (2009) showed that parts of the Cuilcagh dyke which were indistinguishable geochemically could be differentiated in terms of their susceptibility. The susceptibility contrast between aeolian infill and limestone rock allowed the mapping of collapse features in the limestone near Cookstown, northern Ireland (Gibson et al., 2004). Magnetic investigations have taken place in the Lough Neagh region of Northern Ireland. Thompson et al. (1975) showed that the magnetic signal in Lough Neagh sediments was carried by titanomagnetite from the basalts. The concept of a widespread phenomenon termed ‘magnetic enhancement’ is discussed later in the chapter. However, work by

Dearing and Flowers (1982) shows that this does not occur in the Lough Neagh vicinity. At the time of writing, a Ph.D. is being undertaken in National University of Ireland, Galway which is investigating correlations between 'heavy metals' and magnetic susceptibility (Golden et al., 2012; 2015, 2017). The National Roads Authority of Ireland requires surveys to be undertaken to determine if a planned route will damage an unknown archaeological feature. Of the 167 available survey reports for the time period 2001-2010, 160 used magnetometry and 35 measured volume susceptibilities (Bonsall, 2014). The magnetic fabrics (anisotropy of magnetic susceptibility) of some Caledonian granites in Galway and Donegal have been investigated. The mean susceptibility values for the Trawenagh Bay granite in Donegal ranges from 4×10^{-6} (S.I.) to 3500×10^{-6} (S.I.), (Stevenson and Owens, 2006). In an earlier study, King (1966) reported that the Donegal granites are markedly less magnetic than the Galway granites. Geophysics has been employed extensively for archaeological studies in Ireland (Bonsall, 2014; Gibson, 2005, 2007b; Gibson and Breen, 2005).

Gibson et al. (2004) used ERT to map an unknown cave in Co. Cork and discovered a 200m long, 70m wide and 25m deep collapse structure beside site K1. The depression is infilled with low resistivity glacial sediments which are an order of magnitude lower than the Carboniferous limestone. ERT has been employed in a number of archaeological projects in Ireland. Barton and Fenwick (2005) produced a resistivity cross-section across the Iron Age Rathcroghan mound in Co. Roscommon while O'Rourke and Gibson (2009) used ERT to define the defences at Rattin Castle Tower House, County Westmeath. Gibson (2012) obtained cross-sections across the Leamonaghan togher and Gibson and George (2006) used ERT to investigate a church at Clonard monastic site. For the latter two, a series of closely spaced lines of electrical resistivity data were collected and the data merged to yield areal depth slices.

A considerable amount of geomorphological research in Ireland has been carried out on features related to the last glacial event in Ireland and ERT has often formed a major component of this work. Pellicer and Gibson (2011) and Pellicer et al. (2012a, 2012b) have mapped the internal structure of glacial sediments in County Offaly using geophysics, created a database of typical signatures for eskers, lacustrine sediments and

other glacial deposits and produced an evolutionary glacial model for the Irish midlands. Similar work was carried out on post glacial sediments on Bull Island, Co. Dublin (Gibson et al., 2012) and on Clare Island, Co. Mayo (Coxon et al., 2013). Engineering geophysics is generally undertaken by commercial companies such as Apex Geoservices or Minerex though ERT work on landfill sites has been undertaken in academia (George and Gibson, 2000; Gleeson, 2003; Murphy, 2002).

3.9 Magnetic characteristics of Irish rocks

A fundamental control on the magnetic susceptibility of soils is the nature of the parent material which controls, to a large extent, the amount of iron minerals in the soil (Blundell et al., 2009; Fialova et al., 2006). In general, soils derived from rocks with a high magnetic content will usually have a higher susceptibility than soils derived from rocks with few magnetic grains. However, the situation in Ireland is further complicated by glacial activity within the last 2 million years. Vast amounts of till have been moved large distances and deposited far from their original source. For example, granite from Galway has been found in the Slieve Bloom Mountains (120 km farther east) and granite from the Scottish Island of Ailsa Craig is found along the eastern coast of Ireland including Wicklow. In this latter case, the Irish Sea ice sheet has transported the material many hundreds of kilometres. No comprehensive data on the magnetic susceptibility of Irish rocks have been published except for small localised studies (King, 1966; Stevenson and Owens, 2006). As part of this research, in conjunction with my supervisor Dr. Paul Gibson, the magnetic susceptibility of the main Irish rocks was measured.

Serpentinite is known to be a highly magnetic rock (Toft et al., 1990, Seeds and Poole, 1946) and the most magnetic rocks measured in Ireland are the serpentinites of the Slishwood Formation and Deer Park Complex of Counties Sligo and Mayo which form part of an ophiolitic melange (Lemon, 1966; MacDermot et al., 1996; Morris et al., 1995). Magnetic susceptibility values for the serpentinite average $4264 \times 10^{-8} \text{m}^3\text{kg}^{-1}$ with a range of $2901\text{-}6246 \times 10^{-8} \text{m}^3\text{kg}^{-1}$. Up to 14% magnetite content has been recorded at some locations (Hardman and Hull, 1883). Total field magnetic surveys over the Deer Park Complex in Clew Bay yielded anomalies of up to 10,000 nT, (Gibson et al., 1996b). Although highly magnetic, the serpentinite bodies are very small; however, the Tertiary

basalts in NE Ireland, which contain up to 3% magnetite, cover an area of more than 3000 km². For most of NE Ireland, the basalts are divided into older Lower basalts separated from the Upper younger basalts by a 4m thick interbasaltic laterite bed rich in iron and aluminium. In north Antrim, the Causeway basalt is in between the Lower and Upper layers.

The susceptibility of the Lower and Causeway basalts were measured and the former is less magnetic (average $231.2 \times 10^{-8} \text{ m}^3\text{kg}^{-1}$, range $191.3\text{-}267.9 \times 10^{-8} \text{ m}^3\text{kg}^{-1}$) than the latter (average $701.7 \times 10^{-8} \text{ m}^3\text{kg}^{-1}$, range $648\text{-}752.2 \times 10^{-8} \text{ m}^3\text{kg}^{-1}$). The intervening laterite is even more magnetic (average $1133.4 \times 10^{-8} \text{ m}^3\text{kg}^{-1}$, range $828.1 - 1453.9 \times 10^{-8} \text{ m}^3\text{kg}^{-1}$). The basalts were fed by dolerite dykes, virtually all of which have a NW-SE trend in northern Ireland. The Ballintoy dyke has an average susceptibility of $780.5 \times 10^{-8} \text{ m}^3\text{kg}^{-1}$, range $525.7\text{-}1169.9 \times 10^{-8} \text{ m}^3\text{kg}^{-1}$ and the Cuilcagh dyke has an average susceptibility of $1311.8 \times 10^{-8} \text{ m}^3\text{kg}^{-1}$, range $991.4\text{-}1537.1 \times 10^{-8} \text{ m}^3\text{kg}^{-1}$. The latter was studied in detail by Gibson et al., (2009) who found that different segments of the dyke had different magnetic properties. Gabbro from Carlingford has a susceptibility of $352.6 \times 10^{-8} \text{ m}^3\text{kg}^{-1}$ and a range $191.8\text{-}492.8 \times 10^{-8} \text{ m}^3\text{kg}^{-1}$.

Other older igneous rocks which are located west of the study area or within the western part of it may have been a significant source of magnetic grains to the soils. The basalt of the Carboniferous volcano at Croghan Hill has an average susceptibility of $294.4 \times 10^{-8} \text{ m}^3\text{kg}^{-1}$ and a range $213\text{-}342.6 \times 10^{-8} \text{ m}^3\text{kg}^{-1}$. The Hill of Allen which forms part of the Kildare Inlier in western Kildare is formed of a series of basalt lava flows, Plate 3.8. The Hill of Allen basalts have an average susceptibility of $1498.1 \times 10^{-8} \text{ m}^3\text{kg}^{-1}$ and a range $1207.6 - 1660.7 \times 10^{-8} \text{ m}^3\text{kg}^{-1}$. This was an unexpected result and is higher than the other basalts analysed in this study. The other basalts are considerably younger than the Hill of Allen basalt and would thus be less altered. However, it is clear that parent primary material is present within the study area which could be a major source of magnetic grains for the soils.

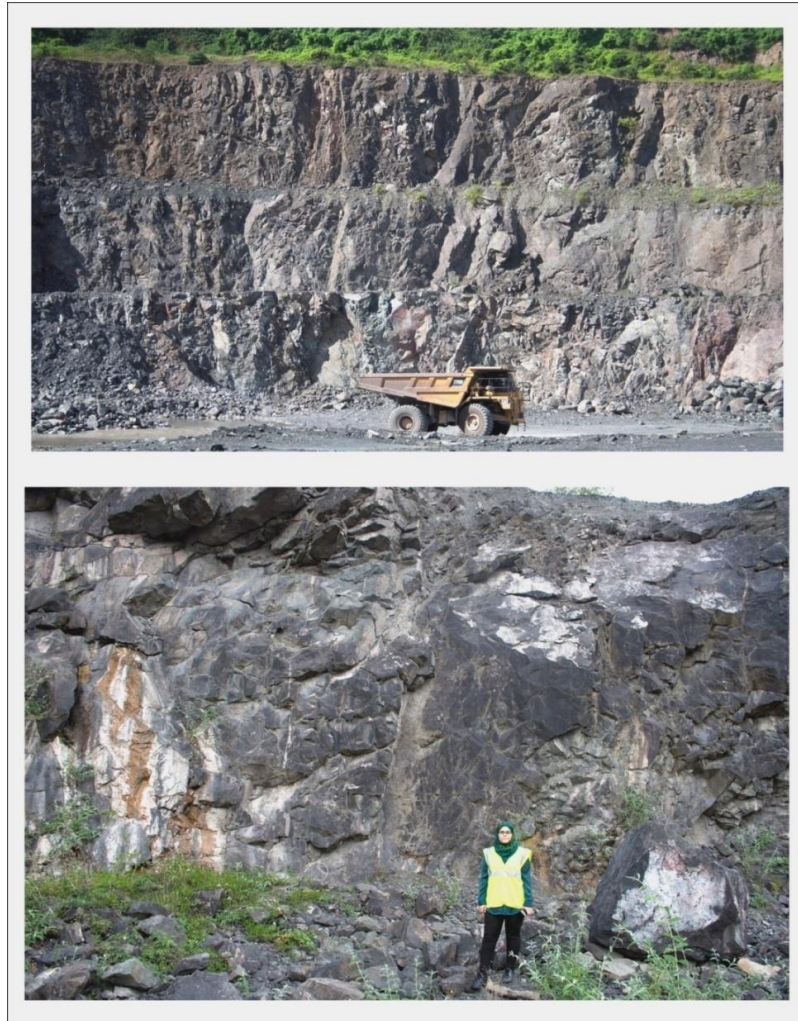


Plate 3.8: Hill of Allen basalts in study area.

Within Co. Wicklow there are outcrops of igneous (mainly granite); sedimentary (greywacke) and metamorphic (slate and schist) rocks. In general, igneous rocks are more magnetic than metamorphic, which in turn are more magnetic than sedimentary ones, though there is often a large overlap in the ranges, Figure 3.6. Basic (mafic) igneous rocks such as basalt are more magnetic than acid (felsic) igneous ones. The former contains ferrimagnetic minerals whereas the latter are mainly formed of diamagnetic minerals such as quartz and feldspar and paramagnetic minerals, such as biotite mica.

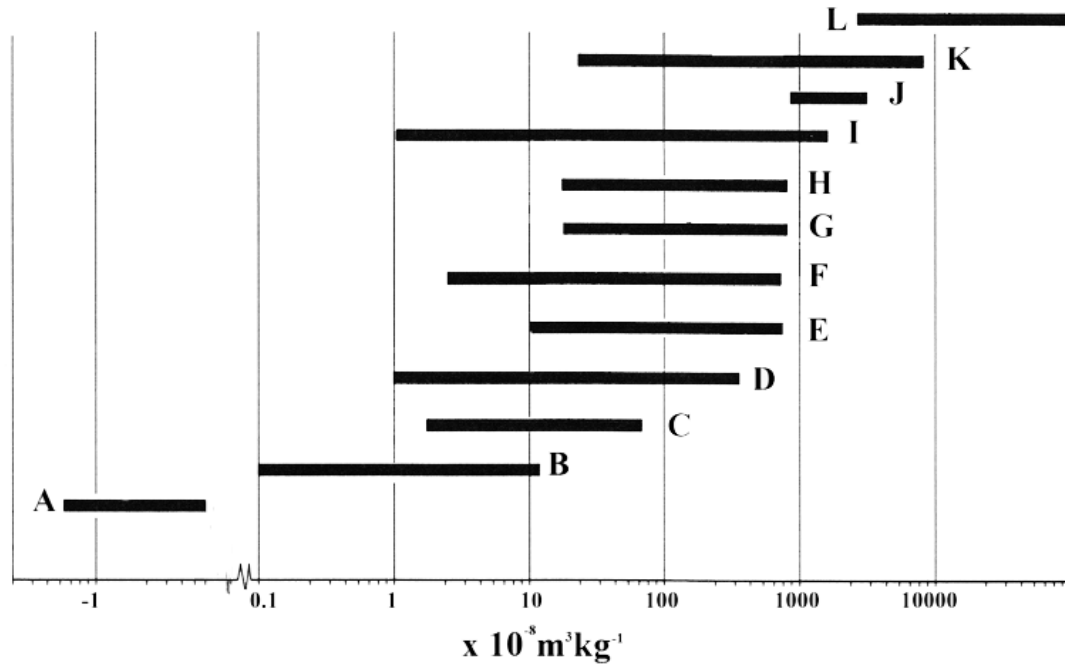


Figure 3.6: Magnetic susceptibility ranges for different lithologies and superficial deposits. A: diamagnetic minerals; B: sedimentary rocks; C: fine/medium metamorphic rocks; D: paramagnetic minerals; E: coarse metamorphic rocks; F: acid igneous rocks; G: canted antiferromagnetic minerals; H: intermediate igneous rocks; I: topsoils; J: mafic/ultramafic rocks; K: burned soils; L: ferrimagnetic minerals. Modified after Dearing (1994).

The magnetic susceptibility for granites from different parts of Ireland were obtained: Cushendun, Galway and Wicklow Caledonian granites and the Tertiary Mourne granites. The Cushendun granite has an average susceptibility of $38.7 \times 10^{-8} \text{ m}^3\text{kg}^{-1}$ and a range of $28.1\text{-}63.7 \times 10^{-8} \text{ m}^3\text{kg}^{-1}$. Although the susceptibility of the Galway (and other) granites is relatively low, locally very high values may be obtained. In the Mace Head region of Carna, there are magnetite-pyrite ‘orbs’ up to 5 cm across (Feely, 2002). A sample was analysed for this thesis which had a susceptibility of $19000 \times 10^{-8} \text{ m}^3\text{kg}^{-1}$. The Wicklow granite has a very low susceptibility ($4.3 \times 10^{-8} \text{ m}^3\text{kg}^{-1}$). The Bray Group and also the Kilcullen Group within the study area consist to a large extent of greywackes which average around $9.0 \times 10^{-8} \text{ m}^3\text{kg}^{-1}$. The susceptibility of a number of schists and slates from different localities was measured. The schists have a higher average susceptibility of $26.4 \times 10^{-8} \text{ m}^3\text{kg}^{-1}$ and a range of $22.1\text{-}31.3 \times 10^{-8} \text{ m}^3\text{kg}^{-1}$. The slates have an average susceptibility of $14.2 \times 10^{-8} \text{ m}^3\text{kg}^{-1}$ and a range of $11.9\text{-}19.3 \times 10^{-8} \text{ m}^3\text{kg}^{-1}$. Most of the metamorphic and metasedimentary rocks that formed during the Caledonian Orogeny

have relatively low magnetic susceptibility values. Limestone is the underlying bedrock for a large part of Kildare and quartzite crops out in north Wicklow (Great Sugar Loaf Mountain). Both lithologies have virtually zero susceptibility. Thin shale layers often separate the limestone beds. These dark layers often contain pyrite which has oxidised where exposed, Plate 3.9. However, even then their susceptibility is very low, c. $3.8 \times 10^{-8} \text{ m}^3\text{kg}^{-1}$.



Plate 3.9: Formation of iron oxide in shales near site K1.

Two other potential local sources of magnetic minerals can be found in the Wicklow region. Firstly, there are a large number of small igneous intrusions in this region, such as the doleritic Tallaght Hills dykes and the dioritic and doleritic intrusions in the Duncannon Group of SE Wicklow (McConnell and Philcox, 1994). Secondly, mineralisation associated with the igneous and metamorphic processes of the Caledonian Orogeny produced magnetic minerals. Siderite and haematite are found at Glendalough and Ballycorus, magnetite has been found in the Goldmines River and the Ballard iron deposit consists of magnetite. In addition, Tichborne (1885) reported that the rich magnetite vein he found near Avoca ‘could be traced for some two miles or more’. In conclusion, although many of the rocks within the study are paramagnetic, there also exists a range of lithologies which contain ferrimagnetic minerals which can contribute to the magnetism of the soils. Such ‘primary magnetism’ is not the sole contributor to

soil magnetism, pedogenic processes can result in the formation of secondary magnetic grains which are of great significance.

3.10 Magnetic characteristics of soils

Some of the earliest magnetic susceptibility studies of soils were undertaken by Le Borgne (1955) in France. Since then, it has been studied in a large number of countries, e.g. England (Dearing et al., 1996b), China (Lu and Bai, 2008), USA (Royall, 2001), Wales (Dearing et al., 1997), Russia (Semenov and Pakhotnova, 1998), Austria (Hanesch and Scholger, 2005), Iran (Karchegani et al., 2011), Canada (de Jong et al., 2000), Poland (Strzyszez and Magiera, 2001), Albania (Hounslow and Chepstow-Lusty, 2004) and Bulgaria (Jordanova et al., 1997). However, notwithstanding the large number of studies, it is difficult to provide a representative table of magnetic susceptibility values for different soils for a number of reasons.

- Firstly, some workers have recorded volume susceptibility whereas others provide results of mass specific susceptibility.
- Secondly, different units may be used and/or different types of equipment have been employed such as Bartington Instruments, Digico, susceptibility bridge, KLY2 Kappabridge or the Sapphire SI-2 magnetic susceptibility meter. The measured susceptibility is dependent on the frequency at which the equipment operates which can vary for different manufacturers.
- Thirdly, in some instances, the published results refer to a bulk sample whereas in other cases, it is a specific particle size fraction.
- Fourthly, terminology regarding soil types is not standardised and site specific samples are collected. For example, Hanesch and Scholger, (2005) collect data on ‘anthrosols’ whereas Semenov and Pakhotnova (1998) make measurements on ‘solonetz’, terms which cannot be reconciled with the 10 Great Soil Groups in Ireland discussed earlier.

Soils exhibit a range of susceptibility values that extends over at least 3 orders of magnitude, Figure 3.6. A feature of such magnetism, is that topsoils generally are more

magnetic than subsoils - a characteristic termed magnetic enhancement (Alekseeva et al., 2007; Le Borgne, 1955; Dearing, 1994). Various studies and hypotheses have been proposed to explain this behaviour. Because magnetite and other magnetic iron oxides are resistant to weathering, their concentration may increase in the upper layer of soil and thus yield higher susceptibility values. An increase in the concentration of such primary minerals tends to occur when the underlying rock is magnetic. However, such enhancements are also seen where the parent rock is not magnetic and the resultant soils are more magnetic than the rock (Dearing et al., 1996b; Hanesch and Scholger, 2005; Mileti et al., 2013; Singer and Fine, 1989; Singer et al., 1996), implying there is a source of secondary ferrimagnetic minerals. Possible sources are pollution and burning, though such effects tend to be localised.

The susceptibility for some parent rocks and their overlying soils (not within the study area) were measured to ascertain if the soils in Ireland also exhibited magnetic enhancement. Chalk on the north Antrim coast and limestone from the Burren both have a susceptibility close to zero. Their respective soils have values of $130 \times 10^{-8} \text{ m}^3\text{kg}^{-1}$ and $14.5 \times 10^{-8} \text{ m}^3\text{kg}^{-1}$. However, in the case of Antrim basalts, the reverse is the case. The Lower and Causeway basalts ($231.2 \times 10^{-8} \text{ m}^3\text{kg}^{-1}$, and $701.7 \times 10^{-8} \text{ m}^3\text{kg}^{-1}$ respectively), have overlying lower soil susceptibilities of $70.2 \times 10^{-8} \text{ m}^3\text{kg}^{-1}$ and $223 \times 10^{-8} \text{ m}^3\text{kg}^{-1}$. This is in contrast to the work carried out by Singer and Fine (1989) who found that the susceptibility of soils over basalts were higher than the parent rock.

The magnetic susceptibility results for the research area will be presented in Chapters 4 and 5, however, it is useful to consider, in general terms how the susceptibility of soils from other areas compares with the Irish research. The discussion here only relates to 'natural' magnetic susceptibility and not the susceptibility due to anthropogenic pollution. Landgraf and Royall (2006) mapped the spatial distribution of susceptibility for a fallow pasture area underlain by limestone in the USA. A similar situation exists for central and eastern Kildare. Their susceptibility values ranged from $115\text{-}200 \times 10^{-8} \text{ m}^3\text{kg}^{-1}$. However, virtually all the Kildare results are significantly lower than this, often by at least one order of magnitude. Peat, as it is formed of diamagnetic organic material has a magnetic susceptibility value of 0 except where polluted by anthropogenic activity

(Rothwell and Lindsay, 2007; Strzyszez and Magiera, 2001). Peat within the study area was virtually non-magnetic. Calcareous marl, underlying the peat was paramagnetic ($5 \times 10^{-8} \text{ m}^3\text{kg}^{-1}$). Water-logged gley soils generally yield low susceptibility values (de Jong et al., 2000). This is supported by work from Austria where gleys have a susceptibility of c. $10\text{-}15 \times 10^{-8} \text{ m}^3\text{kg}^{-1}$ (Hanesch and Scholger, 2005). Dearing et al., (1996b) report that a typical brown earth from England has a susceptibility of $149 \times 10^{-8} \text{ m}^3\text{kg}^{-1}$. This is considerably more than that found by Hanesch and Scholger (2005) for equivalent soils (cambisol), where readings were about 33% of the English values.

3.11 Summary

In Chapter 3, some of the background literature relevant to this research was discussed. The chapter could be conveniently divided into two themes: firstly, various relevant landscape characteristics of the study area were discussed and secondly there was a focus on the geophysical techniques used in the current research. Landscape characteristics were considered in chronological order and from regional to local. A range of igneous sedimentary and metamorphic rocks of various ages, each of which forms roughly one third of the rock skeleton, underlies the study area. Overlying the rocks are till and fluvio-glacial deposits of varying thickness deposited in the later phase of the Midlandian glaciation. Till is the most extensive deposit in Kildare and Wicklow, though hummocky sand and gravel is prevalent in eastern Kildare. Glacial landforms such as corries and meltwater channels occur in the Wicklow mountains and eastern Wicklow respectively.

Soil development began in Ireland at the beginning of the Holocene, approximately 10,000 years ago partially through the interaction of leaching and gleyisation to yield 10 Great Soil Groups for Ireland namely: Podzols, Brown podzols, Brown earths, Grey Brown Podzols, Blanket Peat, Gleys, Basin Peats, Rendzinas, Regosols and Lithosols. The soils of County Kildare were mapped in some detail in the period 1959-1985 however, County Wicklow was not. 19 Soil Series and 6 Soil Complexes are recognised in Co. Kildare, though 8 make up 73% of the area. The Grey Brown podzol Great Soil Group in County Kildare is formed of seven soils series which combined account for 46.2% of land surface of Kildare. Four complex soils form about 23% of Kildare's soil

and the Gley Group (6 series) makes up about 12% of Kildare, similar in area to the peat areas.

According to the EPA, the main soils are: Alluvium (abbreviated to ALLUV), Deep Well Drained Mineral soil (abbreviated to DWDM), Deep Poorly Drained Mineral soil (abbreviated to DPDM), Shallow Poorly Drained Mineral soil (abbreviated to SWDM) and Peat. Six soil types predominate in Wicklow: ADPDM: Acid Deep Poorly Drained Mineral soil; ASWDM: Acid Shallow Well Drained Mineral soil; ADWDM: Acid Deep Well Drained Mineral soil, BSWDM: Basic Shallow Well Drained Mineral soil; ASP: Acid Shallow partially Podzolic and BP: Blanket Peat.

Two different geophysical techniques were employed for this research (Magnetic methods and Resistivity methods) which have been used in natural and anthropogenic pollution studies. An analysis of the magnetic susceptibility of the main types of rocks in Ireland showed that some could be a source of primary magnetic grains, most especially the Hill of Allen basalt which is very magnetic. However, soil susceptibility values that are higher than their underlying rocks indicate that secondary magnetic enhancement is important in Ireland.

CHAPTER 4

MAGNETIC AND ELECTRICAL RESISTIVITY RESULTS

FOR COUNTY KILDARE

4.1 Introduction

The main results of the research in County Kildare are presented in this chapter which, for a number of reasons, commences with a discussion of the particle size distribution for the various soils that are found in the county. Firstly, particle size analysis is a commonly applied procedure used in the classification of soils and it is important to ascertain if it can provide useful discriminating information in the study area. Visual analysis of the $>2000\mu\text{m}$ fraction for the same soil type for example often revealed clast size/type differences. Secondly, the relative particle size distribution combined with the magnetic susceptibility of the various fractions control the bulk magnetic susceptibility. The concept of a 'particle size' does not apply to peat soils as they consist of fibrous vegetable matter. Consequently, particle size analysis was not carried out on peat soils. The discussion on particle size (section 4.2) is followed by sections relating to the magnetic characteristics of Kildare soils:

- Section 4.3. Statistical characteristics of the bulk magnetic parameters (χ : low and high frequency magnetic susceptibility and $\chi_{fd}\%$ (frequency dependent magnetic susceptibility) and K: volume susceptibility).
- Section 4.4. Spatial variability of the magnetic parameters (χ : low and high frequency magnetic susceptibility: $\chi_{fd}\%$ (frequency dependent magnetic susceptibility) and K (volume susceptibility) of the Kildare soils.
- Section 4.5. Variation of volume magnetic susceptibility with temperature (K-T) for specific soil types.
- Section 4.6. Assessment of remanent magnetism measurements.
- Section 4.7. Statistical characteristics of the magnetic parameters of individual Kildare soils.

- 4.8 Characteristics of the magnetic parameters of grain size fractions for individual soils.

The chapter concludes with a section on 2D electrical resistivity tomography results. This section, as well as detailing the resistivity variations at a number of sites, considers the effects of different electrode arrays, azimuthal variations and resistivity-depth models. For this research, approximately 85,000 mass and volume magnetic susceptibility measurements were taken and over 1800 histograms were produced and analysed. If 6 are shown per page this would result in 300 pages of histograms. In addition, there would be approximately 100 pages of K-T results and 300 pages of resistivity figures/results. These 700 pages combined with text and other diagrams would result in a thesis of over 1000 pages. Consequently, only a few representative samples of the results are shown rather than all of them. However, the results, discussions and conclusions are based on the analysis of all data. The rest of the graphs and histograms are shown in separate folders on the accompanying CD as supplementary figures and the relevant figure contains the letter 's', e.g. File 4.1s.docx.

As discussed in Chapter 2, the graphical representations of the results were analysed at different dynamic ranges, thus, for example, the K–T graphs were viewed over short temperature ranges which allowed the subtler trends to be determined.

4.2 Particle size distribution and clastic characteristics of County Kildare soils

According to the EPA five soil types dominate County Kildare, see Figure 4.1 and Table 4.1. The majority of soils are basic, reflecting the underlying limestone lithology. However, peat deposits are acidic as are some soils along the Kildare-Wicklow border where greywacke is found. The soils are termed:

- Alluvium (abbreviated to ALLUV).
- Deep Well Drained Mineral soil (abbreviated to DWDM).
- Deep Poorly Drained Mineral soil (abbreviated to DPDM).
- Shallow Poorly Drained Mineral soil (abbreviated to SWDM).
- Peat.

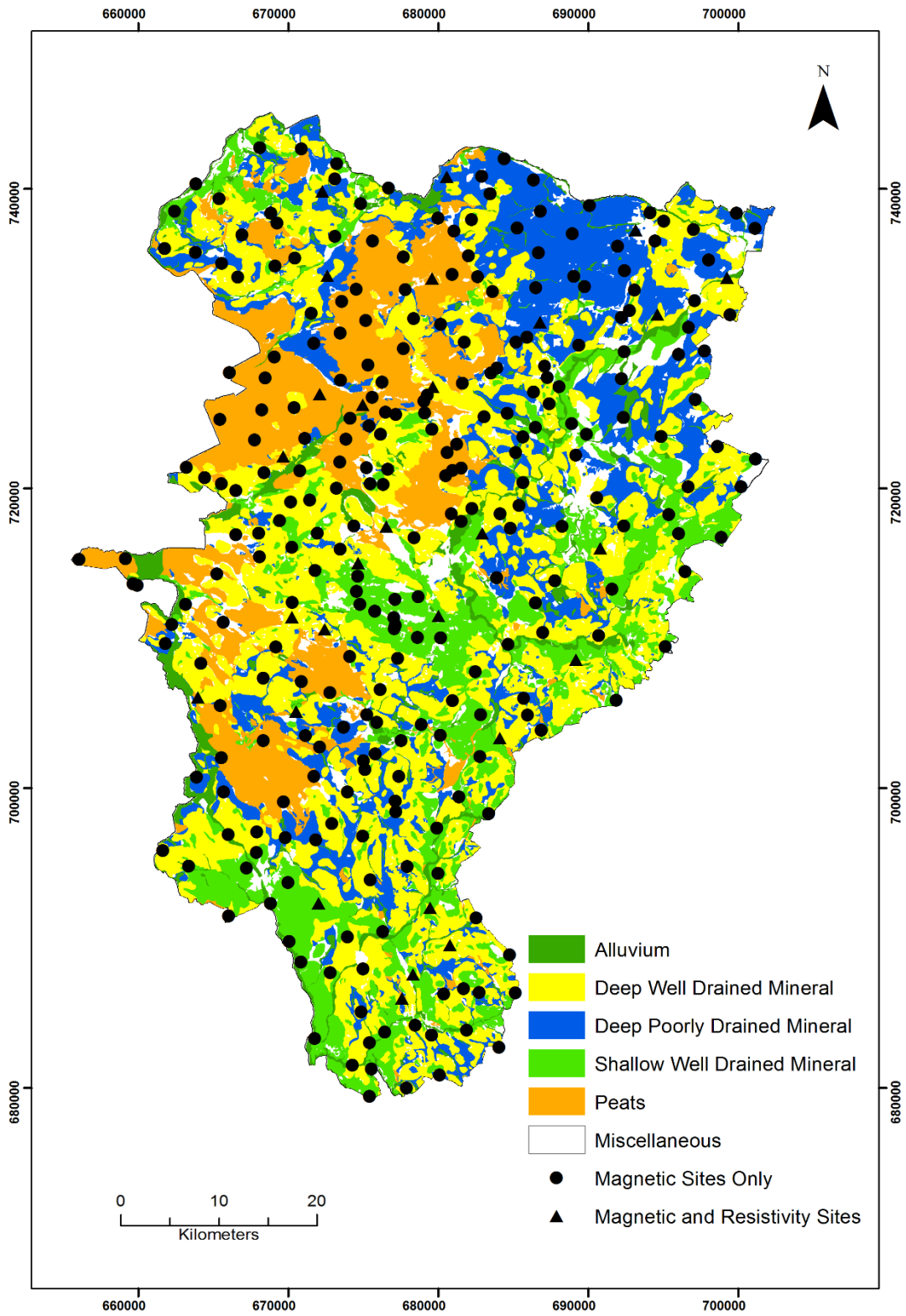


Figure 4.1: The geographical locations of the soil types and sites where data were collected.

Code of Soil	Group of Soils	No.	Code of Samples
ALLUV	Alluvium	20	9,12,31,37,43,58,76,93,151,171,172,202,209,228,229,234,247,255,276,293.
DWDM	Deep Well Drained Mineral	112	2,5,8,15,16,19,20,22,24,26,27,32,39,44,60,61,62,67,68,70,71,72,73,75,78,83,84,85,88,89,91,92,94,97,98,100,101,106,107,108,112,115,116,117,118,119,120,122,126,128,136,137,139,140,141,143,147,148,153,154,156,157,158,159,162,163,165,167,168,169,170,173,174,177,180,184,185,186,188,194,196,197,201,205,211,223,230,231,232,233,246,248,249,251,252,253,256,257,258,269,270,272,273,275,279,281,282,286,287,288,290,295,298.
DPDM	Deep Poorly Drained Mineral	59	1,3,4,6,11,21,33,35,36,40,63,69,79,80,81,82,86,90,95,96,103,105,110,111,123,125,127,129,130,135,142,152,161,166,179,187,190,191,192,193,203,204,206,207,208,210,212,216,217,218,219,220,221,245,254,289,291,292,294.
SWDM	Shallow Well Drained Mineral	64	13,14,17,18,23,25,29,30,34,46,47,48,49,50,51,52,53,54,55,56,57,59,64,65,66,102,104,113,114,121,131,132,133,134,138,160,164,175,176,178,181,182,183,213,214,222,250,260,261,262,263,264,265,266,267,271,274,277,278,280,283,285,296,300.
P	Peats	29	41,42,87,109,124,148,149,150,155,189,195,198,199,200,224,225,226,227,235,236,237,238,239,240,241,242,243,244,299.
MIS	Miscellaneous	16	7,10,28,38,45,74,77,99,144,145,146,215,259,268,284,297.

Table 4.1: Kildare sites by soil type.

Analysis of the clasts in the >2000µm sieve reflect to a large extent the nature of the underlying lithology. Most sites contain limestone fragments 0.5-5cm across which tend to be subrounded to subangular. Some samples taken near the Kildare Inlier contain sandstone clasts. K300 was obtained from the top of the Hill of Allen, above a basalt quarry. The soil layer is very thin and it contains large (up to 3 cm) angular basalt clasts. Soils located near the eastern Kildare border contain angular greywacke fragments.

Soils in east Kildare/west Wicklow border all contain limestone clasts with some also having greywackes pebbles, often large (>3cm) and platy whereas most of the clasts from southern Kildare contain greywacke and granite. Sample K118 has a 2 cm clast of rotted granite and has a pebble which showed a contact between granite and greywacke. The presence of granite is not unexpected as it forms the bedrock for this area. K176 contains a well rounded 2cm diameter quartz pebble, the only such one found in the 300 Kildare sites. It has possibly been transported by water during the deglaciation of the area. Its source is most likely the Wicklow granite to the east. Table 4.2 shows that the main soil series in county Kildare have a remarkably similar particle size distribution pattern with the 600-250µm range being the predominant one (average for Kildare 26.8%). See also File 4.1s.docx in particle size folder on CD.

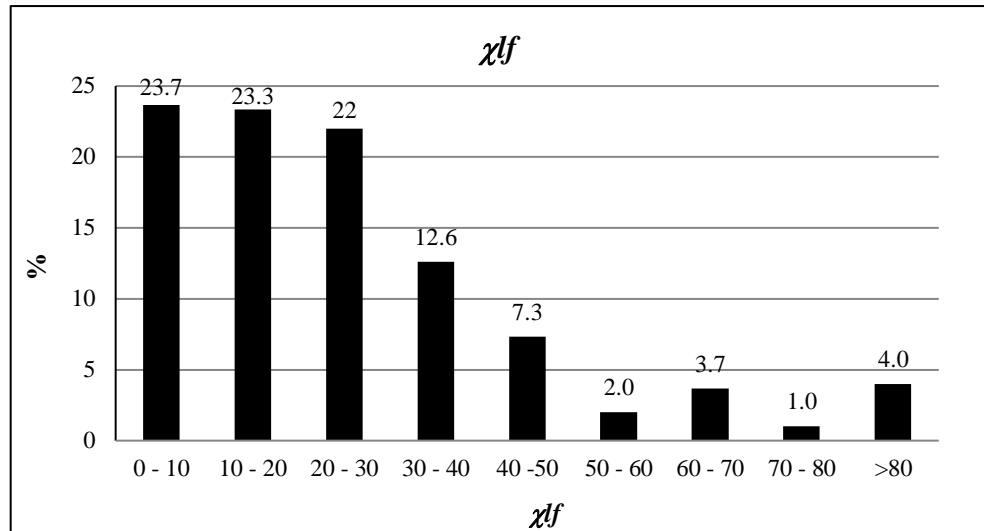
Type of Soil	>2000 µm	2000- 900 µm	900- 600 µm	600- 250 µm	250- 125 µm	125- 63µm	<63 µm
Alluvium	11.2	12.1	13.4	26.2	14.2	14.3	8.6
Deep Well Drained Mineral	10	13.2	12	26	14.8	15.2	8.7
Deep Poorly Drained Mineral	10.9	11.4	12.2	28.3	14.5	14.1	8.7
Shallow Well Drained Mineral	10	12.7	13.1	27.3	14.2	14.6	8.1
Kildare	10.5	11.7	12.3	26.8	14.9	14.9	8.9

Table 4.2: Average percentage of sample in each size fraction for Kildare soils.

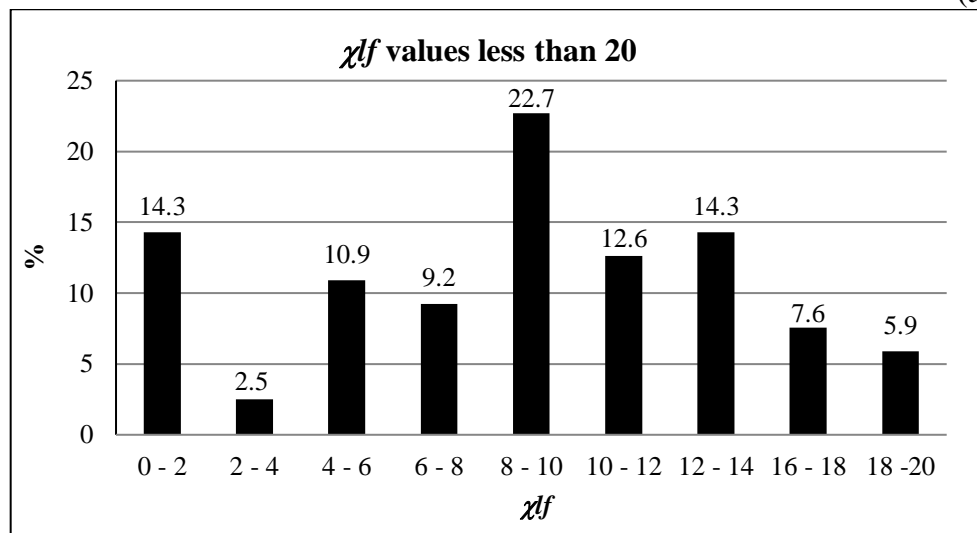
4.3 Statistical characteristics of the bulk magnetic parameters of the Kildare soils

300 soil samples were magnetically analysed using the techniques and procedures discussed in Chapter 2 and their statistics are shown in Table 4.3. Four versions were calculated, one which includes all samples, a second which excludes peat samples, a third which includes all samples except K300 and a fourth which excludes peat and K300. The reason for this is because the magnetic susceptibility of peat is virtually zero and including a large number of samples with a zero in a statistical analysis can greatly skew the results. Also, the χ_{lf} value of K300 is about 20 times greater than the average and including it in calculations can cause major distortions. For example, from Table 4.3 the standard deviation is about 24, kurtosis about 8.2 and skewness is 2.4 when K300 is excluded and 41, 125.6 and 9.6 when it is included. The χ_{lf} values range from 0 to $604.7 \times 10^{-8} \text{ m}^3\text{kg}^{-1}$ with a mean value of $26.7 \times 10^{-8} \text{ m}^3\text{kg}^{-1}$, Table 4.3a. Discounting the peat values, the mean susceptibility value for soil in Kildare rises slightly to $28.1 \times 10^{-8} \text{ m}^3\text{kg}^{-1}$. An χ_{lf} of $>10 \times 10^{-8} \text{ m}^3\text{kg}^{-1}$ indicates that the soil contains ferrimagnetic minerals such as magnetite or maghemite. 76% (80% excluding peat) of the soil samples contain ferrimagnetic minerals. As there are very few magnetic rocks in Kildare, this indicates widespread secondary enhancement in the county.

The average $\chi_{fd}\%$ value of 5.3% indicates that the average soil sample in Kildare contains about 35-40% SP grains. The standard deviation for K (volume susceptibility) is lower than that of the mass specific susceptibility showing slightly less variability. Kurtosis is a measure of the peakedness of a distribution, high values having a sharper peak than a normal distribution. χ_{lf} and K are both positive (with the latter being much less than the former) giving a leptokurtic distribution (a more acute peak around the mean than a normal distribution). The -0.28 values for $\chi_{fd}\%$ (platykurtic distribution) is very close to what is expected for a normal distribution. The χ_{lf} and K magnetic data are positively (right) skewed thus the right-hand side of histogram is longer than the left side. In this instance the median is less than the mean value. For $\chi_{fd}\%$, the distribution is slightly negatively skewed.



(a)

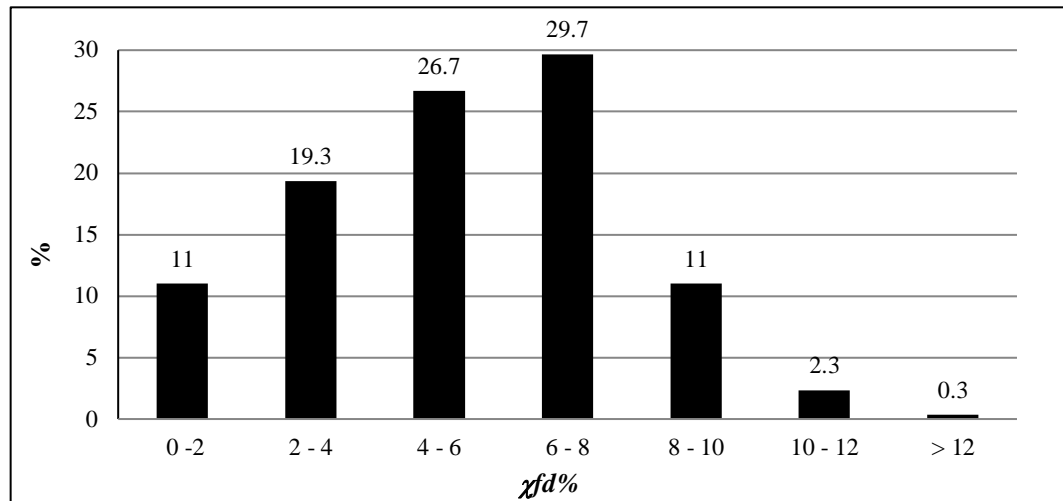


(b)

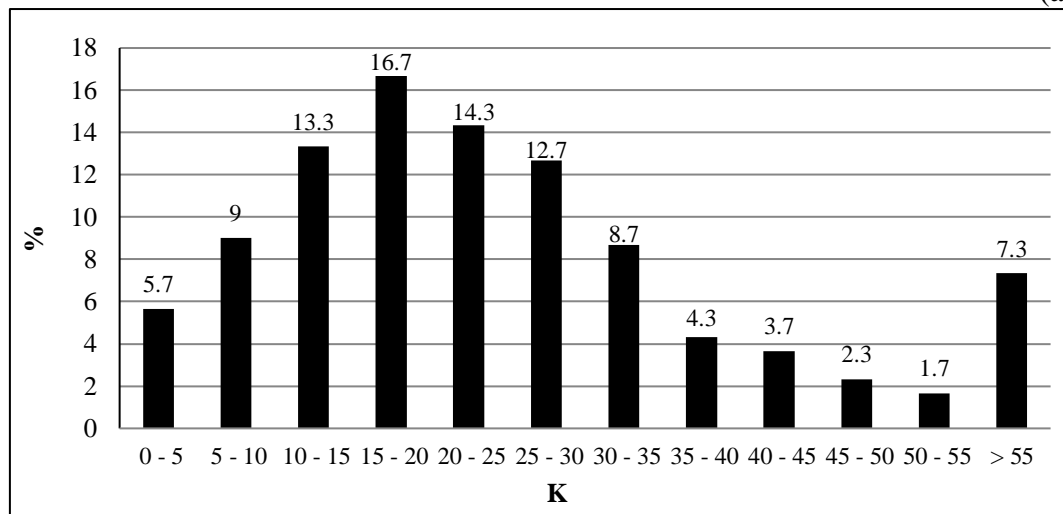
Figure 4.2: Histogram plot of (a) all χ_{lf} and (b) detail of χ_{lf} from $0-20 \times 10^{-8} \text{ m}^3\text{kg}^{-1}$.

A histogram plot for all χ_{lf} is shown in Figure 4.2a. The histogram is clearly non-normal with 66% of the data being less than $30 \times 10^{-8} \text{ m}^3\text{kg}^{-1}$. There is a marked drop in values greater than this and only 4% of the data are $>80 \times 10^{-8} \text{ m}^3\text{kg}^{-1}$ indicating that although 76% of the samples contain ferrimagnetic minerals, they do not contain significant amounts. 44% of the χ_{lf} values are less than $20 \times 10^{-8} \text{ m}^3\text{kg}^{-1}$, Figure 4.2b. 14% of these are in the $0-2 \times 10^{-8} \text{ m}^3\text{kg}^{-1}$ range because of the peat samples. In the $<20 \times 10^{-8} \text{ m}^3\text{kg}^{-1}$ range, the maximum (22.7%) occur between $8-10 \times 10^{-8} \text{ m}^3\text{kg}^{-1}$. The frequency dependent susceptibility data for Kildare ($\chi_{fd}\%$) shows a steady increase between 0-8% followed by a marked reduction in higher values, Figure 4.3a. Most data are in the 6-8%

range (29.6%) though statistically the average value is in the 4-6% range (5.3%, see Table 4.3).



(a)



(b)

Figure 4.3: Histogram of (a) $\chi_d\%$ and (b) volume susceptibility $K (\times 10^{-5})$.

The volume susceptibility measurements taken with the Bartington MS2D ring probe vary from $0-340.9 \times 10^{-5}$ (S.I.). The highest value was obtained at site K300 (Hill of Allen) and is an extreme outlier as the average volume susceptibility is 26×10^{-5} . The volume susceptibility distribution is positively skewed rising quickly and dropping off more gradually, Figure 4.3b. The most populous range is $15-20 \times 10^{-5}$ which has 16.7% of the samples while 7.3% of the data are $>55 \times 10^{-5}$.

All Samples	<i>χ^2_f</i>	<i>χ^2_{hf}</i>	<i>$\chi^2_{fd}\%$</i>	K
Mean	28.5	27	5.3	26.2
Median	21.6	20.2	5.5	21.1
Standard Deviation (SD)	41.3	40.4	2.6	25.5
Skewness	9.6	10.1	0.017	76.8
Kurtosis	127.1	137.7	-0.3	77.6
Shapiro-Wilk (W)	0.31	0.41	0.98	0.58
Excluding Peat Including K300	<i>χ^2_f</i>	<i>χ^2_{hf}</i>	<i>$\chi^2_{fd}\%$</i>	K
Mean	30.1	28.5	5.6	27.6
Median	22.6	20.9	5.8	22.4
Standard Deviation (SD)	42.1	41	2.3	32
Skewness	9.9	10.1	0.079	7.1
Kurtosis	125.6	135.7	-0.35	80.6
Shapiro-Wilk (W)	0.41	0.39	0.99	0.55
All Sample and Peat except K300	<i>χ^2_f</i>	<i>χ^2_{hf}</i>	<i>$\chi^2_{fd}\%$</i>	K
Mean	26.7	25.1	5.3	25.32
Median	21.6	20.2	5.5	21.15
Standard Deviation (SD)	24.4	22.9	2.5	17.9
Skewness	2.4	2.3	-0.16	1.7
Kurtosis	8.2	7.3	-0.28	3.9
Shapiro-Wilk (W)	0.79	0.8	0.99	0.86
All Samples excluding Peat and K300	<i>χ^2_f</i>	<i>χ^2_{hf}</i>	<i>$\chi^2_{fd}\%$</i>	K
Mean	28.1	26.5	5.6	26.7
Median	22.6	20.9	5.8	22.4
Standard Deviation (SD)	24.3	22.8	2.3	17.4
Skewness	2.4	2.3	0.08	1.9
Kurtosis	8.5	7.5	-0.35	4.3
Shapiro-Wilk (W)	0.78	0.78	0.99	0.83

Table 4.3: Statistics for the bulk Kildare soils.

The median may sometimes give a better representation of the ‘average’ as the median value is the value above and below which there are equal numbers of measurements (Theakstone and Harrison, 1970). Note, the small change in median values for the 4 variations in Table 4.3. The interquartile range Q1-Q3 ($10.7-34.2 \times 10^{-8} \text{ m}^3\text{kg}^{-1}$ for the mass specific susceptibility and $14.2-30.7 \times 10^{-5}$ for K, the volume susceptibility) is the range which contains 50% of the samples. The interquartile range Q1-Q3 for $\chi_{fd}\%$ data is 3.7-7.3%.

A Shapiro-Wilk test (confirmed by a Lilliefors test) was performed on the data (Seaby et al., 2007) to ascertain if they conformed statistically to a normal distribution. This returns a parameter W which is the squared correlation coefficient between the data and their corresponding normal scores. If $W = 1$ then there is a perfect fit to a normal distribution. All the χ_{lf} , $\chi_{fd}\%$ and K data (including peat) for Kildare exhibit a significant deviation from a normal distribution. In addition, they do not exhibit a log normal distribution. ($W = 0.96, 0.77$ and 0.32 for $\log \chi_{lf}$, $\log \chi_{fd}\%$ and $\log K$ respectively).

Various authors have postulated correlations between χ_{lf} and $\chi_{fd}\%$ - some positive (Huo et al. 2010; Mokhtari et al., 2011; Dearing et al., 1996a), some negative (Lu and Bai, 2008; Lu et al., 2008) whilst other have reported no correlation (van Dam et al., 2004). A scatterplot of χ_{lf} and $\chi_{fd}\%$ (sample K300 omitted) is shown in Figure 4.4a. A Spearman rank coefficient of 0.18 indicates there is no significant correlation between χ_{lf} and $\chi_{fd}\%$. The correlation between χ_{lf} and K (sample K300 excluded) is a strong positive correlation, (Spearman rank coefficient of 0.69), Figure 4.4b.

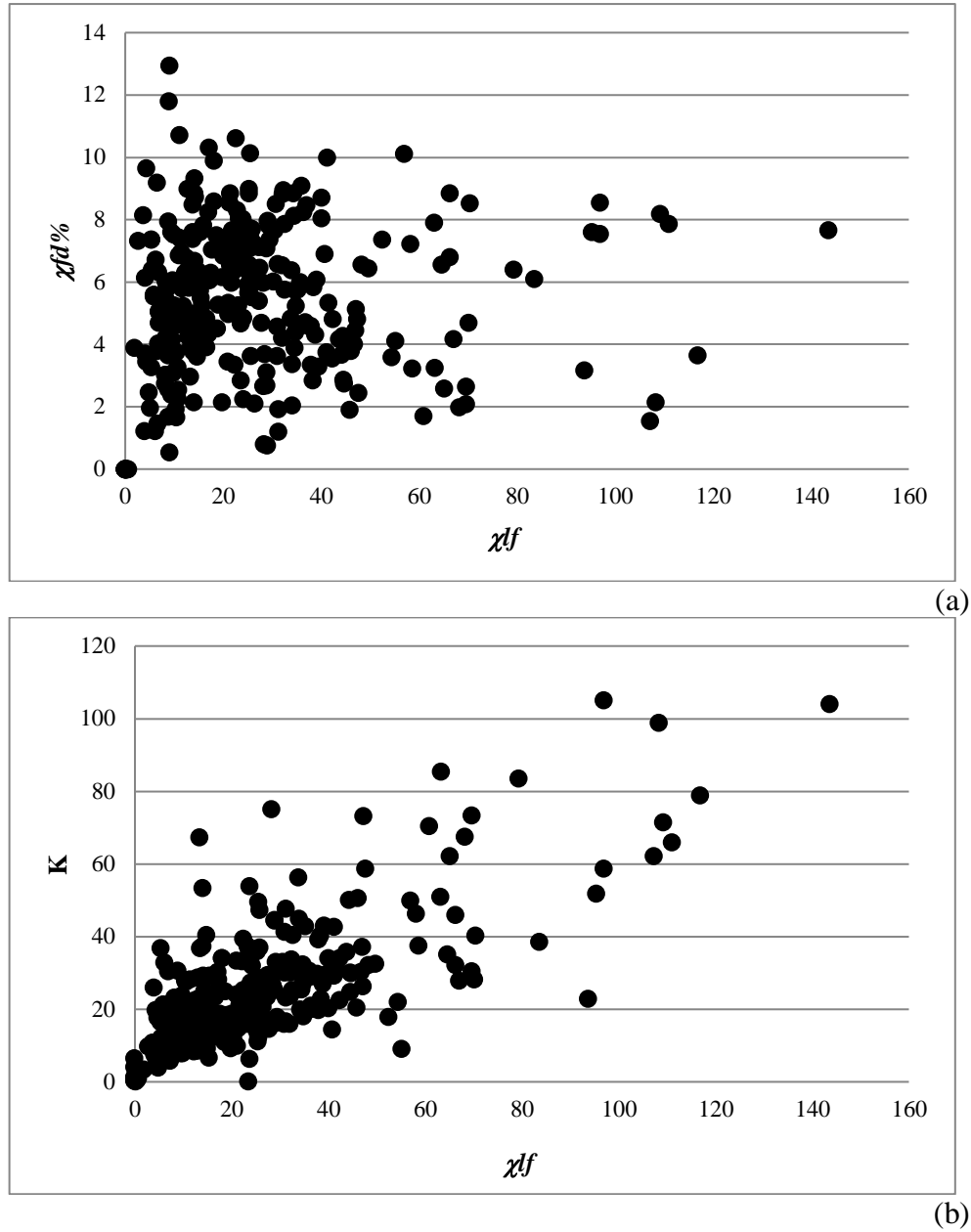


Figure 4.4: (a) Plot of χ_{lf} and $\chi_{fd}\%$ and (b) between χ_{lf} and K . (χ_{lf} unit $\times 10^{-8} \text{m}^3 \text{kg}^{-1}$) and (K unit $\times 10^{-5}$).

4.4 Spatial variability of the bulk magnetic parameters of the Kildare soils

In order to determine the spatial variability of magnetic parameters such as K , $\chi_{fd}\%$ or χ_{lf} it was first necessary to interpolate the irregularly spaced data to a regular grid of nodes from which the image could be produced. This was accomplished using SURFER 11 from Golden Software Inc. However, there are a number of interpolation methods

(e.g. kriging, radial basis function, inverse distance to a power, nearest neighbour, minimum curvature), each of which calculates grid node values using different algorithms and thus yields slightly different results (Golden Software Inc., 2013). Consequently, a range of image maps were created using the same data but with different gridding techniques and the results compared with the raw data to ascertain which preserved the integrity of the collected data. Minimum curvature smoothed the data out, can give high magnitude artefacts where there is no data (like kriging) and produces 'z' values outside the range of measured values.

The gridding algorithm employed in this research was the inverse distance squared, one in which data were weighted such that the influence of one point relative to another declines with distance from the grid node. Bourne (1993) employed the same algorithm to grid irregularly spaced magnetic susceptibility data for the Aylmer and St. Sebastian granitic plutons in Canada. This approach does not extrapolate beyond the 'z' limits but tends to produce 'bulls eyes' because it does not smooth the data. However, from a research point of view, these outlier anomalies are important because they indicate significant deviations from the background. Although less aesthetically pleasing as an image which varies smoothly, the inverse distance squared is more useful and preserves the integrity of the field data. Thus, data were gridded using the appropriate algorithm and then exported as tiff files to ArcMap Geographic Information Systems. An Arcmap shape file of Kildare was used with the 'extraction by mask' utility to produce the Kildare files.

Soils in areas of Kildare which have a susceptibility of $<10 \times 10^{-8} \text{ m}^3\text{kg}^{-1}$ generally only contain diamagnetic and paramagnetic minerals whereas higher values are associated with ferrimagnetic minerals (Dearing, 1999b). Blue and red regions in Figure 4.5 show the ($<10 \times 10^{-8} \text{ m}^3\text{kg}^{-1}$) and ($>10 \times 10^{-8} \text{ m}^3\text{kg}^{-1}$) magnetic regions respectively. There is a significantly greater concentration of low magnetism areas in the northern half of Kildare reflecting to a large extent the geographical position of the peat bogs.

The mass specific magnetic susceptibility for Co. Kildare shows a very pronounced variation, Figure 4.6. Low values ($0-20 \times 10^{-8} \text{ m}^3\text{kg}^{-1}$) predominate in the northwest due mainly to peat outcrops and cover an area of c. 241 km². A second smaller low

susceptibility east-west zone is located south of Irish Transverse Mercator northing 715000 (79 km²). The highest susceptibility values ($>60 \times 10^{-8} \text{ m}^3\text{kg}^{-1}$) are shown in red and are found at 3 locations, one in the north of the county and two in the south. The northern one is associated with the Kildare Inlier while the southern ones mainly relate to the DWDM and SWDM soils.

There is no significant spatial correlation between magnetic susceptibility and frequency dependent susceptibility - compare Figures 4.6 and 4.7. Low values of $\chi_{fd}\%$ (circa 0-2% representing up to 10% SP grains) do correspond to low susceptibility in the northeast however, the area covered is much less (41 km²). However, the high $\chi_{fd}\%$ values in the northeast are associated with low-medium susceptibility values and the high susceptibility over the Kildare Inlier has medium $\chi_{fd}\%$ values (3.5 $\chi_{fd}\%$ - 25% SP minerals). The largest areas of high $\chi_{fd}\%$ are located in the southern part of the county (140 km²). The soils from this region (and the extreme northeast) contain up to 60% of SP minerals.

The volume susceptibility data acquired with the Bartington MS2D probe shows a pattern that is consistent with the mass specific susceptibility data, Figure 4.8. Peat areas give the lowest values ($0-10 \times 10^{-5}$) and the Kildare Inlier stands out as an area of high susceptibility. High susceptibility values tend to cover a larger area in the volume susceptibility map compared with the mass specific susceptibility one. Figure 4.9 represents the relative standard deviation (calculated from the 20 volume susceptibility measurements made at each site with the MS2D probe). The highest values shown in red are a statistical artefact because measured values over peat are so low (c. zero) that very small absolute changes result in large relative variations. The southern third of the county displays a low relative standard deviation (blue), showing there is a less variable signature in this region. A NE-SW trending low zone is also evident in central Kildare where varied types of soil exist.

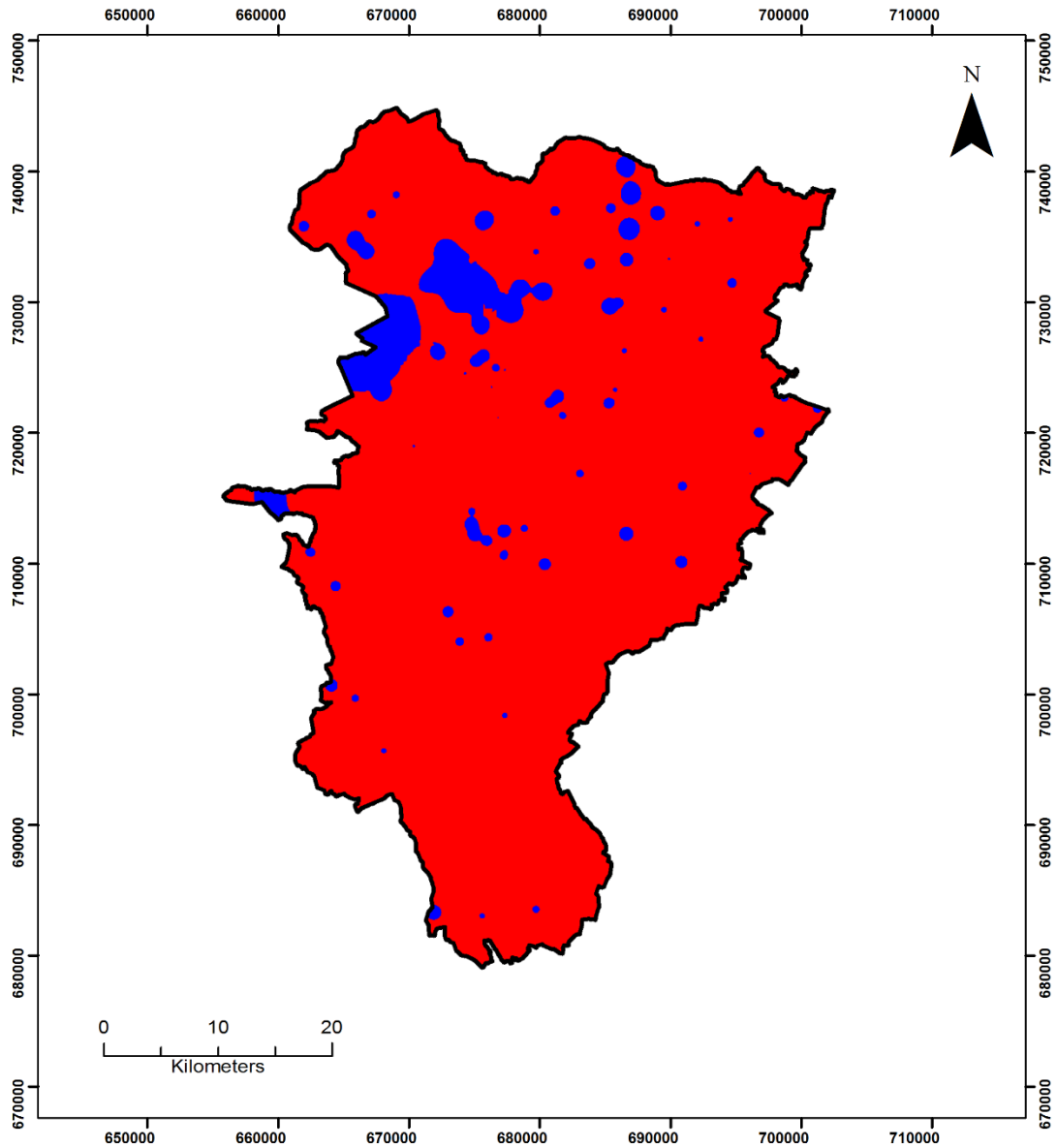


Figure 4.5: Magnetic susceptibility map of Kildare in which blue shows areas $<10 \times 10^{-8} \text{ m}^3 \text{ kg}^{-1}$ and red shows areas $>10 \times 10^{-8} \text{ m}^3 \text{ kg}^{-1}$.

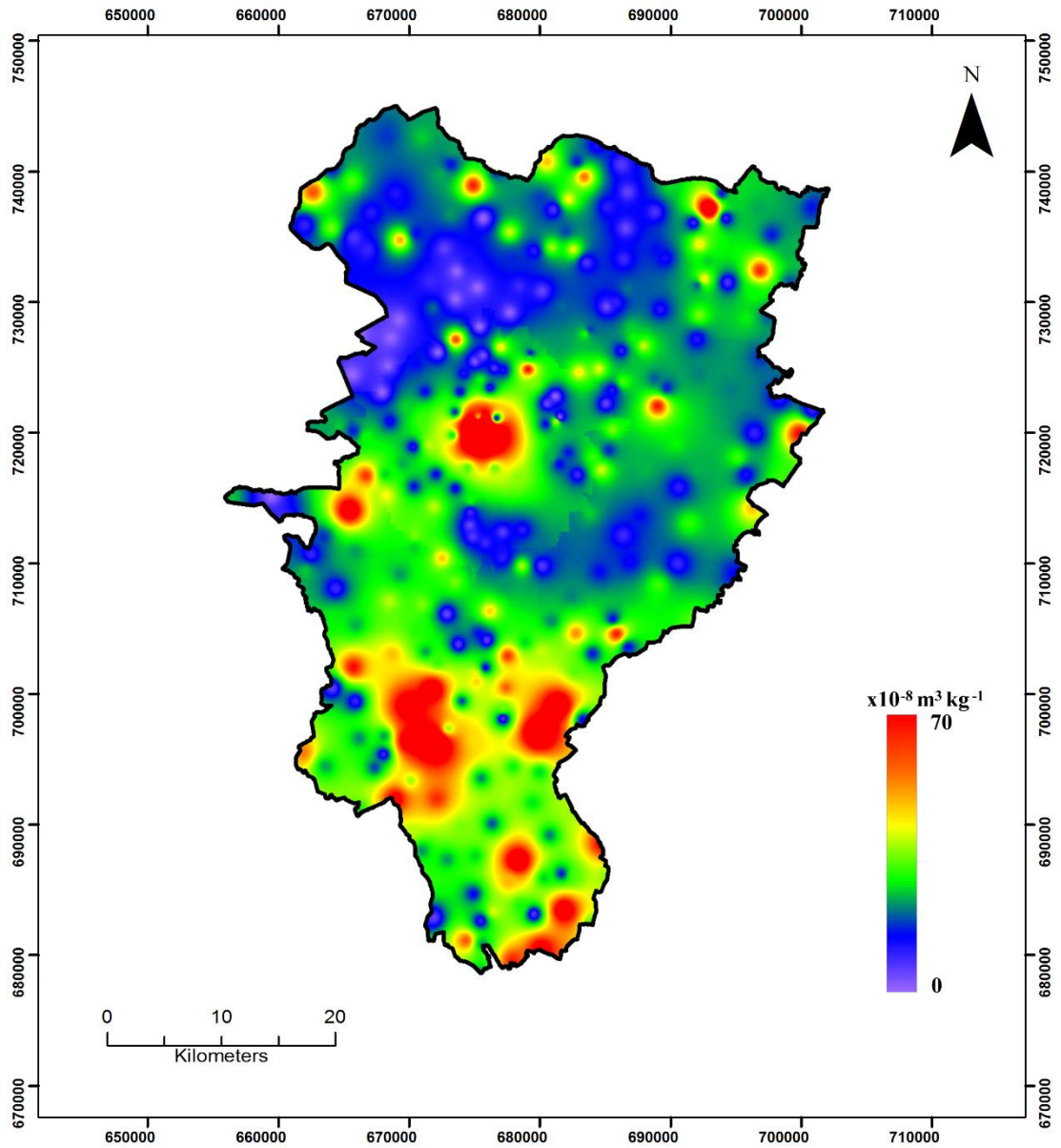


Figure 4.6: Magnetic susceptibility map of Kildare (χ_f).

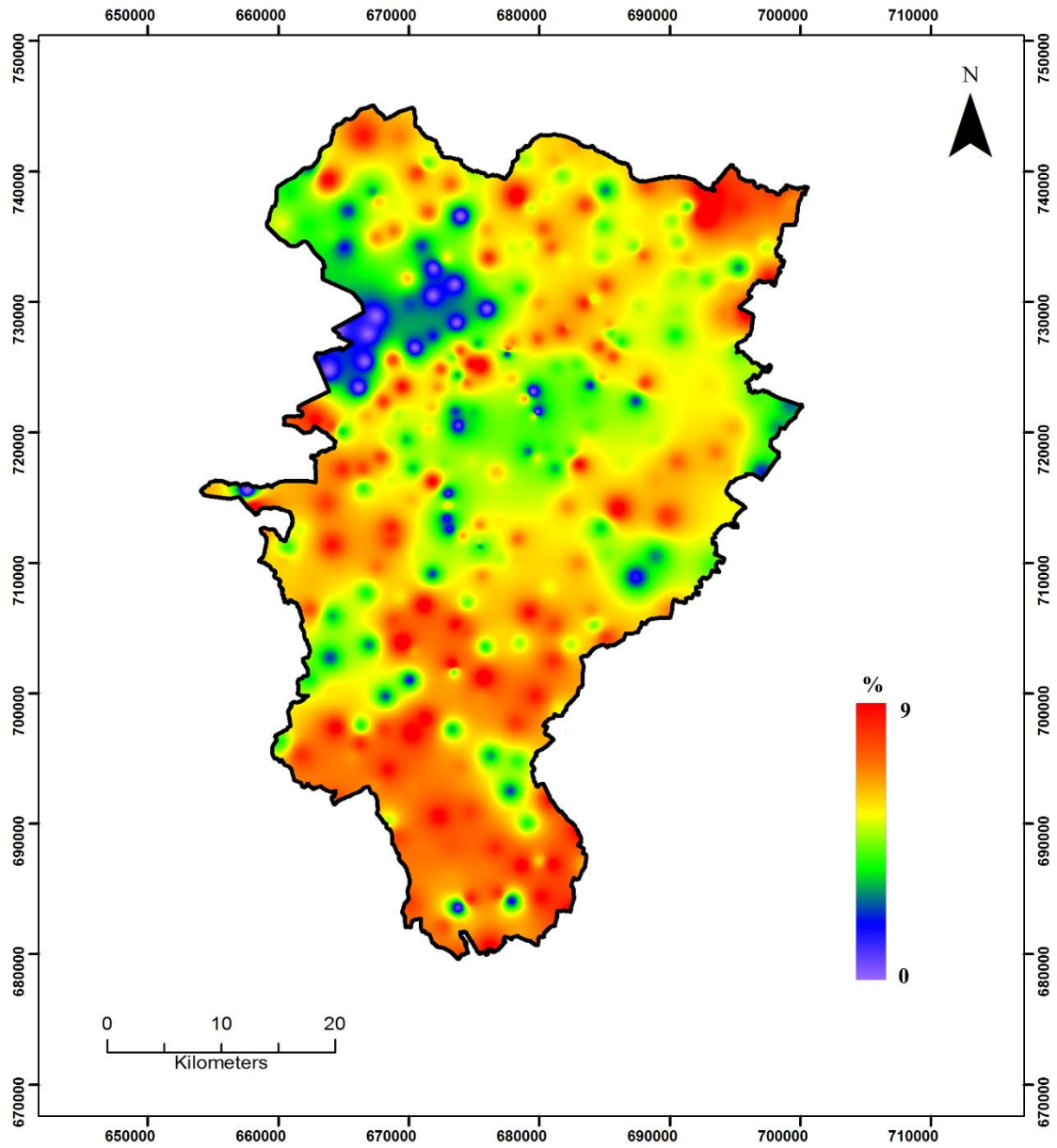


Figure 4.7: $\chi^2 d\%$ map of Kildare.

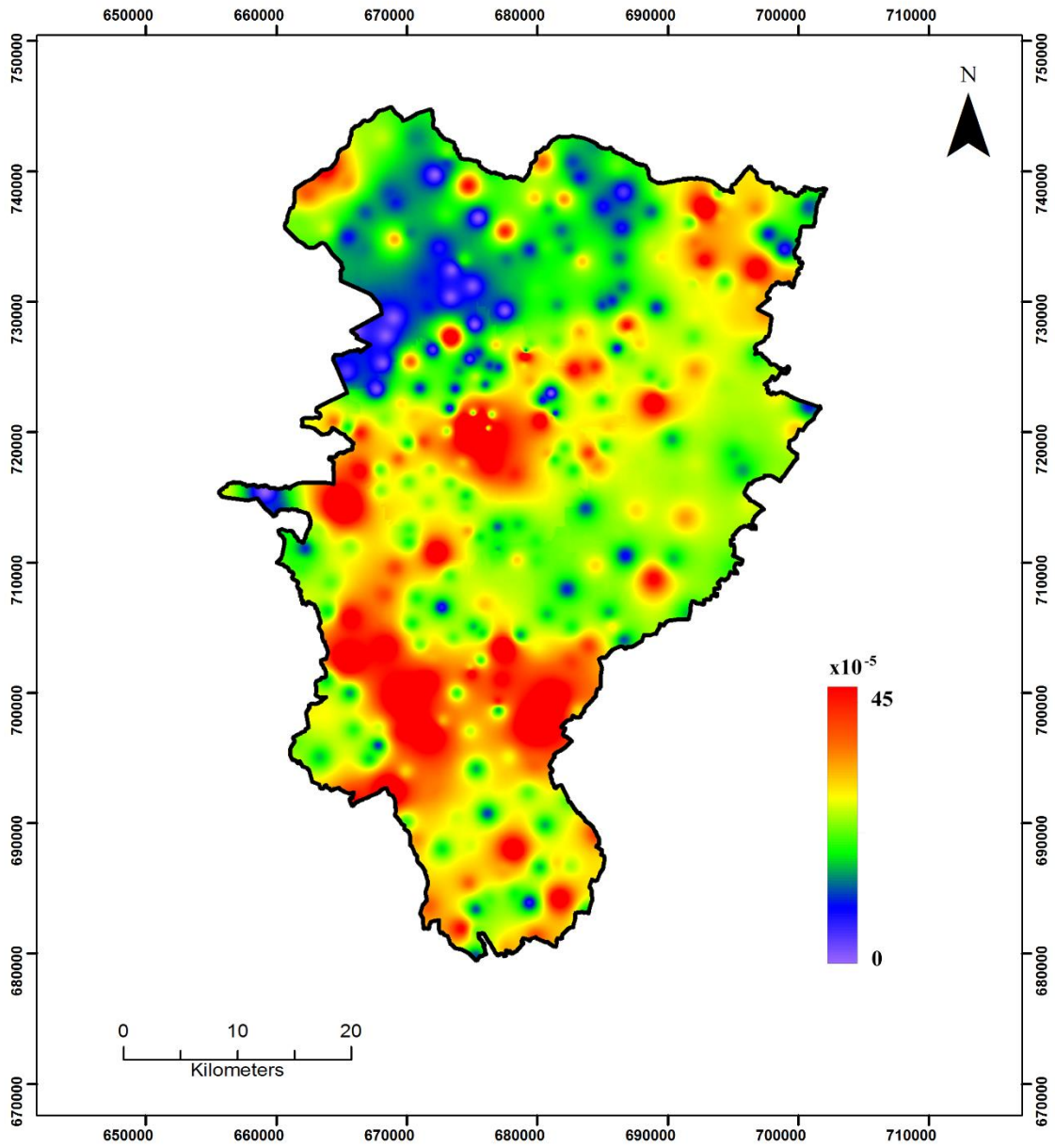


Figure 4.8: Magnetic susceptibility map of Kildare (K).

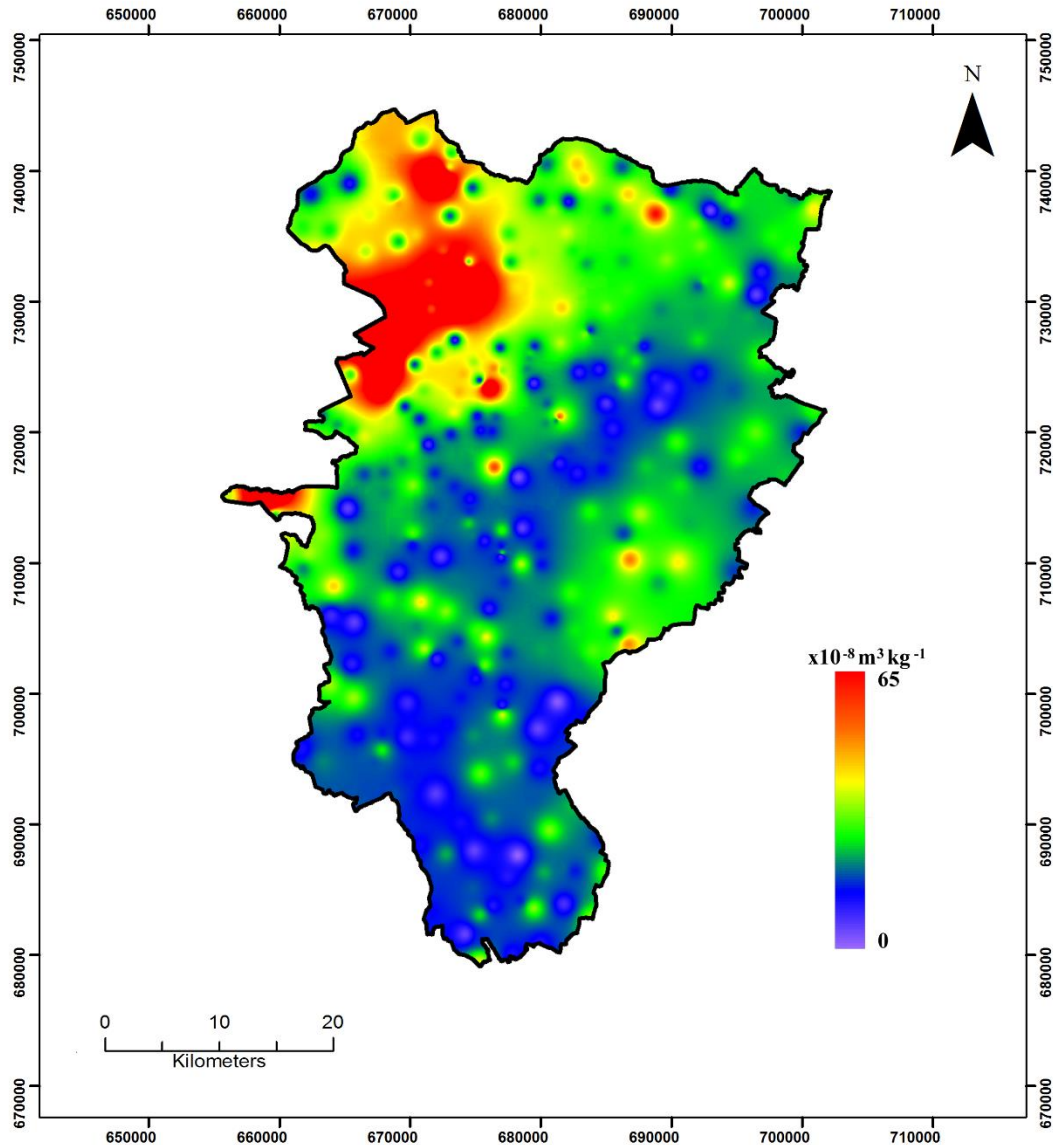


Figure 4.9: Relative standard deviation (χ_{lf}) for Kildare.

4.5 K-T data analysis

The results of measuring the variation of susceptibility with temperature (K-T) are presented in graphical format in this section. 100 sites (33% of the total) were analysed. The sites were chosen to represent the various soils that are present in Kildare and ensured a good spatial distribution. A range of K-T characteristics were employed in this comparative study in order to determine further information on the properties of the magnetic grains most especially whether they were superparamagnetic (SP), multidomain (MD) or single domain (SD) in character.

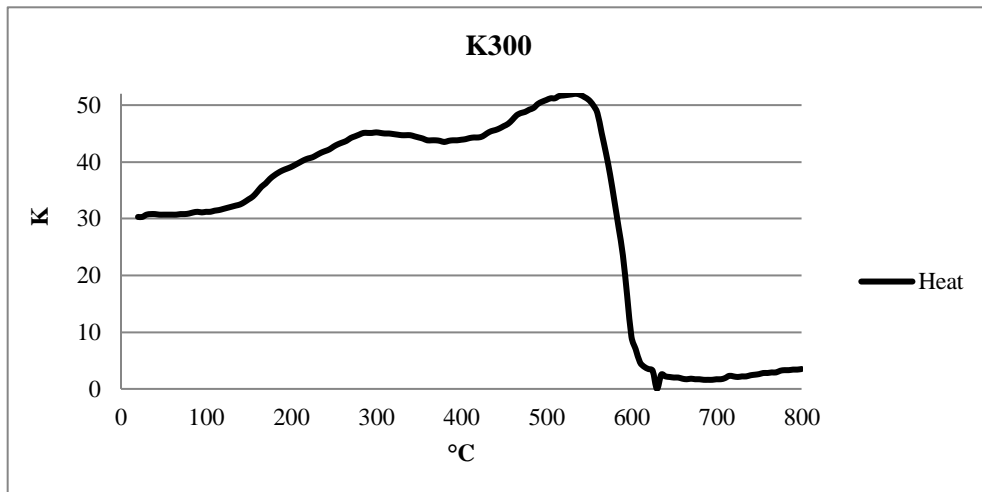
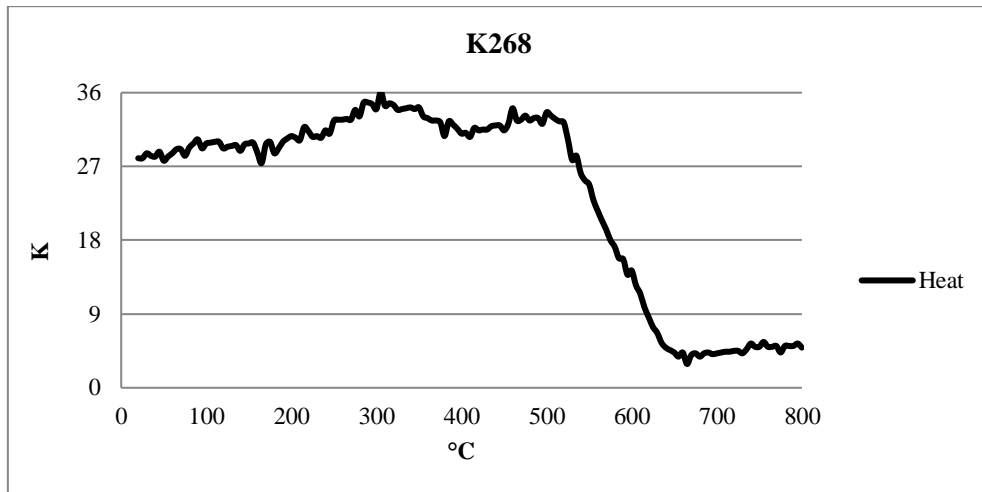
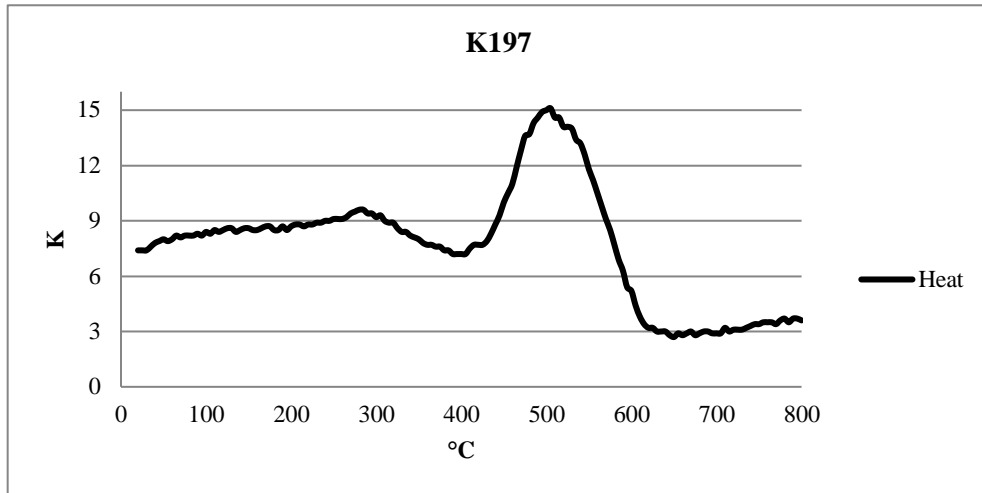


Fig 4.10: Typical K-T graphs for Kildare.

The general shape of the heating curve graph

It is possible to differentiate between soils which contain titanium poor titanomagnetites and titanium rich Fe-Ti oxides. The former yields K-T graphs in which the susceptibility remains constant or increases gradually between 20°C and 500°C whereas the shape of the latter is totally different. Titanium rich Fe-Ti oxides produce graphs in which the susceptibility increases between 20-120°C and then plummets sharply to about 33% of its room temperature value (Chadima, 2016).

The slope of the Curie temperature decrease, which occurs at about 500°C, can be relatively shallow (wide) or steep (narrow). Steep slope is believed to be indicative of a small range of mineral types/sizes whereas a wide slope indicates a mixture of mineral types/sizes. The observed Curie temperatures can be affected by a combination of magnetic mineral types, compositions, sizes and shapes. The slope itself (in detail) may not be a single line but formed of segments possibly reflecting different mineral arrangements. Chadima (2016), for example, shows that the slope is vertical for pyrrhotite when it is in a monoclinic form (ferrimagnetic) with a Curie temperature of 325°C but the slope is formed of two steps when the mineral assemblage is composed of a mixture of monoclinic and hexagonal pyrrhotite. The K-T graph changes its slope at different temperatures depending on whether existing minerals have been converted to new minerals with a susceptibility that is different from the original.

The general shape of the cooling curve graph

The cooling curve tends to have fewer 'characteristics' than the heating one. As each sample begins the cooling cycle in the same paramagnetic state at 800°C and new magnetite is formed at temperatures lower than the 585°C Curie point, one would intuitively expect them all to be similar. However, the cooling slope and temperature of maximum susceptibility may vary, also whether the curve is horizontal below the Curie temperature or has a slight gradient. The relative size of the cooling and heating curves is important. Very infrequently the heating curve is greater or a similar size to the cooling one indicating that magnetite is being dissolved in a less magnetic host mineral. In addition, the cooling curve gradient may begin to increase at a lower or higher

temperature than the heating curve gradient. Various authors have attempted to explain the mechanism for the growth of magnetite minerals from other minerals as cooling proceeds. Chadima (2016) states the high K values on cooling curves are due to ‘complex alteration’. Hrouda et al (2003) states that the formation of new magnetite ‘cannot be ascribed to one particular alteration process’. Lu et al (2008) states there is ‘thermally induced conversion from iron containing silicates/clay minerals to new magnetite’.

The presence/absence shape of the Hopkinson Peak

A substantial number of the Kildare samples exhibit a Hopkinson peak, with different characteristics. Vahle and Contny (2005) give a good explanation on susceptibility controls at temperatures $< T_C$ (Curie temperature) which depend on the ratio of $MS(T)/K(T)$, where $MS(T)$ is the spontaneous magnetization and $K(T)$ is the magnetocrystalline anisotropy. Both parameters decrease with increasing temperature. At low temperatures, they cancel out and magnetic susceptibility remains nearly constant. If $K(T)$ decreases faster than $MS(T)$, the thermal fluctuation at T close to T_C causes magnetic susceptibility to increase, producing the Hopkinson peak.

This effect is common for natural magnetite (Thompson et al., 1975). Studies of synthetic minerals showed that a sharp Hopkinson peak indicate a narrow particle size distribution and the concept of relative peak height (RPH) – the height of the peak relative to minimum susceptibility (pre-heating) was presented by Mahmood and Bsoul, (2012). For most Kildare soils with a Hopkinson peak, RPH was in the 1.7-3 range. In virtually all cases in this study this minimum susceptibility was the room temperature susceptibility. The Hopkinson effect is enhanced with decreased grain size, though SP grains do not exhibit the Hopkinson effect. It is most pronounced for SD grains and considerably more muted for MD grain size (Dunlop and Ozdemir, 1997). T_{max} (the temperature at which the highest susceptibility is obtained) is lower, the finer the magnetic grain size (Liu et al., 2005).

Three typical K-T curves for the Kildare soils are illustrated in Figure 4.10. K197 has a very prominent Hopkinson peak which is absent from the other two. Approximately 80% of the soils in Kildare possess a Hopkinson peak. From its $\chi_{fd}\%$ value, K197 contains c.

50% SP grains, and because of its Hopkinson peak it also contains a large percentage of SD minerals, the remainder being MD in character.

Neither of the other 2 sites has a Hopkinson peak. K300 is the most magnetic site in the study area and has less than 5% SP grains. Its lack of a Hopkinson peak indicates few SD grains thus it is formed of mainly large MD grains. K268, on the other hand has about 60% SP and the rest would be MD. Other subtle differences can be discerned. The gradient of the slope for K300 is steeper than that for K268 and for the latter the susceptibility values start to decrease at a slightly lower temperature and become paramagnetic at a higher temperature. It is possible that the MD magnetic grains in K300 are approximately the same size, as one would expect a steep curve as they would all reach T_C at approximately the same time. 100 K-T heating and cooling curves are displayed in the supplementary material CD (File 4.2s.docx in K-T folder). Many cooling curves follow a similar trend. As temperature decreases there is a marked increase in susceptibility as new magnetite grows, which levels off around 300°C. For some samples, the cooling curve starts to increase at a slightly higher temperature than the minimum on the heating curve - see K17 and K18. The susceptibility for the cooling curve is often 5-15 times greater than the heating curve though for site K268, both curves are similar, note also the shallower cooling curve slope which starts to rise at a lower temperature. Neither K138 or K279 (non-Hopkinson peak soils) exhibit a susceptibility cooling curve which is considerably greater than the heating one, unlike the other soils. The decrease in susceptibility over a very wide temperature range from 180-580°C for K170 is unlike all other sites. It may contain hexagonal pyrrhotite (T_C of 270°C) and a range of other magnetic minerals of different sizes.

4.6 Measurement of remanent magnetic declination and inclination angles

Earlier it was stated that in order to confidently use the results of the remanent magnetism measurements it was necessary to ensure that they were due to natural processes and not affected by anthropogenic activity. A determination has to be made that when declination and inclination values are outside a specified range, they are not caused by natural processes and hence the results are unreliable. Although the present declination for the study area is 356°, geomagnetic secular variation i.e. the very rapid variation with time

of the direction (and magnitude) of the geomagnetic field has to be considered. This secular variation is due to high frequency non-dipole changes. Declination during the course of the 20th century varied by about 30° for Ireland and for the period 1600-1950 it was between 335°- 5° in England (Malin and Bullard, 1981). In Oregon (another northern hemisphere location), detailed measurements show that for the last 10,000 years the declination range was 348°- 20°. Similarly, the declination in Bulgaria was in the 327°-23° range over the last 8,000 years (Kovacheva et al.,1998) and 350°-42° in England over the last 3000 years (English Heritage, 2008). Allowing for a margin of error, declination values outside the 315°-55°range would be expected to have been influenced by non-natural processes. Inclination variations tend to cover a smaller range than declination. For England between 1600-1950, it ranged from 67°-75°, between 56°-73° in the last 3000 years, between 47°-72° for the last 8,000 years in Bulgaria and for the last 10,000 years in Oregon 40°-70°. Inclinations of <30° indicate unreliable results. 260 orientated samples (10 each at 26 Kildare sites) were analysed and the statistical results and lower area stereoplots for 4 of these are shown below, Figure 4.11. Other stereoplot examples and their statistical characteristics can be seen in the supplementary CD material (File 4.3s.docx, folder stereoplots).

K5

Normal Polarity Directions: Declination= 354.6°, Inclination= 72.2°, Alpha (95%) =10.8°, k= 18.99, n= 10, R= 9.5734, R-bar= 0.9573, Spherical Variance= 0.0427, csd(37%)= 18.59°, csd(5%)= 32.13° ,Rayleigh Test: Uniformity rejected at 99% probability Fisher Model: fit not acceptable (rejected at 95% probability).

K81

Normal Polarity Directions: Declination= 334.4°, Inclination= 68.8°, Alpha(95%)= 39.9°, k= 2.90, n= 9, R= 5.9503, R-bar= 0.6611, Spherical Variance= 0.3389, csd(37%)= 47.58°, csd(5%)= 82.23° Rayleigh Test: Uniformity rejected at 99% probability Fisher Model: fit acceptable (95% probability).

K220

Normal Polarity Directions: Declination= 343.3°, Inclination= 72.2°, Alpha (95%)= 5.1°, k= 91.55, n= 9, R= 8.9223, R-bar= 0.9914, Spherical Variance= 0.0086, csd(37%)= 8.47°, csd(5%)= 14.63° Rayleigh Test: Uniformity rejected at 99% probability Fisher Model: fit acceptable (95% probability).

K143

Normal Polarity Directions: Declination= 338.7°, Inclination= 71.0°, Alpha (95%)= 10.6°, k= 19.62, n= 10, R= 9.5872, R-bar= 0.9587, Spherical Variance= 0.0413, csd(37%)= 18.28°, csd(5%)= 31.60° Rayleigh Test: Uniformity rejected at 99% probability Fisher Model: fit acceptable (95% probability).

The Fisher mean direction for K5 is similar to today's current position. A relatively high 'k' concentration factor of 18.99 shows a low scatter (supported by the R-bar value of 0.9573 exhibiting a compact grouping), Figure 4.11. However, K5 contains 2 points where the declinations are outside the expected range for undisturbed ground (declinations of 231.6° and 99.7°). The stereoplot for K81 is much more scattered than that of K5 even though the normal polarity directions are reasonably close. The stereoplot shows 2 data points having declinations (61.7° and 72.7°) outside the expected range indicating some disturbance at the site. Note also the much lower 'k' factor and lower R-bar. 5 points have declinations outside the 315°-55° range and one point (shown as open triangle) has a negative inclination (-5.9°) which would be expected for a soil which formed just south of the equator, if it developed naturally with no disturbance. One point has a declination of 267.3° and an inclination of 14.9°, both of which are outside expected normal ranges.

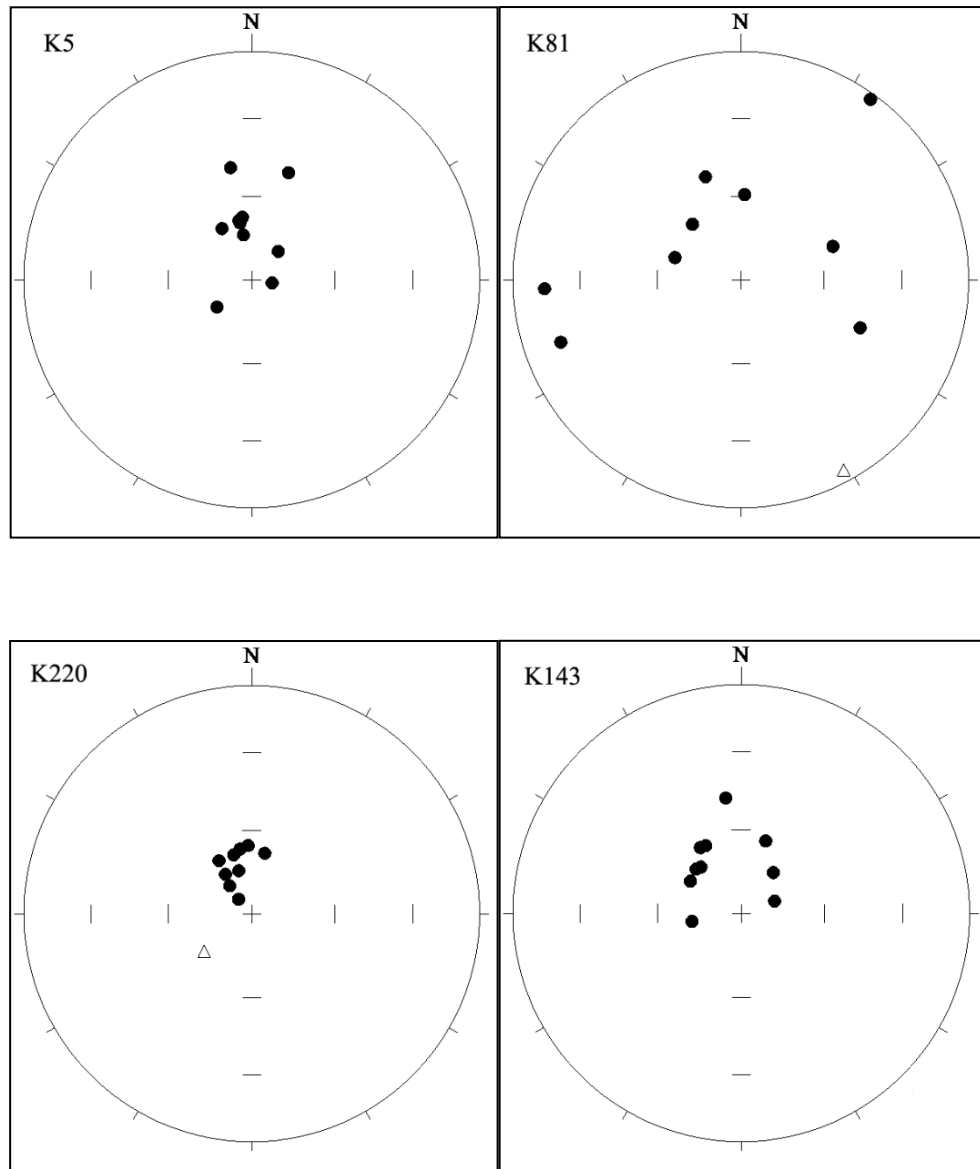


Figure 4.11: Sample Stereoplots.

K220 has a much tighter grouping than K5 or K81 (very high 'k' and R-bar factors). Note these have been calculated on the normal polarity data, Figure 4.11. There is evidence of disturbance at this site as one of the data points has a negative inclination (open triangle symbol). All data points for K143 have positive inclinations within the expected range but 3 are outside the declination range and grouping is quite weak. However, the scatter is much greater for K209 with even the average normal polarity declination being outside the undisturbed range. Both R-bar and 'k' are low. The soil at site K150 is disturbed and most of the measured inclinations are negative (reverse

polarity). It is possible to calculate the average normal and reverse polarity vector directions but the results are meaningless. Other sites such as K26 and K2 have predominantly positive inclinations but the stereoplots show, they are widely scattered and display no evidence of clustering, File 4.3s.docx. Some sites yield inclinations where negative polarities occur predominantly (K36, K221, K189, K89) or exclusively (K16). Site K1 appears to be undisturbed, it has a normal polarity declination of 0.6° and an inclination of 71.8° , and is tightly clustered $k = 101.05$, $R\text{-bar} = 0.9920$. CSD (37%) and CSD (5%) (which are the radii of the cones which contains 63% and 95% of the data respectively) are very low for K1 compared with other sites.

43% of the inclination angles measured in this study yielded negative polarities and in all likelihood were as a result of the soil being turned over by ploughing. A further 8% were positive but less than 30° . Other samples had declinations which also indicated disturbance. Only 1 out of 26 sites (K1, which represents <4% of the sites investigated) had 10 samples which appear to be non-disturbed. The results discussed here exhibit no geographical or soil distribution pattern. The conclusion drawn here is that it is not possible to use directional declination and inclination data obtained from the near surface as a soil discriminator in Kildare because of the widespread human interference in the top soil layer which makes the results of such a survey unreliable.

4.7 Statistical characteristics of the magnetic parameters of individual Kildare soils

The statistical analysis of magnetic parameters in earlier sections applied to the bulk data. Analysis was also carried out on individual soils for comparative purposes. The lowest χ/f for the main Kildare soils (DPDM) ranges from $3.68 - 180.06 \times 10^{-8} \text{ m}^3\text{kg}^{-1}$ though 50% of the data are within the 8.88 to $27.91 \times 10^{-8} \text{ m}^3\text{kg}^{-1}$ range and its mean is $16.62 \times 10^{-8} \text{ m}^3\text{kg}^{-1}$, the lowest for any Kildare soil (except peat), Table 4.4. Such poorly drained soils tend to yield reducing conditions which tend to limit the growth of magnetic iron oxides. As reported in Chapter 3, gleys in Austria are c. $10\text{-}15 \times 10^{-8} \text{ m}^3\text{kg}^{-1}$ (Hanesch and Scholger, 2005). Alluvium and DWDM soils have a similar mean though the latter is slightly higher ($28.7 \times 10^{-8} \text{ m}^3\text{kg}^{-1}$). The highest average χ/f is associated with the SWDM soil ($40.93 \times 10^{-8} \text{ m}^3\text{kg}^{-1}$) though its interquartile range is quite low. The highest

χ_{lf} in the study area ($604.72 \times 10^{-8} \text{ m}^3\text{kg}^{-1}$ for K300) is a SWDM soil. The frequency dependent magnetic susceptibility is very similar for all soils (except peat where it is zero) averaging around 5.7%. The highest $\chi_{fd}\%$ is 5.94, for Alluvium. The Shapiro-Wilk test shows that the χ_{lf} values deviate significantly from a normal distribution.

Alluv	K	χ_{lf}	χ_{hf}	$\chi_{fd}\%$
Mean	22.42	18.67	17.58	5.94
Median	19.50	13.46	12.98	5.59
Standard Deviation (SD)	12.56	13.45	12.66	2.59
Skewness	1.12	1.72	1.67	1.05
Kurtosis	1.01	2.86	2.53	1.53
Shapiro-Wilk (W)	0.89	0.8	0.8	0.92
Minimum	5.68	5.45	5.05	2.15
1st Quartile	15.80	9.86	9.47	4.18
2nd Quartile	19.51	13.46	12.99	5.60
3rd Quartile	25.59	22.37	20.83	7.38
Maximum	53.175	58.24	54.04	12.95
DWDM				
DWDM	K	χ_{lf}	χ_{hf}	$\chi_{fd}\%$
Mean	27.26	28.70	27.02	5.83
Median	24.64	25.54	23.62	6.02
Standard Deviation (SD)	14.23	17.68	16.79	2.29
Skewness	1.38	1.21	1.26	-0.02
Kurtosis	2.83	1.58	1.76	-0.89
Shapiro-Wilk (W)	0.9	0.9	0.89	0.97
Minimum	6.58	5.08	4.98	0.53
1st Quartile	16.88	14.51	13.84	3.77
2nd Quartile	24.62	25.54	23.59	6.01
3rd Quartile	33.69	36.13	33.47	7.63
Maximum	85.22	93.80	90.82	10.72

DPDM	K	χ^2_f	χ^2_{hf}	$\chi^2_{fd}\%$
Mean	15.41	16.62	15.88	5.54
Median	19.25	14.97	14.02	5.25
Standard Deviation (SD)	16.25	25.14	23.53	2.32
Skewness	2.31	4.00	3.84	0.22
Kurtosis	5.67	19.43	17.64	-0.50
Shapiro-Wilk (W)	0.71	0.52	0.53	0.98
Minimum	0.05	3.68	3.38	1.46
1st Quartile	11.33	8.88	8.21	3.67
2nd Quartile	19.25	14.97	14.02	5.25
3rd Quartile	28.97	27.91	26.18	6.59
Maximum	83.02	180.06	162.48	11.79
SWDM				
SWDM	K	χ^2_f	χ^2_{hf}	$\chi^2_{fd}\%$
Mean	33.81	40.93	39.06	5.51
Median	22.53	25.54	23.82	5.97
Standard Deviation (SD)	43.49	76.55	75.84	2.15
Skewness	5.89	6.59	6.73	-0.77
Kurtosis	40.49	48.31	49.92	-0.31
Shapiro-Wilk (W)	0.41	0.34	0.33	0.92
Minimum	10.08	3.99	3.94	0.44
1st Quartile	17.67	14.07	13.34	4.51
2nd Quartile	22.53	25.54	23.83	5.97
3rd Quartile	32.90	38.12	36.24	7.36
Maximum	340.92	604.72	602.03	8.54

Table 4.4: Statistical data for main Kildare soils.

4.8 Characteristics of the magnetic parameters of grain size fractions for individual soils

4.8.1 Statistical characteristics

Earlier magnetic sections have considered bulk properties of all the soils in Kildare or the bulk magnetic properties of individual soils. However, particle size analysis was also carried out and in this section, the magnetic statistics of individual fractions are determined, Table 4.5:

<i>xf</i>	>2000 µm	2000- 900 µm	900-600 µm	600-250 µm	250-125 µm	125-63 µm	<63 µm
Min	2.3	2.3	2.1	2.8	2.8	3.1	3.4
Q1	11.7	14.5	14.2	12.4	12.2	11.5	12.7
Q2	20.9	24.9	24.2	22.3	21.2	21.9	23.2
Q3	40.1	41.0	38.7	33.5	34.2	34.0	37.4
Max	400.6	178.2	189.1	180.3	159.2	182.6	196.0
Max with K300	929.2	480.8	354.3	239.2	225.8	307.4	307.4
Mean	36.9	32.3	30.9	28.3	28	28.5	30.5
Median	20.9	24.9	24.2	22.3	21.1	21.9	23.2
SD	49	27.2	26.4	24.6	24.3	25.6	28.2
Skew	3.6	2.4	2.8	2.6	2.4	2.6	2.7
Kurtosis	17.4	8.2	10.6	9.2	7.4	9.2	9.6
W	0.61	0.79	0.75	0.75	0.77	0.74	0.72
<i>xfd%</i>	>2000 µm	2000- 900 µm	900-600 µm	600-250 µm	250-125 µm	125-63 µm	<63 µm
Min	0.0	0.0	0.0	0.0	0.0	0.0	0.0

Q1	2.9	3.2	3.8	3.5	4.0	3.8	3.4
Q2	5.1	5.4	5.7	6.1	6.2	6.0	6.2
Q3	8.0	7.1	7.5	7.9	8.1	8.0	8.3
Max	13.9	14.1	13.3	14.0	13.9	12.9	12.7
Max with K300	13.9	14.1	13.3	14.0	13.9	12.9	12.7
Mean	5.3	5.4	5.6	5.8	5.9	5.9	5.9
Median	5.1	5.4	5.7	6.1	6.2	6	6.2
SD	3.2	2.9	2.6	2.9	2.8	2.8	3
Skew	0.4	0.4	0.04	0.05	-0.01	-0.06	-0.2
Kurtosis	-0.6	-0.2	-0.3	-0.6	-0.4	-0.6	-0.8
W	0.97	0.98	0.99	0.98	0.99	0.99	0.97

Table 4.5: Individual fractional statistics for Kildare soils (excluding peat).

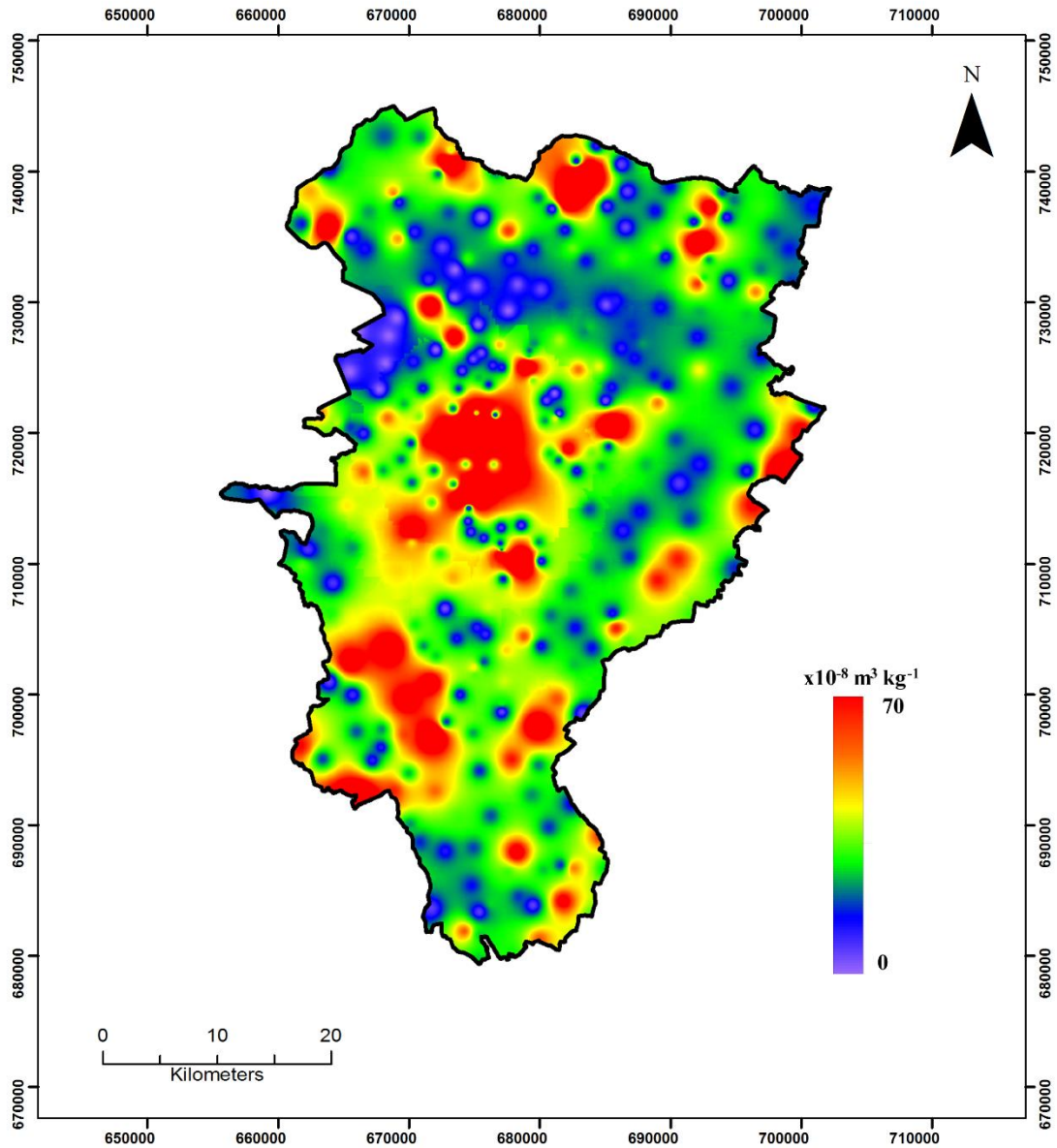
There is a reasonable consistency for some of the fractional susceptibility data. The minimum susceptibility value is similar for all fractions as is the Shapiro-Wilk index (none of the data are normally distributed). The interquartile range (Q1-Q3) is similar for all fractions though the range tends to be slightly lower for the smaller fraction sizes: ($>2000\mu\text{m}$: $11.7\text{-}40.1 \times 10^{-8} \text{ m}^3\text{kg}^{-1}$, $<63\mu\text{m}$: $12.7\text{-}37.4 \times 10^{-8} \text{ m}^3\text{kg}^{-1}$). Skewness is also reasonably similar (slightly higher for largest sieve) and the median is always less than the mean indicating the data are positively (right) skewed, thus the right hand side of histogram is longer than the left side. There is however, a marked difference for the $>2000\mu\text{m}$ sieve for some of the susceptibility statistics. The maximum value is over 100% greater than the values for the other sieves and the standard deviation is much larger (49 as opposed to about 26). As mentioned earlier, a high kurtosis value gives a sharper peak than a normal distribution would for a histogram. Again, the $2000\mu\text{m}$ sieve is significantly higher than other sieve data. The $\chi_{fd}\%$ data are very consistent for all fractions though the interquartile range is largest for the largest sieve size and there is a

general small increase in the mean and median values with decreasing grain size fraction indicating an increase in SP grains.

4.8.2 Spatial variation for individual fractional sizes

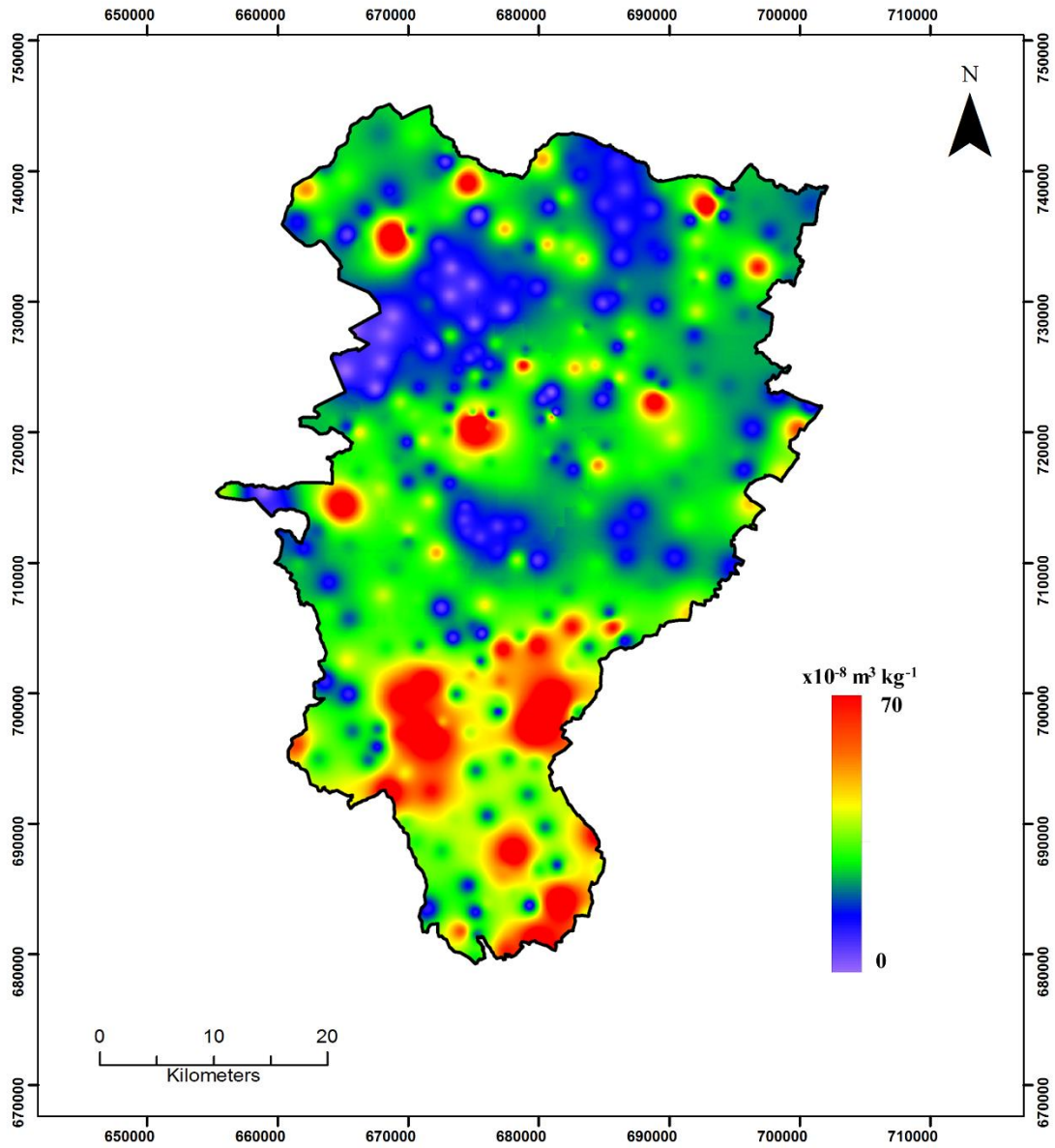
Figure 4.6 showed the spatial variation of χ_{lf} , in which the highest values are in red. However, one red part of the map may be due to a very high magnetic susceptibility in one sieve whereas another red region is due to a very high susceptibility in a different sieve fraction. Spatial maps were constructed for the 7 different sieve fractions, two of which are shown in Figure 4.12.

For gridding purposes, a value of 0 was allocated to all peat samples for all fractions. The $>2000\mu\text{m}$ spatial map shows very high magnetic values are associated with a much larger area centred on the Kildare Inlier than any other fraction. The area of high magnetic susceptibility on the $<63\mu\text{m}$ is c. 8.3 km^2 but 76.1 km^2 on the $>2000\mu\text{m}$ map. A very prominent N-S trending low magnetic zone (not associated with peat deposits is present on the small grain size maps but not the larger grain sizes. High value zones on the northern Kildare border are much more prominent on the $>2000\mu\text{m}$ sieve than on the other smaller ones. There is less variation between the fractions in the southern part of the county; however, even here differences are observable. The southwest magnetic high varies in area from 41 km^2 - 52 km^2 - 45.1 km^2 - 29 km^2 - 27.9 km^2 - 31.3 km^2 - 40.5 km^2 from highest to lowest fraction. High susceptibility for the $>2000\mu\text{m}$ fraction for the Kildare Inlier does not have a complementary high $\chi_{fd}\%$. NW Kildare and the southern quarter of the county are associated with high $\chi_{fd}\%$ for the finer sieve fractions, Figure 4.13.



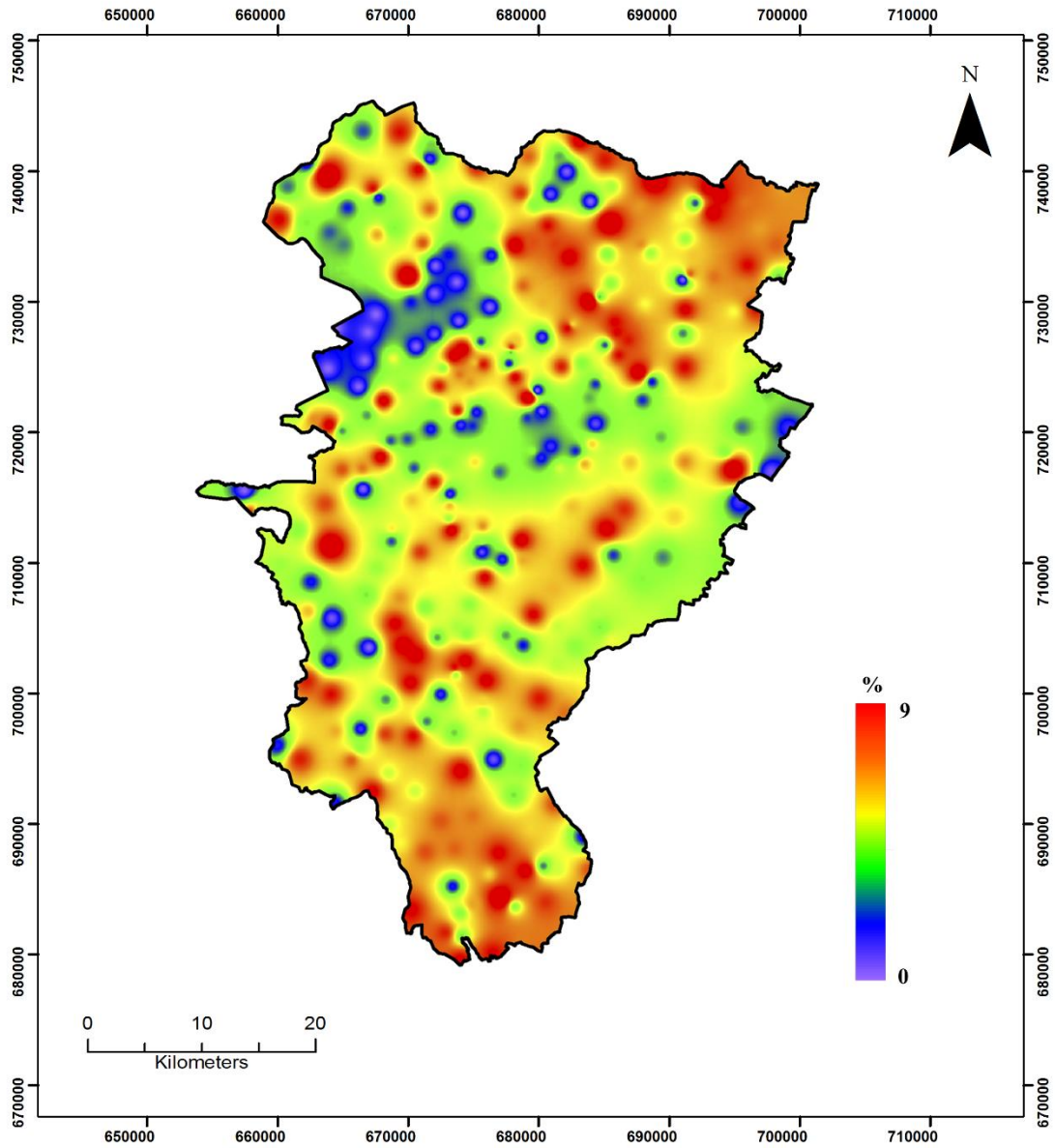
(a)

Figure 4.12: Spatial maps of Kildare showing variation in susceptibility for (a) 2000µm and (b) <63µm fractions.



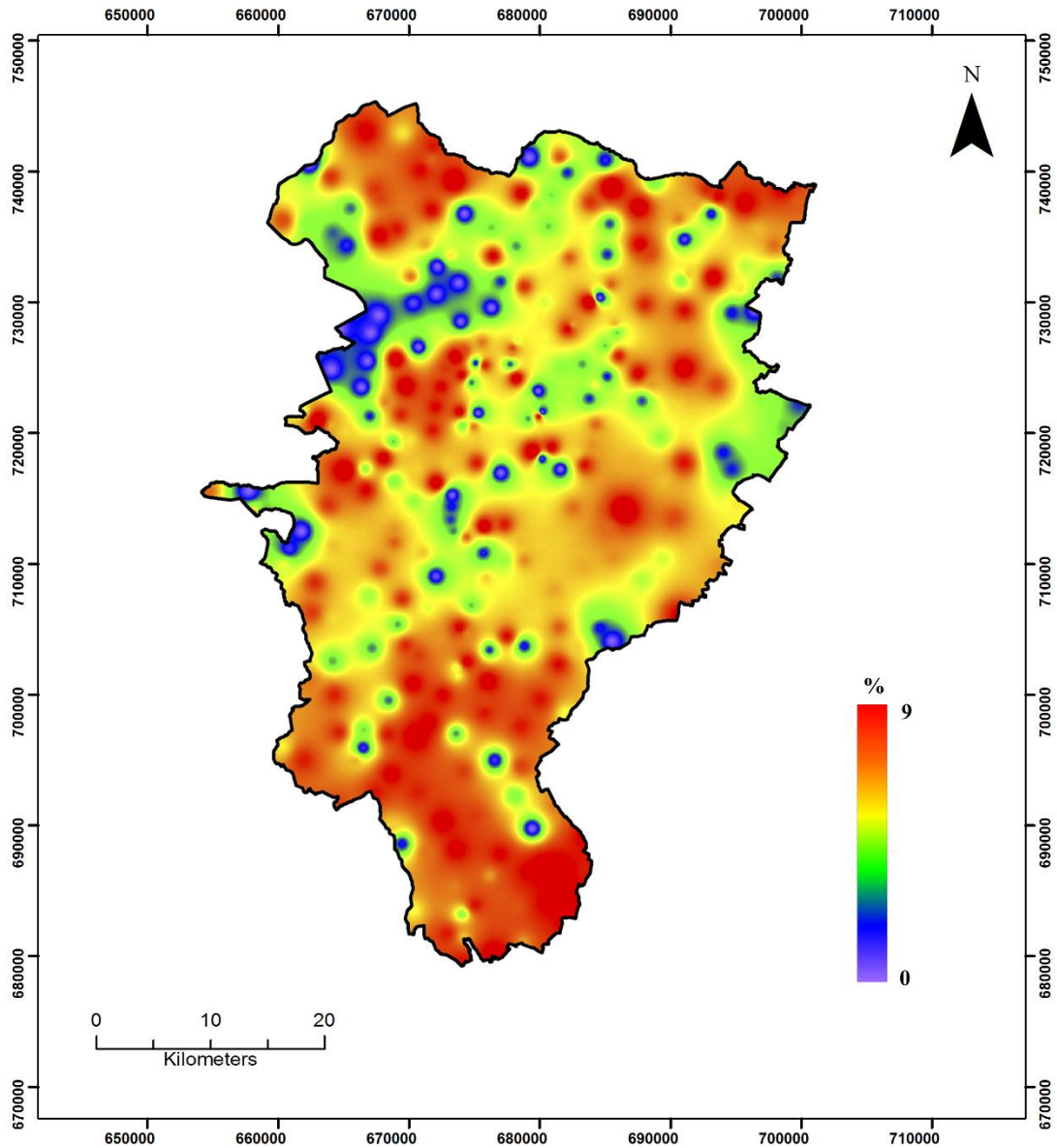
(b)

Figure 4.12: Continued.



(a)

Figure 4.13: Spatial maps of Kildare showing variation in $\chi_{fd}\%$ for (a) 2000 μm and (b) <63 μm fractions.



(b)

Figure 4.13: Continued.

4.8.3 Variation of χ_{lf} and $\chi_{fd}\%$ with particle size

As mentioned in the introduction to this chapter, not all data collected and analysed is presented here. Figure 4.14 shows the variation in susceptibility and percentage frequency dependent susceptibility (χ_{lf} and $\chi_{fd}\%$) for 6 of the 300 Kildare sites. Other examples can be found at File 4.4s.docx in histograms folder on CD. Two aspects of the histograms are immediately obvious. Firstly, the absolute magnetic susceptibility values

can vary greatly. The variation in absolute values is not as extreme for the percentage frequency dependent susceptibility because the range is 0-14%. Secondly, a number of susceptibility distribution patterns can be observed. K5 and K18 display a negative χ_{fd} ramp, (as particle size increases, susceptibility decreases), the opposite of K14. Some soils have a predominant fraction (K34), while others do not (K2). Two conclusions can be drawn from this study: Firstly, it is evident that different fractional sizes can carry different magnetic signals. Secondly, soil types have a range of different χ_{fd} and $\chi_{fd}\%$ patterns. Figure 4.15 shows the χ_{fd} and $\chi_{fd}\%$ distribution patterns for all of Kildare. χ_{fd} varies from $30.5\text{-}36.9 \times 10^{-8} \text{ m}^3\text{kg}^{-1}$ while $\chi_{fd}\%$ increases from 5.3-5.9% as particle size decreases.

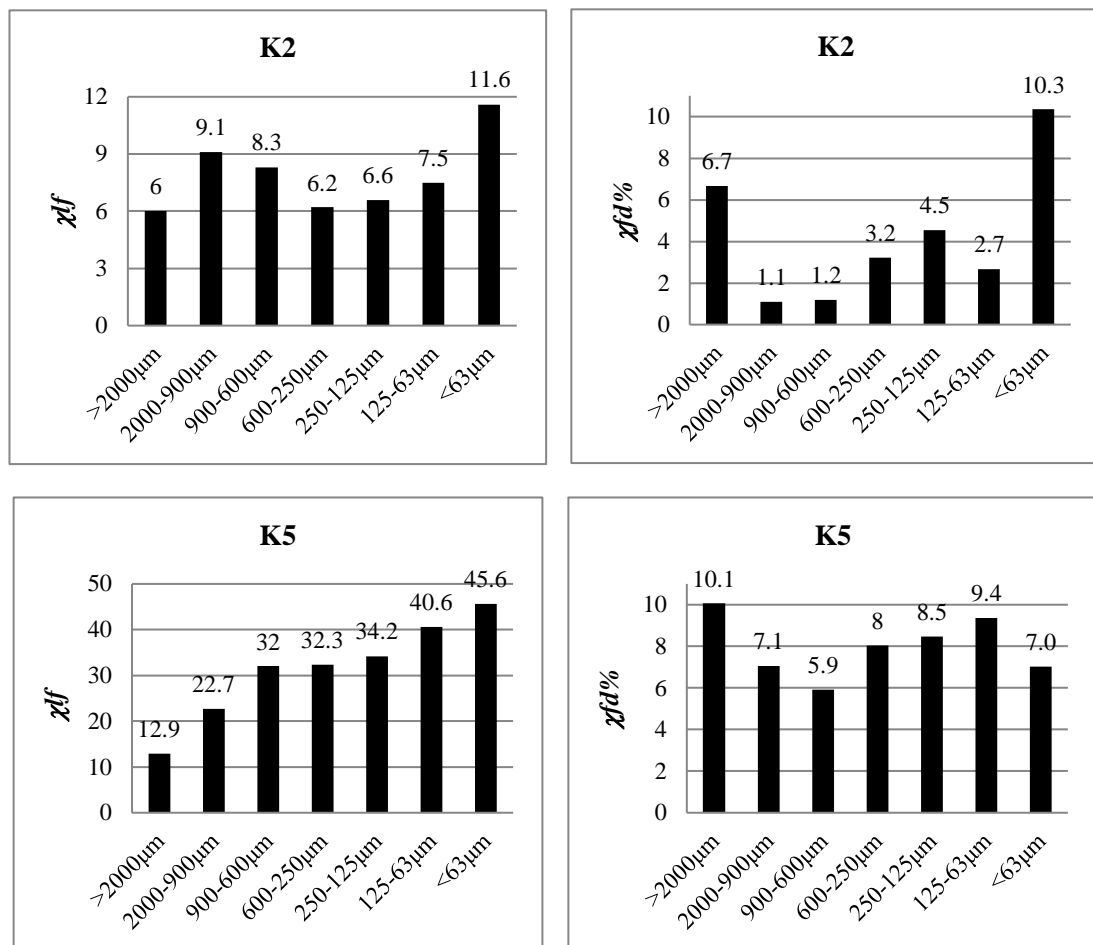


Figure 4.14: Typical χ_{fd} and $\chi_{fd}\%$ histograms for the Kildare soils.

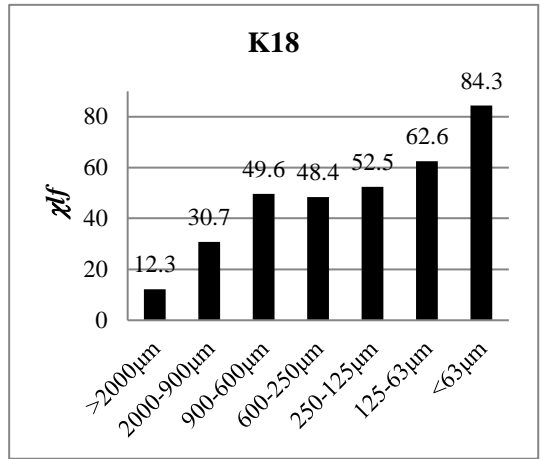
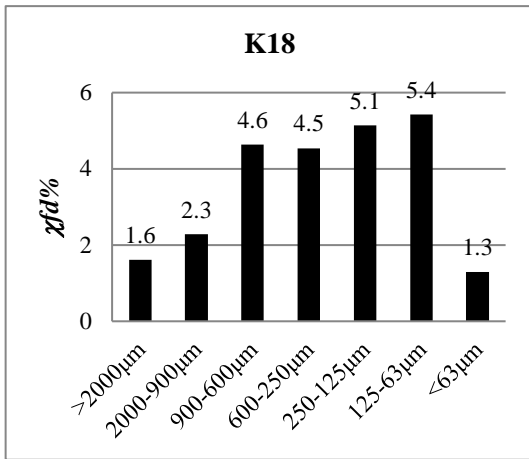
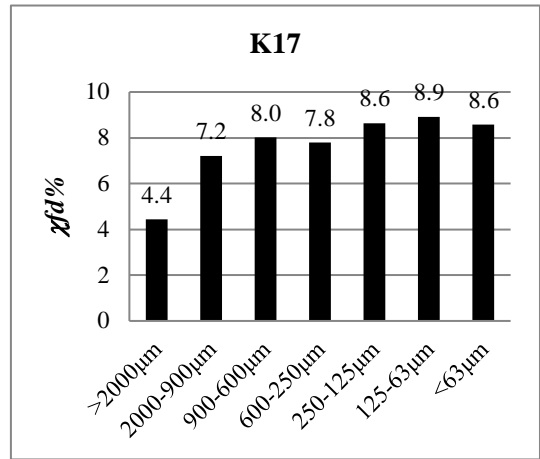
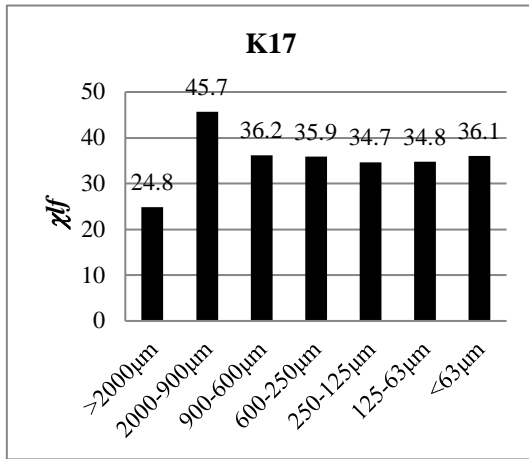
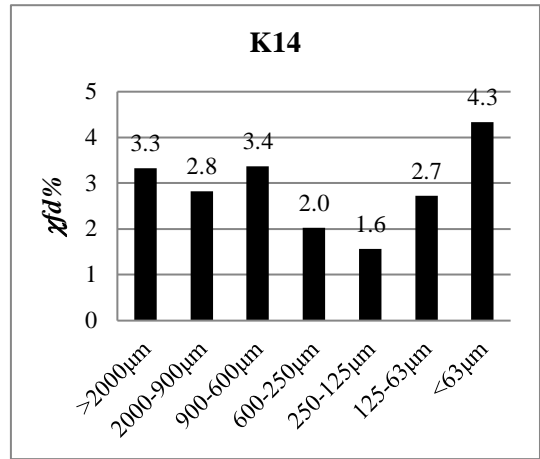
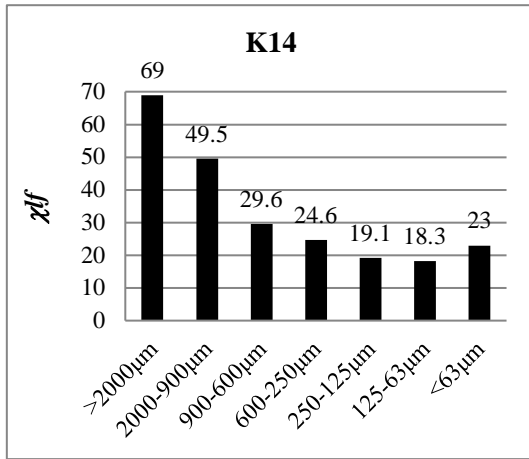
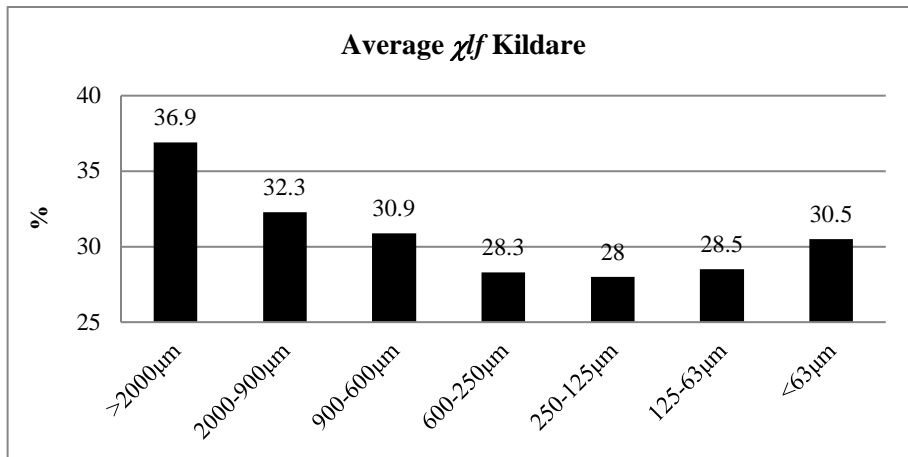
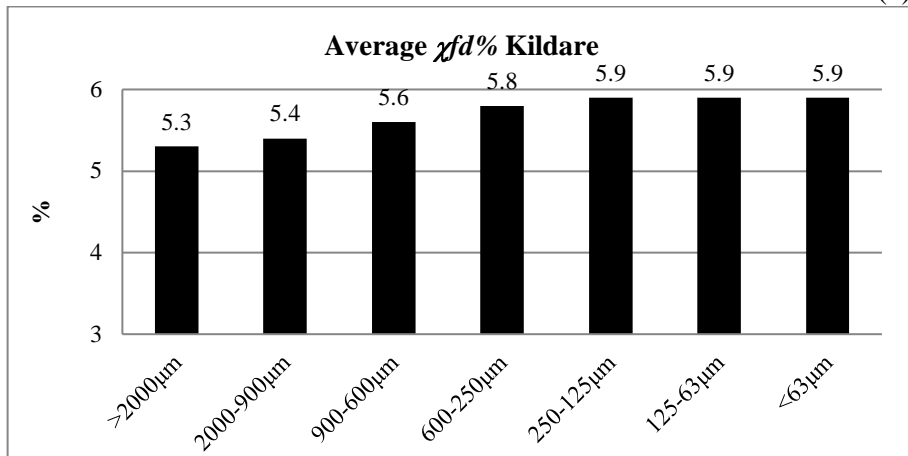


Figure 4.14: Continued.



(a)



(b)

Figure 4.15: Average (a) χ_{lf} and (b) $\chi_{fd}\%$ for Kildare.

4.9 Resistivity data for Co. Kildare

Resistivity data were collected at 28 of the 300 Kildare sites which encompassed a range of soil types and a wide geographical spread, Figure 4.1. The results for each resistivity site are displayed in a standard manner in order to allow direct comparison. The dynamic range scale is the same for all model sections (10-800 ohm-m) and is plotted on a semi-logarithmic scale, similar to other resistivity data. The results are discussed in Chapter 6. Three Wenner-Schlumberger resistivity examples are shown here - see File 4.5s.docx in resistivity data folder for all data which includes:

N-S and W-E Dipole-Dipole resistivity model sections.

N-S and W-E Wenner-Schlumberger resistivity model sections.

N-S and W-E Dipole-Dipole and Wenner-Schlumberger variation of average model resistivity with depth below the surface.

Resistivity sections are shown thus: K2 DD (N-S) which is the north-south Dipole-Dipole resistivity model for site K2. WS refers to Wenner-Schlumberger data and a (W-E) section is one oriented west-east. If the soil profile was made up of horizontal layers of constant thickness and resistivity, then a W-E resistivity section would be similar to a N-S section. A pronounced pattern of very high surface resistivity underlain by a low resistivity zone below which the resistivity increase is evident for K81, Figure 4.16. The average resistivity model profiles confirm this low resistivity 'sandwich' with values of c. 44 ohm-m at 1.5m, 313 ohm-m at the surface and 201 ohm-m at depth. The W-E and N-S model profiles are very similar (Figure 4.19).

The resistivity section for K189 is in marked contrast to that of K81. Resistivity values are low for this peaty site (c. 30-70 ohm-m), most likely due to its high water content and zonation is not very evident. Figure 4.17. There is a significant variation between the W-E average resistivity model profile and the N-S one. There is little change in the average model resistivity with depth, near the surface for the N-S line, it is c. 76 Ohm-m, increasing to 87 Ohm-m at 1.25m then decreasing to 68 Ohm-m at a depth of 2.25m, Figure 4.19. For the E-W average resistivity, there is a significant variation. Near the surface resistivity is relatively high (109 Ohm-m) at mid depth much lower (42 Ohm-m at 1.25m) and then increases greatly at depth (162 Ohm-m at 2.25m). indicating a large degree of heterogeneity. K89 is another site where there is a poor correlation between the N-S and W-E sections, Figure 4.18. The resistivity range is low (mainly 100-200 Ohm-m, shown in green) and the site lacks layering. The average resistivity model profiles show that at depths less than 1.4m, the W-E resistivity values are greater than the N-S ones but the situation is reversed at depths greater than 1.4m, Figure 4.19.

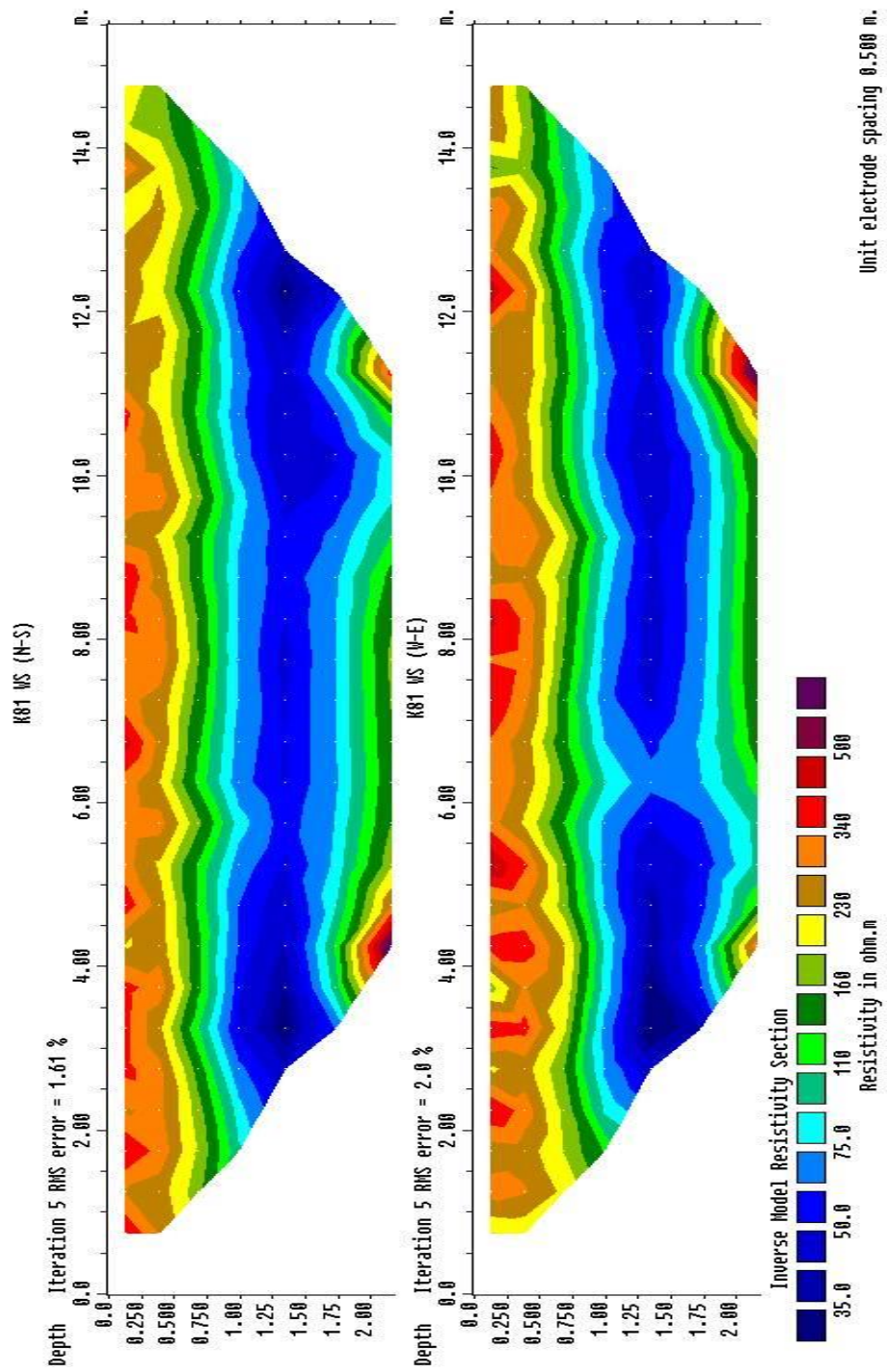


Figure 4.16: Resistivity model for site K81.

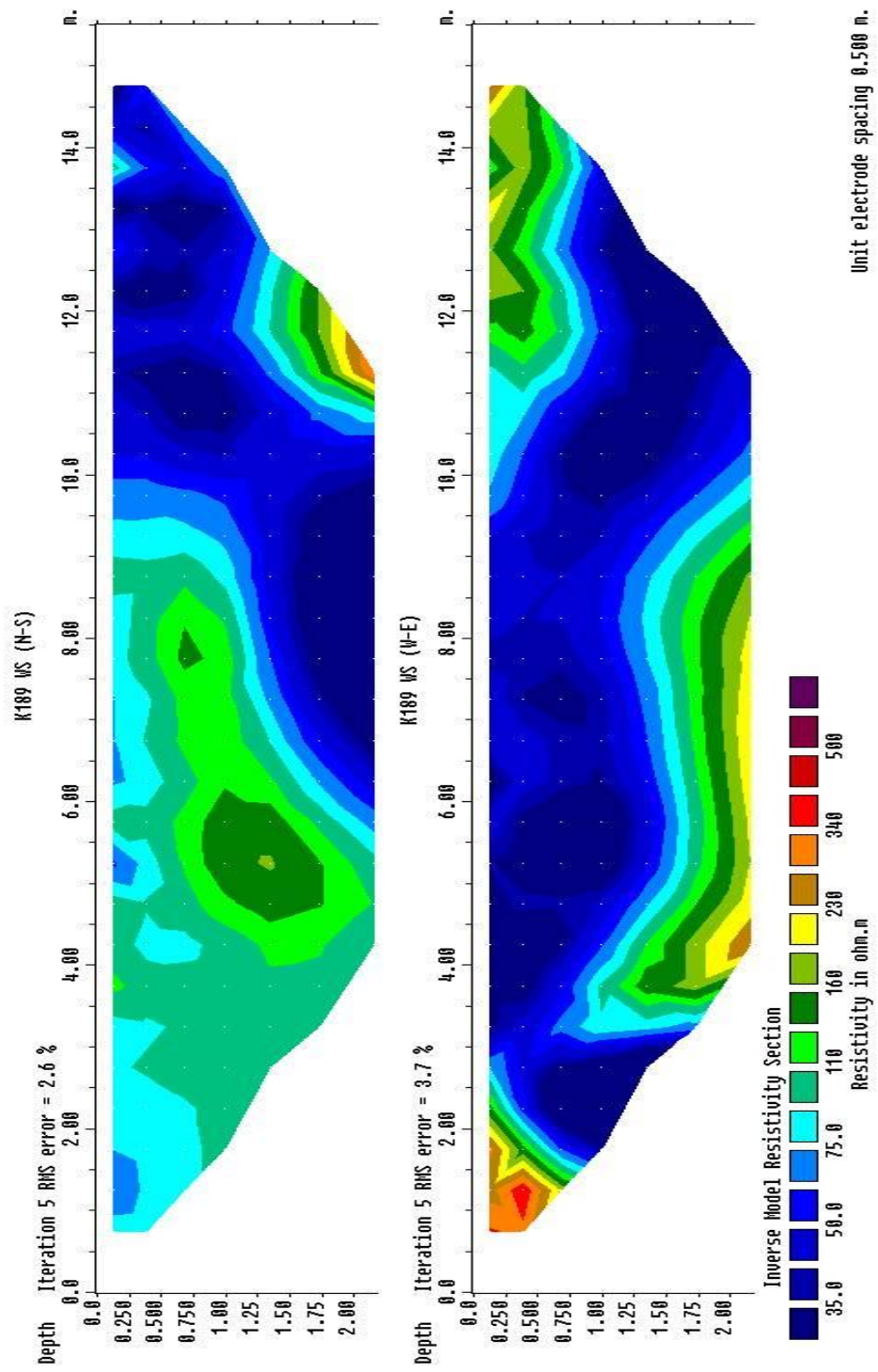


Figure 4.17: Resistivity model for site K189.

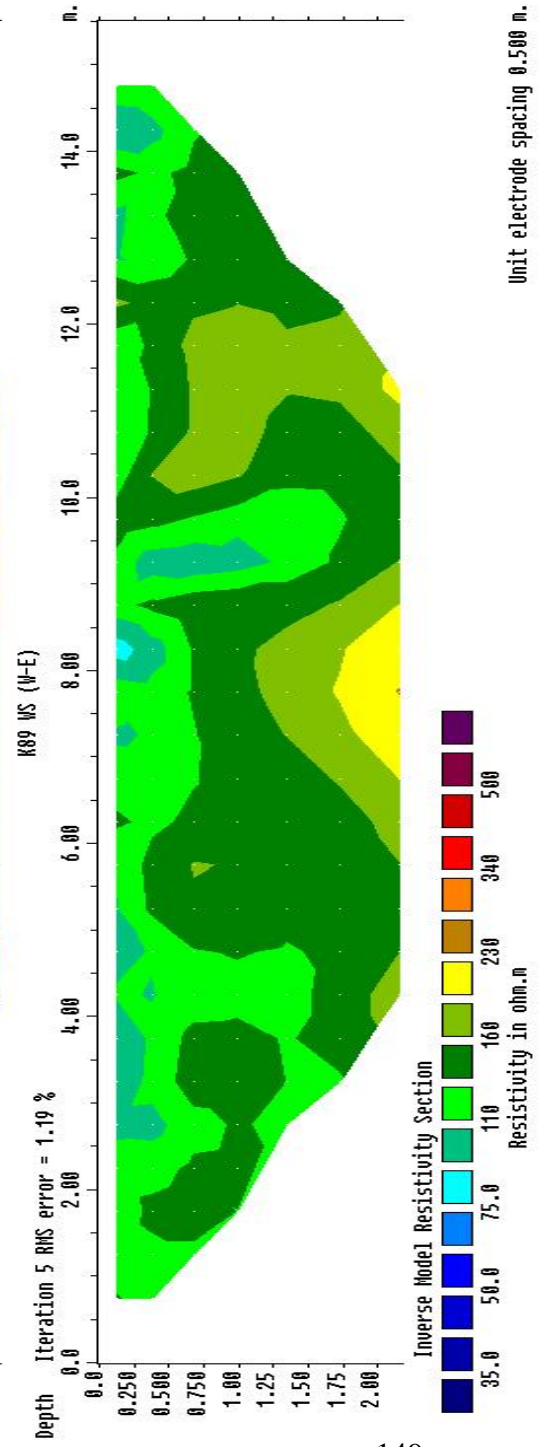
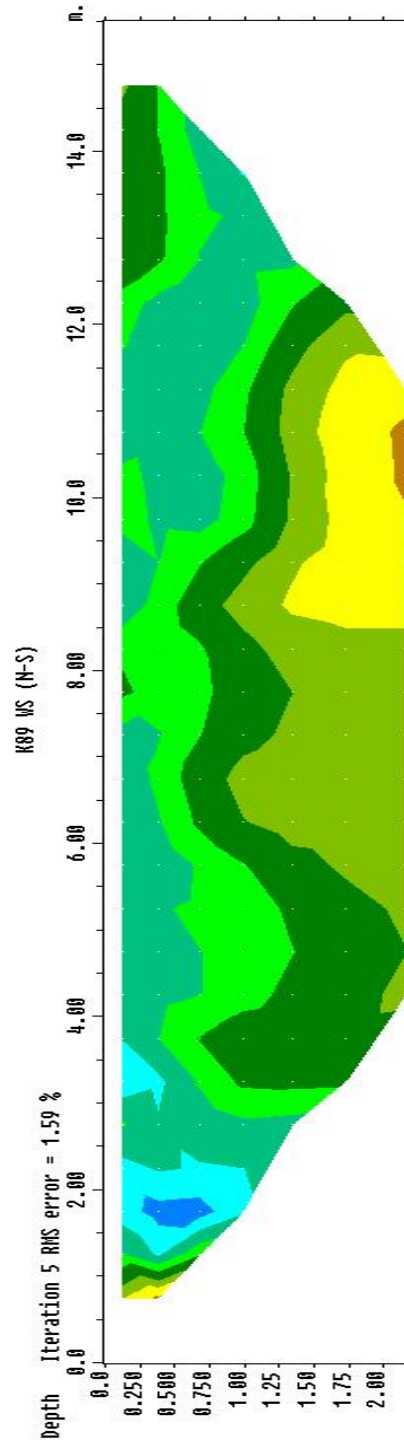


Figure 4.18: Resistivity model for site K89.

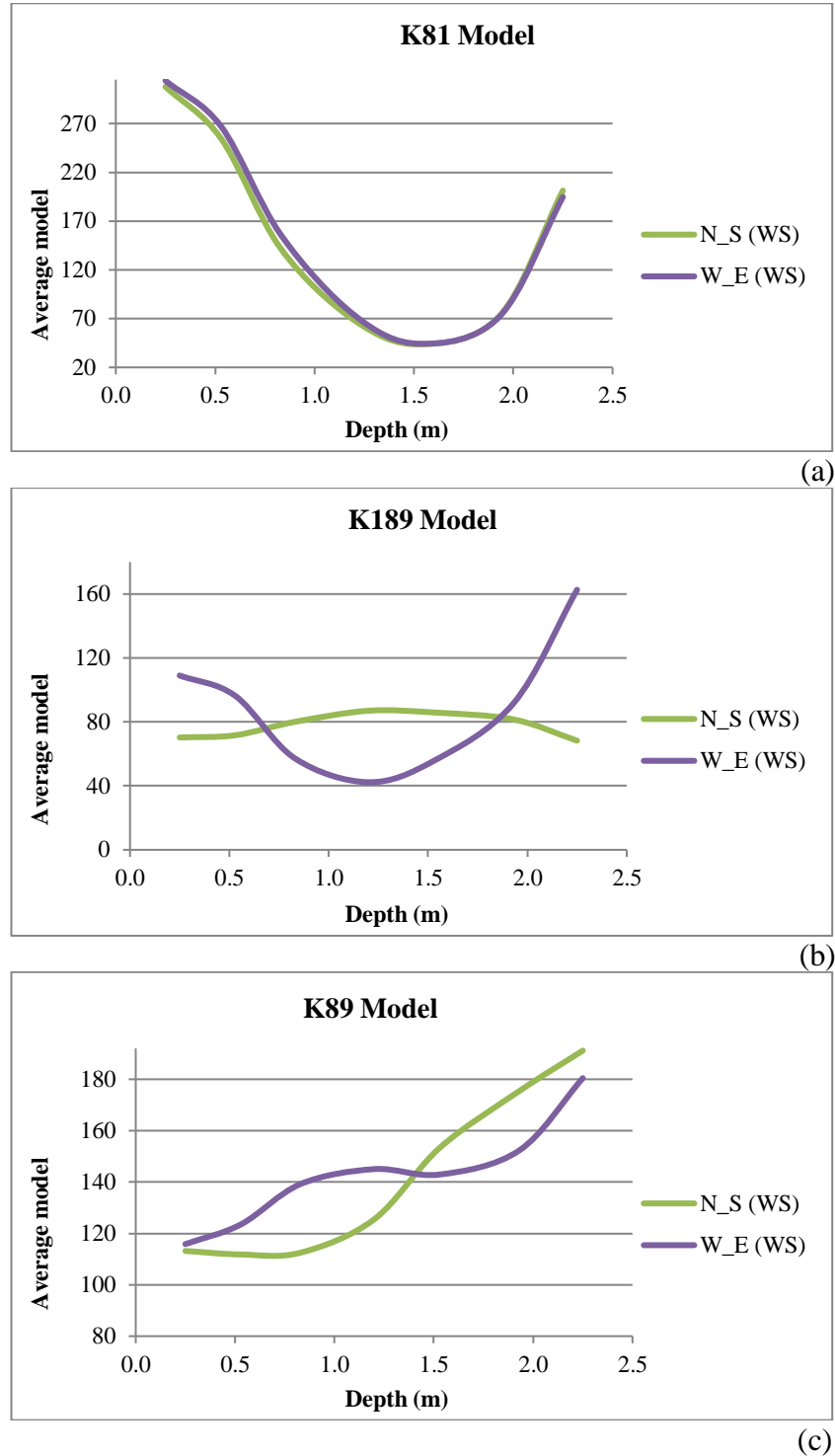


Figure 4.19: Average resistivity model for (a) K81, (b) K189

and (c) K89.

4.10 Summary

The average bulk soil χ_{lf} value is $26.7 \times 10^{-8} \text{ m}^3\text{kg}^{-1}$ though it ranges from 0 to $604.7 \times 10^{-8} \text{ m}^3\text{kg}^{-1}$ with about 76% of the samples containing ferrimagnetic minerals indicating widespread secondary enhancement for County Kildare. 66% of the bulk soil χ_{lf} data is less than $30 \times 10^{-8} \text{ m}^3\text{kg}^{-1}$ and only 4% are $>80 \times 10^{-8} \text{ m}^3\text{kg}^{-1}$. For K, the average is 25.3×10^{-5} and for $\chi_{fd}\%$ the mean is 5.3% thus the average soil sample in Kildare contains about 35-40% SP grains.

Approximately 75-80% of the sites for which K-T data were obtained were characterised by a Hopkinson peak of varying size. A typical profile shows a gradual increase in susceptibility values from 20°C to about 300°C where there is a small increase for a short temperature range followed by a small decrease, before the Hopkinson peak. Analysis of the declination and inclination remanent magnetism data for a number of soils showed that it was not possible to use near surface directional declination and inclination data as a soil discriminator because of the widespread human interference in the top soil layer which makes the results unreliable.

Regarding the spatial variability of K, $\chi_{fd}\%$ and χ_{lf} in Kildare, low values ($0-20 \times 10^{-8} \text{ m}^3\text{kg}^{-1}$) of mass specific magnetic susceptibility predominate in the northwest (due mainly to peat) and cover c. 241 km². The highest mass specific magnetic susceptibility values ($>60 \times 10^{-8} \text{ m}^3\text{kg}^{-1}$) are found at 3 locations, one in the north of the county (Kildare Inlier) and two in the south. Low values of $\chi_{fd}\%$ (0 -2% representing up to 10% SP grains) are located in the northwest and high $\chi_{fd}\%$ values in the northeast. The Kildare Inlier has medium $\chi_{fd}\%$ values (3.5 $\chi_{fd}\%$ - 20% SP minerals). The largest areas of high $\chi_{fd}\%$ are in the southern part of the county. This region (and the extreme northeast) contains up to 60% of SP minerals. The volume

susceptibility data shows a similar pattern to the mass specific susceptibility data with peat areas giving the lowest values ($0-10 \times 10^{-5}$). Regarding the particle size distribution of χ_{lf} and $\chi_{fd}\%$ for Kildare soils, it was found that the same soil types can have different absolute susceptibility values and different susceptibility patterns.

Analysis of resistivity data showed that some sites were non-homogenous, i.e. the W-E profile was markedly different from N-S ones whereas others were virtually identical. 13% of Kildare sites have a maximum model resistivity > 1000 Ohm-m. A 'trough' resistivity profile is relatively common for Kildare in which the resistivity is higher at the surface and at depth compared with mid-depth. The results are discussed further in Chapter 6.

CHAPTER 5

MAGNETIC AND ELECTRICAL RESISTIVITY RESULTS FOR COUNTY WICKLOW

5.1 Introduction

This chapter is the ‘Wicklow equivalent’ of Chapter 4. There are 6 main soil types in Wicklow according to the Environmental Protection Agency:

ADPDM: Acid Deep Poorly Drained Mineral soil.

ASWDM: Acid Shallow Well Drained Mineral soil.

ADWDM: Acid Deep Well Drained Mineral soil.

BSWDM: Basic Shallow Well Drained Mineral soil.

ASP: Acid Shallow partially Podzolic.

BP: Blanket Peat.

For brevity, these soils will be referred to by their acronyms. As in Chapter 4, the concept of a particle size does not apply to peat and its magnetic susceptibility is virtually zero. This chapter is divided into sections similar to those employed for Kildare data to provide consistency though there will be none on remanent magnetism measurements as they could not be relied on to yield consistent results.

A discussion on particle size distribution and clast analysis (section 5.2) is followed by 5 sections relating to the magnetic characteristics of the main Wicklow soils.

- Section 5.3. This section considers the main statistical characteristics of the bulk magnetic parameters χ : low and high frequency magnetic susceptibility, $\chi_{fd}\%$: frequency dependent magnetic susceptibility and K: volume susceptibility.
- Section 5.4. Spatial variability of the magnetic parameters (χ_{lf} , $\chi_{fd}\%$ and K) of the Wicklow soils is discussed.
- Section 5.5. Determination of variation of volume magnetic susceptibility with temperature (K-T) for Wicklow soil types.

- Section 5.6. Statistical characteristics of the magnetic parameters of individual Wicklow soils.
- Section 5.7. Determination of the variation in χ_{lf} and $\chi_{fd}\%$ for individual particle size ranges for main soils.

The chapter concludes with the results of 2D electrical resistivity tomography measurements at different Wicklow sites (section 5.8) and summary (section 5.9).

5.2 Particle size distribution and clastic characteristics of County Wicklow soils

Table 5.1 gives the main soil groups in County Wicklow and the sites where soil was collected (W1-W250). The geographical locations of the soil type sites are shown in Figures 5.1. The ADPDM soil is located mainly along the Wicklow coast and extends for the length of the county and its clastic host fragments reflect this geographical position. Most samples contain angular greywacke, most probably from the underlying Ordovician metasediments. Clasts are 1-3 cm in size with the smaller ones being more rounded.

For a poorly sorted soil sample, no fraction would predominate and each of the 7 sieves would have about 14.5% of the data. 34.4% of the ADPDM samples have the 600-250 μ m range as the predominant one. The ASWDM soils (48 samples analysed) are mainly located east/southeast of the Wicklow Mountains with fewer sites to the west. Some sites showed the presence of both greywacke and granite. The shape of the clasts was mainly subangular or planar. Subangular quartzite was found in W133 and W225 and schist in W184. The >2000 μ m fraction is the most predominant one in 27.6% of the samples. 38.4% of the sample sites were taken within the ADWDM soil type. This soil is the most spatially diverse of all the soils, occurring east and west of the Wicklow mountains. The types of clasts in this soil varied greatly but again greywackes from the Ordovician and Cambrian metasediments predominated. The clasts were mostly subangular in shape and the size was variable, up to 5cm.

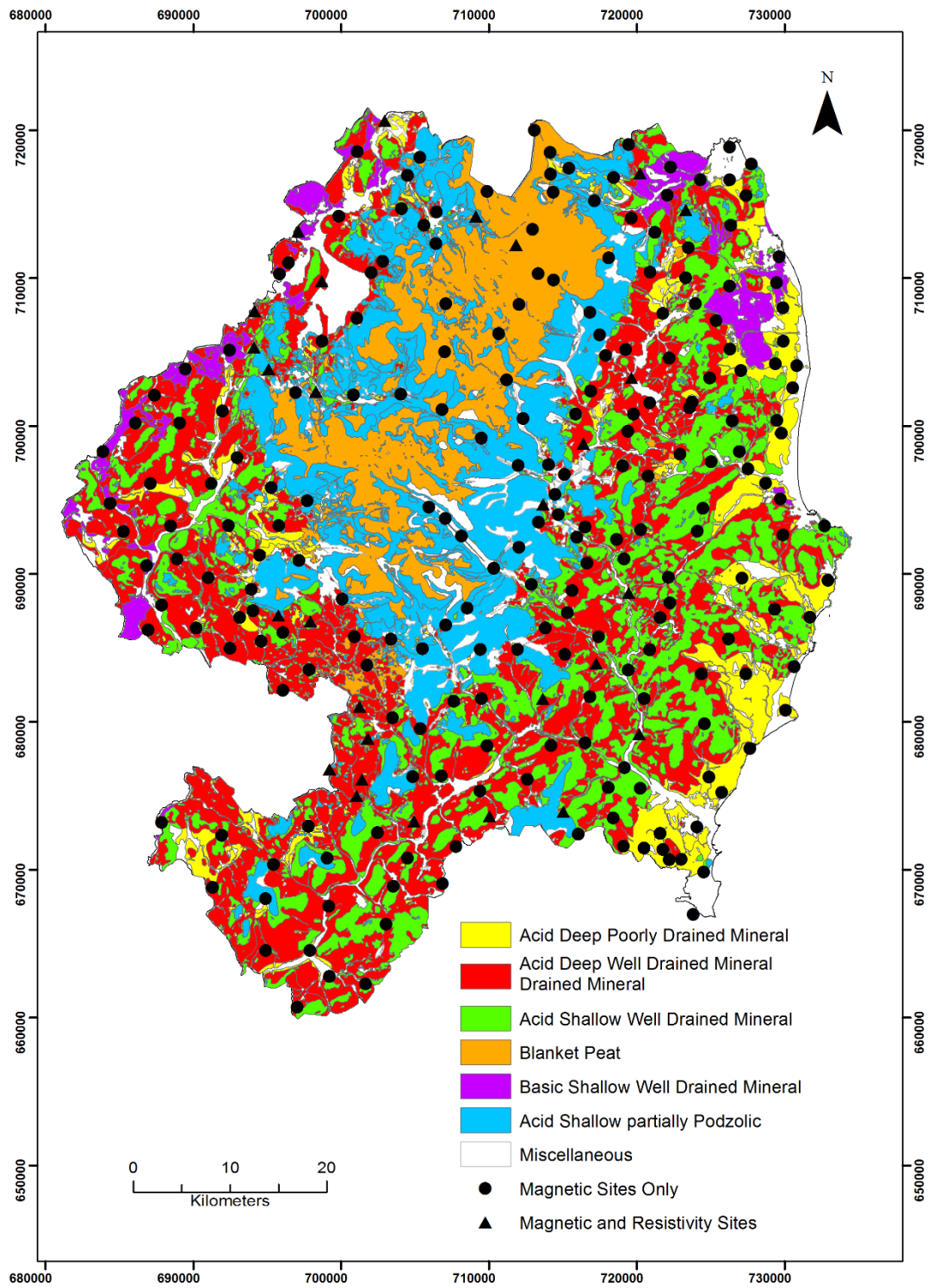


Figure 5.1: The geographical locations of magnetic and resistivity sites.

Code of Soil	Group of Soils	No.	Code of Samples
ADPDM	Acid Deep Poorly Drained Mineral	33	1,37,40,64,82,86,89,90,92,96,99,100,101,102,106,108,110,111,112,115,116,117,118,140,141,163,182,219,224,235,238,241,247.
ADWDM	Acid Deep Well Drained Mineral	96	4,6,7,8,12,14,15,16,36,41,44,47,48,49,50,51,52,54,57,58,59,61,62,63,65,66,68,72,74,76,77,80,81,85,87,88,119,123,124,126,127,129,130,131,134,135,138,145,146,147,151,152,154,158,159,161,162,164,165,173,176,177,178,179,181,183,185,186,187,189,190,192,193,194,195,196,201,202,203,207,209,213,215,216,217,218,222,223,226,227,231,234,239,242,248,249.
ASWDM	Acid Shallow Well Drained Mineral	48	5,11,17,39,43,53,55,56,67,75,79,83,91,93,94,98,120,122,125,128,132,133,136,137,139,142,143,144,148,157,160,172,175,184,188,197,198,199,200,204,206,208,210,211,212,220,225,250.
BP	Blanket Peat	11	25,26,27,28,29,30,31,34,46,245,246.
BSWDM	Basic Shallow Well Drained Mineral	12	2,3,78,84,103,149,150,153,155,156,221,233.
ASP	Acid Shallow partially Podzolic	30	9,10,18,20,21,24,32,33,35,38,42,70,71,166,167,168,169,170,171,174,180,191,214,228,229,230,236,237,240,243.
MIS	Miscellaneous	20	13,19,22,23,45,60,69,73,95,97,104,105,107,109,113,114,121,205,232,244.

Table 5.1: Soil groups in County Wicklow.

BSWDM samples were analysed from both NE Wicklow and from the Kildare-Wicklow border. The vast majority of these samples contained greywacke from nearby host Silurian, Ordovician and Cambrian lithologies. The shape range is subrounded to subangular and up to 3cm in size. 30 samples (12%) of ASP soil were obtained and analysed. A range of different types of rock fragments and minerals

was found in this soil. Subrounded rotted granite and/or mica flakes were common. For ADPDM, ASWDM, ADWDM and BSWDM, the dominant range is 600-250 μm , averaging around 17.5%. The >2000 μm range is dominant for ASP soils, closely followed by 600-250 μm (16.5%). The average particle size distribution for all Wicklow soils combined showed little variation for most sizes though 600-250 μm is slightly more prominent (17.7%). For Kildare, the 600-250 μm range is much more dominant (27.9%), thus, in general, the Kildare soils are better sorted than the Wicklow ones.

5.3 Statistical characteristics of the magnetic parameters of the Wicklow soils

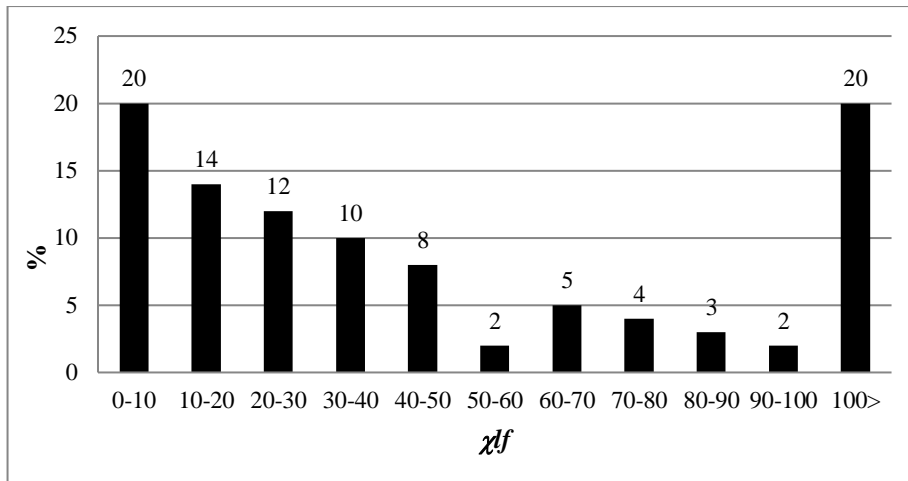
250 soil samples were magnetically analysed using the techniques and procedures discussed in Chapter 3 and their statistics are shown in Table 5.2 and relevant histograms in Figure 5.2.

Bulk Wicklow	χf	χhf	$\chi fd\%$	K
Mean	64.8	59.8	5.7	24.3
Median	31.1	29.5	5.9	21.1
Stan. dev.	87.1	79.5	3	13.3
Skewness	2.6	2.6	-0.18	0.89
Kurtosis	7.9	8.1	-1.1	0.2
Shapiro-Wilk	0.68	0.68	0.96	0.93
Minimum	0	0	0	3.3
1st Quartile	12.9	12.5	3.2	14
2nd Quartile	31.1	29.5	5.9	21.1
3rd Quartile	76.8	71.2	8.3	32.1
Maximum	536.1	484.7	12.3	66.9

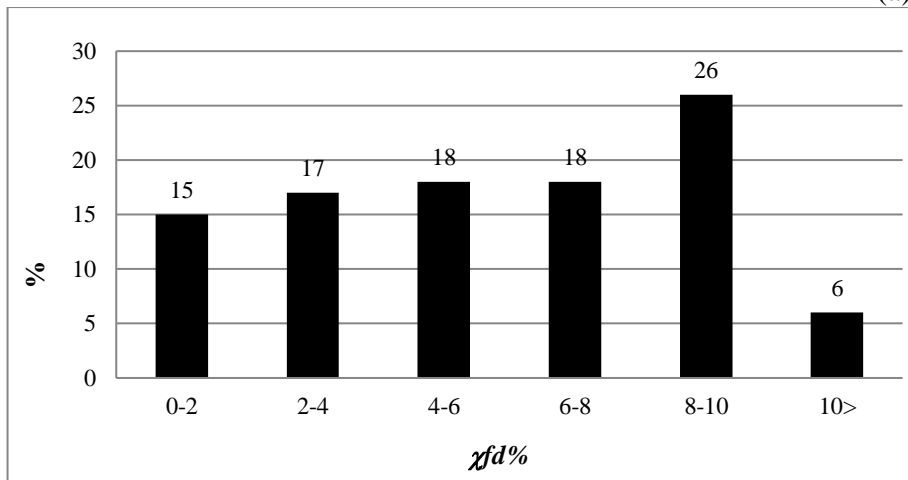
Table 5.2: Statistics for the bulk Wicklow soils.

The χf values range from 0 to $536.1 \times 10^{-8} \text{ m}^3\text{kg}^{-1}$ with a mean value of $64.8 \times 10^{-8} \text{ m}^3\text{kg}^{-1}$, Table 5.2. As discussed earlier if $\chi f > 10 \times 10^{-8} \text{ m}^3\text{kg}^{-1}$ then the soil contains

ferrimagnetic minerals such as magnetite or maghemite. 80% of the soil samples contain ferrimagnetic minerals and because there are few magnetic rocks in Wicklow and those that are there occupy a small area, there is widespread secondary enhancement in the county.

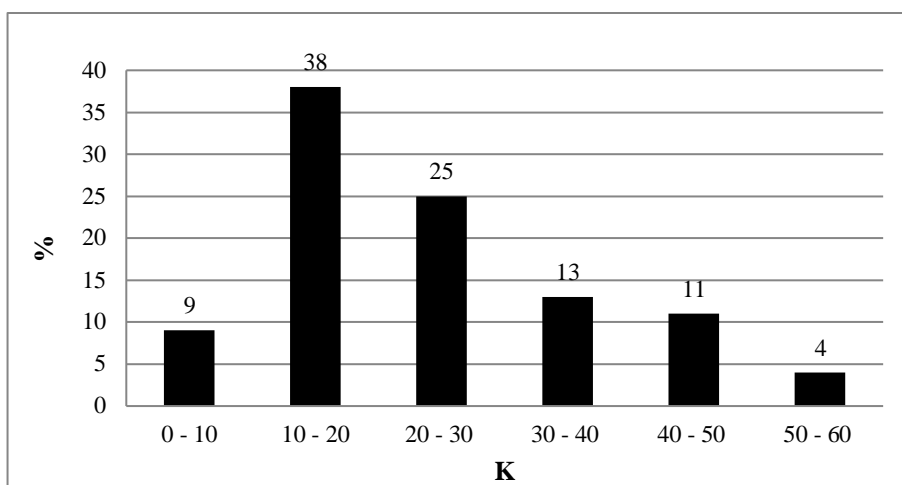


(a)



(b)

Figure 5.2: Histogram plot of (a) χ_f , (b) $\chi_{fd}\%$ and (c) volume susceptibility (K).



(c)

Figure 5.2: Continued.

The average $\chi_{fd}\%$ value of 5.7% indicates that the average soil sample in Wicklow contains about 40% SP grains. The mean and standard deviation for K (volume susceptibility) is significantly lower than that of the mass specific susceptibility. The kurtosis values for χ_{lf} and K are both positive (with the former being much larger than the latter) giving a leptokurtic distribution (a more acute peak around the mean than a normal distribution). The χ_{lf} and K magnetic data are positively (right) skewed, thus the right hand side of histogram is longer than the left side. In this instance the median is less than the mean value. For $\chi_{fd}\%$, the distribution is slightly negatively skewed. All measured magnetic parameters deviate significant from a normal distribution according to the Shapiro-Wilk test. The very high standard deviations are probably due to the non-normal distribution. The χ_{lf} histogram shows a distinctly uniform decreasing pattern as χ_{lf} increases, Figure 5.2a. 20% of the samples are less than $10 \times 10^{-8} \text{ m}^3\text{kg}^{-1}$ and exhibit paramagnetic behaviour. However, this pattern is disrupted by the very large increase (20% of the data) for values $>100 \times 10^{-8} \text{ m}^3\text{kg}^{-1}$. The $\chi_{fd}\%$ data are approximately constant (c. 17%) for ranges 0-2%, 2-4%, 4-6% and 6-8% though there is a marked increase in the 8-10% range, i.e. 32% of the samples contain about 65-70% SP grains. Very few of the samples have more than 75% SP grains. The volume susceptibility graph has some similarities with the mass specific susceptibility. As K values increase the percentage decreases. However, there

are differences. There is no prominent increase at the highest susceptibility and also there are much fewer samples with a very low susceptibility. A distinct pattern can be observed on the χ_{lf} - $\chi_{fd}\%$ graph, Figure 5.3. χ_{lf} is less than $100 \times 10^{-8} \text{ m}^3\text{kg}^{-1}$ for 200 of the Wicklow sites and there is a uniform range of $\chi_{fd}\%$ from 0-10%. 17.8% of these samples have a $\chi_{fd}\%$ value $>8\%$. However, of the 50 sites where $\chi_{fd}\%$ is $>100 \times 10^{-8} \text{ m}^3\text{kg}^{-1}$, 87.5% of the values have a $\chi_{fd}\%$ value $>8\%$. In other words, the highest susceptibility values in Wicklow are associated with the highest $\chi_{fd}\%$ values. This pattern is discussed in Chapter 6.

The interquartile range Q1-Q3 ($12.9\text{-}76.8 \times 10^{-8} \text{ m}^3\text{kg}^{-1}$ for the mass specific susceptibility and $14.0\text{-}32.1 \times 10^{-5}$ for K, the volume susceptibility) is the range which contains 50% of the samples. If a box-whisker plot of the data were constructed it would be seen that the whiskers for χ_{lf} are markedly asymmetric with the left-hand one being considerably shorter than the right one. However, the left hand one ($0\text{-}12.9 \times 10^{-8} \text{ m}^3\text{kg}^{-1}$ range) contains 25% of the data whereas the right-hand range is $77.1\text{-}169.2 \times 10^{-8} \text{ m}^3\text{kg}^{-1}$ and only contains 14.8% of the data.

For the bulk magnetic data for Wicklow, there is a statistically significant correlation between χ_{lf} and $\chi_{fd}\%$. (Spearman rank coefficient 0.62. The correlation between χ_{lf} and K is also a significant one, Figure 5.3b, (Spearman rank coefficient of 0.69).

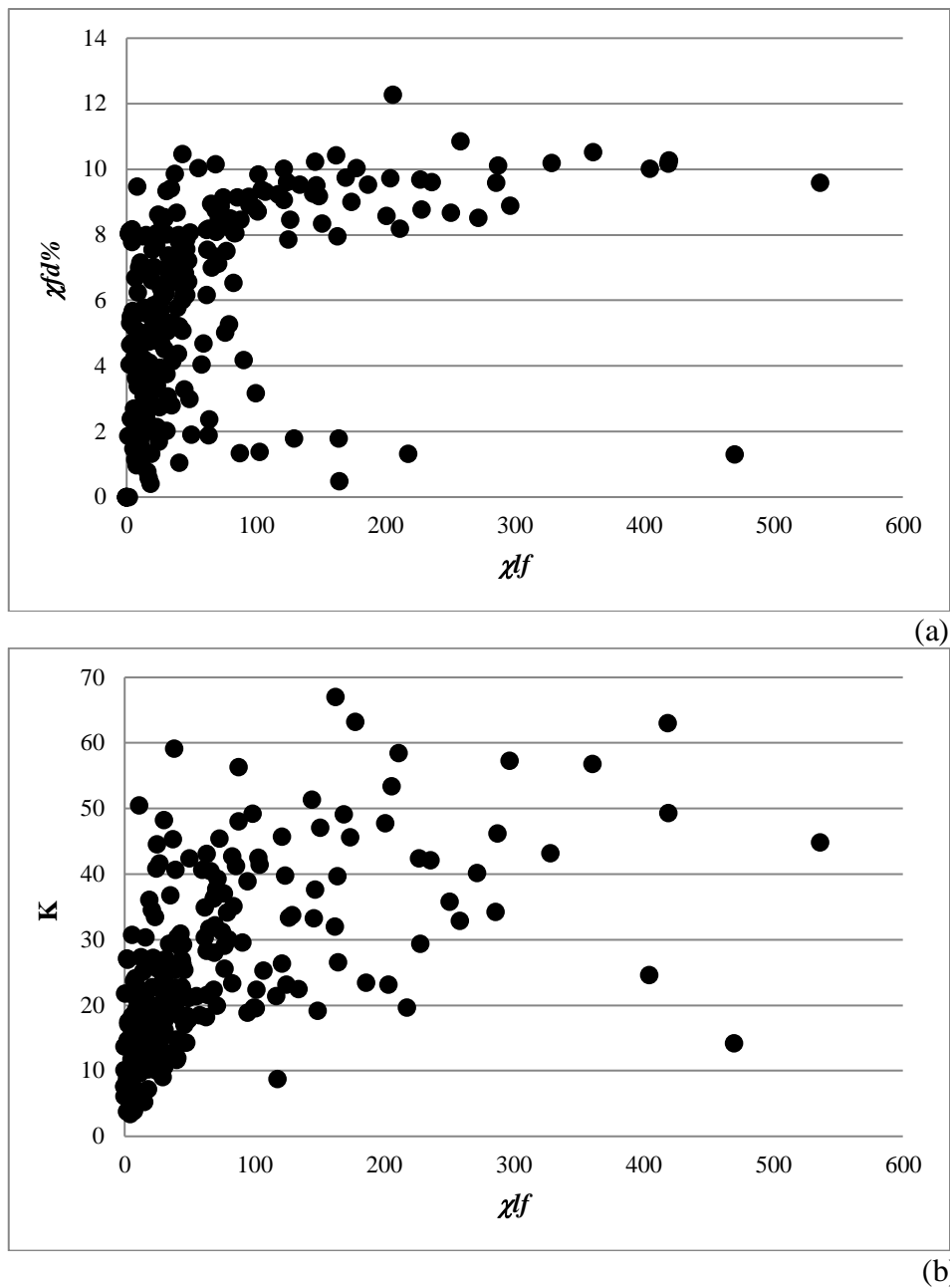


Figure 5.3: Correlation between (a) χ_{lf} and $\chi_{fd}\%$ and (b) between χ_{lf} and K.

5.4 Spatial variability of the bulk magnetic parameters of the Wicklow soils.

Six spatial maps were produced from the Wicklow magnetic data, most of which are similar to those discussed in section 4.4 in Chapter 4, namely:

- Map of low frequency mass susceptibility data (threshold image) - Figure 5.4.
- Map of low frequency mass susceptibility data - Figure 5.5.
- Map of low frequency susceptibility data – high values - Figure 5.6.
- Map of volume susceptibility data (K) - Figure 5.7.
- Map of frequency dependent susceptibility data - Figure 5.8.
- Map of relative standard deviation data – Figure 5.9.

There is a very distinct prominent spatial dimension to the susceptibility threshold image, in which regions dominated by ferrimagnetic minerals are shown in red ($>10 \times 10^{-8} \text{ m}^3\text{kg}^{-1}$) and areas where diamagnetic and paramagnetic minerals predominate are in blue, ($<10 \times 10^{-8} \text{ m}^3\text{kg}^{-1}$), Figure 5.4.

The diamagnetic/paramagnetic zone trends NNE-SSW and is confined almost exclusively to the western half of the county. It is confined to areas where the underlying bedrock is Caledonian granite (see Figure 3.1, Chapter 3 for comparison). However, the low values are mainly concentrated in the northwest apart of the county, being absent for the southern granites. When Figure 5.5 is compared with the soils map of Wicklow, there is a very good correlation of the low susceptibility values with blanket peat (light brown) and shallow acid partially podzolic soils (blue).

The blanket peat is formed of vegetable matter and contains no magnetic minerals and the podzolization process produces intensely leached soils in which iron is removed from the upper layers. As samples were obtained from the top 10-15cm, again one would not expect magnetic minerals from these soils. The highest susceptibility values are located in the eastern half of the county where the host rocks are Ordovician metasediments and the soil types are ASWDM and ADWDM, Figure 5.5. The spatial pattern for χ_{lf} data for the range $100\text{-}500 \times 10^{-8} \text{ m}^3\text{kg}^{-1}$ is shown in Figure 5.6. Most of the county has values less than $100 \times 10^{-8} \text{ m}^3\text{kg}^{-1}$ as evidenced by the purple/mauve background colour, with the highest values in the east/southeast. High susceptibility values (shown red) are recorded east of Avoca. Sheppard and McConnell (2014) show this as an area with copper-lead-zinc-iron mineralization.

Figure 5.6 shows a NNE-SSW trending 20 km long high susceptibility zone extending from E714690 N685926 to E719874 N706847. This coincides with the mineral deposits in the Glendalough area (Downes and Platt, 1978). The highest values measured in Wicklow are located at E724580 N693979 ($536.1 \times 10^{-8} \text{ m}^3\text{kg}^{-1}$). These are not associated with any known mineral deposits. However, based on the results presented here it is possible that there are unknown mineral deposits in this area. In the extreme south of the county some smaller anomalies (green) are associated with tin-arsenic mineralization.

The spatial pattern for volume susceptibility (K) is similar to that for (χ/f) in that the highest values are in the east/southeast part of the county, Figure 5.7. Average values of around 22×10^{-5} predominate in the west. $\chi/d\%$ data mirrors the χ/f distribution to a large extent, Figure 5.8. Very low values (0-2%) are rare and occur mainly in the north central part of the county in peat areas. Intermediate values (shown in green) are generally confined to the west/northwest, whereas the higher values are in the east/southeast and coincide with high χ/f locations. The relative standard deviation map gives low values in the areas where K is highest indicating less variability between the K values obtained using the Bartington MS2D loop sensor, Figure, 5.9.

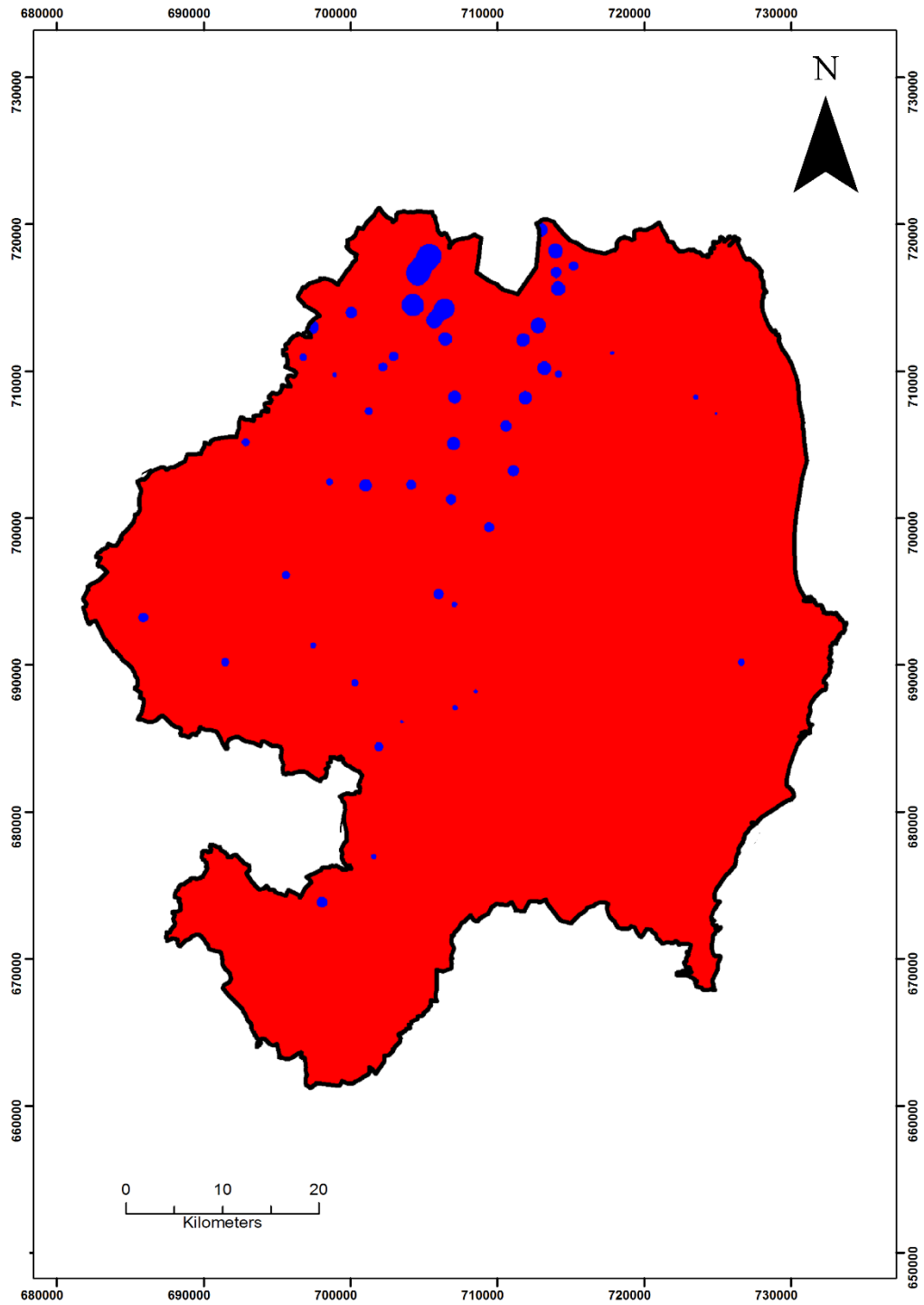


Figure 5.4: Magnetic susceptibility threshold map of Wicklow in which blue shows areas $<10 \times 10^{-8} \text{ m}^3\text{kg}^{-1}$ and red shows areas $>10 \times 10^{-8} \text{ m}^3\text{kg}^{-1}$.

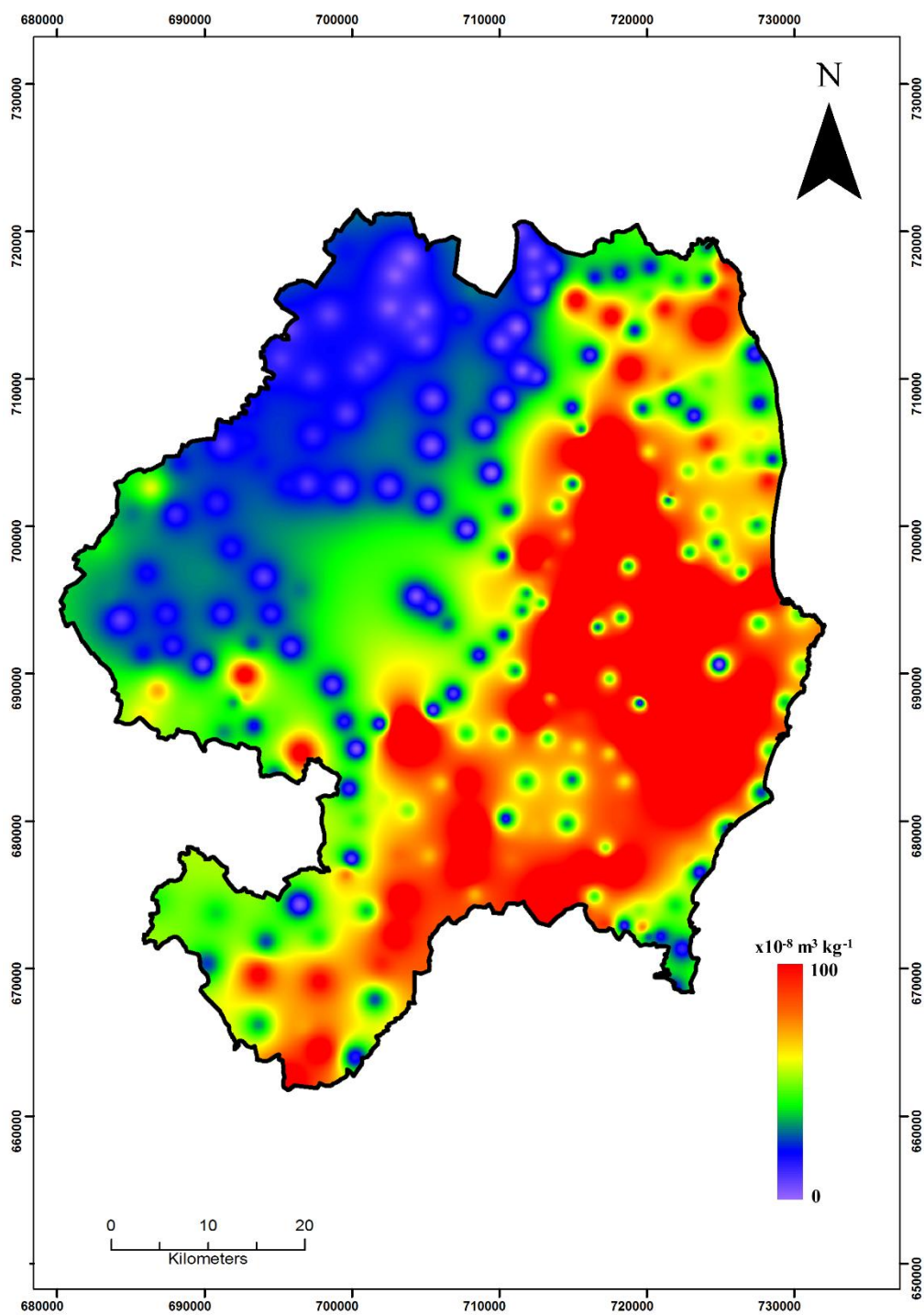


Figure 5.5: Magnetic susceptibility map of Wicklow ($\chi_l f$).

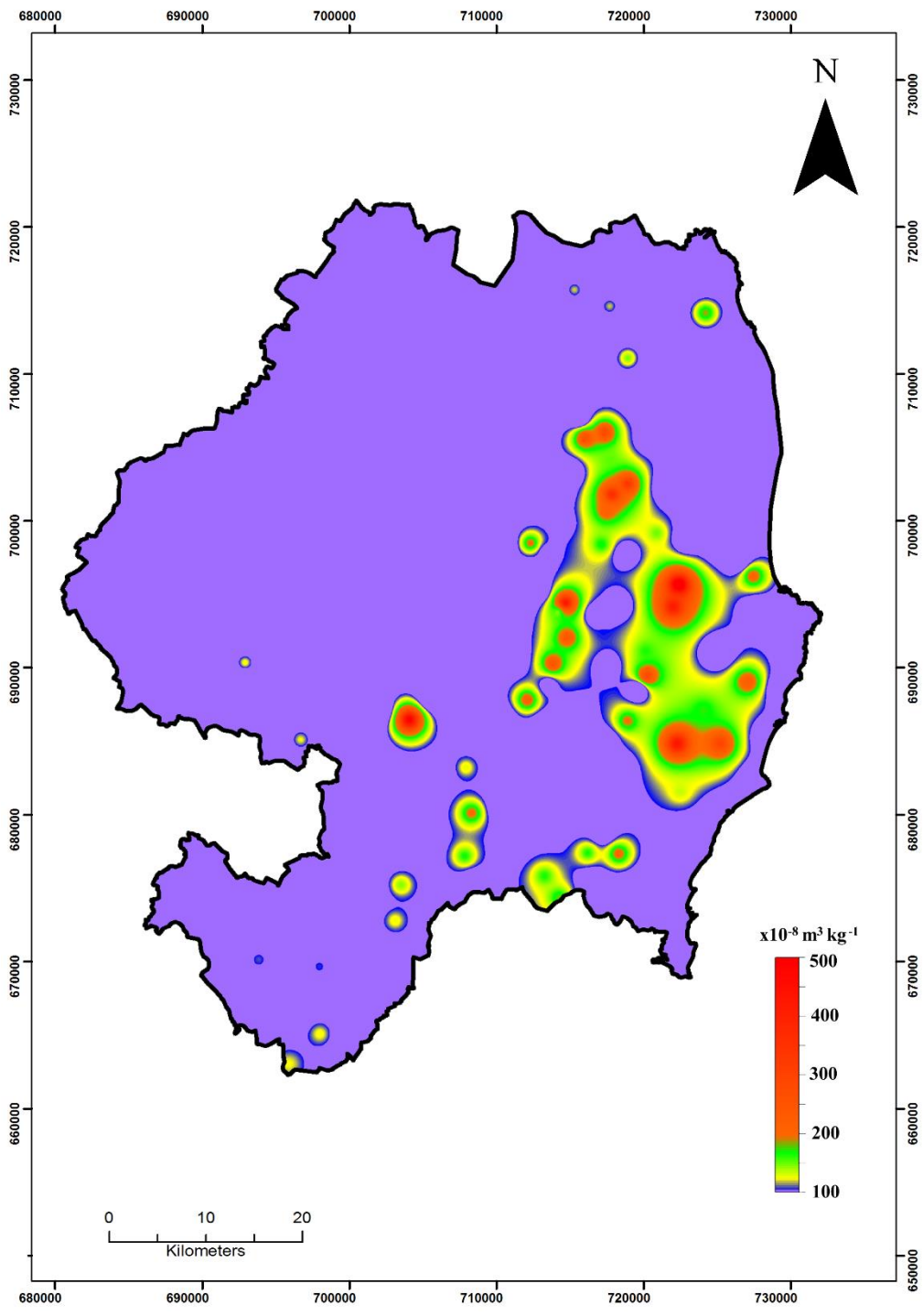


Figure 5.6: Magnetic susceptibility map of high values in Wicklow (*xlf*).

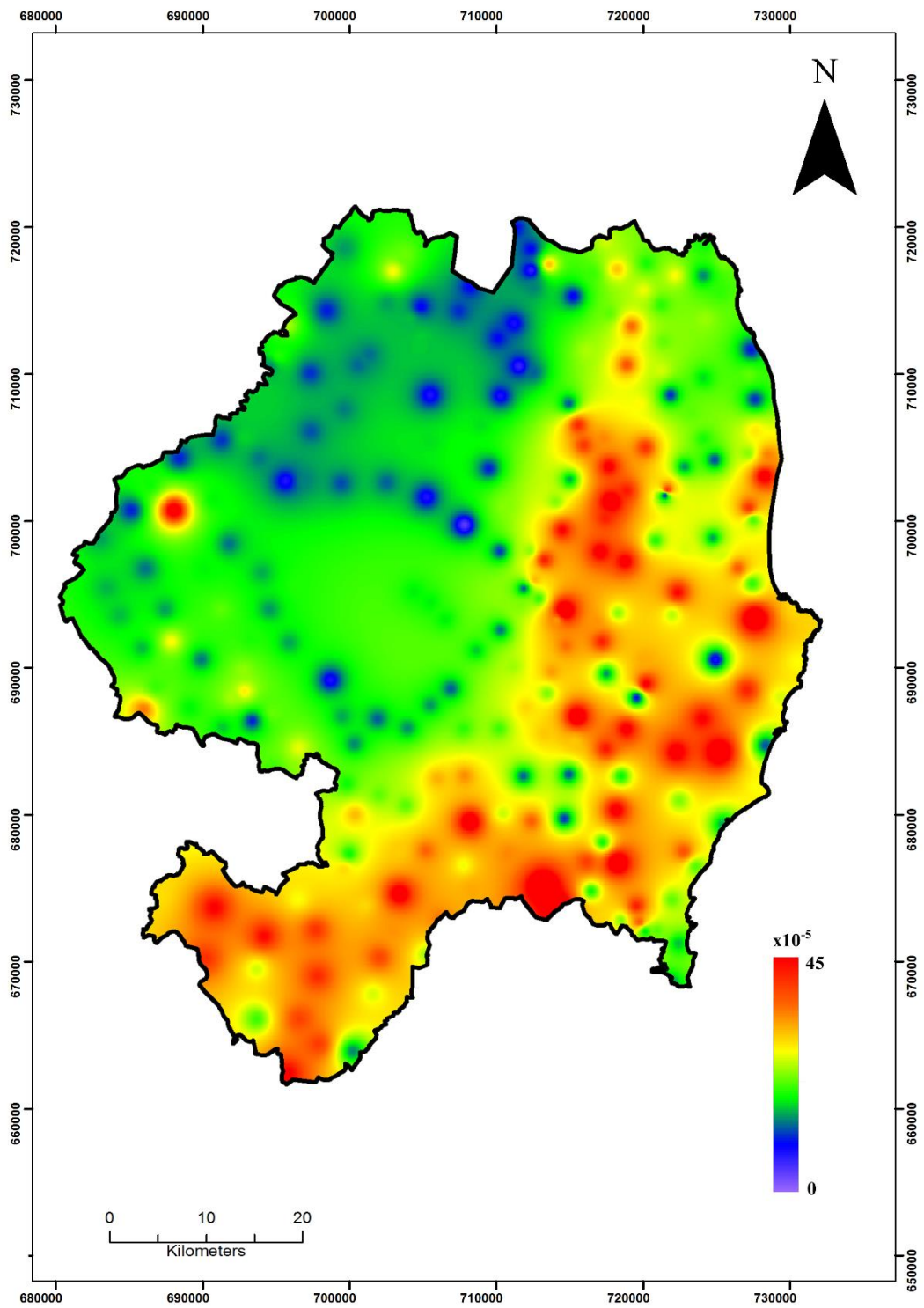


Figure 5.7: Magnetic susceptibility map of Wicklow (K).

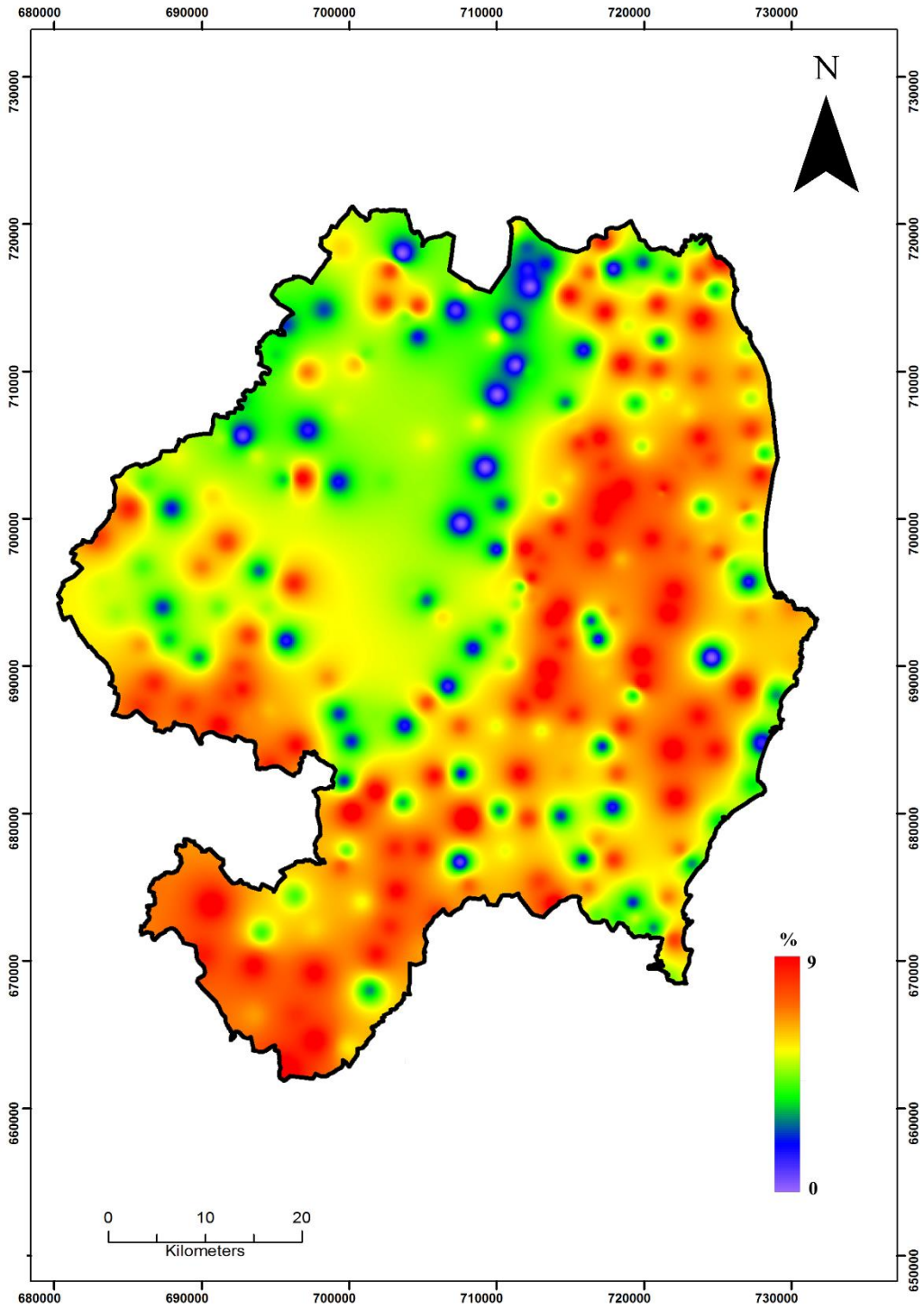


Figure 5.8: $\chi d\%$ map of Wicklow.

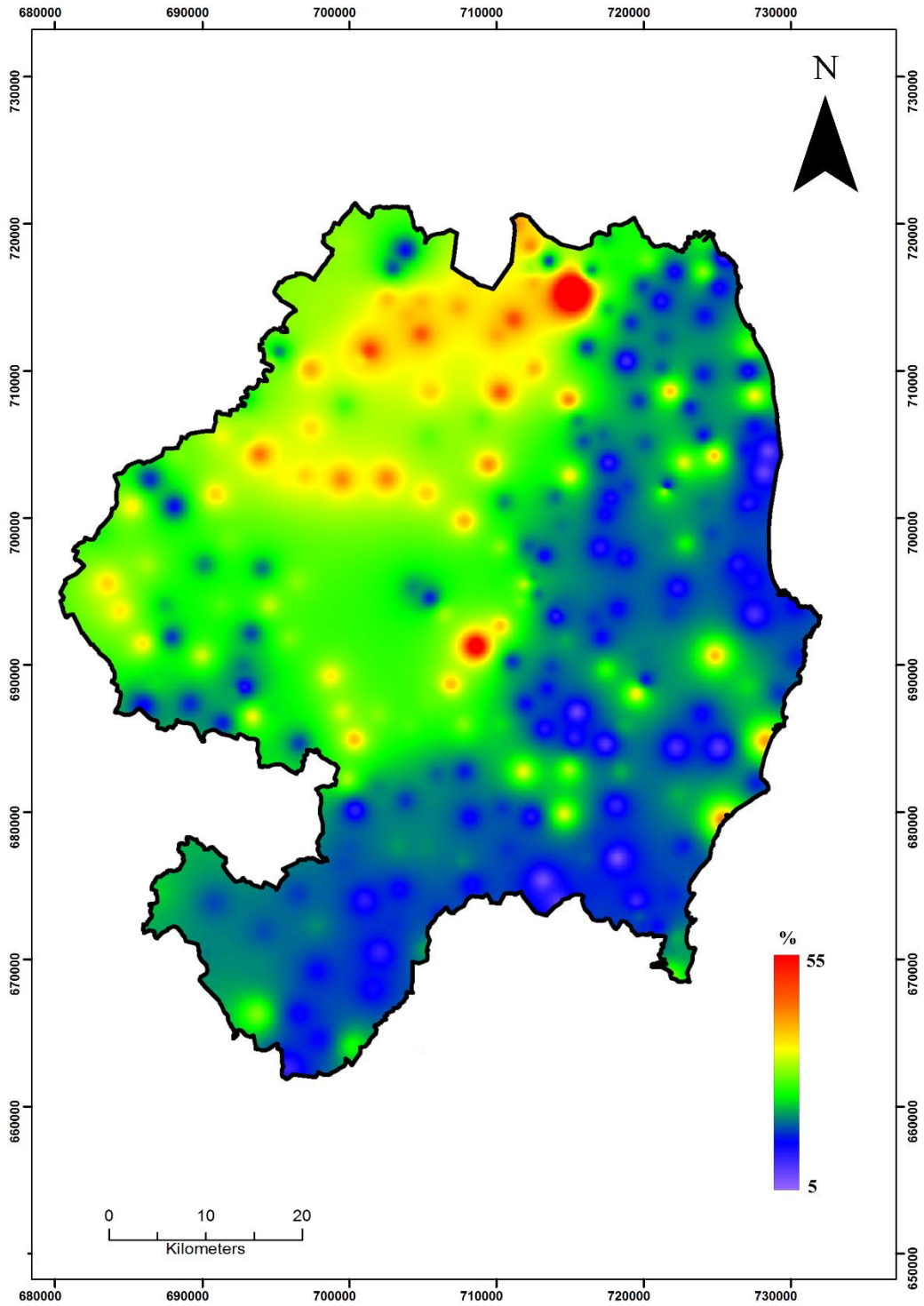


Figure 5.9: Relative standard deviation map (χ^2) of Wicklow.

5.5 K-T data analysis

Three sample K-T heating curves are shown in Figure 5.10, see File 5.1s.docx for all 100 Wicklow heating and cooling curves (in K-T folder in supplementary material). The Hopkinson peak is very pronounced for site W224, its relative peak height is greater than 6, one of the highest in the study area. Its $\chi_{fd}\%$ value means it has 60% SP grains which combined with the Hopkinson peak (high SD contents) means it contains very few MD grains. However, W84 has 55% SP grains and the remaining 45% are MD as it lacks a Hopkinson peak. W122 contains 75% SP, with most of the remainder being MD. Susceptibility decreases over a wide temperature range, beginning at 270°C. The Curie temperature of pyrrhotite is 270°C (Table 2.5), thus it is most likely present in this sample.

All the 14 ADPDM soils for which K-T data were obtained were characterised by a Hopkinson peak, though the peaks for some are poorly developed. RPH is mainly in the 2-3 range (average 2.3) but is highest (5.46) for K17 indicating conversion of a significant amount of SD grains to SP grains. The $\chi_{fd}\%$ data indicate sites with high susceptibilities: W238 ($117.8 \times 10^{-8} \text{ m}^3\text{kg}^{-1}$); W118 ($90.7 \times 10^{-8} \text{ m}^3\text{kg}^{-1}$); W100 ($98.9 \times 10^{-8} \text{ m}^3\text{kg}^{-1}$) and W86 ($94 \times 10^{-8} \text{ m}^3\text{kg}^{-1}$) generally have poorly developed Hopkinson peaks whereas lower susceptibility sites W90 ($46.2 \times 10^{-8} \text{ m}^3\text{kg}^{-1}$); W92 ($44.3 \times 10^{-8} \text{ m}^3\text{kg}^{-1}$); W106 ($34.8 \times 10^{-8} \text{ m}^3\text{kg}^{-1}$); W141 ($50 \times 10^{-8} \text{ m}^3\text{kg}^{-1}$) and W224 ($30.9 \times 10^{-8} \text{ m}^3\text{kg}^{-1}$) have better developed ones. Regarding the cooling curves for the ADPDM soils (shown in File 5.1s.docx), in general they are all fairly similar, but in detail, 3 differences can be observed.

- The temperature at which the maximum magnetic susceptibility is attained on the cooling cycle varies quite greatly. Most are within the 200-400°C range. However, W118 is greater than 400°C and W100 is less than 200°C.
- W100 is also unique for this soil type in that the susceptibility starts to increase at a lower temperature than the heating curve whereas for most sites the curves coincide (though the opposite is the case for W86).

- The cooling curve susceptibility is 5-10 times greater than the heating curve susceptibility at room temperature except for W100 again where the factor is considerably less (2.2).

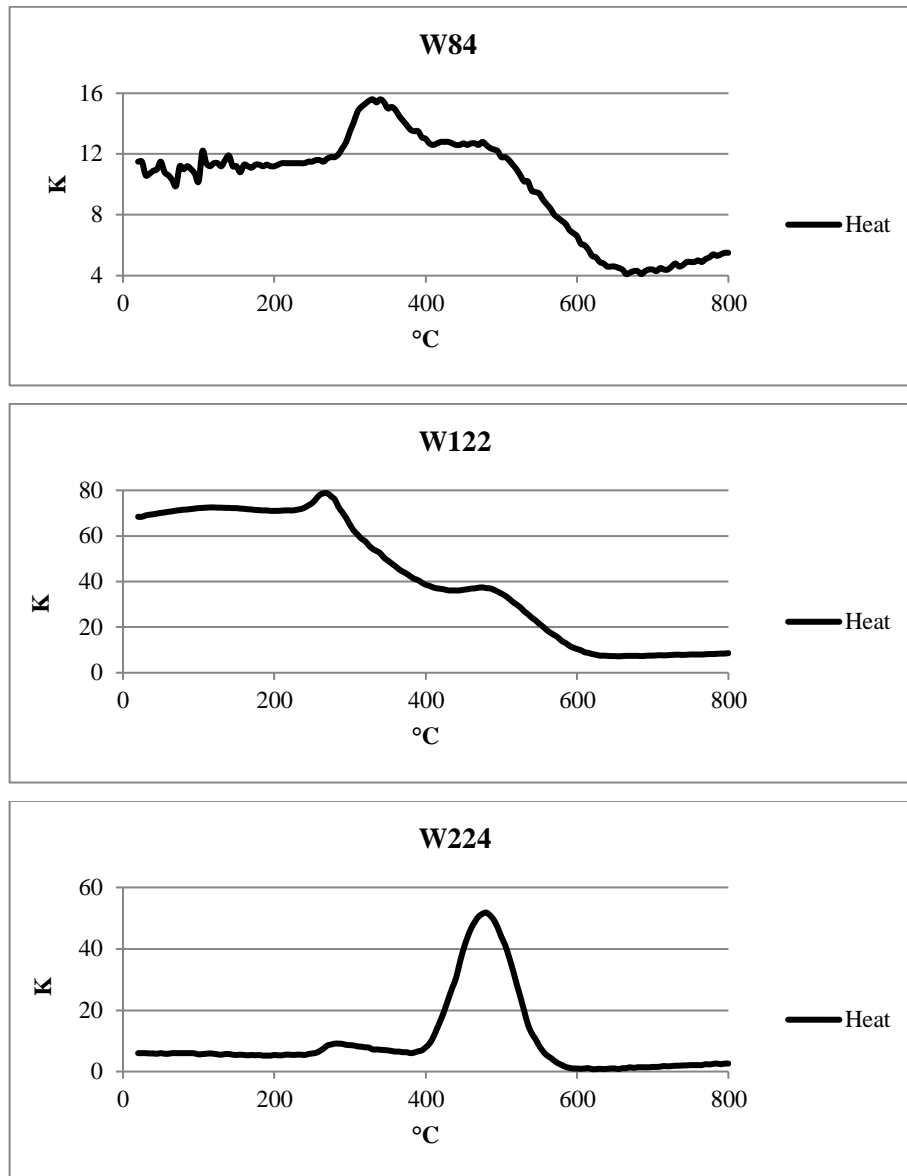


Figure 5.10: Typical Wicklow K-T heating curves.

There is considerably more variability for the ASWDM K-T data than for the Kildare soils discussed in Chapter 4. For Kildare, the majority of soils display a prominent Hopkinson peak with RPH>1.5-2. A few ASWDM soils are similar (W120, W137).

However, a large proportion of the sites (77%) have either a very weakly developed Hopkinson peak or none at all. A large proportion of samples with a weak Hopkinson peak have high susceptibility values and high $\chi_{fd}\%$ showing that they contain c. 70-80% SP grains. The ADWDM soils are similar to those discussed above for ASWDM in that most of the sites (82%) have either a very weakly developed Hopkinson peak or none at all. The RPH values for these sites are generally close to 1. BSWDM soils show a range of K-T profiles mainly with a well developed Hopkinson peak. The average RPH of 2.9 is the highest of all Wicklow soils. 62% of the ASP soils are associated with a pronounced Hopkinson peak.

5.6 Statistical characteristics of the magnetic parameters of individual Wicklow soils

The χ_{lf} values for ADPDM range from 0 to $129.3 \times 10^{-8} \text{ m}^3\text{kg}^{-1}$ with an average value of $41 \times 10^{-8} \text{ m}^3\text{kg}^{-1}$, which is greater than any main Kildare soil, Table 5.3. The average $\chi_{fd}\%$ value of 5.5% indicates that the soil sample in Wicklow contains about 40% SP grains. 50% of the mass specific susceptibility samples are within the interquartile range Q1-Q3 ($18.2\text{-}49 \times 10^{-8} \text{ m}^3\text{kg}^{-1}$). The Shapiro-Wilk test for χ_{lf} and $\chi_{fd}\%$ shows that both deviate from a normal distribution but K does not deviate significantly from such a pattern. The ADWDM χ_{lf} values are in the $1.9\text{-}419.1 \times 10^{-8} \text{ m}^3\text{kg}^{-1}$ range with a mean value of $84.8 \times 10^{-8} \text{ m}^3\text{kg}^{-1}$, which is twice that of ADPDM and of an average Kildare soil, Table 5.4. The mean $\chi_{fd}\%$ value of 6.9% indicates that the average ADWDM soil sample in Wicklow contains about 50% SP grains. 50% of the samples are within the interquartile range Q1-Q3 ($20.2\text{-}121.1 \times 10^{-8} \text{ m}^3\text{kg}^{-1}$) for the mass specific susceptibility. The Shapiro-Wilk test for χ_{lf} , K and $\chi_{fd}\%$ shows that all deviate from a normal distribution. There is a strong correlation between $\chi_{fd}\%$ and χ_{lf} and between χ_{lf} and K.

ADPDM	χ_{lf}	χ_{hf}	$\chi_{fd}\%$	K
Mean	41	38.5	5.5	23.6

Median	30.8	29	5.4	21.9
Standard Deviation	33.8	31.6	2.6	9.7
Skewness	1.2	1.2	-0.2	0.65
Kurtosis	0.52	0.78	-1.2	0.24
Shapiro-Wilk	0.87	0.87	0.93	0.96
Minimum	0	0	0	7.5
1st Quartile	18.2	17.3	3.5	17.7
2nd Quartile	30.8	29	5.4	21.9
3rd Quartile	49	47.4	7.8	27
Maximum	129.3	127	9.2	49.2

Table 5.3: Statistical data for ADPDM soils.

ADWDM	χ_{lf}	χ_{hf}	$\chi_{fd}\%$	K
Mean	84.8	77.4	6.9	28.6
Median	45.5	42.6	7.7	27.6
Standard Deviation	92.6	83.23	2.8	9
Skewness	1.6	1.6	-0.45	0.38
Kurtosis	1.9	1.9	-0.91	0.26
Shapiro-Wilk	0.79	0.79	0.94	0.96
Minimum	1.9	1.7	0.8	5.2
1st Quartile	20.2	19	5	15.4
2nd Quartile	45.5	42.6	7.7	27.6
3rd Quartile	121.4	109.6	9.2	40.5
Maximum	419.1	376.1	12.3	67

Table 5.4: Statistical data for ADWDM soils.

The ASWDM χ_{lf} values are in the 2.5- 536.1 $\times 10^{-8}$ m³kg⁻¹ range with the latter being the second highest recorded value in the research area, only sample K300 was greater. The average value of 93.2 $\times 10^{-8}$ m³kg⁻¹ is also the highest mean value, Table 5.5. The mean $\chi_{fd}\%$ value of 6.2% indicates that the average ASWDM soil sample in Wicklow contains about 45% SP grains. 50% of the samples are within the

interquartile range Q1-Q3 ($27.3-109 \times 10^{-8} \text{ m}^3\text{kg}^{-1}$) for the mass specific susceptibility. The Shapiro-Wilk test for χ_{lf} , K and $\chi_{fd}\%$ is similar to ADWDM in that all deviate from a normal distribution.

ASWDM	χ_{lf}	χ_{hf}	$\chi_{fd}\%$	K
Mean	93.2	86.2	6.2	28.3
Median	55.7	52.6	6.9	22.6
Standard Deviation	108.9	98.3	2.9	15
Skewness	2.5	2.5	-0.45	0.92
Kurtosis	7.1	6.9	-1	-0.07
Shapiro-Wilk	0.7	0.71	0.93	0.89
Minimum	2.5	2.2	0.49	9.9
1st Quartile	27.3	25.8	4.1	18.2
2nd Quartile	55.7	52.6	6.9	22.6
3rd Quartile	109	105.2	8.5	39
Maximum	536.1	484.7	10.2	63.2

Table 5.5: Statistical data for ASWDM soils.

The BSWDM soil χ_{lf} values are in the $6.9-40.34 \times 10^{-8} \text{ m}^3\text{kg}^{-1}$ range with an average value of $20.7 \times 10^{-8} \text{ m}^3\text{kg}^{-1}$, Table 5.6. The average $\chi_{fd}\%$ value of 4.6% shows a typical soil BSWDM sample in Wicklow contains about 35% SP grains. 50% of the samples are within the interquartile range Q1-Q3 ($12.2-34 \times 10^{-8} \text{ m}^3\text{kg}^{-1}$) for the mass specific susceptibility. The Shapiro-Wilk test for χ_{lf} , K and $\chi_{fd}\%$ shows that all deviate from a normal distribution. The χ_{lf} values for ASP are in the $1.7-107.2 \times 10^{-8} \text{ m}^3\text{kg}^{-1}$ range with an average value of $20.4 \times 10^{-8} \text{ m}^3\text{kg}^{-1}$, very similar to BSWDM, Table 5.7. The mean $\chi_{fd}\%$ value of 4.1% is the lowest for any Wicklow soil and indicates that a typical ASP soil sample in Wicklow contains about 30% SP grains. 50% of the mass specific susceptibility samples are within the interquartile range Q1-Q3 ($5.9-26.9 \times 10^{-8} \text{ m}^3\text{kg}^{-1}$). The Shapiro-Wilk test for χ_{lf} and K deviate from a normal distribution but $\chi_{fd}\%$ does not.

BSWDM	χ_f	χ_{hf}	$\chi_{fd}\%$	K
Mean	20.7	19.6	4.6	16.6
Median	19.4	18.1	4.7	15.7
Standard Deviation	13.3	12.3	2.2	5
Skewness	0.89	0.82	0.35	0.99
Kurtosis	-0.27	-0.43	-1.2	0.77
Shapiro-Wilk	0.89	0.89	0.92	0.91
Minimum	6.9	6.5	1.3	10.2
1st Quartile	12.2	11.9	2.1	14.5
2nd Quartile	19.4	18.1	4.7	15.7
3rd Quartile	34	32.4	5.6	19
Maximum	40.34	37.1	8	27

Table 5.6: Statistical data for BSWDM soils (exc. W103).

ASP	χ_f	χ_{hf}	$\chi_{fd}\%$	K
Mean	20.4	19.1	4.1	16.6
Median	11.8	11.7	4.5	16.3
Standard Deviation	23.5	221.4	2.7	8
Skewness	2.5	2.4	0.3	1.2
Kurtosis	6.8	6.4	-1	2.4
Shapiro-Wilk	0.7	0.72	0.92	0.93
Minimum	1.7	1.7	0	3.8
1st Quartile	5.9	5.8	1.7	12.2
2nd Quartile	11.8	11.7	4.3	16.3
3rd Quartile	26.9	25.3	5.7	19.6
Maximum	107.2	97.2	9.3	41.5

Table 5.7: Statistical data for ASP soils (exc. W167).

5.7 Characteristics of the magnetic parameters of grain size fractions for individual and bulk Wicklow soils

5.7.1 Statistical characteristics

A very good consistency between fractions exists for the susceptibility data, Table 5.8. The mean susceptibility value is similar for all fractions, only ranging from 65.5-

$67.4 \times 10^{-8} \text{ m}^3\text{kg}^{-1}$ and the median value does not vary much. The Shapiro-Wilk index is virtually identical and this test shows that none of the data are normally distributed. The interquartile range (Q1-Q3), where 50% of the data lie, is similar for all fractions though the range tends to be higher for the smaller fraction sizes:($>2000\mu\text{m}$: $13.4-71.7 \times 10^{-8} \text{ m}^3\text{kg}^{-1}$ and $<63\mu\text{m}$: $13.5-82.1 \times 10^{-8} \text{ m}^3\text{kg}^{-1}$).

Skewness is also reasonably similar (it is slightly higher for largest sieve) and the median is always less than the mean indicating the data are positively (right) skewed, thus the right hand side of histogram is longer than the left side. The difference between the mean and median is considerably greater for Wicklow than for Kildare. The kurtosis is also significantly greater. The high positive values indicate a sharper peak than a normal distribution (a leptokurtic distribution).

The $\chi fd\%$ data are very consistent for all fractional sizes. There is a general small increase in the mean (and median) values with decreasing grain size fraction indicating an increase in SP grains. The same results were found for the Kildare soils.

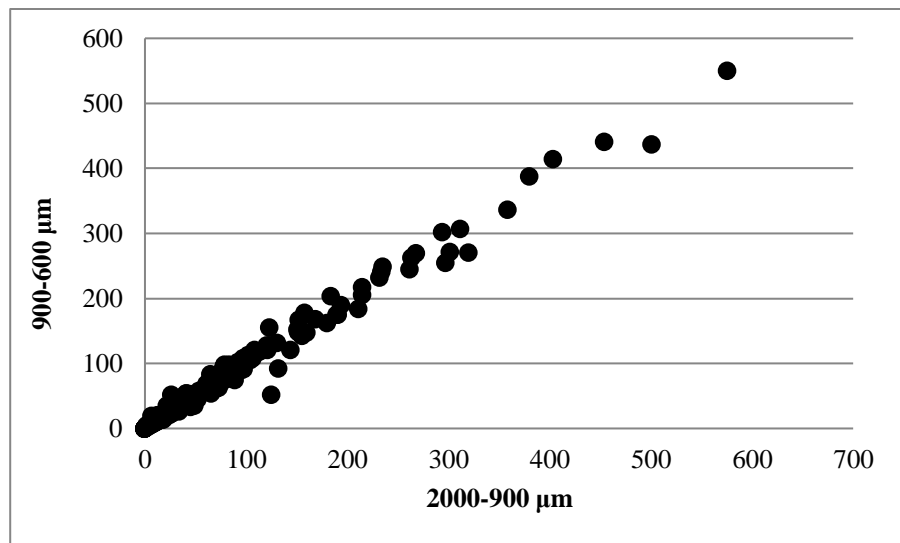
<i>χf</i>	>2000μm	2000-900 μm	900-600 μm	600-250 μm	250-125 μm	125-63 μm	<63 μm
Min	0	0	0	0	0	0	0
Q1	13.4	13.5	12.2	13	12.6	13.2	13.5
Q2	32.2	33.4	32	33.2	33.5	31.8	33.3
Q3	71.7	83.4	75.3	78.9	80.6	79.2	82.1
Max	630.8	588.5	546.8	562.3	583.5	576.1	549.7
Mean	65.9	67.4	67	66.9	66.8	66.1	65.5
Median	32.2	33.4	32	33.2	33.5	31.8	33.3
SD	93.7	89.2	92.6	91.7	91.4	89.9	86.2
Skewness	2.9	2.5	2.7	2.7	2.7	2.7	2.6
Kurtosis	10	7.8	8.2	8.4	8.8	8.6	7.9
W	0.65	0.7	0.68	0.67	0.68	0.68	0.68
<i>$\chi fd\%$</i>	>2000	20-900	900-600	600-250	250-125	125-63	<63

Min	0.0	0.0	0.0	0.0	0.0	0.0	0.0
Q1	2	2.8	2.9	3.2	3.3	3.2	3.5
Q2	5	5.6	6	6.2	6	6.2	6.2
Q3	7.9	8.5	8.5	8.7	8.8	8.8	8.7
Max	13.3	14.5	12.1	13.5	15.9	14	13
Mean	5.1	5.5	5.5	5.8	5.9	5.9	5.9
Median	5	5.6	6	6.2	6	6.2	6.2
SD	3.4	3.4	3.2	3.3	3.4	3.3	3.3
Skewness	0.05	-0.06	-0.18	-0.14	-0.18	-0.14	-0.15
Kurtosis	-1.1	-0.9	-1.2	-1.1	-0.9	-1	-0.9
W	0.96	0.96	0.95	0.96	0.95	0.96	0.97

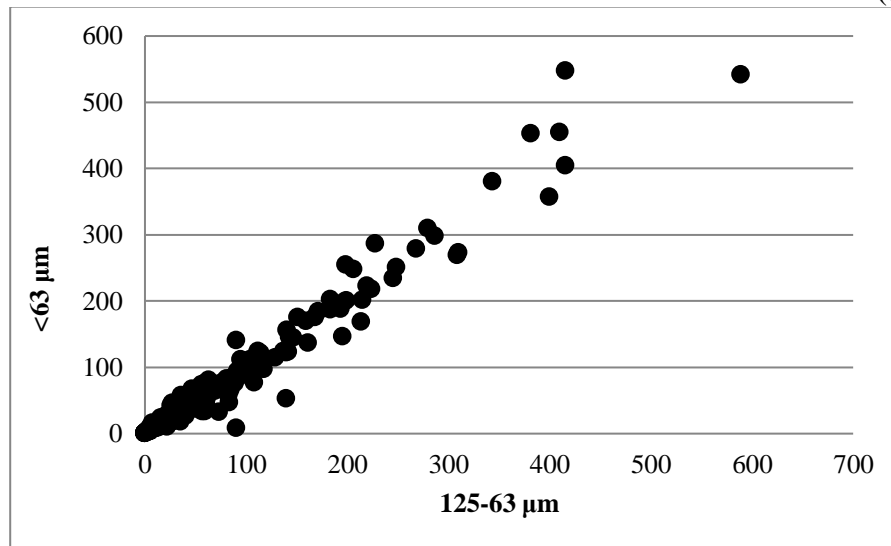
Table 5.8: Individual fractional statistics for all Wicklow soils.

5.7.2 Spatial variation for individual fractional sizes

In the corresponding section, in Chapter 4 (section 4.8.2), the spatial variability of magnetic susceptibility with respect to the 7 grain size fractions were examined. No such equivalent examples are shown here. The close correspondence between the statistical parameters of the individual fractions (Table 5.8), means that any such maps would be very similar and look very like the bulk susceptibility image given in Figure 5.5. For example, the correlation between 2000-900 μm and 900-600 μm fractions and 125-63 μm and <63 μm are illustrated in Figure 5.11. The gradient is very close to 1 for both graphs and the correlations are 0.96 and 0.99 respectively. Correlations between other fractions are also very similar: 600-250 μm and 250-125 μm fractions (0.97) and 2000-900 μm and 250-125 μm (0.96). The poorest but still strong correlation is with the >2000 μm fraction.



(a)



(b)

Figure 5.11: Correlation between (a) 2000-900 μm and 900-600 μm fractions and (b) 125-63 μm and <63 μm for all Wicklow soils.

5.7.3 Particle size distribution of χ_{lf} and $\chi_{fd}\%$ for main Wicklow soils

In this section, the χ_{lf} and $\chi_{fd}\%$ distribution patterns for different particle sizes are examined. File 5.2s.docx, in the histograms folder, illustrates over 100 examples of

the variation in susceptibility and percentage frequency dependent susceptibility respectively (χ_{lf} and $\chi_{fd}\%$) for different fractional sizes for Wicklow soils.

Approximately 34% of the ADPDM samples have a susceptibility histogram in which one (or at the most two) sieves predominate – most often the $>2000\mu\text{m}$ one. In general, the largest fraction is about twice the others. Susceptibility histogram ramp patterns are rare, either negative or positive. 41% of the $\chi_{fd}\%$ histograms are roughly constant for all fractions

The absolute χ_{lf} values for ASWDM soil vary greatly from $2 \times 10^{-8} \text{ m}^3\text{kg}^{-1}$ (W11) to $200 \times 10^{-8} \text{ m}^3\text{kg}^{-1}$ (W120). The average value of $93.2 \times 10^{-8} \text{ m}^3\text{kg}^{-1}$ is the highest average value in Wicklow. Only about 12% have a dominant fraction, less than half that of ADPDM. Negative and positive ramp distributions are more common though. 40% of the $\chi_{fd}\%$ histograms are relatively uniform.

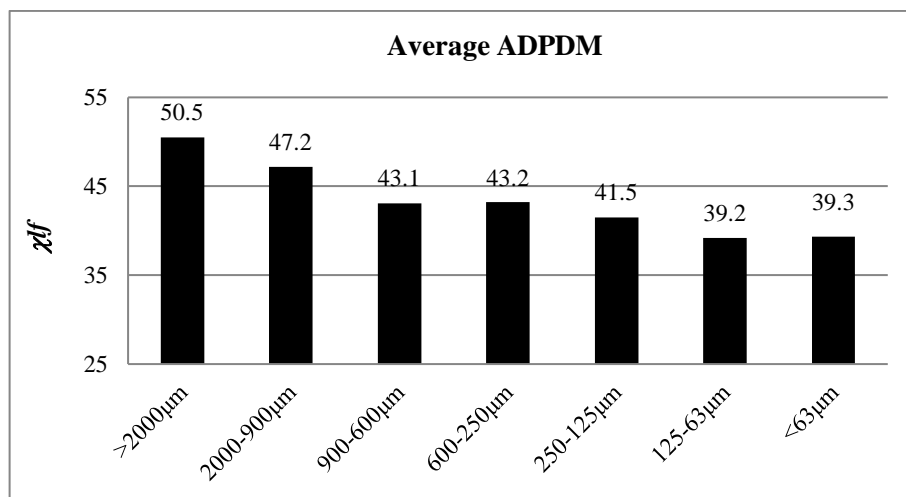
96 of the 250 Wicklow sites were taken on ADWDM soil. 11.5% were characterised by a dominant susceptibility sieve – mainly the $>2000\mu\text{m}$. A negative susceptibility ramp (susceptibility increases as particle size decreases) is shown by some sites with no positive ones being observed. Approximately uniform responses for all or most sieves is common and again the $\chi_{fd}\%$ histograms are relatively uniform.

For BSWDM soils some ramps are evident but not common. The histograms do not readily fall into any set patterns. There is a massive variation in susceptibility for ASP soils. 19% of the samples have a dominant sieve size, which is variable, some $\chi_{fd}\%$ histograms are approx. constant for all or most sieves. There is a very variable response in general for $\chi_{fd}\%$ histograms, most likely due to the low susceptibility values and precision of the Bartington MS2 meter, see W239 and W236 for example.

Figures 5.12 and 5.13 show histograms of the average susceptibility and frequency dependent susceptibility respectively for the 7 different fractional sieve sizes for the 5 main Wicklow soil groups. For ADPDM and BSWDM, the larger fractions have the highest susceptibilities, by a factor of around 25%, when compared to the lowest

values. For the other soils, the susceptibility difference between different fractions is quite low. The ranges between the highest and the lowest for ADWDM is ($85-89 \times 10^{-8} \text{ m}^3\text{kg}^{-1}$) and for ASP is ($35-39 \times 10^{-8} \text{ m}^3\text{kg}^{-1}$) only represent a 5% difference. ASWDM soils vary a bit more, but most sieves yield an average susceptibility of c. $93 \times 10^{-8} \text{ m}^3\text{kg}^{-1}$. When all Wicklow soils are analysed, the susceptibility data show a remarkable uniformity with all values in the $68-70 \times 10^{-8} \text{ m}^3\text{kg}^{-1}$ range. It can be concluded that in general, for Wicklow soils, all fraction sizes contribute equally to the measured susceptibility.

The frequency dependent susceptibility for the Wicklow soils does not vary greatly between fractional sizes for any individual soil type, Figure 5.13. For all the soils combined, the range is 5.1-5.9%. The 4 smaller sieve sizes all have greater % values than the larger sieves, but the difference is not great. The lowest % is for the $>2000\mu\text{m}$ fraction. This sieve often contains rock fragments which tend to have low % values. Although the variation is small, the trend is pronounced (Pearson coefficient of $R=0.91$, a very strong correlation) it can be concluded that for the Wicklow soils, the smaller fraction sizes contribute slightly more to the measured frequency dependent susceptibility than larger grain fractions.



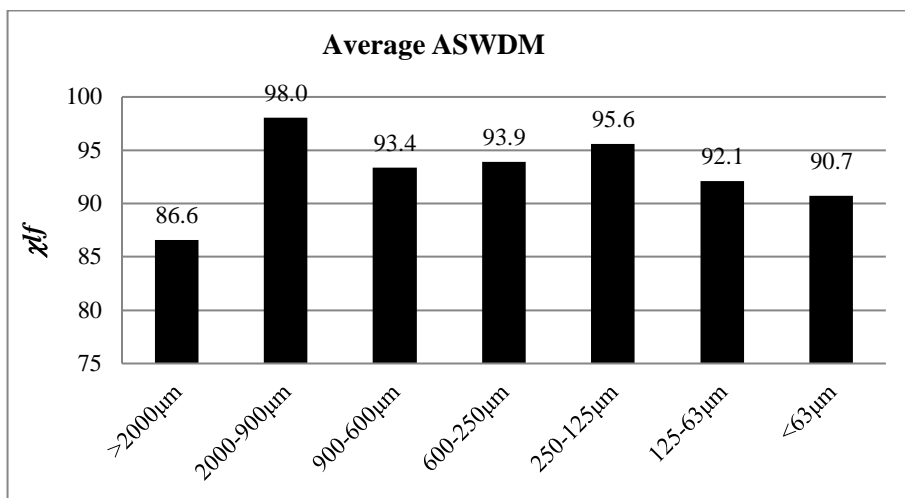
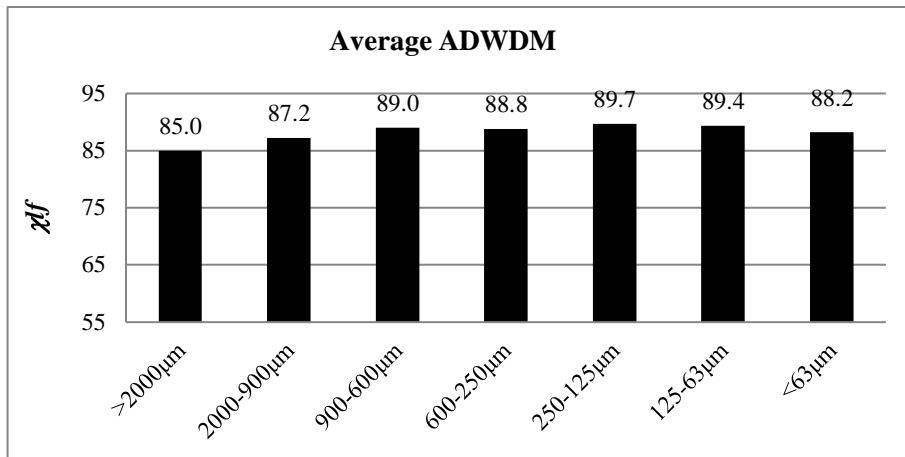
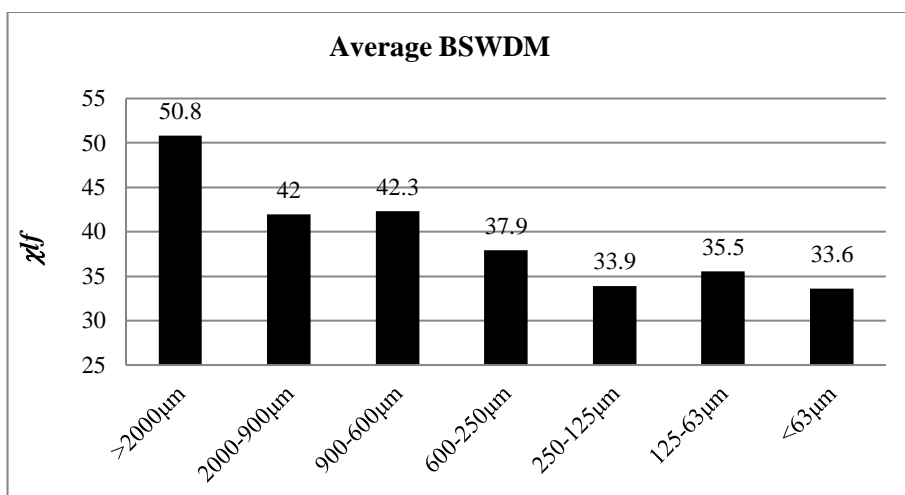


Figure 5.12: Average susceptibility for the main Wicklow soil types.



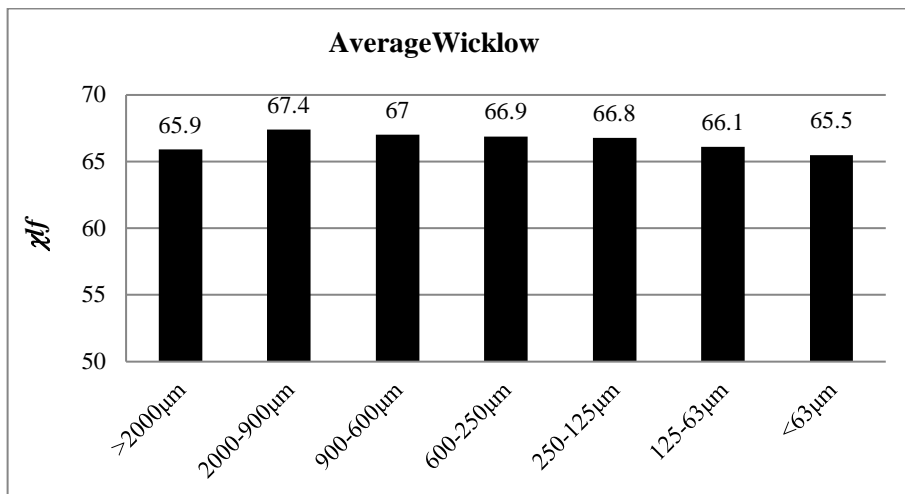
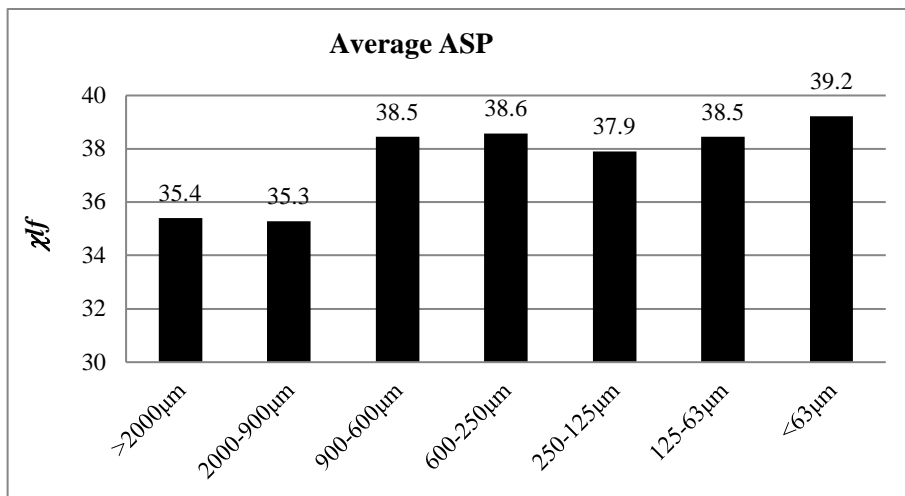
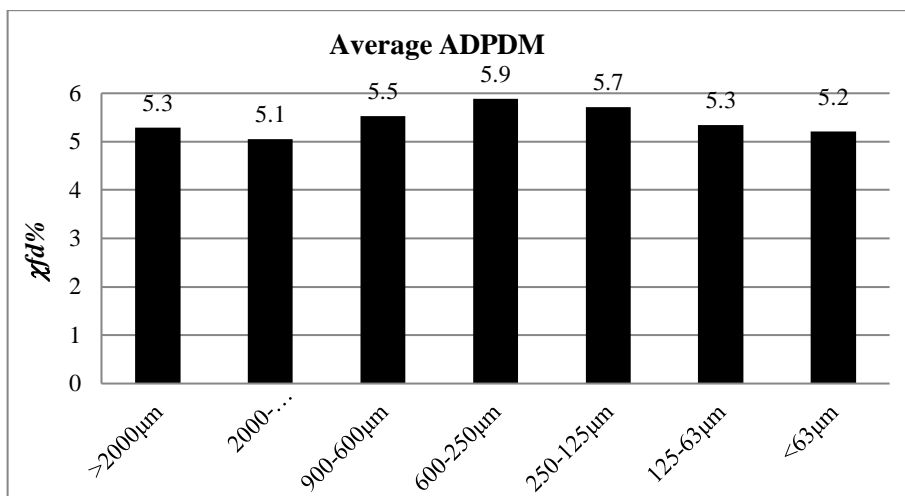


Figure 5.12: Continued.



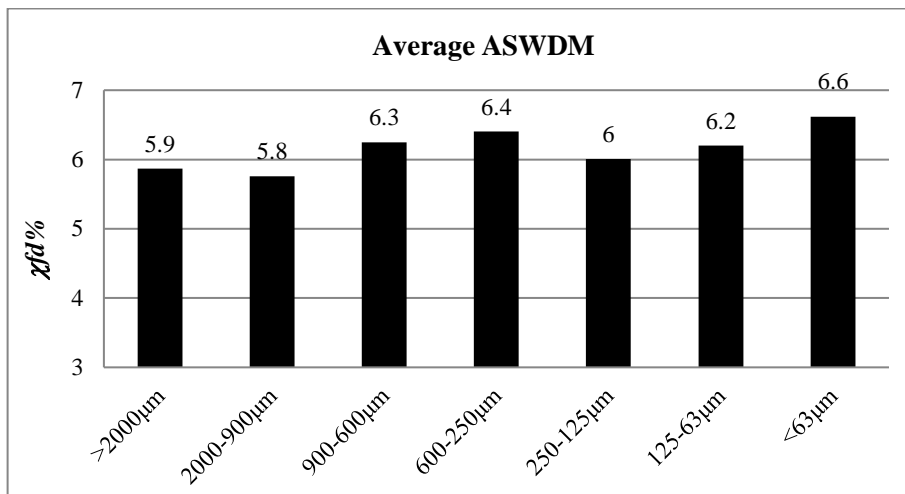
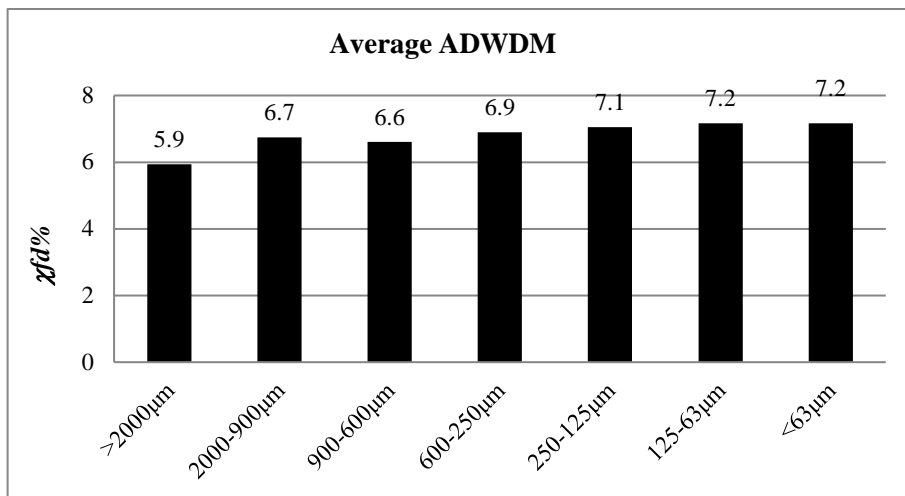
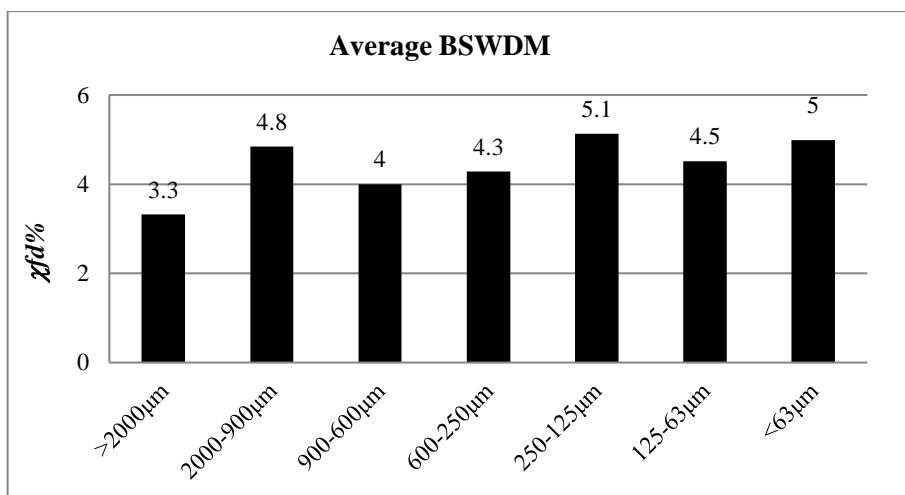


Figure 5.13: Average $\chi_{fd}\%$ for the main Wicklow soil types.



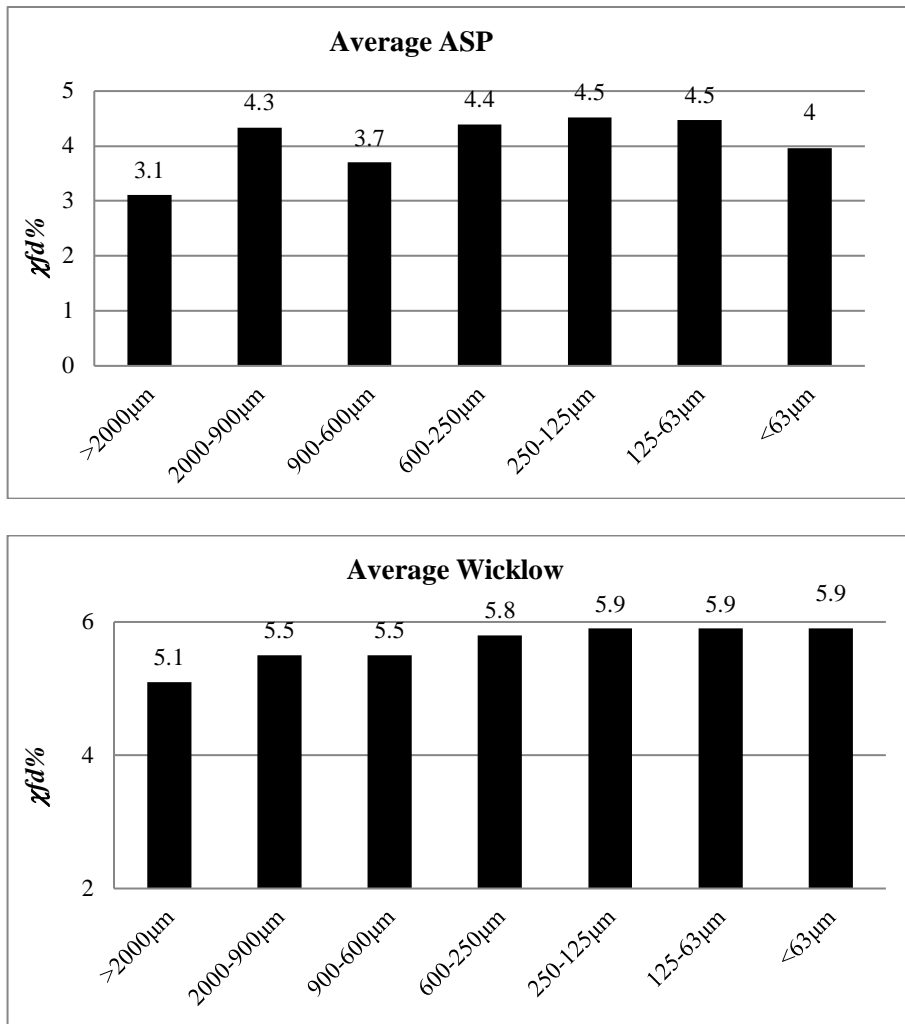


Figure 5.13: Continued.

5.8 Resistivity results for Co. Wicklow sites

The resistivity data collected in County Wicklow are considered in this section and the results displayed in the same format as that used in County Kildare. The locations of the 29 resistivity sites are given in Figure 5.1. Two examples are shown in this section, the others are in File 5.3s.docx within the resistivity data folder. The same dynamic range as that employed in Chapter 4 is used in order to facilitate comparisons. However, an examination of File 5.3s.docx shows that this is not the optimum display range for some sites which have a high resistivity. In these circumstances, the Wenner-Schlumberger sections will continue to employ the same

range as used in Kildare, but the Dipole-Dipole sections will use an enhanced dynamic range for display purposes. The results along with those collected in Kildare are discussed in Chapter 6.

Two 2D resistivity examples are shown here, W79 (Figure 5.14) and W210 (Figure 5.15) and average model profiles for both are displayed in Figure 5.16. The former lacks sub-horizontal layering and resistivity is mainly in the range 300-600 Ohm-m, Figure 5.14. Average resistivity gradually increases to a depth of 1.5m below which there is a steeper gradient. The N-S and W-E average model resistivity are quite different showing that this site is non-homogeneous.

Site W210 displays a sharp contact between zones of different resistivity. An upper thin low resistivity layer (100 Ohm-m) is underlain by a 500 Ohm-m layer, Figure 5.15. The average model profile shows that the maximum resistivity is attained at a depth of 1.5m, below which resistivity values decrease. In this instance the N-S and W-E average model resistivity are very similar.

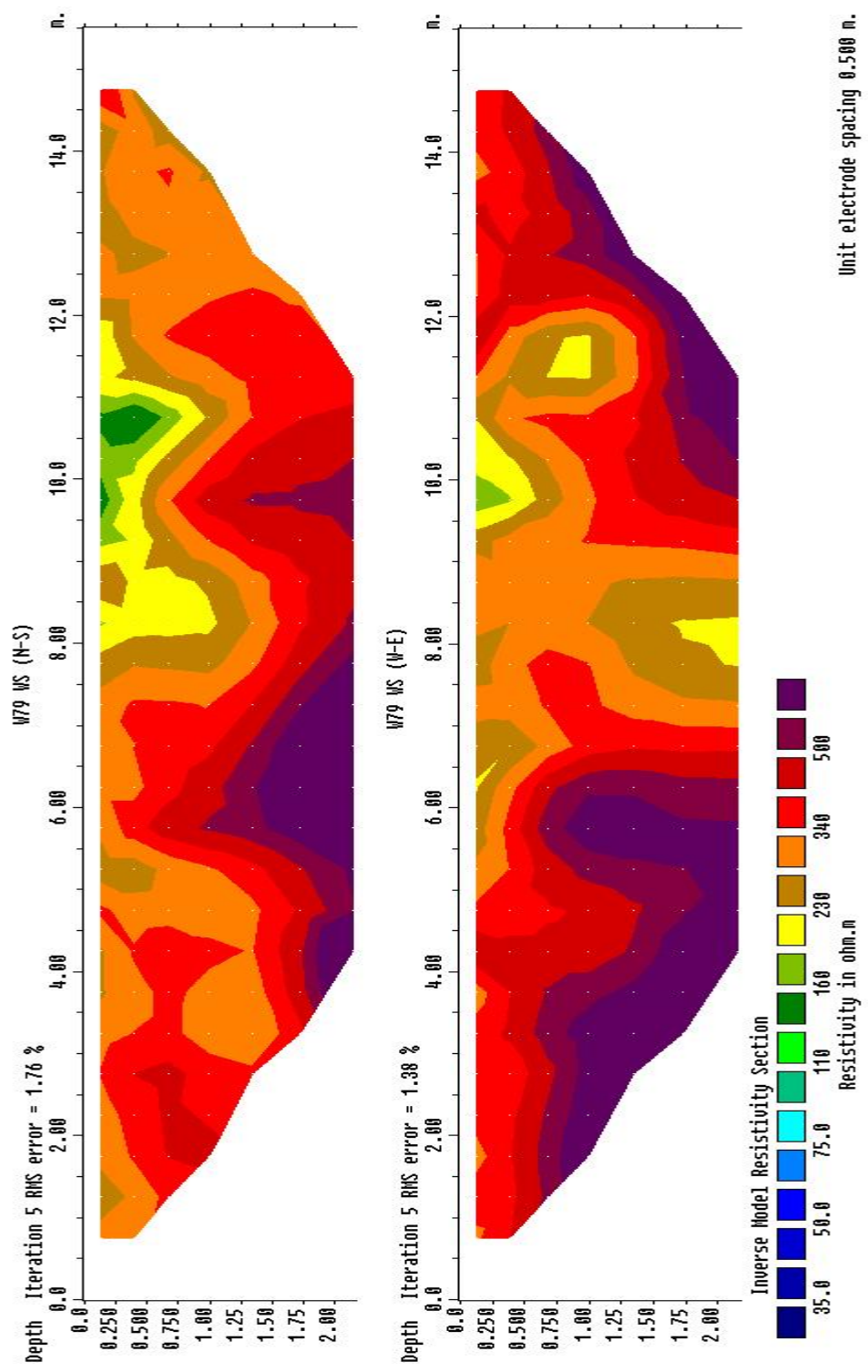


Figure 5.14: 2D resistivity model for site W79.

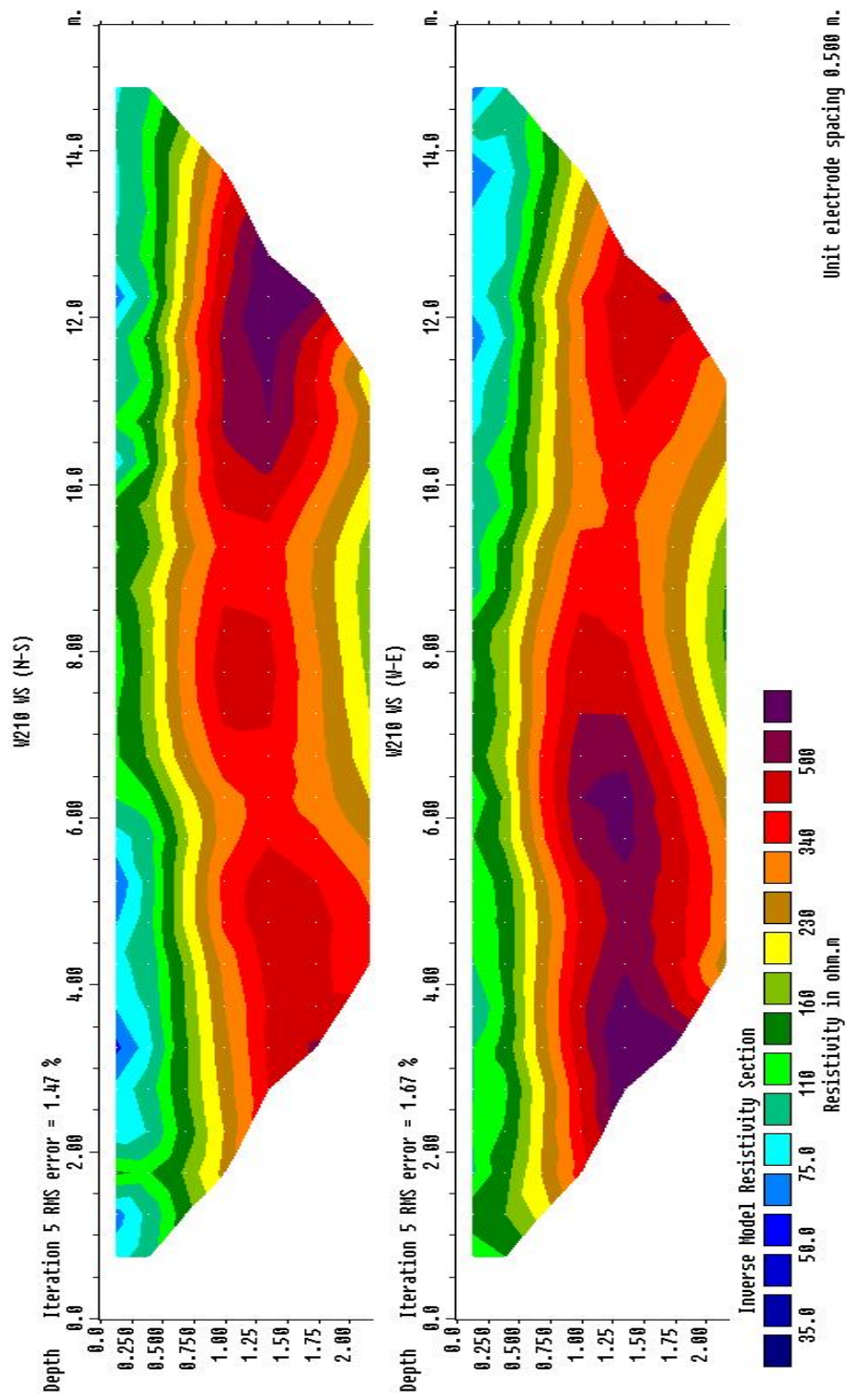


Figure 5.15: 2D resistivity model for site W210.

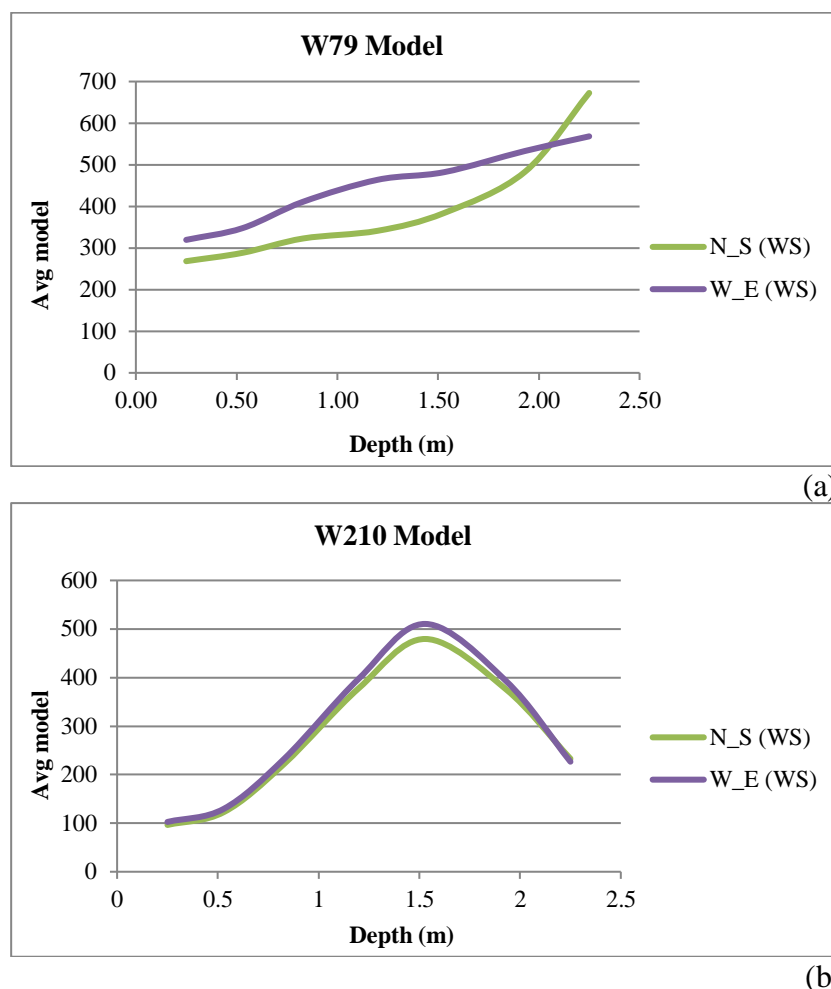


Figure 5.16: Average resistivity model for (a) W79 and (b) W210.

5.9 Summary

The average bulk soil χ_{lf} value for Wicklow is $64.8 \times 10^{-8} \text{ m}^3\text{kg}^{-1}$ though it ranges from 0 to $536.1 \times 10^{-8} \text{ m}^3\text{kg}^{-1}$. 80% of the samples contain ferrimagnetic minerals indicating widespread secondary enhancement. Although there tends to be fewer samples with higher values, 20% are $>100 \times 10^{-8} \text{ m}^3\text{kg}^{-1}$. The frequency dependent susceptibility data for Wicklow ($\chi_{fd}^{\%}$) is approximately constant between 0-8% and then increases in the 8-10% range (26%) but drops off sharply above this.

Discounting BP, the mean χ_{lf} falls into one of 3 categories. The statistics for ASP and BSWDM are very similar and they have the lowest χ_{lf} , of around $20 \times 10^{-8} \text{ m}^3\text{kg}^{-1}$ and contain about 25-30% SP grains, Table 5.9. The average χ_{lf} for ADPDM soils is about twice that of ASP and BSWDM and they have about 40% SP grains. ADWDM and ASWDM soils in turn possess an average χ_{lf} about twice that of ADPDM. The $\chi_{fd}\%$ are also the highest (50% SP grains).

Type of Soils	Average		
	χ_{lf}	$\chi_{fd}\%$	K
ADPDM	42	5.6	23.6
ADWDM	84.8	6.9	28.6
ASWDM	93.2	6.2	28.3
BSWDM	37.1	4.2	16.6
ASP	35.4	3.9	16.6
BP	3.6	0	3

Table 5.9: Average χ_{lf} , $\chi_{fd}\%$ and K for Wicklow soils.

Spatial analysis of the Wicklow data show that the lowest χ_{lf} values are associated with blanket peat and ASP soils and the highest (in the east/southeast) with ASWDM and ADWDM soils. Most of Wicklow has values less than $100 \times 10^{-8} \text{ m}^3\text{kg}^{-1}$ with the highest within a narrow zone where mineralization is known. The spatial pattern of K mirrors that of χ_{lf} (highest values are in the east/southeast). Very low $\chi_{fd}\%$ values (0-2%) are not common and are found mainly in the north central peat part of the county. Intermediate values (5-7%) are generally found in west/northwest Wicklow, whereas the higher values (>8%) are associated with high χ_{lf} locations in the east/southeast.

All sampled ADPDM soils displayed a Hopkinson peak, though in the case of 38.5% of the samples, it was poorly developed. Poorly developed Hopkinson peaks tend to be associated with high susceptibility sites whereas lower susceptibility sites have better developed ones. A large proportion of ASWDM soils (77%) have either a very weakly developed Hopkinson peak or none at all. 82% of ADWDM soils have similar characteristics to those discussed above for ASWDM. BSWDM soils mainly show a well developed Hopkinson peak as do 62% of the ASP soils.

Resistivity data were collected for 29 sites in Wicklow using the same array formats and orientations as those employed for Co. Kildare. Two 2D resistivity models examples were considered. One, displayed distinct layering and the site appeared homogeneous but the other (W79) lacked such layering and is non-homogeneous. The resistivity results are discussed in Chapter 6.

CHAPTER 6

Analysis and Discussion of Results

6.1 Introduction

Up to now, the study area has been investigated either in terms of County Kildare or County Wicklow. This is an important methodological approach as it allows comparisons to be made between each county, in terms of, for example, magnetic properties. However, magnetic properties do not change at county borders, thus in order to determine regional variations or patterns, the study area is considered in this chapter as an entity. The chapter is divided into 6 major sections which reflect the main aims and objectives of the research.

- Section 6.2 Spatial variation of the magnetic susceptibility, frequency dependent susceptibility and volume susceptibility of the study area.
- Section 6.3 Characteristics of the magnetic properties of the soils of the study area.
- Section 6.4 Assessment of correlation between magnetic susceptibility and frequency dependent susceptibility for the soils of the study area.
- Section 6.5 Electrical resistivity properties of the soils of the study area.
- Section 6.6 Analysis of GIS database using principal component multivariate analysis.
- Section 6.7 Discussion on the biogeoscientific processes that result in different magnetic and electrical properties of soil.

6.2 Spatial variation of the magnetic susceptibility, frequency dependent susceptibility and volume susceptibility of the study area

The spatial variability for low frequency magnetic susceptibility, frequency dependent susceptibility and volume susceptibility of the study area is shown in Figures 6.1, 6.2 and 6.3 respectively. Broadly, the magnetic susceptibility shows a

general pattern of values increasing from the northwest (blue) to the southeast (red), Figure 6.1. The range extends over 2 orders of magnitude. Apart from the Kildare Inlier, the northern two thirds of Kildare have a low susceptibility, similar to northwest Wicklow. The southern third of Kildare has mainly a medium susceptibility (green) of c. $50 \times 10^{-8} \text{ m}^3\text{kg}^{-1}$, with some small isolated high susceptibility regions. The NE-SW trending boundary in central Wicklow, separating low from high susceptibility areas, from a soil perspective coincides with the ASP (low) –ADWDM/ASWDM (high) boundary and from a rock perspective separates the Caledonian granite (low) from Ordovician metasediments (medium/high). The zone of highest values forms a broad arc extending from southeast Wicklow northwards. It dies out in the north underlain by Cambrian metasediments. Low (blue) and high (red) susceptibility regions cover areas of c. 1700km^2 and 800 km^2 respectively.

The obvious zoning seen in Figure 6.1 is not as prevalent for the $\chi_{fd}\%$ data, Figure 6.2. Lowest values are in the peat regions of the study area but intermediate values (4.5%, shown green) predominate for much of Kildare and western Wicklow. These soils are composed of c. 35% SP magnetic grains. Southern Kildare and eastern Wicklow have high $\chi_{fd}\%$ values, indicating >60% SP content. Volume susceptibility variations for the study area are shown in Figure 6.3. It has obvious correlations with Figure 6.1 (χ_{lf}) in that peat areas are low and that eastern Wicklow is characterized by an arc of higher K values shown in red. The central part of the study area (western Wicklow and eastern Kildare) contains very few high readings and is characterized by intermediate values.

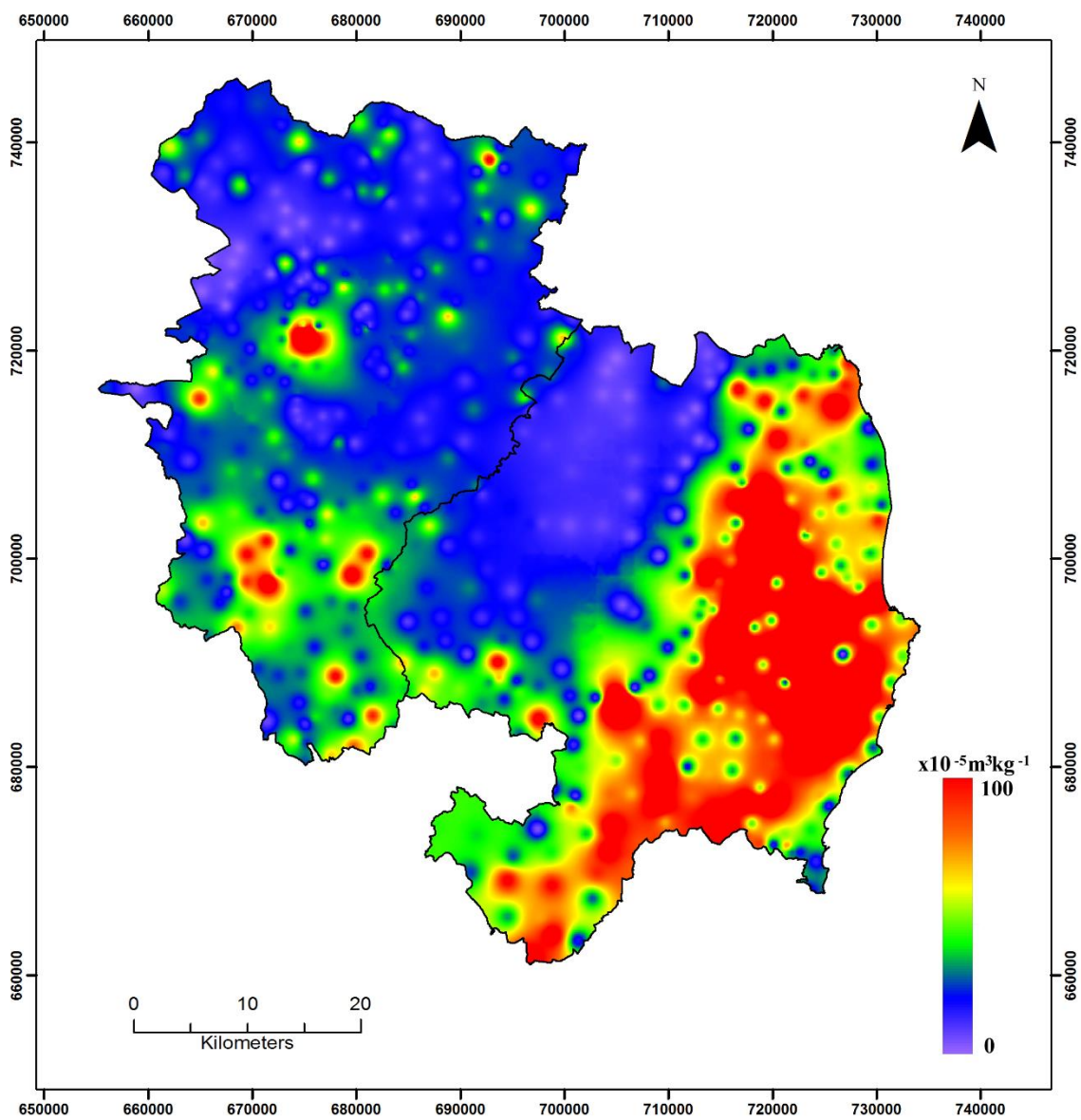


Figure 6.1: Spatial variability for low frequency magnetic susceptibility.

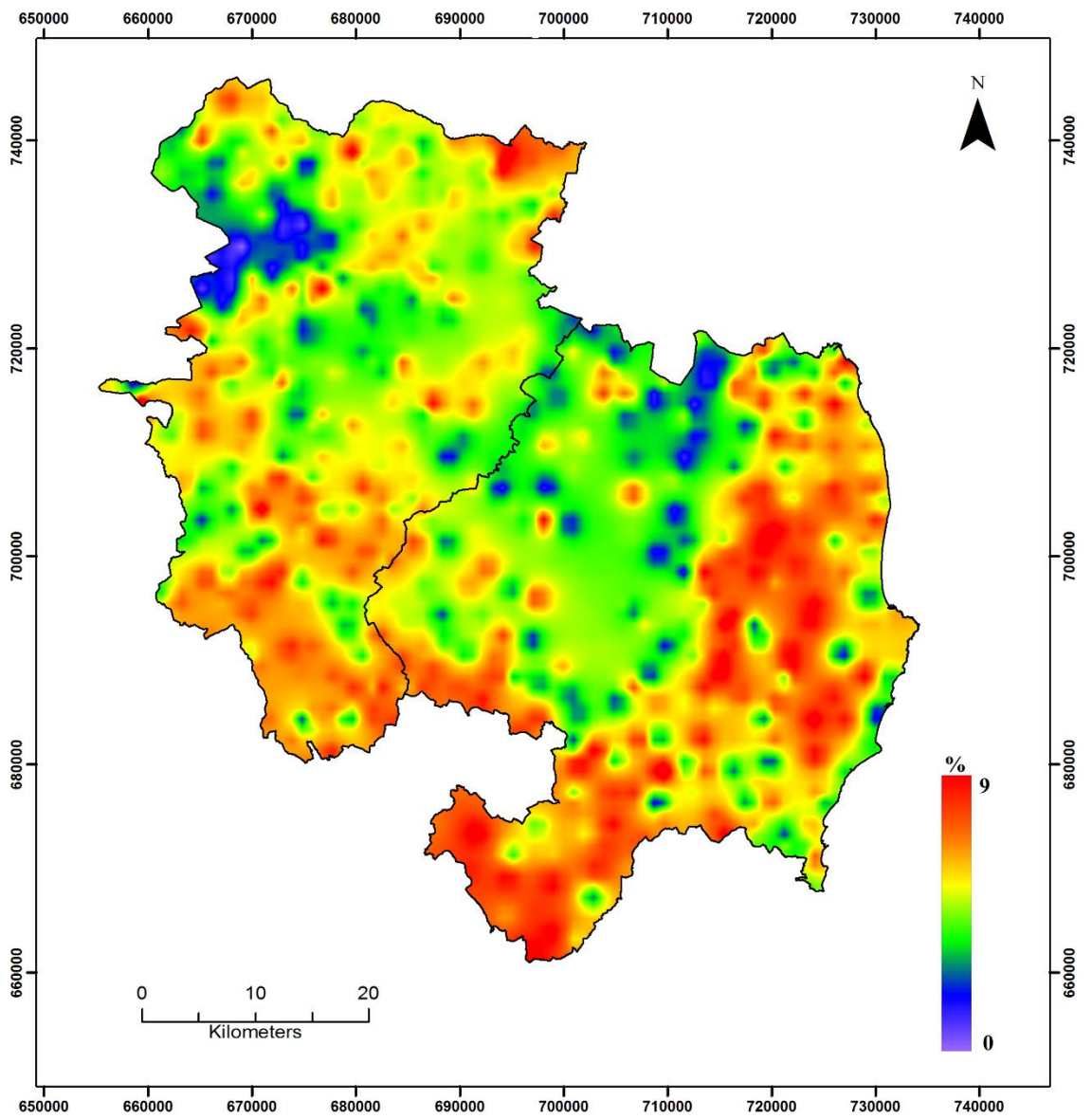


Figure 6.2: Spatial variability for frequency dependent susceptibility.

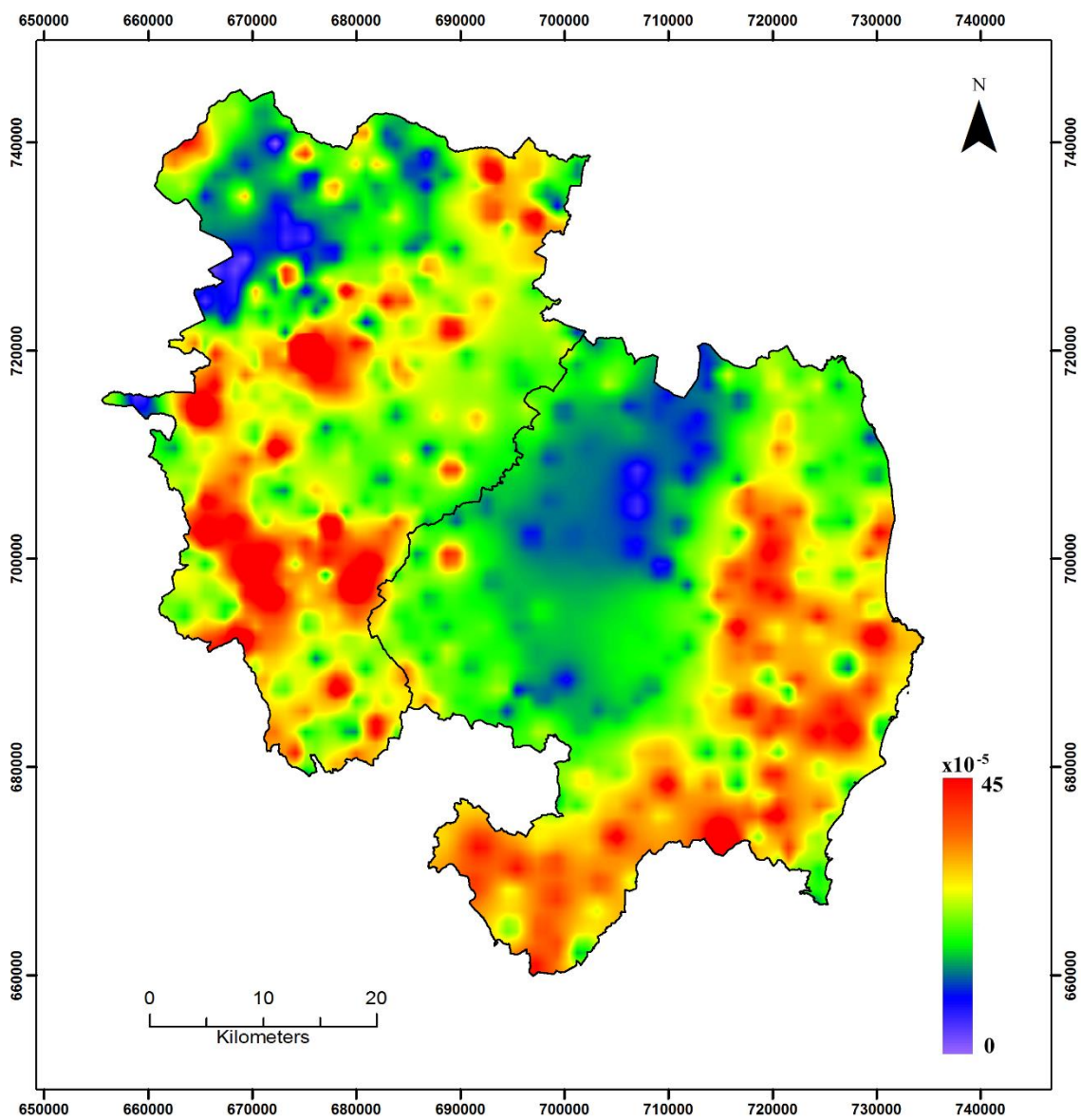


Figure 6.3: Spatial variability of volume susceptibility.

6.3 Characteristics of the magnetic properties of the soils of the study area

Table 6.1 provides some statistical parameters of the study area which in general can be considered a weighted average of the two counties.

	χ_{lf}	χ_{hf}	$\chi_{fd}\%$	K
Mean	45	41.9	5.3	25.4
Median	24.6	23	5.7	21.1
Standard deviation	68.5	63.4	2.8	20.9
Skewness	4	4.2	-0.14	7
Kurtosis	21.1	23.6	-0.8	95.6
Shapiro-Wilk	0.56	0.56	0.98	0.64
Minimum	0	0	0	0
1st Quartile	11.1	10.7	3.4	14.1
2nd Quartile	24.6	23	5.7	21.1
3rd Quartile	44.7	42.6	7.8	31.8
Maximum	604.7	602	12.9	340.9

Table 6.1: Statistical characteristics of the study area, (χ_{lf} and χ_{hf} unit: $\times 10^{-8} \text{m}^3 \text{kg}^{-1}$, **K** unit: $\times 10^{-5}$).

The study area mean of $45 \times 10^{-8} \text{m}^3 \text{kg}^{-1}$ and standard deviation of 68.5 is between the equivalent values for Wicklow $64.8 \times 10^{-8} \text{m}^3 \text{kg}^{-1}$ and $87.1 \times 10^{-8} \text{m}^3 \text{kg}^{-1}$ and Kildare $28.5 \times 10^{-8} \text{m}^3 \text{kg}^{-1}$ and $41.3 \times 10^{-8} \text{m}^3 \text{kg}^{-1}$ respectively. The very high standard deviation values are highly anomalous and are most likely as a result of a non-normal distribution of the magnetic values (Shapiro-Wilk value of 0.56, Table 6.1). 50% of the susceptibility values are within (Q1-Q3): $11.2-44.7 \times 10^{-8} \text{m}^3 \text{kg}^{-1}$. 23.6% of the Kildare soils (including peat) have a susceptibility $< 10 \times 10^{-8} \text{m}^3 \text{kg}^{-1}$ and thus contain diamagnetic and paramagnetic minerals only (no ferrimagnetic minerals). This percentage is very similar to County Wicklow, where c. 20% of the samples are $< 10 \times 10^{-8} \text{m}^3 \text{kg}^{-1}$. However, only 2.6% of the Kildare soils have a susceptibility $> 100 \times 10^{-8} \text{m}^3 \text{kg}^{-1}$, the corresponding percentage for Wicklow soils is 19.2%.

Based on magnetic values, a soil can be classified into one of nine types, Table 6.2. The middle of the medium range is the average susceptibility for Kildare and Wicklow, $45 \times 10^{-8} \text{ m}^3\text{kg}^{-1}$. The medium range is $30\text{-}60 \times 10^{-8} \text{ m}^3\text{kg}^{-1}$, values greater than $60 \times 10^{-8} \text{ m}^3\text{kg}^{-1}$ are high and those less than $30 \times 10^{-8} \text{ m}^3\text{kg}^{-1}$ are considered low. $30 \times 10^{-8} \text{ m}^3\text{kg}^{-1}$ and $60 \times 10^{-8} \text{ m}^3\text{kg}^{-1}$ are very close to the mean susceptibility of Kildare and Wicklow respectively. 59% of the samples have a low susceptibility, 20.9% a medium one and 20.1 % a high one. The mean $\chi_{fd}\%$ of 5.5 for the study area is considered to be close to the middle of the medium range which extends from 3.5-7.5%. Values greater than 7.5% are high and those less than 3% are considered low. 25.6% of the samples have a low $\chi_{fd}\%$, 46% a medium one and 28.4% a high one.

Rank	χ_{lf}	$\chi_{fd}\%$	Soil type
Soil type A	Low	Low	PEAT, ASP, BSWDM
Soil type B	Low	Medium	ADPDM, ASP, BSWDM, ALLUV, DWDM, DPDM, SWDM
Soil type C	Low	High	ADPDM
Soil type D	Medium	Low	
Soil type E	Medium	Medium	
Soil type F	Medium	High	ADWDM
Soil type G	High	Low	
Soil type H	High	Medium	ASWDM
Soil type I	High	High	ASWDM, ADWDM

Table 6.2: Soil type characterisation based on χ_{lf} and $\chi_{fd}\%$.

Peat deposits from both Kildare (raised bog) and Wicklow (blanket bog) belong to Soil Type A, i.e. low χ_{lf} and $\chi_{fd}\%$. In general, the χ_{lf} is around $0\text{-}7 \times 10^{-8} \text{ m}^3\text{kg}^{-1}$ for Kildare but tends to be slightly higher in Wicklow. The rainfall and steep slopes in Wicklow have probably resulted in fine rock material being washed down and incorporated in the peat, which, as it is 100% organic, should be non-magnetic. The average χ_{lf} for peat in England and Wales is $17 \times 10^{-8} \text{ m}^3\text{kg}^{-1}$ (Blundell et al., 2009a).

80% of the Alluvium soils are within the low susceptibility category and 20% in the medium and 0% in the high. 65% of the χ_{fd}° values are within the medium range, 20% in the high and 15% in the low. The Alluvium soil belongs mainly to Soil Type B, i.e. low χ_{lf} and medium χ_{fd}° , as does DWDM, DPDM, SWDM.

In Wicklow, ADWDM soils mostly have a high susceptibility (42.8%), though, a good proportion have a medium one (35.4%). 53.2% also have a high χ_{fd}° (30.2% medium). Of those ADWDM soils with a high susceptibility, 92.7% also have a high χ_{fd}° . It mostly falls within Soil Type I but a good proportion is Soil Type F. ASP and BSWDM soils have certain similarities in that they are both Soil Type A or B. ASWDM soils differ greatly from the two discussed above, they fall, almost equally, within Soil Type H and I. 12.5% of sites which have a high susceptibility have a low χ_{fd}° , all of which, bar one, is in the southeast within the Avoca mineralisation zone. Such high susceptibility MD grains are associated with heavy metal contamination/pollution (Lu et al., 2009) or highly magnetic clasts. The latter situation is evident for sample K300 as the basaltic Kildare inlier yielded the highest bulk susceptibility value in study area, but has a χ_{fd}° of 0.44%. Also, other magnetic rocks in Ireland have low χ_{fd}° values (serpentinite χ_{fd}° of 0.5%, gabbro χ_{fd}° of 1.2% and basalt χ_{fd}° of <1%). Such rocks do not exist around Avoca, so the observed pattern of high susceptibility, low χ_{fd}° sites originates from localities such as the Ballard iron deposit or long magnetite veins near Avoca (Tichborne (1885)) or possibly anthropogenic activity in the exploitation of the mineral deposits. ADPDM soils fall mostly within Soil Type B but a good proportion are of Soil Type C.

In conclusion, apart from peat (all Soil Type A), Soil Type B (low χ_{lf} and medium χ_{fd}°) predominates, especially in Kildare though a proportion of SWDM falls within Soil Type E. For Wicklow, the situation is more varied. ADPDM soils (Type B and C) contrast with ASWDM soils (almost equally Soil Type H and I) and ADWDM soils mostly falls within soil Type I but a good proportion are in soil Type F. ASP and BSWDM are Soil Type A or B, Table 6.2.

6.4 Assessment of correlation between magnetic susceptibility and frequency dependent susceptibility for the soils of the study area.

Correlation has 2 components: polarity and strength. Polarity can be either positive (+) - both parameters increase - or it can be negative (-), as one parameter increases, the other decreases. The strength can be ascertained by the Spearman rank. From earlier work, there is no significant correlation between χ_{lf} and $\chi_{fd}\%$ for Kildare (Spearman rank of 0.17) but for Wicklow there is a significant correlation between χ_{lf} and $\chi_{fd}\%$ (Spearman rank of 0.62) as there is for the study area as a whole (Spearman rank of 0.42). This conclusion however, may mask important variations for the soils. The DWDM, DPDM, SWDM and Alluvium soils of Kildare show no significant correlation between χ_{lf} and $\chi_{fd}\%$ (Spearman rank of 0.08, 0.001, 0.05, - 0.008 respectively). Neither do the ADPDM and BSWDM Wicklow soils (Spearman rank of 0.3, 0.17 respectively) but there is a significant correlation for the Wicklow ASP, ASWDM and ADWDM soils (Spearman rank of 0.38, 0.49, 0.75 respectively).

A concept in multi-frequency magnetic susceptibility measurement is that of ‘delta χ ’ where $\Delta\chi = (\chi_{lf} - \chi_{hf})$, (Quijano et al., 2011). This is also given the symbol $\chi_{fd}\%$ (Dearing et al., 1996b). From equation 2.2, Chapter 2, $\chi_{fd}\%$ and $\Delta\chi$ can be related thus: $\chi_{fd}\% = 100\Delta\chi / \chi_{lf}$. From this equation it may seem that as $\Delta\chi$ increases, so will $\chi_{fd}\%$. However, Table 6.3 lists 3 different scenarios, in which $\Delta\chi$ always increases. However, in case A, $\chi_{fd}\%$ remains constant, for B it decreases and for C it increases.

	χ_{lf}	χ_{hf}	$\Delta\chi$	$\chi_{fd}\%$
A	10	9	1	10
	100	90	10	10
	1000	900	100	10
B	10	9	1	10

	100	92	8	8
	1000	950	50	5
C	10	9	1	10
	100	88	12	12
	1000	850	150	15

Table 6.3: Hypothetical variation of $\Delta\chi$ with $\chi fd\%$.

Also from the above equation, it is evident that when χlf is 100, $\chi fd\% = \Delta\chi$ and at higher values, $\Delta\chi$ is greater than $\chi fd\%$. About 1 in 5 (18.8%) of the Wicklow sites have $\Delta\chi$ greater than $\chi fd\%$ and the corresponding equivalent for Kildare is 1 in 37 (2.6%).

At this time, it is worth reconsidering the 3 parameters which control susceptibility (type, concentration and magnetic state). The type of magnetic mineral in the soil is important as some, such as magnetite and maghemite are much more magnetic than others. Over 78% of the study area soils contain such minerals and this is supported by K-T curve data. Variation in the amount (concentration) of such minerals in samples is an obvious factor in determining the susceptibility value but of more relevance to the current discussion is the magnetic state of these minerals. SP grains are significantly more magnetic than MD or SD ones (Worm, 1998). Dunlop and Ozdemir (1997) report that SP susceptibility is two orders of magnitude higher than SD or MD behaviour and that ‘even a small fraction of SP material in a sample will tend to dominate the induced magnetisation’.

Thus, a high susceptibility could be due to a large concentration of MD minerals or a smaller concentration of SP grains. The two highest susceptibility values in the study area exemplify this: K300 has a susceptibility of $604.7 \times 10^{-8} \text{ m}^3\text{kg}^{-1}$ and contains about 2% SP grains, thus the high susceptibility is because of a high concentration of MD and SD magnetite (from the Kildare Inlier). Indeed, the K-T graph obtained for this sample is virtually identical to the K-T curve of MD magnetite (Chadima, 2016). However, W204 has a susceptibility of $536.1 \times 10^{-8} \text{ m}^3\text{kg}^{-1}$ but contains about 75% SP grains, thus the high susceptibility is due to a smaller amount of magnetite but it

is in SP format. The susceptibility of primary magnetic grains (i.e. broken up clasts from the host rock) is carried by frequency independent SD or MD grains (Dearing et al., 1996b).

This was confirmed by the author who magnetically analysed Irish rocks and discovered they have very low $\chi_{fd}\%$ values, i.e. contain few frequency dependent SP grains. SP grains form within the soil due to pedogenic processes and are secondary ferrimagnetic minerals (SFMs). This is also supported by other findings in this research. Over 76% of the Kildare soil samples and 80% of the Wicklow soil contain ferrimagnetic minerals, however the host rocks are virtually non-magnetic, i.e. the soils acquired their SFMs by pedogenic processes. See further discussion in section 6.7.

There is a marked difference in $\Delta\chi$ values for the two highest susceptibility samples, $2.7 \times 10^{-8} \text{ m}^3\text{kg}^{-1}$ for K300 and $51.4 \times 10^{-8} \text{ m}^3\text{kg}^{-1}$ for W204. A graph of $\Delta\chi$ (y axis) against χ_{lf} (x axis) can yield useful information about the relative importance of amount or domain state of magnetic grains in controlling the susceptibilities for the study area soils. For a soil with no SP grains, $\chi_{lf} = \chi_{hf}$ and $\Delta\chi = 0$, ($0\chi + 0$) thus all points would lie along the x axis and have zero gradient. However, a plot of $\Delta\chi$ and χ_{lf} for Kildare and Wicklow data shows that an increase in low frequency susceptibility (χ_{lf}) is related to an increase in the difference between low and high frequency ($\Delta\chi$), Figure 6.4. This difference increases with an increase in the quantity of SP grains. This linear correlation is taken to indicate that with increasing magnitude, the susceptibility is increasingly controlled by the fine (SP) pedogenic magnetic fraction (Foster et al., 1994). For Kildare, the Spearman rank coefficient = 0.87 and for Wicklow it is 0.94.

The correlation coefficient is stronger for Wicklow, compared with Kildare thus (in general) the effect of SP grains is more important in explaining the high susceptibility values for Wicklow than greater amounts of magnetic minerals.

Figure 6.5 - a plot of χ_{lf} against $\Delta\chi$ for all the study area data – shows a strong correlation of 0.92 and that most data (c. 89%) lie along the dipping alignment, i.e. the greater the amount of SP grains the higher the susceptibility. About 11% of the data (including peat which contains no magnetic grains of any size) do not conform to this alignment and for these, higher susceptibility values are due to them containing more magnetic minerals. When $\chi_{fd}\%$ is plotted against χ_{lf} (Figure 6.6a), the resultant diagram is very similar to that shown in Figure 5.3a, in that susceptibility values $<80 \times 10^{-8} \text{ m}^3\text{kg}^{-1}$ have a range of $\chi_{fd}\%$ values while those that are higher are associated mainly with high $\chi_{fd}\%$ values. A similar pattern was uncovered for Welsh topsoils, Figure 6.6b (Dearing et al., 1996b) and for Chinese loess, Figure 6.6c and Foster et al., (1994) concluded that ‘the fine-grained ferromagnetic mineral fraction is largely responsible for the climatically controlled susceptibility enhancement in the loess sediments’.

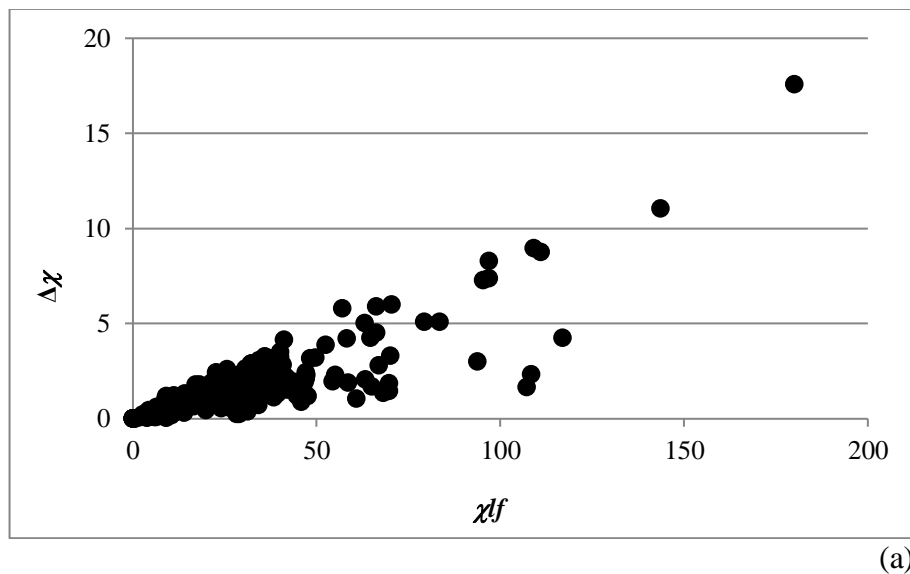
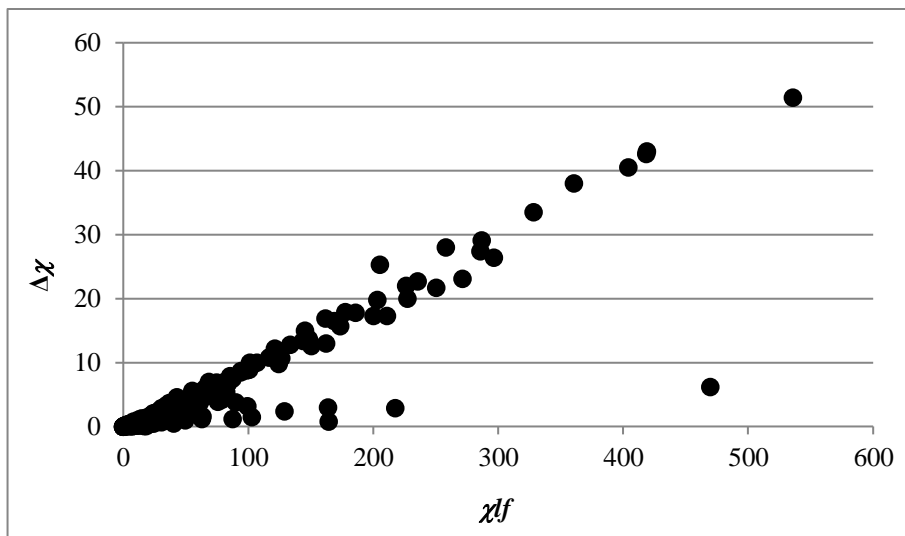


Figure 6.4: Plot of $\Delta\chi$ and χ_{lf} for (a) Kildare and (b) Wicklow data.



(b)

Figure 6.4: Continued.

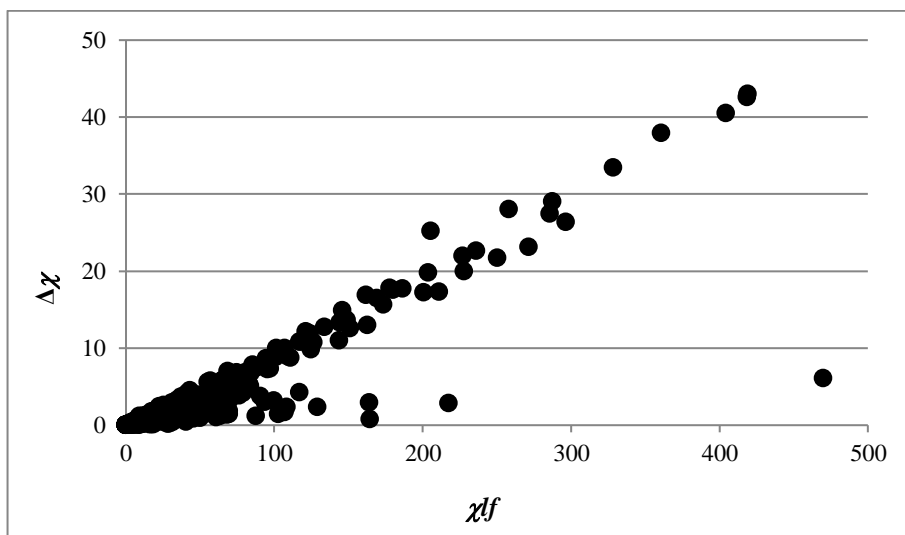
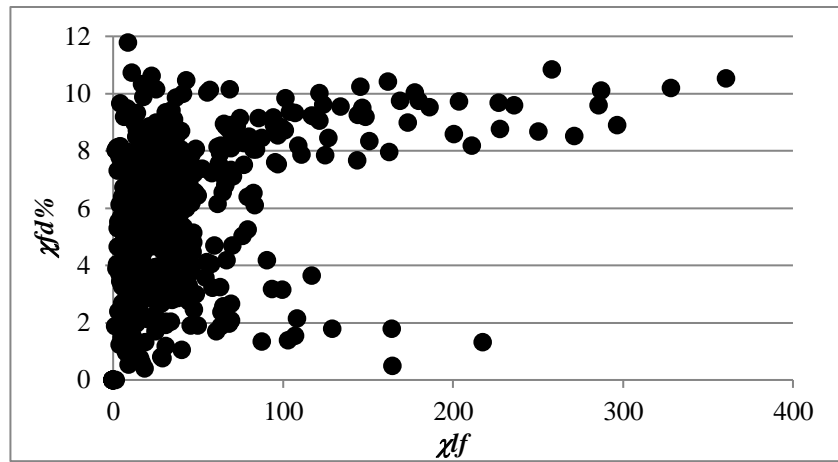
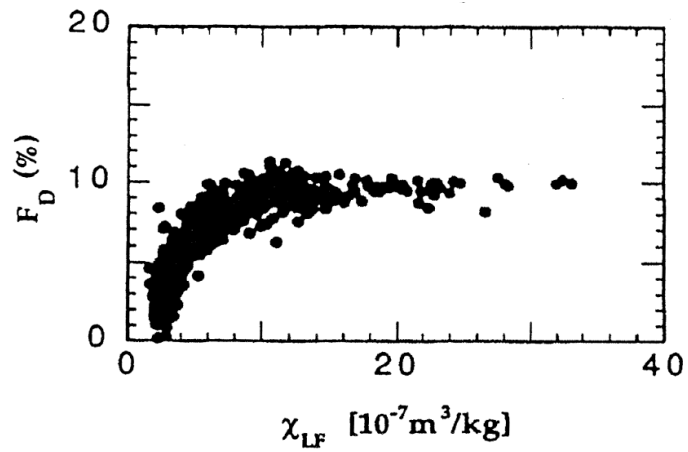


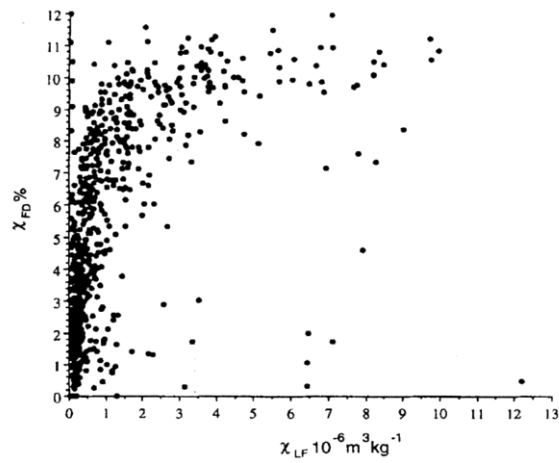
Figure 6.5: Plot of χlf against $\Delta\chi$ for all the study area soils.



(a)



(b)



(c)

Figure 6.6: (a) Plot of $\chi_{fd}\%$ against χ_{lf} for the study area, (χ_{lf} unit: $\times 10^{-8} \text{m}^3 \text{kg}^{-1}$), (b) Similar plot for Welsh topsoils (Dearing et al. (1996b) and for (c) Chinese loess (Foster et al., 1994).

6.5 Electrical resistivity properties of the soils of the study area

6.5.1 Introduction

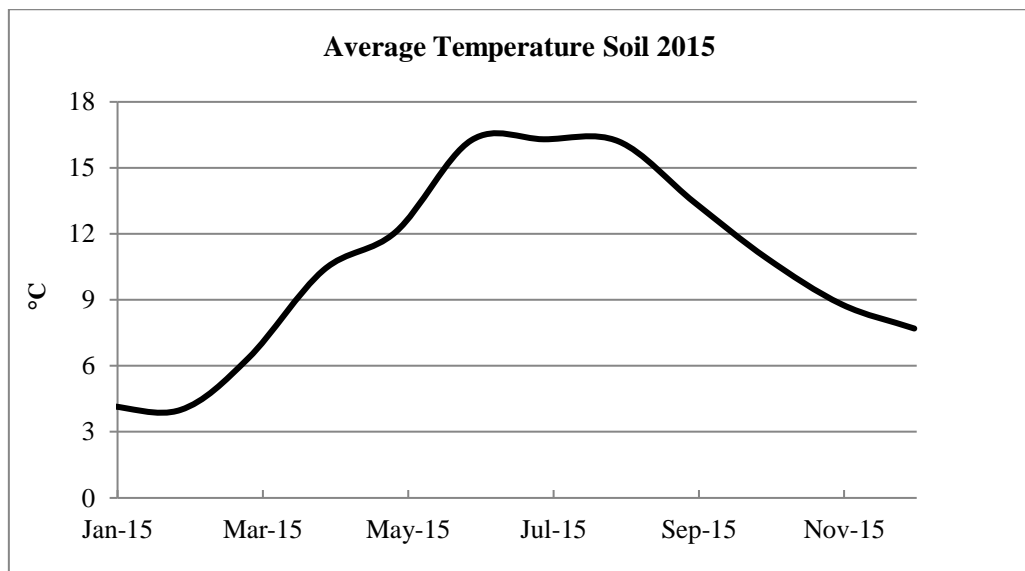
In order to directly compare the electrical resistivity properties of different soils, various external factors have first to be considered. One of these (as discussed in section 2.3.2, Chapter 2) is temperature, and all the resistivity images within this research have been normalized to 10°C. However, precipitation varies throughout the year and this can have a significant effect on resistivity. Historically, the driest month in Ireland is April and December is the wettest. An inverse relationship exists, the more water, the lower the resistivity. Temperature and precipitation variations in 2014/15 were shown in Figure 2.9 and, whereas temperature varies smoothly, precipitation is much more variable. To determine the degree to which precipitation can affect resistivity, data were collected at Site K1 at monthly intervals during 2015. Data were collected using Wenner-Schlumberger and Dipole-Dipole arrays but as the results are similar, only data from the former array are presented. The temperature and precipitation changes during this time interval are shown in Figure 6.7. Again, temperature variation is smooth and precipitation very variable. Rainfall in December 2015 was three times the average and the highest ever recorded for that month.

6.5.2 Time lapse resistivity results

A number of features can be observed from Figure 6.8 which illustrates the average 2015 monthly modelled resistivity variations near the surface (0.5m) and at 2m depth.

- Resistivity is greater at depth as was the case for most of the profiles collected in Kildare due possibly to more compaction and less moisture filled pore space. Also, the influence of high resistivity bedrock may be a factor.
- A similar variation is observed at both depths. Resistivity is lowest during the winter months (January and December) and highest in the summer (June, July and August). The difference between summer and winter is more pronounced for the shallow profile most likely because evapotranspiration will have a greater affect in the near surface layer.

- A time lag would be expected between changes at the surface and at depth (Pellicer, 2010). For example, precipitation would cause a decrease at the surface quickly, but it would take some time for the moisture to penetrate to depth. The highest resistivity near the surface is in July and drops back to low values by September whereas for the 2m profile, resistivity is still high in September and decreases in October. If data were collected weekly rather than monthly (and if the data were obtained at greater depth) the time lag would be more obvious.



(a)

Figure 6.7: (a)Temperature and (b) precipitation changes during time lapse experiment.

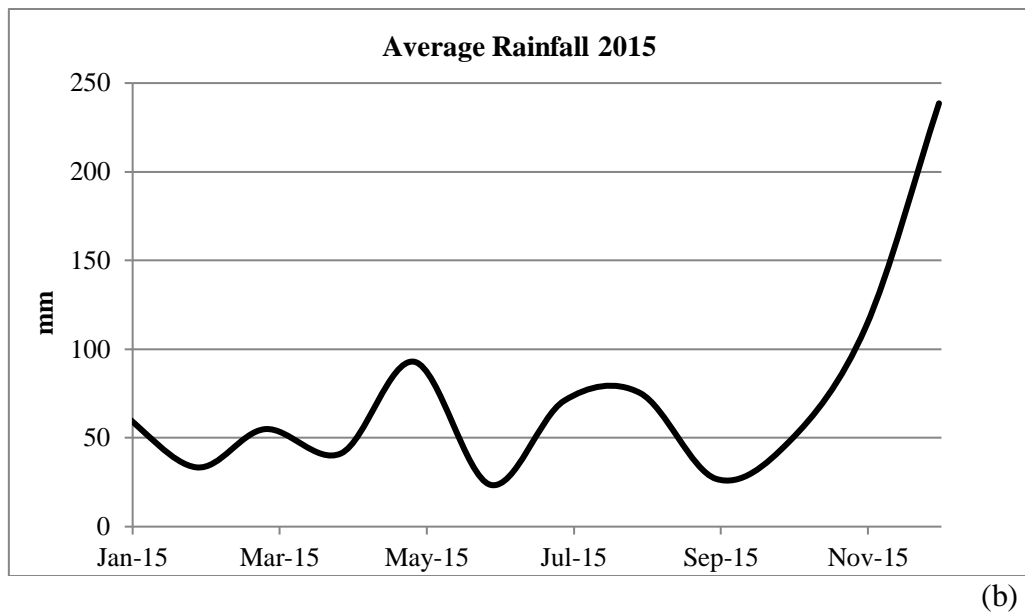


Figure 6.7: Continued.

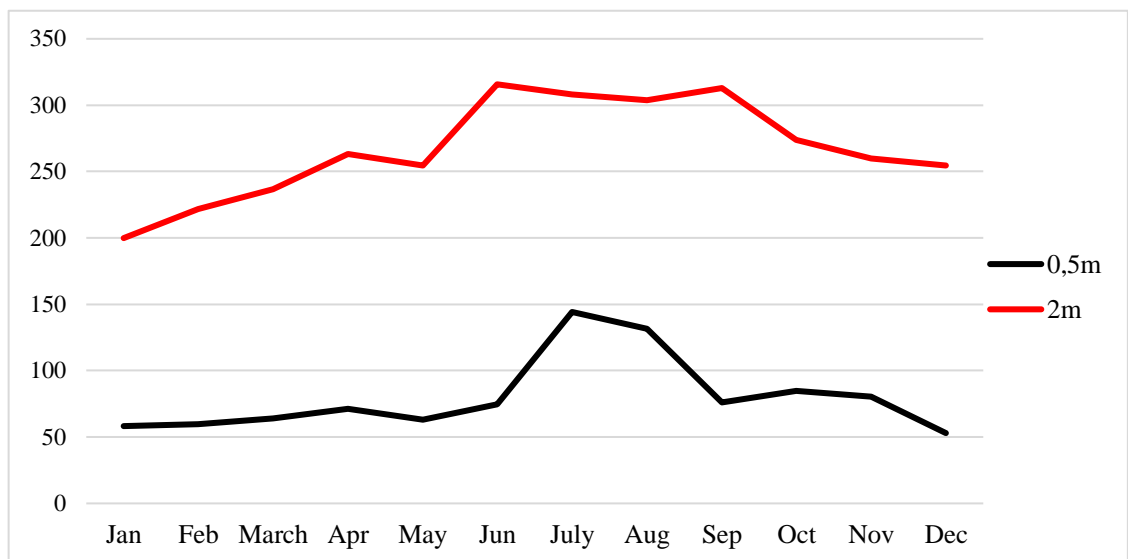
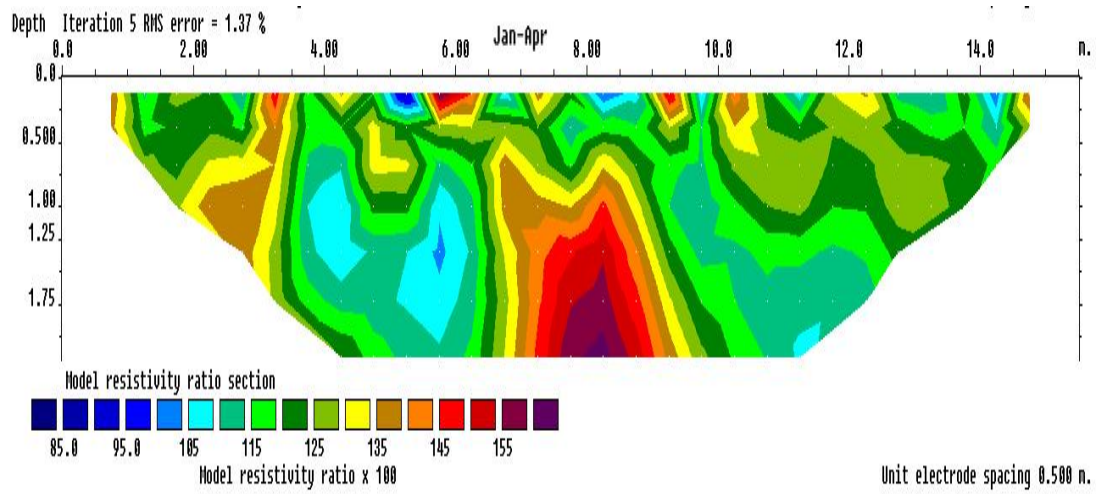


Figure 6.8: RES2DINV modelled resistivity profiles from near the surface (0,5m) and 2m depth for one year.

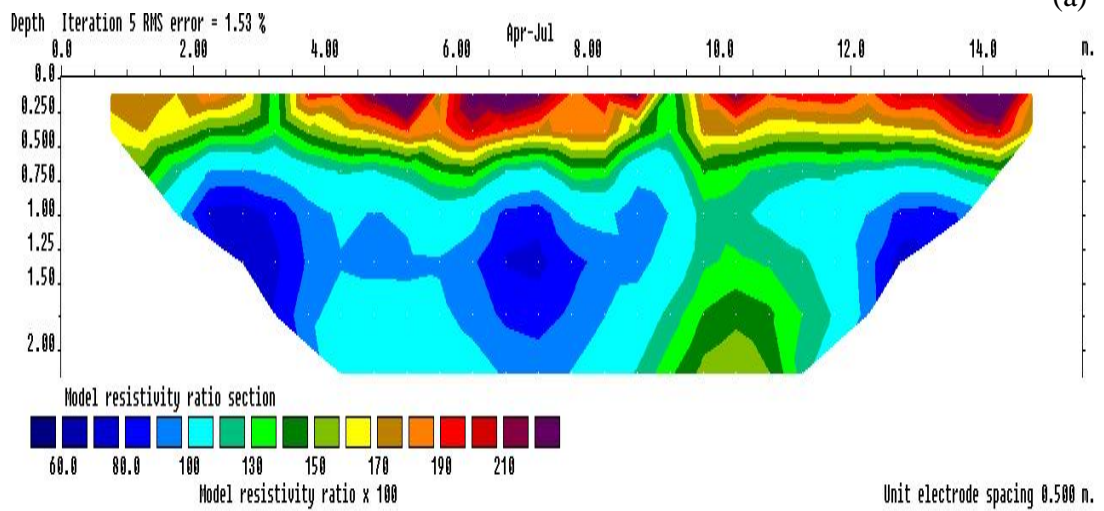
Figures 6.9 and 6.10 show the time lapse images between January-April, April-July, July-October and October-December in resistivity ratio format. Thus, a value of 100 means there has been no change in resistivity between the 2 dates, when resistivity ratio >100, the later (second) resistivity is > than (first) earlier resistivity.

Virtually all the January-April time lapse image is > 100 , thus resistivity has increased in April compared to January. This is what would be expected as the winter rains decrease as one enters spring. Most of the image is green, showing an increase of 5-25%. For April to July, a thin upper surface layer (brown-red) is evident where resistivity has increased greatly underlain by blue showing a 0-20% decrease, Figure 6.9. The higher temperature in summer (and less rainfall) results in increased evapotranspiration and the surface layers dry out, giving a higher resistivity. Between July and October, the time lapse image is essentially the inverse of the April-July image, a decrease in the upper layer (blue) and an increase at depth of up to 20%, Figure 6.10. The October to December image shows a decrease (in places up to 60% of October values) for most of the subsurface as shown by the blue, green and yellow colours. This is due to increased winter rainfall.

A number of conclusions can be taken from this investigation. Firstly, time lapse studies add an extra dimension to the information that can be obtained from resistivity. These traverses are only 16.5m in length, thus the temperature and precipitation conditions along their length are constant. However, there are often marked differences in changes in resistivity at the same level which could indicate facies change, different degrees of compaction or pore space volume. Secondly, in the study area, resistivity values in summer can be up to 100% higher than those in winter. For example, a resistivity of 43 Ohm-m was allocated to a model block in December and a value of 110 Ohm-m to the same block in July. This latter conclusion may seem to make direct comparisons between resistivity lines acquired on different dates impossible; however, it shows that one should plan resistivity surveys so that time lapse studies do not encompass the extremes. The Wicklow resistivity data (shown in Chapter 5) were collected between 23rd April 2015 and 8th June 2015 (80% in May alone). Thus, whereas 43 Ohm-m and 110 Ohm-m were allocated in December and July, 67 Ohm-m (April) and 63 Ohm-m (June) were the values of the same model block when data were collected.



(a)



(b)

Figure 6.9: Time lapse image for site K1 for (a) January-April and (b) April-July periods in resistivity ratio format.

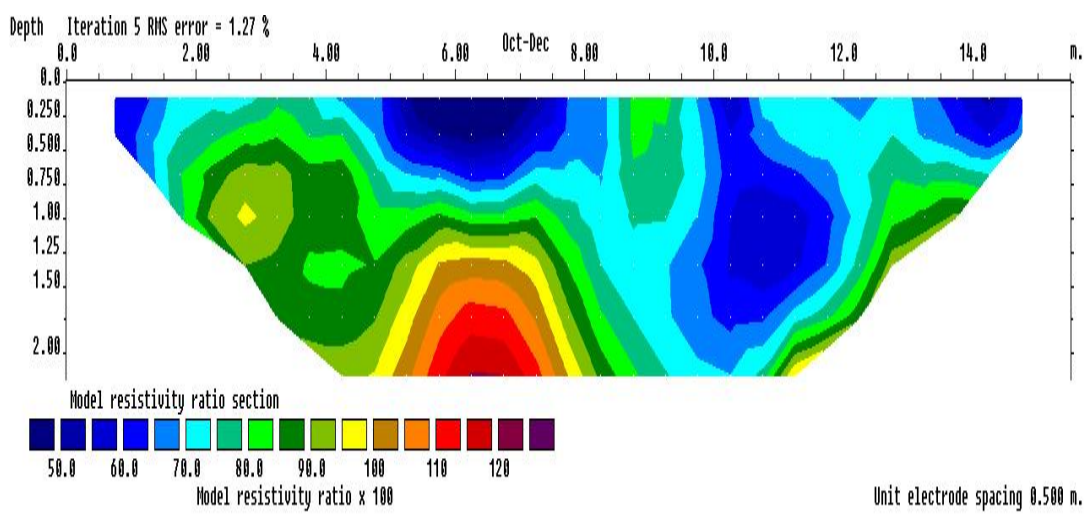
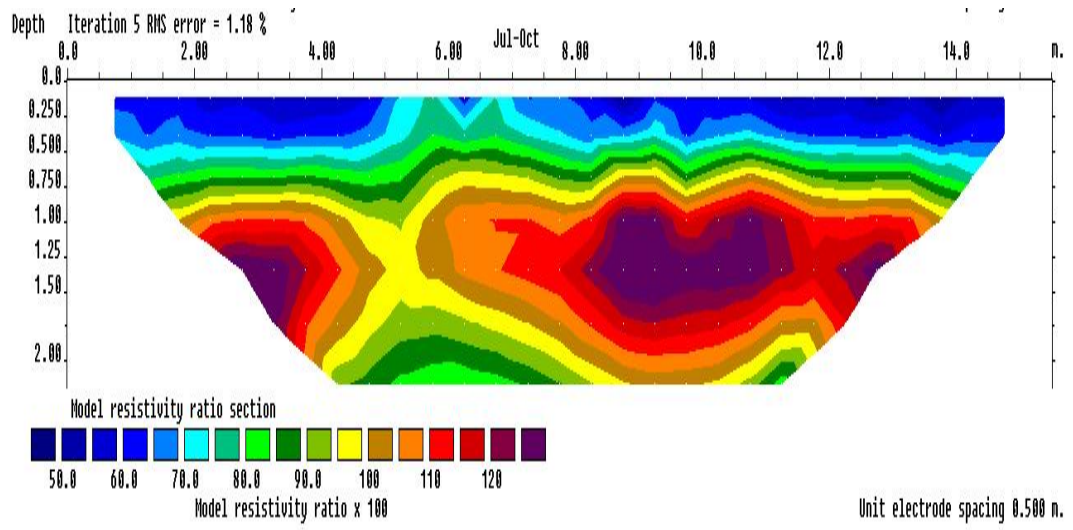


Figure 6.10: Time lapse image for site K1 for July-October and October-December periods in resistivity ratio format.

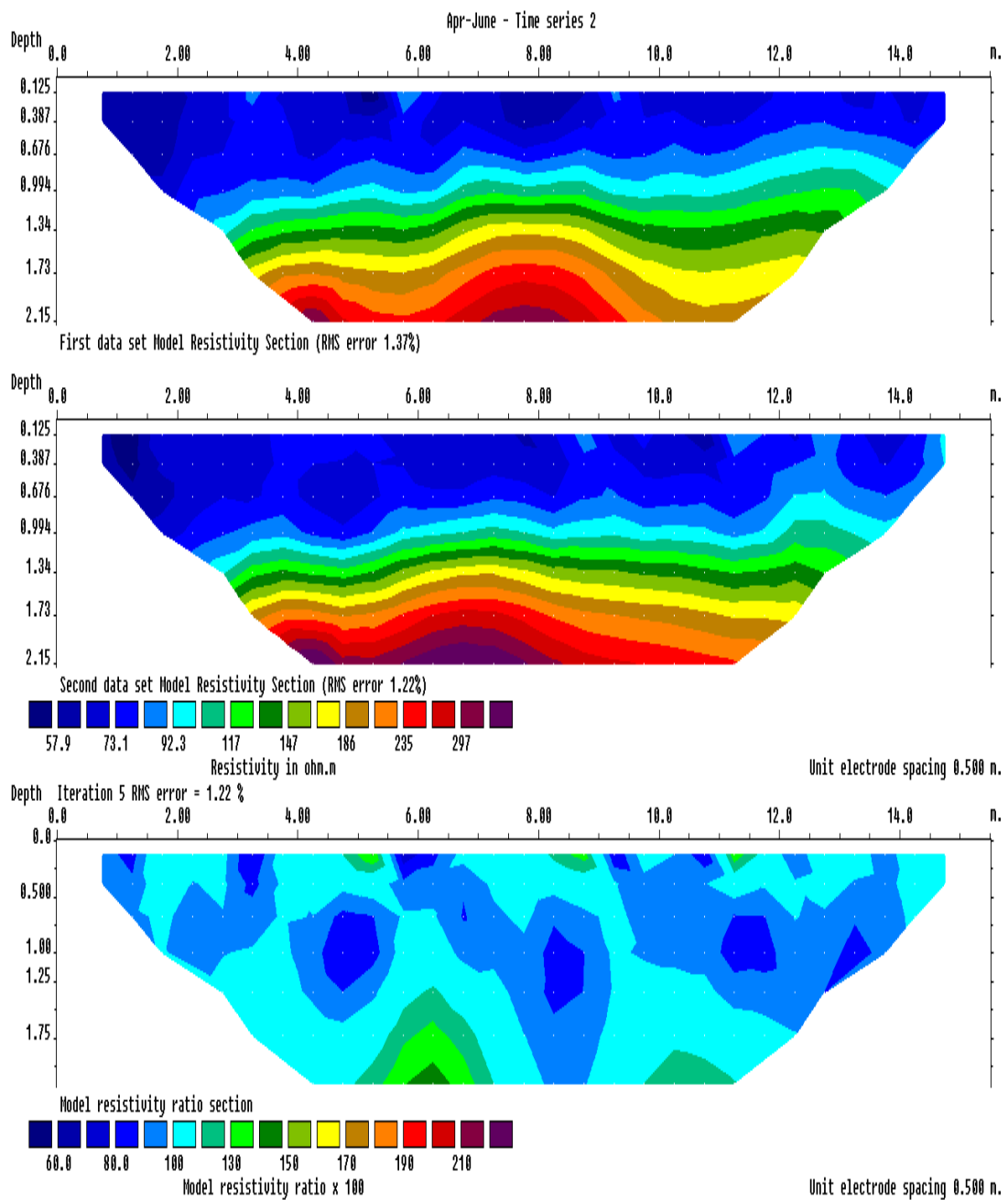


Figure 6.11: Time lapse image and the separate April and June models.

Figure 6.11 shows the time lapse image alongside the separate April and June models and there is very little difference between them – thus Wicklow results are comparable. 96% of the Kildare resistivity data were collected in July to September 2014 (72% in September alone) and are directly comparable with each other. Most of the Wicklow data were gathered in May and the Kildare data in September and comparing equivalent months, one would expect May data (Wicklow) to be about 77.7% of the September data (Kildare).

6.5.3 Analysis of resistivity in the study area.

Resistivity data were collected at 28 Kildare and 29 Wicklow sites and in this section three aspect of the data are analysed. Firstly, the absolute values provide information on the types of sediments which may be present within the top 2m. Well-drained coarse sediments such as fluvio-glacial sands will have much higher resistivity values than poorly sorted fine-grained clays (Pellicer, 2010). Secondly, the subsurface patten of resistivity may prove useful. Do the beds dip? does resistivity increase or decrease downwards? Do any trends exist? The third aspect considered here is that of spatial distribution. Is resistivity higher (or lower) in any particular part of the study area?

Data were collected in both Dipole-Dipole and Wenner-Schlumberger format. Generally, the model pseudosections and inverse model shapes for the arrays were similar. However, although the shapes were similar, the absolute values differed with the Dipole-Dipole resistivity values being less than the Wenner-Schlumberger ones. As Wenner-Schlumberger data were never less than Dipole-Dipole data, this appears to be an artifact of the modelling program and should always be borne in mind if one is comparing data obtained by a third party using a different array. The ‘n’ factor for the array type may also differ and should always be included with the metadata. As discussed in Chapter 2. The ‘n’ factor for this research for Dipole-Dipole ($c2-p1/c2-c1$) for levels 1, 2, 3 was 0.33, 0.66, 1 and for Wenner-Schlumberger 0.5, 1. 1.5 ($c1-p1)/(p1-p2)$).

Site	Minimum	Maximum	Soil type
------	---------	---------	-----------

K12	114.52	1335.3	ALLUVIUM
K209	55.02	134.26	ALLUVIUM
K1	31.75	297.2	DPDM
K81	31.29	716.21	DPDM
K 220	77.9	176.77	DPDM
K221	40.41	276.45	DPDM
K36	56.8	296.4	DPDM
K2	48.89	260.02	DWDM
K89	68.53	237.69	DWDM
K143	46.38	337.12	DWDM
K180	58.87	227.94	DWDM
K186	59.17	407.15	DWDM
K230	81.41	241.81	DWDM
K298	88.13	494.71	DWDM
K139	43.281	494.71	DWDM
K16	145.31	878.41	DWDM
K117	45.41	150.11	DWDM
K150	43.44	155.28	PEAT
K53	131.93	1092.4	SWDM
K14	128.32	348.73	SWDM
K46	241.83	1242.9	SWDM
K250	83.37	1159.5	SWDM
K114	36.64	176.91	SWDM
K178	66.66	278.66	SWDM
K271	55.13	322.23	SWDM
K138	26.17	397.97	SWDM
K189	15.45	334.12	PEAT
W247	94	1861	ADPDM
W4	151.7	1934.3	ADWDM
W14	70.5	214.7	ADWDM

W15	383.4	10088	ADWDM
W47	206.6	3028	ADWDM
W48	210.9	2580	ADWDM
W49	188.68	3391.5	ADWDM
W51	146.5	642.9	ADWDM
W119	110	344.5	ADWDM
W126	148.25	1630	ADWDM
W135	143.3	1932	ADWDM
W146	106.6	1527.6	ADWDM
W173	173.15	3141.4	ADWDM
W181	99.76	268	ADWDM
W187	332	19817	ADWDM
W192	248.33	916.4	ADWDM
W216	93.3	238	ADWDM
W217	102.4	252.36	ADWDM
W234	266	9665	ADWDM
W248	295.29	3885	ADWDM
W249	297.7	2448	ADWDM
W35	261	9765.5	ASP
W38	68.17	3028	ASP
W17	409.9	15259	ASWDM
W79	131.56	1113	ASWDM
W210	56	706	ASWDM
W250	220	6992	ASWDM
W2	120.5	237.2	BSWDM
W34	119	5309	PEAT

Table 6.4: Minimum and maximum model resistivity (unit: Ohm-m) values for Kildare and Wicklow soils.

Analysing Table 6.4, which give the minimum and maximum Wenner-Schlumberger model resistivity for soils in Kildare and Wicklow, shows a pronounced difference between the two counties. The maximum model resistivity for Wicklow is significantly greater than that of Kildare. Only 14.8% of Kildare sites have a maximum model resistivity > 1000 Ohm-m, whilst the corresponding percentage for Wicklow is 66%. All Wicklow soils (except BSWDM for which only one traverse was acquired) have at least one site >1000 Ohm-m. Average resistivity are given in Table 6.5. The minimum values for Kildare and Wicklow are similar, but there is more than an order of magnitude difference for the maximum values.

Average Minimum Resistivity	Average Maximum Resistivity	Soil type
74.4	469.4	All Kildare
181	3869.8	All Wicklow
204.5	6017.5	ASWDM
120.5	237.2	BSWDM
164.6	5227.45	ASP
94	1861	ADPDM
188.7	3397	ADWDM
84.7	734.5	ALLUV
47.8	304.6	DPDM
96.2	627	SWDM
68.3	372.6	DWDM

Table 6.5: Average minimum and maximum model resistivity values. (resistivity unit: Ohm-m).

Similarly, with individual soil types, those in the western half of the study area have an average maximum modelled resistivity value that is markedly lower than those in the east. Precipitation will relatively easily soak into a soil; one would expect a low near surface resistivity. As soil depth increases, one intuitively assumes so will compaction, reducing pore space. Thus, less water will penetrate to depth and thus a

higher resistivity should be found. A good proportion of the study area soils have this type of pattern. However, many profiles, especially in Wicklow (50% of Wicklow sites) have low resistivity near the surface, a higher mid depth resistivity and a lower resistivity at depth. This trend is rare in Kildare: (K230). There is little resistivity variation with depth for some sites: (W216 and W2) whilst others display a mid-depth resistivity layer that is lower than the resistivity at depth or at the surface. This 'trough' profile is uncommon in Wicklow. A high near surface resistivity decreasing with depth pattern is probably due to a well draining surface layer. There is an obvious pattern for resistivity for ADWDM soils in Wicklow. 60% of ADWDM sites have low resistivity near the surface, a higher mid depth resistivity and a lower deep resistivity and 15% have an increasing resistivity with depth profile. All these sites are associated with high maximum model resistivity. ADWDM sites in which resistivity decrease with depth or remains approximately constant have a maximum model resistivity that is an order of magnitude lower.

The resistivity data were analysed to ascertain if there was any spatial context to (a) absolute values and (b) resistivity patterns. In addition, any patterns regarding the magnetic parameters of the sites were also investigated. Sites K180, K230 and K178 are close to each other but one has a 'trough' resistivity pattern, one has an increasing resistivity with depth pattern and the third a low resistivity near the surface, a higher mid depth resistivity and a lower deep resistivity pattern. A similar spatial study of Wicklow data produced no correlation.

The spatial variation of level 1 modelled average resistivity is displayed in Figure 6.12. The lowest resistivity is 56.8 Ohm-m and is at site K199 and the highest in Wicklow (1169 Ohm-m at site W250). The highest values are located in southwest Wicklow and extend in a broad zone north-eastward along the axis of the Wicklow Mountains. A narrower northwest trending high resistivity zone extend across central Kildare. This trend is discussed in section 6.7.

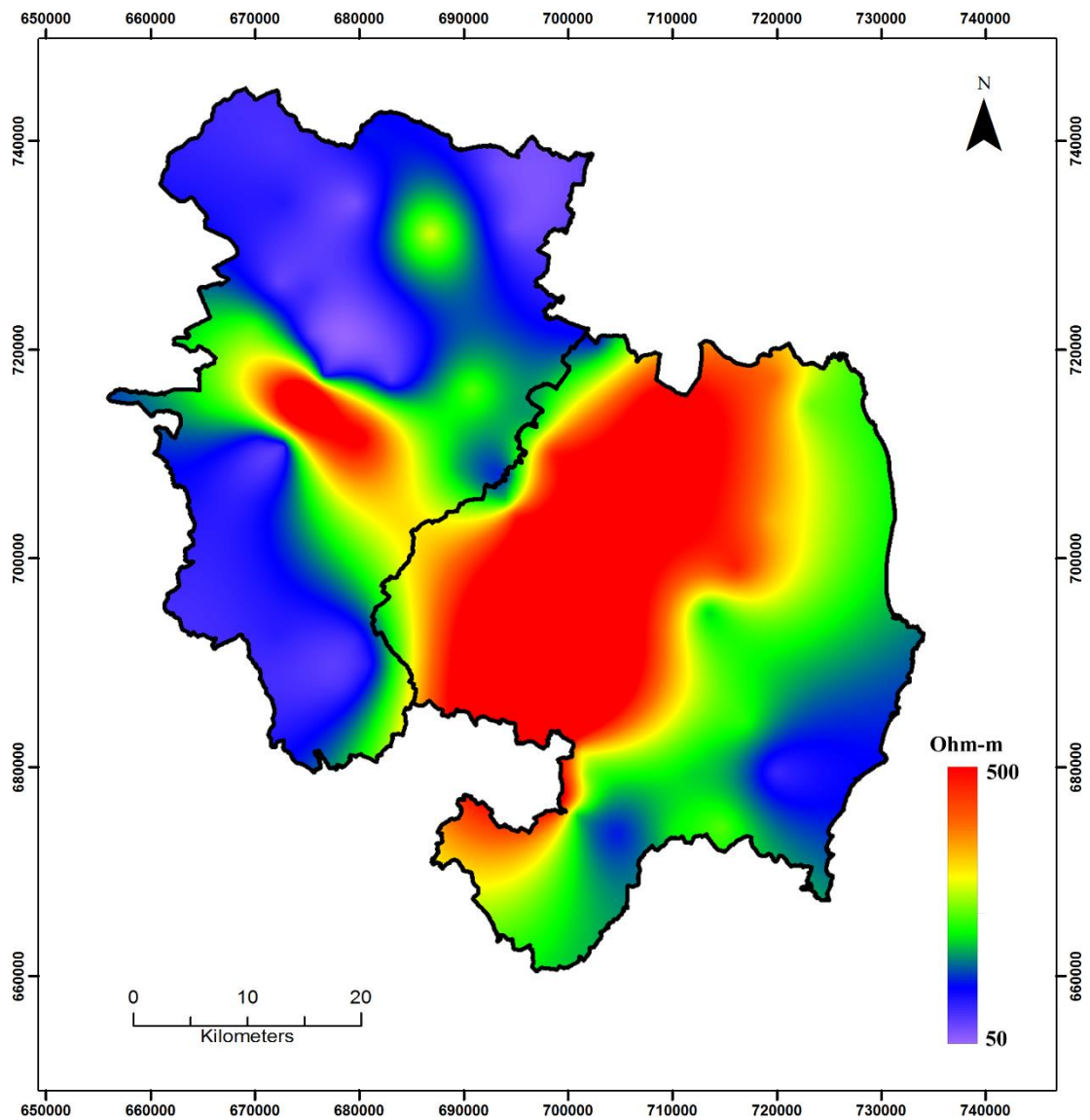


Figure 6.12: Spatial variation of modelled average resistivity for topmost soil layer (50 cm).

6.6: Principal Component Multivariate Analysis of GIS database

During the course of this research, the spatial variation of a number of parameters have been determined. These are mass specific magnetic susceptibility, frequency dependent magnetic susceptibility, volume magnetic susceptibility (Figures 6.1-6.3) and modelled layer 1 resistivity (Figure 6.12). These were input into an Arcmap GIS

database as individual layers. However, other data for the study area were available to the author and these were also input into the database. These included a digital elevation model, a soils map, a geological map and a glacial landforms map. In addition, the Geological Survey of Ireland provided 9 geochemical datasets:

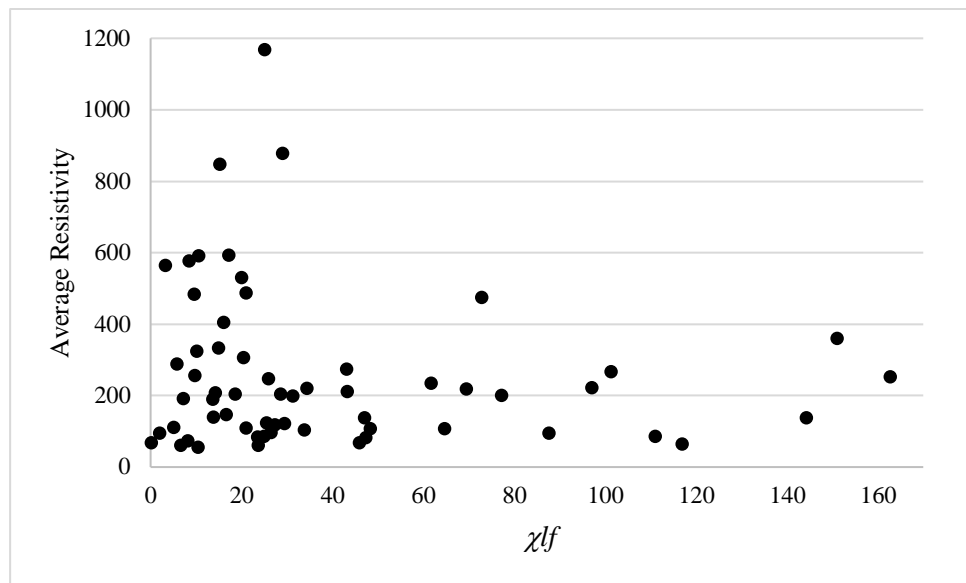
- Iron whose concentration varies from 1.3-3.2% with very low values throughout the study area except in SE Wicklow.
- Lithium whose concentration varies from 9.9-74.3 ppm (parts per million) with low values in Kildare and high values over the Caledonian granite in Wicklow.
- Nickel whose concentration varies from 11.2-46.1 ppm with the high values in NE Kildare, medium in SE Wicklow.
- Copper whose concentration varies from 11.4-31.1 ppm with very high values in NE Kildare and low everywhere else.
- Zinc whose concentration varies from 69.1-165.1 ppm, very high in NE Kildare and low everywhere else.
- Uranium whose concentration varies from 1.2-5.5 ppm with the highest values in south Kildare and SW Wicklow, low values elsewhere.
- Tin whose concentration varies from 0.8-7 ppm, low in Kildare and high in Wicklow
- Lead whose concentration varies from 21.2-64.6 ppm, very high values in east Wicklow, medium in NE Kildare and low in east Kildare.
- Mercury whose concentration varies from 0.08-0.2 ppm with low Kildare values and high in central Wicklow.

Thus, the GIS database is composed of 17 variables which may possibly be correlated. Principal Component Analysis (PCA) is a statistical method in which the possibly correlated variables are converted into a set of variables whose correlation is zero, called principal components. It is a statistical technique used to determine the relatedness of variables. The results are given in terms of a correlation matrix, eigenvalues and an eigenvector matrix. The variance of the database is redistributed

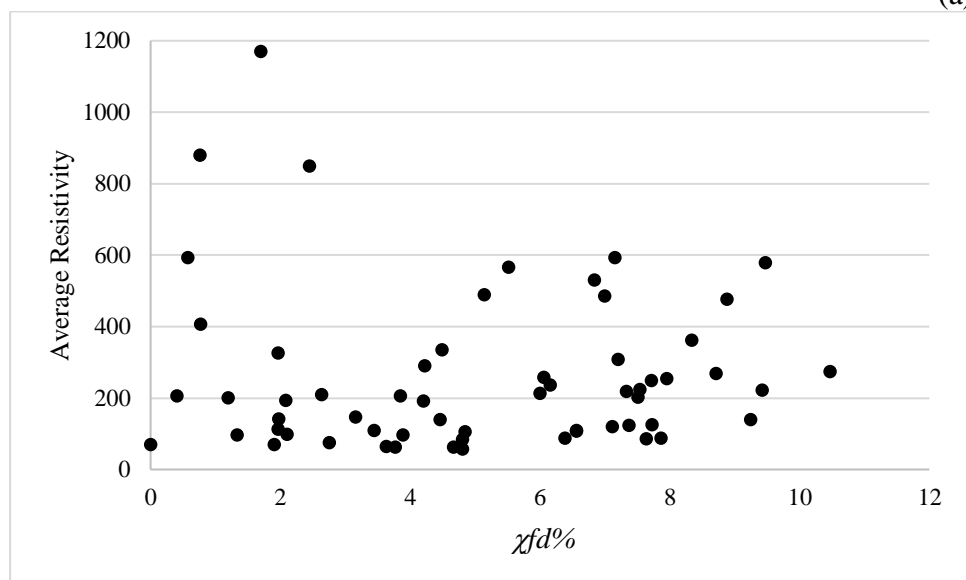
such that the first principal component (PC1) has the greatest variance (accounts for most of the database variability) with higher principal components having progressively lower variances (smaller eigenvalues).

The correlation matrix shows that the highest correlation that χ_{lf} has with any other variable is with iron (Fe). The positive value of 0.60 is strong and not unexpected, soils with high concentrations of iron have a greater capacity to form ferrimagnetic minerals which would be reflected in higher values of χ_{lf} . The other geochemical elements (copper, lithium, tin, lead, mercury, uranium) have a weaker positive relationship with χ_{lf} , though in the case of nickel and zinc, the correlation is negative. The strong positive correlation of χ_{lf} and K (0.52) is also expected. One of the aims of this research was to determine if a correlation existed between mass specific magnetic susceptibility and percentage frequency dependent susceptibility (χ_{lf} and $\chi_{fd\%}$). Earlier work in this chapter showed that neither DWDM, DPDM, SWDM and Alluvium soils of Kildare nor ADPDM and BSWDM Wicklow soils show a significant correlation between χ_{lf} and $\chi_{fd\%}$ but there is a significant correlation for the Wicklow ASP, ASWDM and ADWDM soils. This variation is reflected in the positive correlation value of 0.47 between χ_{lf} and $\chi_{fd\%}$ which is reasonably strong.

The correlation between χ_{lf} and resistivity and $\chi_{fd\%}$ and resistivity is statistically virtually zero. Magnetic and resistivity data were collected at 57 sites within the study area. The average of the modelled resistivity for layer 1 (nearest the surface) was plotted against χ_{lf} and $\chi_{fd\%}$, Figure 6.13. These graphs support the conclusion there is no correlation. However, see discussion in next section.



(a)



(b)

Figure 6.13: Plot of (a) χ_{lf} data against average modelled resistivity data and (b) $\chi_{fd}\%$ against average modelled resistivity for layer 1.

The correlation between χ_{lf} and topography is also virtually zero. This may seem an anomalous result because the soils with the highest χ_{lf} values are in Wicklow where the highest elevations are found. However, this trend is balanced by the presence of blanket peat (χ_{lf} values close to zero) at high elevations in the Wicklow Mountains. Also, the correlation between χ_{lf} and geology and glacial sediments is very weak

(0.08). There is however, a good correlation (0.4) between χ_{lf} and soils, thus the latter are an important determining factor in susceptibility.

A strong positive correlation (0.6) exists between resistivity and topography. Resistivity has a strong negative correlation (-0.63 and -0.42) with nickel and zinc respectively and a strong positive one (0.68) with lithium, uranium (0.5) and tin (0.62). It also has a good correlation with soils (0.47) showing that soil characteristics influence the resistivity. Soils and iron content are highly correlated (0.69). Based on the eigenvectors for the GIS database PC1 accounts for 86.68% of the database variability, PC2 for 13.03%, and PC3 for 0.21% with the higher PCs combined accounting for only 0.08% of the variability. Figure 6.24 shows an image in which PC1 is projected in red, PC2 in green and PC3 in blue light. This image encompasses 99.92% of the variance of the 17 layers database.

Black areas display the lowest variance in the study area, and many of them are the peatlands of western Kildare. These are very flat areas with low concentrations of geochemical elements and are associated with very low χ_{lf} and $\chi_{fd}\%$ values. Blue/green regions have low to medium variance and dominate Kildare and north Wicklow. Yellow/red on Figure 6.24 represents high variance regions and is most evident in the southern part of Wicklow. This is an area of high variability: iron concentration is high but copper and zinc concentrations are low. It is an area of high $\chi_{fd}\%$ for soils with large amounts of SP grains and low $\chi_{fd}\%$ for non-frequency dependent soils.

The results discussed here show that geophysical magnetic and resistivity data such as those collected in this research can be combined with geochemical data such as those given in the Geochemical Atlas of Ireland (Fay et al., 2007) and statistically analysed to yield a much more informative useful digital database. The geochemical samples for the Atlas were taken at a depth of 10cm, similar to the magnetic data. Only 1310 soil samples were obtained for geochemical analysis for the Republic of Ireland, whilst 550 soil samples were taken in Kildare and Wicklow for this study.

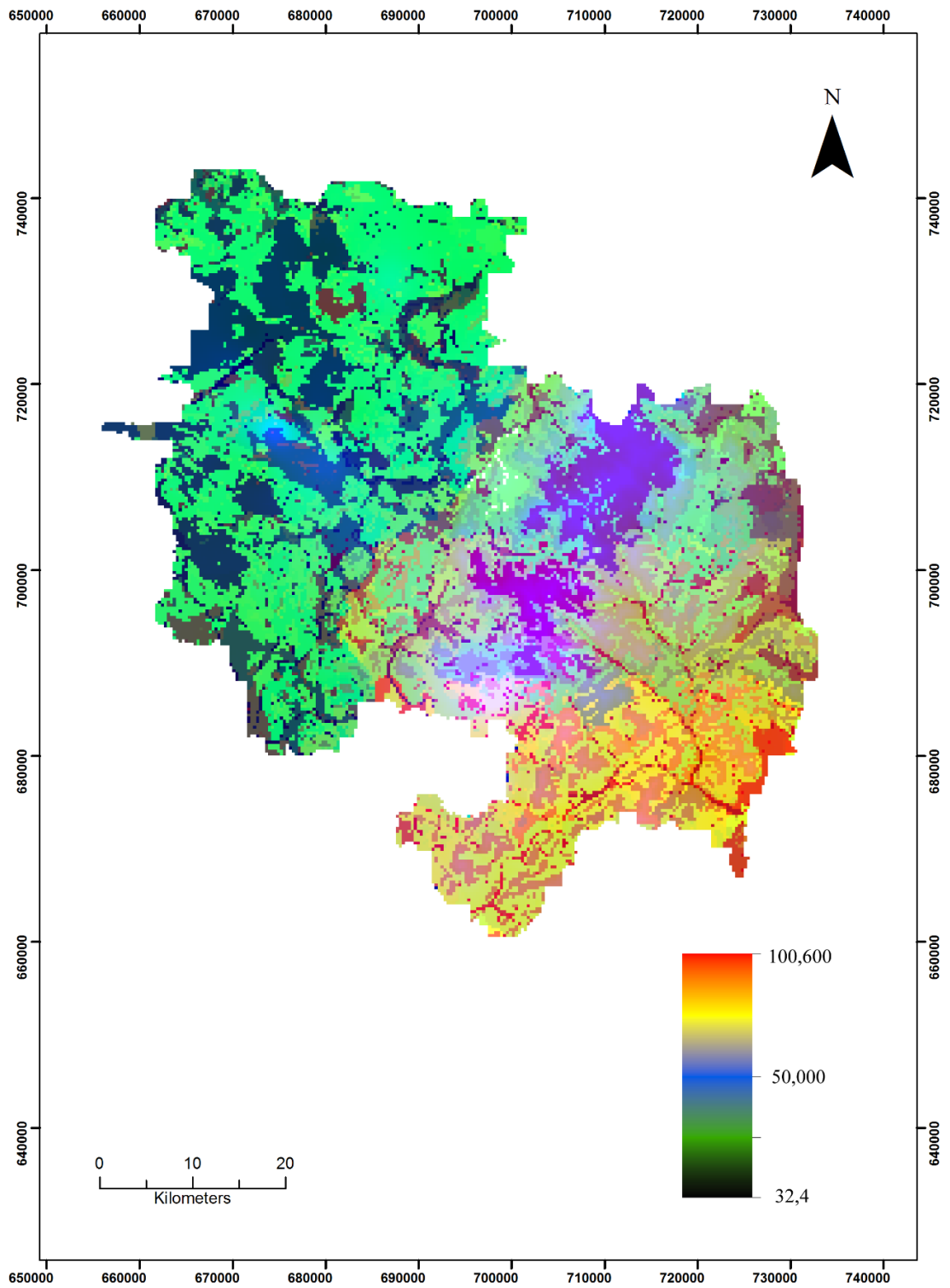


Figure 6.14: Principal components map of study area in which PC1 is projected in red, PC2 in green and PC3 in blue light.

6.7 What are the biogeoscientific processes that result in different magnetic and electrical properties of soil?

In this final section, potential biogeoscientific reasons for the observed magnetic and resistivity properties are discussed. The average magnetic and resistivity characteristics of 11 different soil types were investigated in this thesis, Table 6.6. Various hypotheses have been suggested in order to explain the presence and enhancement of ferrimagnetic grains in soils (Dearing et al., 1996b). These include:

- Concentration of primary ferrimagnetic minerals from parent material.
- Accumulation of airborne magnetic particulates, generally from a pollution source.
- Magnetotactic bacteria which produce SD magnetite.
- Formation of ferrimagnetic minerals from weakly magnetic minerals due to fire.
- A ‘fermentation’ process, in which anaerobic microbial Fe reduction is followed by formation of magnetite or maghemite.

Some of these hypotheses such as pollution sources or effects of fire may be relevant in small localised areas but they cannot explain the magnetic patterns observed in this study. Similarly, concentrations of magnetotactic bacteria are too low to be a major source of magnetism (Dearing et al., 1996a).

In general terms, one can consider three broad interconnected controlling factors for the magnetic and resistivity variability seen in this study: variations in the physical environment, changes in the chemical environment and changes in the biological environment. Changes in the physical environment include different bedrock types, porosity and permeability of soil/sediment, extent of vadose zone or variability in slope which can control drainage (Karchegani et al., 2011). In the chemical environment, fluid composition, chemical processes, temperature, moisture content, redox status and organic matter content may vary (Maher, 1988) while bacterial activity can alter the biological environment.

Type of Soils	Minimum Resistivity	Maximum Resistivity	Average Resistivity of layer 1	Average χf	Average $\chi f d\%$
ALLUV	84.77	734.78	160.5	18.67	5.94
DWDM	68.54	372.97	139.69	28.66	5.83
DPDM	47.63	352.61	134.92	26.14	5.31
SWDM	96.26	627.41	267.00	40.94	5.52
PEAT	29.5	244.6	92.5	5.2	0
ADPDM	94.00	1861.00	141.39	42.24	5.62
ADWDM	188.72	3397.23	330.43	84.83	6.89
ASWDM	204.37	6017.50	528.45	93.22	6.24
BSWDM	120.50	237.20	193.65	37.12	4.28
ASP	164.59	5227.45	350.07	35.38	3.98

Table: 6.6: Magnetic and resistivity characteristics of study area soils. (χf unit: $10^{-8} \text{m}^3 \text{kg}^{-1}$) and (Resistivity unit: Ohm-m).

Blundell et al. (2009a), in a major study of English and Welsh soils, found that the most important factors controlling the spatial variability of magnetic susceptibility were parent material and drainage while climate, relief and micro-organisms were much less important. Based solely on the magnetic properties of the bedrock within the study area, it would be expected that the magnetic susceptibility of the overlying soils would be very low. This is because the parent bedrock is mainly non-magnetic limestone and greywacke. The only magnetic bedrock in the study area, site K300, was a small basalt outcrop. However, the magnetic measurements made in this research, have shown that 80% of the study area contain ferrimagnetic minerals and the soils' magnetic content is often significantly higher (at least an order of magnitude in many locations) than that of the bedrock. Thus, it can be concluded that, in general, the 'parent material' in the research area is not a major contributor to the soil's magnetic properties. This is an important finding as 'parent material' is often cited as

a major factor to explain soil magnetism (Blundell et al., 2009a; Hanesch and Scholger, 2005). Similar results have been found elsewhere (Mileti et al., 2013; Singer and Fine, 1989). There is no evidence of ‘magnetic depletion’, in which soils’ susceptibility is less than the parent rock susceptibility such as is seen in Bulgaria (Jordanova et al., 1997).

The average soil in the research area contains 40% SP ferrimagnetic minerals which form within the soil due to pedogenic processes and are known as secondary ferrimagnetic minerals (SFMs). Earlier in this chapter (see Figure 6.5) it was demonstrated that for 89% of the magnetic data collected, the greater the amount of SP grains the higher the susceptibility. Only 11% of the data differed and for these, higher susceptibility values are due to them containing more magnetic minerals. It is the environmental factors which control the pedogenic processes which in turn control the formation of secondary SP minerals which ultimately yields a magnetic susceptibility which are important. At sites where these factors operate to a large extent, more SP minerals will be formed. SP minerals are widely believed to have formed by a fermentation process in which secondary iron oxides are formed by biogeochemical transformation (Le Borgne, 1955). This is facilitated by alternating wet and drying cycles within the soil which results in fluctuating reducing and oxidising conditions (redox) which facilitate the formation of SP ferrimagnetic minerals. ((Dearing et al., 1997, Maher, 1998; Maher and Taylor, 1988; Mullins, 1977; Hannam and Dearing, 2008).

The production process is enhanced in organic biologically active topsoils – see Dearing et al. (1996a) and Maher and Taylor (1988). Poorly drained or water-logged soils such as gleys do not exhibit strong SP mineral development which occurs in well-drained soils (Maher 1988). Free draining soils (brown earths or brown podzols) tend to have higher χ_{fd} values (>5%) than gleys (2.6%), (Dearing et al., 1996b). Note from Table 6.6, that Acid Deep Well Drained Mineral (ADWDM) soil and that Acid Shallow Well Drained Mineral (ASWDM) soil have the highest susceptibility and the highest χ_{fd} . As mentioned previously, the study area has an average

background $\chi_{fd}\%$ of 5.5% which is reasonably high. This may be due to the large extent of pasture in the study area. Dearing et al (1996a) reported that ‘Wales has considerably less arable land than England and is dominated by permanent and improved pasture. Under pasture, pedogenic production of SFMs continues undisturbed. In contrast, annual ploughing, more common across England, has a smoothing effect on the vertical distribution of SFMs and may lead to their dilution with subsoil’.

Soils that have been affected by anthropogenic pollution have high magnetic susceptibility values but a low $\chi_{fd}\%$ value as the magnetic grains are quite large, being MD or SD rather than SP. $\chi_{fd}\%$ values are related to the presence of pedogenically derived fine-grained magnetite (Maher and Taylor, 1988; Dearing et al., 1996b), thus intuitively older soils should in general have a higher $\chi_{fd}\%$ as the pedological processes which produce the SP magnetite will have operated for longer. This association was confirmed for the Tabernas alluvial fan and lake system in southeast Spain (Harvey et al, 2003).

One major question, regarding magnetic variation remains, why do the high χ_{lf} (typically $>100 \times 10^{-8} \text{ m}^3\text{kg}^{-1}$) and high $\chi_{fd}\%$ ($>8\%$) samples (which lie mostly in the ‘horizontal’ zone of Figure 6.6a), be mostly spatially located in a narrow zone in Figure 5.6, Chapter 5? These high value samples are mostly associated with ADWDM (60.5%) and ASWDM (28%) soils which have the highest χ_{lf} and $\chi_{fd}\%$ readings. However, the same soils are widespread in western Wicklow where they do not possess such high values. It has been argued in the literature, that as SP grains form due to pedogenic processes, as the soil gets older, more SP grains will form which in turn will cause an increase in susceptibility.

This view is supported by soil chronosequences studies in California (Fine et al., 1992, Singer et al., 1989), China (Lu, 2000) and Spain (Harvey et al., 2003). However, Lu et al. (2008b) quoting Vidic and Verosub (1999), claimed that magnetic susceptibility values do not show a statistically positive correlation with soil age for

Slovenian soils. For the present research it would be difficult to argue that the high values zone is because for some unknown reason the ADWDM and ASWDM soils within it are older than other equivalent ones when there is no physical reason why they should be so.

However, the high χ_{lf} and $\chi_{fd}\%$ zone coincides with the most heavily mineralized (and in the 17-19th century, the most heavily industrialized) part of the research area, and in the author's opinion this is no coincidence. The removal of mineralized material from many open cast mines (East Avoca Open Pit, Cronebane Open Pit) and associated processing (smelting, fossil fuel burning) could result in an atmospheric magnetic input to the surrounding soils. However, there still remains a problem. Studies in Britain, China and Europe show that atmospheric polluted magnetic grains are large (generally MD in character) and only yield relatively low $\chi_{fd}\%$ values (< 2-3%), (Blundell et al., 2009b; Lu et al., 2009). It appears more likely that the mineralization in east Wicklow was an initial primary source of metaliferrous atoms into the soil and normal pedogenic processes incorporated this rich supply into a large concentration of SP grains.

Dearing et al. (1996b) record that strongly magnetic soils found over weakly magnetic substrate (as in this study) are due to ultrafine SP grains, similar to the conclusions drawn here. There are undoubtedly higher order site specific controls on magnetic susceptibilities. Weathering can facilitate the concentration of magnetite in silt sized fractions (Maher, 1998) and in this study, the silt sized fraction often had the highest susceptibility.

Earlier in this thesis it was reported that various authors have postulated correlations between χ_{lf} and $\chi_{fd}\%$ - some positive (Huo et al., 2010; Mokhtari et al., 2011; Dearing et al., 1996a), some negative (Lu and Bai, 2008; Lu et al., 2008) whilst others have reported no correlation (van Dam et al., 2004). A positive relationship occurs when pedogenic processes produce highly magnetic SP grains, the more produced, the higher the susceptibility. When SP grains make up 10% of a sample the $\chi_{fd}\%$

value is 2%, if the SP grains make up 50% of a sample the $\chi_{fd}\%$ value is 7% and if SP grains make up 75%, then $\chi_{fd}\%$ value is 10%. Approximately 89% of the samples in this study shows an increase in susceptibility with an increase in SP grains. If a soil is water-logged or possible immature, then conditions are not conducive to SP grain formation, then $\chi_{fd}\%$ is very low and the soil susceptibility is predominantly controlled by parent material and it may be high or low but $\chi_{fd}\%$ is low either way i.e. there is no correlation between χ_{lf} and $\chi_{fd}\%$. Some authors have recorded negative correlations between χ_{lf} and $\chi_{fd}\%$ which appears to be difficult to reconcile with the discussion above. In a study in Hangzhou city, China, Lu and Bai (2008), recorded χ_{lf} of c. $100 \times 10^{-8} \text{ m}^3\text{kg}^{-1}$ for soils with a $\chi_{fd}\%$ value in the 9-12% range, while other soils with a $\chi_{fd}\%$ of 0-3% had a susceptibility χ_{lf} of c. $800 \times 10^{-8} \text{ m}^3\text{kg}^{-1}$. Scanning electron microscopy and X-ray studies showed that the highly magnetic soils contained anthropogenically produced microscopic ‘iron spherules’. As mention earlier in this chapter, 12.5% of sites which have a high susceptibility have a low $\chi_{fd}\%$, all of which, bar one, is in the southeast within the Avoca mineralization zone.

The factors and scientific processes which control the resistivity/conductivity of a soil have been discussed extensively in a general context in section 2.3.2, Chapter 2 and are not repeated here. However, a specific explanation is required to account for the regional shallow level resistivity pattern displayed in Figure 6.12 which shows a northeast trending broad zone of high resistivity. Values are 1-2 orders of magnitude higher within this zone compared to the rest of the study area. The high resistivity zone corresponds spatially with the Wicklow Mountains. This positive correlation of resistivity and topography was also determined statistically (see previous section). Most of the rest of the study area is very flat with low gradients. Precipitation in such areas has ample time to soak into the ground. Dry soils, in which the voids in the vadose zone are air-filled have high resistivity but when they are water-filled, a liquid phase pathway can exist and resistivity is lower. A negative correlation generally exists between resistivity and water content (Liangfu and Bingua, 2012; McCarter, 1984). In the Wicklow Mountains, precipitation runoff is more rapid because of the

steep slopes, and less water soaks in, resulting in air-filled voids and hence a higher resistivity. In the flat lands of Kildare, only 13% of sites have a maximum model resistivity greater than 1000 Ohm-m, and for Wicklow it is 66%.

Figure 6.13 shows a very poor correlation between χ_{lf} and resistivity. However, it must be remembered that this figure shows site magnetic data and for any one soil type there can be a massive variation in χ_{lf} . For example, the minimum susceptibility for ASWDM soil is $2.5 \times 10^{-8} \text{ m}^3\text{kg}^{-1}$ and the maximum is $536.1 \times 10^{-8} \text{ m}^3\text{kg}^{-1}$. Similarly, the range for ADWDM is $1.9 - 419.1 \times 10^{-8} \text{ m}^3\text{kg}^{-1}$. To make a meaningful comparison, average data at the soil type level should be employed. A fundamental question is: should there be any correlation between magnetic and resistivity data as the former depends on microscopic mineral grains whilst resistivity is strongly controlled by soil water content? As discussed earlier in this section, poorly drained or water-logged soils do not exhibit strong SP mineral development which occurs in well drained soils, thus the latter have a higher magnetic susceptibility. Also, the measured resistivity is lower for a water-logged soil (as the voids are water-filled) than for a well drained soil in which the voids near the surface are air-filled. Thus, both magnetic susceptibility and resistivity should be higher for well drained soils and a positive correlation should exist between them. Figure 6.15 shows that a statistically significant positive correlation does exist between the magnetic and resistivity data at the soil type level (Spearman rank of 0.73). The correlation might have been higher with a different sampling procedure for the magnetic data – see section 7.5, Chapter 7 on limitations of the research.

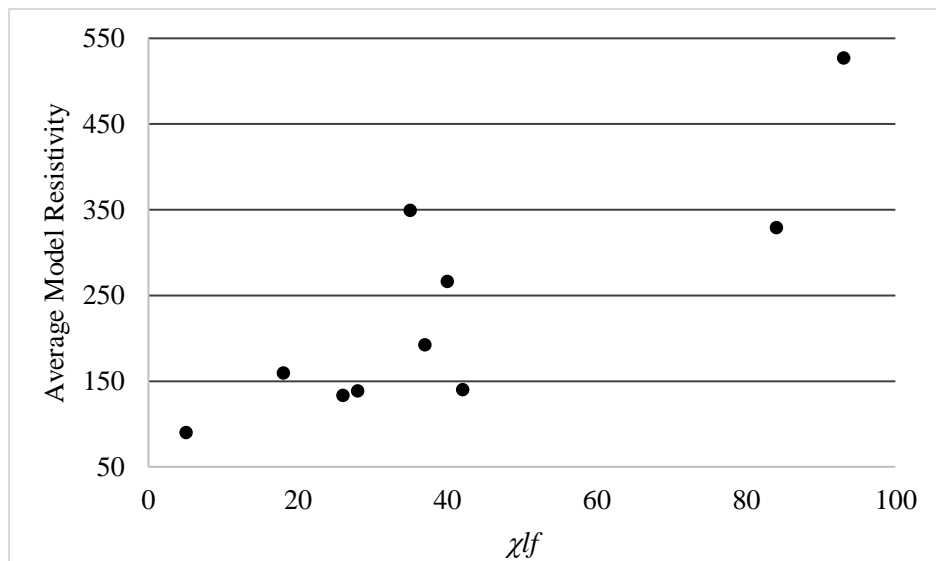


Figure 6.15: Plot of average χ_{lf} data against average modelled resistivity data for layer 1 for soil types listed in Table 6.6.

6.8 Summary

The χ_{lf} variation pattern for the study area is one of values increasing from the northwest to the southeast exhibiting a 2 orders of magnitude range. Most of the northern two thirds of Kildare and northwest Wicklow have a low susceptibility, while the susceptibility of southern Kildare is mainly in the medium range, c. $50 \times 10^{-8} \text{m}^3 \text{kg}^{-1}$. Low from high susceptibility areas are delineated in central Co. Wicklow by a NE-SW trending boundary. The zone of highest values forms a broad arc extending from southeastern Co. Wicklow northwards. Lowest values of $\chi_{fd}\%$ are in the peat but intermediate values ($\chi_{fd}\%$ of 4.5%, c. 35% SP) predominate for much of Kildare and western Wicklow. Southern Kildare and eastern Wicklow have high $\chi_{fd}\%$ values, indicating >60% SP content. Volume susceptibility (K) variations has similarities with the χ_{lf} patterns. The soils in the study area could be classified depending on whether they have high medium or low χ_{lf} and $\chi_{fd}\%$. A plot of $\Delta\chi$ and χ_{lf} shows that an increase in low frequency susceptibility (χ_{lf}) is related to an increase in the difference between low and high frequency ($\Delta\chi$) and this difference increases with an increase in the quantity of SP grains. This linear correlation is taken to

indicate that with increasing magnitude, the susceptibility is increasingly controlled by the fine (SP) pedogenic magnetic grains.

Time lapse resistivity experiments have demonstrated that resistivity values for the same site can vary by 100 per cent over the year and that one should carefully plan extended surveys to minimize temporal variations. The average 2015 monthly modelled resistivity variations show that resistivity is greater at depth and is lowest during the winter months (January and December) and highest in the summer (June, July and August). mostly likely because evapotranspiration will have a greater affect in the summer.

A significant difference in absolute resistivity values exists between Wicklow and Kildare, with the latter being much lower. 13% of Kildare sites have a maximum model resistivity > 1000 Ohm-m, and for Wicklow it is 66%. 50% of Wicklow sites have low resistivity near the surface, a higher mid depth resistivity and a lower deep resistivity, but only 3% of Kildare sites display this 'arch' trend. Conversely a 'trough' profile is uncommon in Wicklow compared with Kildare.

Principal Component Analysis (PCA) was performed on a GIS database composed of 17 variables. The correlation matrix shows that the highest correlation that χ_{lf} has with any other variable is with iron (Fe). The strong positive correlation of χ_{lf} and K (0.52) is also unexpected. There is a positive correlation value of 0.47 between χ_{lf} and $\chi_{fd}\%$ which is reasonably strong. The correlation between χ_{lf} and resistivity and $\chi_{fd}\%$ and resistivity is statistically virtually zero. There is however, a good correlation (0.4) between χ_{lf} and soils, thus the latter are an important determining factor in susceptibility. A strong positive correlation (0.6) exists between resistivity and topography.

Approximately 80% of the study area soils contain ferrimagnetic grains and are considerably more magnetic than their 'parent material' indicating a high degree of secondary enrichment. SP grains are widely believed to have formed by a fermentation process consisting of alternating wet and drying cycles which results in

fluctuating reducing and oxidising conditions. Their formation is enhanced in well-draining soils and is very poorly developed in water-logged soils. In the study area, Acid Deep Well Drained Mineral (ADWDM) soil and Acid Shallow Well Drained Mineral (ASWDM) soil have the highest susceptibility and the highest $\chi_d\%$. At the soil type level, a theoretical positive correlation should exist between magnetic susceptibility and resistivity as values for both should be higher in a well-drained soil and lower in a water-logged soil. Magnetic and resistivity data collected in this thesis confirmed this correlation. The author is unaware of any other scientific literature which has demonstrated this correlation.

CHAPTER 7

Summary and Conclusions

7.1 Introduction

The main results of the research carried out for this thesis are summarised in this chapter. The 6 research aims of this thesis, the 10 objectives needed to fulfil them and the overall research question, first introduced in Chapter 1, are restated here. In section 7.2, each objective is considered individually and the degree to which it was achieved is assessed. A similar exercise is conducted in section 7.3 for the thesis aims. The research question is addressed in section 7.4 and the chapter concludes with a short section on limitations of the research.

7.2 Research objectives fulfilment

Objective 1: Collection of samples from a sufficiently large number of spatially referenced sites for analysis, in the laboratory, of mass specific magnetic susceptibility at high and low frequency and percentage frequency dependent susceptibility.

300 sites were identified for County Kildare and 250 for County Wicklow where soil samples were taken from for laboratory based measurements of magnetic properties. The main soils in the study area had multiple samples taken to ensure representative data were collected, see Tables 4.1 and 5.1. The Irish Grid co-ordinates for all samples were acquired. There is a good spatial coverage of the study area, though the data are more sparse in the highest most inaccessible parts of the Wicklow Mountains. However, these areas have a blanket peat cover which has zero susceptibility. No data could be collected in the military camp.

Objective 1 was successfully completed.

Objective 2: Measurement of volume magnetic susceptibility in the field at spatially referenced sites.

20 volume magnetic susceptibility readings were obtained at each of the 550 sites. Data were collected by the author using a systematic sampling regime with a Bartington MS2D loop probe. The Irish Grid co-ordinates of each site were obtained using a Trimble XT GPS system. Analysis of the 20 samples showed a near normal distribution for the sites.

Objective 2 was successfully completed.

Objective 3: Production of representative soil samples and measurement of their bulk low and high frequency magnetic susceptibility.

It was important that the soil samples collected during this research were representative of the sites, otherwise all findings would be invalidated. Thus, simply taking one sample at each site would not have been appropriate. Thus initially, 3 samples (each about 0.5kg in weight) were collected at each of the 3 corners of a 7m sampling triangle (see Figure 2.2). The samples were taken at a depth of about 10-15 cm. Soil at the surface may have been magnetically contaminated and magnetic susceptibility tends to decrease at greater depths. The 3 samples were air dried then thoroughly mixed. The sample was then ‘coned’ and divided into quarters (A, B, C, D, Figure 2.4). This ensured each quarter contained roughly equal amounts of coarse, medium and fine grained material. Each of the quarters were then mixed and 4 high frequency and 4 low frequency magnetic susceptibility measurements taken. The results were averaged to give a representative low and high susceptibility value for that site. Equal care was taken in the laboratory measurement phase. A Bartington MS2B meter was employed. It was important to ensure consistency throughout the measurement phase which lasted over two years. A calibration sample (330×10^{-5} S. I units) was measured after every 30 samples to ensure no drift had occurred. Also, the orientation of the cylindrical sample was the same for low and high frequency measurements.

Objective 3 was successfully completed.

Objective 4: Fractional analysis of representative soil samples and the measurement of low and high frequency magnetic susceptibility for individual fractions.

Little work on the magnetic susceptibility of specific soil fractional sizes has been done, only one such paper for Ireland was found. Snowball and Thompson (1990) report a decrease in magnetic susceptibility with an increase in grain size near Lough Catherine in Northern Ireland. Bulk samples (from all 550 sites) were divided into 7 fractional sizes, the largest was $>2000\mu\text{m}$ and the smallest $<63\mu\text{m}$. The former represents pebble size, the latter silt grade with intervening ones being coarse to fine sand scale. This approach also allowed the clasts in the sieves to be examined. Most of these were limestone, greywacke or granite and in some sites (e.g. K176, K134, W208) the clasts were different from the underlying rock type. Magnetic laboratory analysis was carried out as discussed in Objective 3.

Objective 4 was successfully completed.

Objective 5: Collection and analysis of K-T data to determine Curie temperatures for magnetic minerals in the soils of the research area to help determine the magnetic mineralogy and magnetic domain format.

The variation in magnetic susceptibility with temperature was measured for the soils from 100 Kildare sites and 100 Wicklow sites, approximately 36% of all sites. A maximum of 10 sites per week could be analysed and this component of the research took six months laboratory work using the Bartington K-T system. The shape of the graphs and Curie temperatures showed which magnetic minerals were present. The degree to which a Hopkinson peak developed, combined with the values (calculated from the low and high frequency MS2B susceptibility) allowed a determination of percentage of MD, SD or SP present in the soil sample. K300 for example has virtually no SP minerals ($<5\%$) because its $\chi_{fd}\%$ is so low (0.44%). Thus, it must be

formed of 95% MD and/or SD ones. However, its K-T graph does not have a Hopkinson peak. Such a peak is formed by the conversion of SD grains to SP ones, thus it contains virtually no SD grains and must be mainly MD in character.

Objective 5 was successfully completed.

Objective 6: Collection and analysis of oriented soil samples for laboratory remanent magnetism, inclination and declination measurement.

10 oriented soil cubes were taken at each of 26 different Kildare sites and their remanent magnetism, inclination and declination obtained using a Molspin spinner magnetometer. The results were disappointing because in only one of the sites could the author be reliably confident that no disturbance was present (K1). It was concluded that it was not possible to use near surface directional magnetic data as a soil discriminator in the study area because of the widespread human interference in the topmost layer making the results of such a survey unreliable.

Thus, although Objective 6 was successfully completed, the results were unreliable.

Objective 7: Formulation of and forward modelling of subsurface resistivity models.

In order to qualitatively understand the apparent resistivity pseudosections that were measured in the field, five simple subsurface model types were constructed which reflected the types of subsurface that might be expected. They were: Two horizontal layer model; Three horizontal layer model; Two vertical fault model; Surface channel model and Deep channel model. Geotomo RES2DMOD software was used in their creation. Various parameters were changed, such as resistivity contrast or thickness of layers and the effect noted. In the case of the 3 layers model, the effects of a middle low or high resistivity layer was analysed. This proved especially fortuitous as a sizeable proportion of both Kildare and Wicklow sites fitted this model. Inversion of the models was also performed to determine any limitations of the program.

Objective 7 was successfully completed.

Objective 8: Acquisition of 2D apparent resistivity pseudosection data using different array types at a representative number of sites and inverse modelling of the results.

Resistivity data were collected at 28 Kildare sites and at 29 Wicklow sites from which 2D apparent resistivity pseudosections were constructed. Data were collected using 2 different array types (Wenner-Schlumberger and Dipole-Dipole) with 2 orientations (N-S and W-E). The data were modelled with Geotomo RES2DINV inversion software using the same input parameters for each site in order to ensure consistency.

Objective 8 was successfully completed.

Objective 9: Determine homogeneity of subsurface soil at a representative number of sites by employing azimuthal resistivity surveying.

Collecting a single line resistivity data does not provide any information on how homogenous the subsurface is. Electrical Resistivity Tomography was carried out at each of the resistivity sites with 2 orientations: north-south and west-east. Similar results would be expected for a uniform subsurface. For the study area, some north-south trends were similar to the west-east ones while others were markedly different indicating a large degree of heterogeneity.

Objective 9 was successfully completed.

Objective 10: Determine the annual temporal degree of resistivity change using time lapse electrical resistivity imaging at a selected site.

In order to be able to directly compare resistivity data which were obtained at different times it was important to determine how resistivity varied temporally. To this end, resistivity data were collected at site K1 each month for one calendar year. The data showed that resistivity values for the same site can vary by 100 per cent

over a year – a significant variation. Changes between adjacent months are considerably less. Resistivity data were collected in this research over as short a time span as possible. The findings here show that one cannot simply compare third party data unless information about when the data were recorded are known.

Objective 10 was successfully completed.

7.3 Research aims fulfilment

Aim 1: To determine if Irish soil types in Counties Kildare and Wicklow have characteristic magnetic or electrical resistivity geophysical properties.

Two aspects of the magnetic characteristics of the Kildare and Wicklow soils became apparent soon after beginning this research. Firstly, average bulk susceptibility values for Wicklow were markedly different from Kildare. 76% of the Kildare samples contain ferrimagnetic minerals (indicating widespread secondary enhancement) with an average Kildare bulk soil χ_{lf} value of $26.7 \times 10^{-8} \text{ m}^3\text{kg}^{-1}$. About 66% of the bulk soil χ_{lf} is less than $30 \times 10^{-8} \text{ m}^3\text{kg}^{-1}$ and 44% of the χ_{lf} values are less than $20 \times 10^{-8} \text{ m}^3\text{kg}^{-1}$. Only about 4% are $>80 \times 10^{-8} \text{ m}^3\text{kg}^{-1}$. Approximately the same degree of secondary enhancement occurs in Wicklow (80%) as in Kildare but the average bulk soil χ_{lf} value is considerably higher: $64.8 \times 10^{-8} \text{ m}^3\text{kg}^{-1}$. Only 2.7% of the Kildare samples are $>100 \times 10^{-8} \text{ m}^3\text{kg}^{-1}$ whereas for Wicklow, the value is 20%. Secondly, there is often a very wide range of susceptibility values for the same soil type. It is evident that the measured susceptibility is very site specific and that it is important to obtain large number of samples for each soil type to determine average values for comparative purposes.

Some soils in both Kildare and Wicklow have an average χ_{lf} value of c. $20 \times 10^{-8} \text{ m}^3\text{kg}^{-1}$. Alluvium: $18.7 \times 10^{-8} \text{ m}^3\text{kg}^{-1}$; BSWDM: $20.7 \times 10^{-8} \text{ m}^3\text{kg}^{-1}$; DPDM: $16.6 \times 10^{-8} \text{ m}^3\text{kg}^{-1}$. Other soils group around $30\text{-}40 \times 10^{-8} \text{ m}^3\text{kg}^{-1}$ such as: DWDM: $28.7 \times$

$10^{-8} \text{ m}^3\text{kg}^{-1}$ and ADPDM: $41 \times 10^{-8} \text{ m}^3\text{kg}^{-1}$. Two Wicklow soils have much higher susceptibilities ADWDM: $84.8 \times 10^{-8} \text{ m}^3\text{kg}^{-1}$ and ASWDM: $93.2 \times 10^{-8} \text{ m}^3\text{kg}^{-1}$.

There tends to be considerably less variation for $\chi_{fd}\%$. Discounting peat, the lowest $\chi_{fd}\%$ values are in Wicklow: ASP (4.1%) and BSWDM (4.6%) and the highest values ADWDM (6.9%) and ASWDM (6.2%). Most other soils average around 5.7%.

The electrical resistivity measured during this research showed distinct differences between Kildare in the west and Wicklow in the east, only 13% of Kildare sites have a maximum model resistivity $>1000 \text{ Ohm-m}$, whilst the corresponding percentage for Wicklow is 66%. The average maximum resistivity value for Kildare was 237.2 Ohm-m and for Wicklow 3869.8 Ohm-m.

There are also differences in the variation of resistivity with depth. 50% of Wicklow sites have a low resistivity near the surface, a higher mid depth resistivity and a lower deep resistivity but only 3% in Kildare have a similar trend. About 33% of Kildare sites display a mid-depth resistivity layer that is lower than the resistivity at depth or at the surface, a pattern that is uncommon in Wicklow.

Aim 1 was successfully completed, Kildare and Wicklow do have different magnetic and electrical resistivity properties.

Aim 2: To produce the first spatially referenced county scale maps of volume magnetic susceptibility (K), mass specific magnetic susceptibility (χ_{lf}) and percentage frequency dependent susceptibility ($\chi_{fd}\%$) in Ireland.

Magnetic susceptibility maps of Kildare and Wicklow were produced which divided the counties into areas which contain ferrimagnetic images and those that do not. Mass specific magnetic susceptibility (χ_{lf}) maps showing the entire range of values were created for Kildare and Wicklow. Equivalent volume susceptibility (K) and percentage frequency dependent susceptibility ($\chi_{fd}\%$) maps were produced. In addition, spatial maps of Kildare for mass specific magnetic susceptibility (χ_{lf}) and for percentage frequency dependent susceptibility ($\chi_{fd}\%$) for the $>2000\mu\text{m}$ and

<63 μ m fractions were produced. Spatial maps of the entire study area (Kildare and Wicklow combined) for χ_{lf} , $\chi_{fd}\%$ and K were produced in Chapter 6 (Figures, 6.1, 6.2 and 6.3 respectively).

Aim 2 was successfully completed.

Aim 3: To determine the magnetic mineralogy and magnetic domain format of the soils of Counties Kildare and Wicklow.

Approximately 80% of the sites investigated in Counties Kildare and Wicklow contain ferrimagnetic minerals (even though most of the bedrock in the counties does not) and analysis of K-T data graphs (Curie temperature) indicate that magnetite is predominant. Dual frequency susceptibility measurements allowed $\chi_{fd}\%$ to be calculated and a determination of the SP percentage in a soil. For example, ASP soils contain on average 25-30% SP grains ($\chi_{fd}\%$ of 4.1) while ADWDM contains about 50% SP grains ($\chi_{fd}\%$ of 6.9). Poorly developed Hopkinson peaks indicate relatively small amounts of SD minerals present, thus for example K300 contains very little SP or SD minerals and is mainly MD in character. About 80% of the Kildare sites for which K-T data were obtained were characterised by a Hopkinson peak of varying size.

ADPDM soils have a Hopkinson peak, though in the case of 38.5% of the samples, it was poorly developed. BSWDM soils mainly show a well-developed Hopkinson peak as do 62% of the ASP soils. A large proportion of ASWDM soils (77%) have either a very weakly developed Hopkinson peak or none at all indicating they contain only a small percentage of SD grains. 82% of ADWDM soils have similar characteristics to ASWDM soils. Only about 37% of Wicklow samples possess a Hopkinson peak.

Aim 3 was successfully completed.

Aim 4: Ascertain if different fractional size ranges carry the same or different magnetic signals.

χ_{lf} and $\chi_{fd}\%$ data were obtained for 7 fractional grain sizes for the main soils within the study area. For most of the Kildare soils it was found that the largest sieve grades and the smallest one ($<63\mu\text{m}$) contain a larger percentage of maximum susceptibilities than average while the mid-range sieves ($125-63\mu\text{m}$, $250-125\mu\text{m}$ and $600-250\mu\text{m}$) contain a lower number of maximums. A similar pattern (higher percentage for larger and smallest sieve sizes, lower percentage of maximum susceptibilities for mid-range ones) could be discerned for 4 of the main Wicklow soil groups (ADWDM, ASWDM, BSWDM and ASP).

When the histograms displaying the variation of χ_{lf} and $\chi_{fd}\%$ with particle size are examined, it is evident that there can be marked differences in magnetic properties for different fractional sizes. When soils are aggregated to the county level some of the differences are averaged out, but differences still exist. For Wicklow the sieve with the highest susceptibility ($2000-900\mu\text{m}$) is only 3% higher than the one with the lowest value ($<63\mu\text{m}$) whereas for Kildare the one with the highest susceptibility ($>2000\mu\text{m}$) is 30% higher than the one with the lowest value ($250-125\mu\text{m}$).

Aim 4 was fully met and it was concluded that different fractional size ranges may carry different magnetic signals.

Aim 5: Within the scientific literature (for different parts of the world) various claims have been made regarding the correlation between mass specific magnetic susceptibility and percentage frequency dependent susceptibility (χ_{lf} and $\chi_{fd}\%$). The existence or otherwise of such correlations for soils within the study area will be evaluated.

An assessment of the correlation between χ_{lf} and $\chi_{fd}\%$ for the soils of the study area was made in section 6.4. Analysis in Chapter 4 showed there is no significant correlation between χ_{lf} and $\chi_{fd}\%$ for Kildare (Spearman rank of 0.17). However, for Wicklow, there is a significant positive correlation between χ_{lf} and $\chi_{fd}\%$ (Spearman rank of 0.62). Similarly, for the study area, there is also a strong positive correlation (Spearman rank of 0.42). In detail, the DWDM, DPDM, SWDM and Alluvium soils

of Kildare show no significant correlation between χ_{lf} and $\chi_{fd}\%$ (Spearman rank of 0.08, 0.001, 0.05, -0.008 respectively). Neither do the ADPDM and BSWDM Wicklow soils (Spearman rank of 0.3, 0.17 respectively) but a significant positive correlation does exist for the Wicklow ASP, ASWDM and ADWDM soils (Spearman rank of 0.38, 0.49, 0.75 respectively).

Plotting $\chi_{fd}\%$ against χ_{lf} for the study area shows that susceptibility values $<80 \times 10^{-8} \text{ m}^3\text{kg}^{-1}$ have a range of $\chi_{fd}\%$ values whilst those that are higher are associated mainly with high $\chi_{fd}\%$ values. This pattern has been found in other parts of the world and interpreted as indicating that the SP mineral fraction is largely responsible for the climatically controlled susceptibility enhancement. Delta χ ($\Delta\chi$) equals $(\chi_{lf} - \chi_{hf})$ and is related thus: $\chi_{fd}\% = 100\Delta\chi / \chi_{lf}$. For Kildare Spearman rank coefficient = 0.87 and for Wicklow it is 0.94. For the study area, 89% of the samples show a strong correlation and for these with increasing magnitude, the susceptibility is increasingly controlled by the SP pedogenic magnetic fraction.

Aim 5 was successfully completed.

Aim 6: Construct and analyse a Geographic Information System (GIS) database for the study area.

A 17 layers georeferenced Arcmap GIS database of the study area was constructed, formed of mass specific magnetic susceptibility data, frequency dependent magnetic susceptibility data, volume magnetic susceptibility data and modelled layer 1 resistivity data. Also, analysed were a digital elevation model, a soils map, a geological map, a glacial landforms map and 9 geochemical datasets (Iron, Lithium, Nickel, Copper, Zinc, Uranium, Tin, Lead and Mercury). Principal Component Analysis (PCA), a statistical method used to determine the relatedness of variables was performed on the data. The results are given in terms of a correlation matrix, eigenvalues and an eigenvector matrix.

The correlation matrix shows that that χ_{lf} has a high positive correlation with iron, volume susceptibility and with $\chi_{fd}\%$. The other elements have a weaker positive relationship with χ_{lf} , though in the case of nickel and zinc, the correlation is negative. The strong positive correlation of χ_{lf} and K (0.52) is also unexpected. The correlation between χ_{lf} and resistivity and $\chi_{fd}\%$ and resistivity is statistically virtually zero as is the correlation between χ_{lf} and topography. Also, the correlation between χ_{lf} and geology and glacial sediments is very weak (0.08). There is however, a good correlation (0.4) between χ_{lf} and soils. A strong positive correlation exists between resistivity and topography, soils and lithium. Soils and iron content are highly correlated (0.69). Correlation between resistivity and geology and glacial sediments is close to zero.

From the eigenvectors, PC1 accounts for 86.68% of the database variability, PC2 for 13.03%, and PC3 for 0.21% with the higher PCs combined accounting for only 0.08% of the variability

Aim 6 was successfully completed.

7.4 Research question: Based upon an extensive study of a variety of soil types, what are the biogeoscientific processes that result in different magnetic and electrical properties of soil?

It is clear from the aims and objectives above that soils with different susceptibilities and/or SP mineral concentrations are responsible for the magnetic variations and variations in subsurface/terrain characteristics have caused the observed resistivity differences. It is however, important that average values be employed in any analysis and that enough data be collected to ensure the results are statistically robust. In general, soils which have lower average χ_{lf} values and less variability in $\chi_{fd}\%$ such as DWDM, DPDM, SWDM, ADPDM, BSWDM and Alluvium soils show no significant correlation between χ_{lf} and $\chi_{fd}\%$ but there is a significant correlation for the ASP, ASWDM and ADWDM soils.

The magnetic properties of the soils in the study area depended overwhelmingly on the formation of superparamagnetic (SP) secondary ferrimagnetic minerals (almost exclusively magnetite). 80% of the study area soils are characterised by a high degree of secondary enrichment. For 89% of the acquired magnetic data, the greater the amount of SP grains the higher the susceptibility. A well-drained soil environment which undergoes fluctuating reducing and oxidising conditions facilitates the formation of SP grains and in this study, was best achieved by Acid Deep Well Drained Mineral (ADWDM) and Acid Shallow Well Drained Mineral (ASWDM) soils. Poorly drained soils have a lower χ_{lf} and $\chi_{fd}\%$. A small percentage of soils had a high χ_{lf} but a low $\chi_{fd}\%$. Such frequency independent soils tend to have an anthropogenic origin and were located around Avoca, a site of former industrial activity.

A high resistivity area coincides with the Wicklow Mountains. High runoff rates on the slopes minimizes infiltration, reducing water content of the vadose zone compared with low slope areas. At the soil type level, a theoretical positive correlation should exist between magnetic susceptibility and resistivity as values for both should be higher in a well drained soil and lower in a water-logged soil. Magnetic and resistivity data collected in this thesis confirmed this correlation.

The research question was fully answered.

7.5 Limitations of the current research

In many research projects, there may be constraints which limit the effectiveness of the study. At its simplest this may involve a lack of access to equipment or one can be forced to compromise due to conflicting requirements. Regarding the former, there are types of magnetic measurements, other than those used in this research which could have provided useful information, however, the author did not have access to the relevant instrumentation. For example, if a soil sample is subjected to a strong increasing magnetic field, it acquires an isothermal remanent magnetisation (IRM).

The maximum value is called the saturation isothermal remanent magnetisation (sIRM) and this varies with magnetic mineralogy and grain size.

Other types of geophysical data could also be acquired. Ground penetrating radar is ideal for detailed work and relies on differences in relative permeability due to variations in grain size, sediment type, water content and porosity. An important parameter in ground penetrating radar is the frequency of the antennae, the higher the frequency, the more the detail but the less the penetration. The resistivity sections imaged 2m depth and such a depth would be required for the radar. Based on work at Maynooth University and experience gained at Minerex geophysical company, such ground penetrating radar should be collected at 5cm intervals using 400-500 MHz antennae.

A compromise had to be made regarding the volume susceptibility measurements. Twenty volume susceptibility readings were collected for each of the 550 sites using a Bartington MS2D instrument (total of 11,000 measurements). Ideally these data should be obtained when the ring probe is in direct contact with the bare soil. However, to totally clear the grass cover from 11,000 patches would have taken a substantial amount of time. Thus, the approach taken for this research was to collect data with and without grass cover for 2 of the 20 readings and determine a 'scaling factor' which was applied to all 20 values. This procedure is based on the assumption that the grass thickness is approximately constant within a site. An alternative approach would have been to only take 2-3 readings per site with and without grass and obtain an average, however, such few readings may not be representative. It should be realised the main reason for collecting volume susceptibility data was to provide real-time information in the field about how magnetic susceptibility varied between sites (this could not be done for the mass specific susceptibility data which was the most important data source for this research). A strong correlation was found between mass specific susceptibility and volume susceptibility suggesting the approach taken, while not ideal, was acceptable.

Resistivity data were collected using a Tigre 32 with 32 electrodes to acquire 2D resistivity data for a 15.5m traverse (0.5m electrode spacing). Ideally data would have been collected in a 3D array. However, the maximum grid I could create with 32 electrodes was 6×5 electrodes. With a 0.5m spacing the area sampled in 3D would have been 2.5×2 m, which is very small. Also, if I wanted to do a Wenner array which uses 4 electrodes, for 1 side of grid, I could only collect 3 readings: electrodes 1,2,3,4 2,3,4,5 and 3,4 5,6. Also with Wenner array, level 1 uses electrodes 1,2,3,4. To go to level 2 (deeper), one uses electrodes 1,3,5,7 but there is no 7 in a row. The only way around this would have been to use a system with considerably more electrodes, but one was not available. In Chapter 6, it was demonstrated that there was a good correlation between average susceptibility and average modelled resistivity for layer 1.

With a 0.5m electrode spacing, the median depth for layer 1 is 25 cm. Ideally, the samples obtained for magnetic measurement should have been taken at a depth of 25cm instead of the 10-15cm depth that was employed. An ideal scenario would be to excavate a 50cm deep trench. In the present research, each site is associated with a single susceptibility value. However, analysis of the susceptibility from the trench wall at different depths would allow the construction of vertical susceptibility profiles which has the potential to provide much more information and the susceptibility values could be averaged to provide a better representative magnetic value for layer 1.

The variation of resistivity was determined at site K1 by collecting data on a monthly basis for one year. This allowed the production of Figure 6.8 which showed that resistivity is lowest during the winter months and highest in the summer because of evapotranspiration. If this was to be repeated, I would collect the data on a weekly rather than on a monthly basis. This would result in a much more detailed picture of resistivity change with time. Resistivity decreases as subsurface moisture increases, but the change is non-linear (Liangfu and Bingua, 2012; McCarter 1984). A major limitation was that no subsurface data on moisture content was collected

simultaneously with the collection of resistivity data. If such data had been collected, the nature of the non-linear relationship could have been investigated. The use of a portable electrical conductivity probe to determine the variations in electrical conductivity of the fluid medium at the time of the ERT measurements would have provided very useful data.

REFERENCES

- Abu-Hassanein, Z. S., Benson, C. H. and Blotz, L. R. (1996). Electrical Resistivity of Compacted Clays. *Journal of Geotechnical Engineering*, 122, pp 397-406.
- Ahmed, S. and Carpenter, P. (2003). Geophysical response of filled sinkholes, soil pipes and associated bedrock fractures in thinly mantled karst, east-central Illinois. *Environmental Geology*, 44(6), pp.705-716.
- Alekseeva, T., Alekseev, A., Maher, B.A. and Demkin, V. (2007). Late Holocene climate reconstructions for the Russian steppe, based on mineralogical and magnetic properties of buried palaeosols. *Paleogeography, Paleoclimatology, Paleoecology*, 249(1-2), pp. 103-127.
- Allied Associates (2000). *Imager-Pro 2000: 2D resistivity imaging control software operating manual*. 34 pages.
- An Foras Taluntais (1970). *Soils of County Kildare*. National Survey of Ireland, 92 pages.
- Archie, G.E. (1942). The electrical resistivity log as an aid in determining some reservoir characteristics. *Transactions of the AIME. Society of Petroleum Engineers*, 146(01), pp 54–62.
- Baharuddin, M., Hashim, R. and Taib, S. (2009). Electrical Imaging Resistivity Study at the Coastal Area of Sungai Besar, Selangor, Malaysia. *Journal of Applied Sciences*, 9(16), pp.2897-2906.
- Baines, D., Smith, D., Froese, D., Bauman, P. and Nimeck, G. (2002). Electrical resistivity ground imaging (ERGI): a new tool for mapping the lithology and geometry of channel-belts and valley-fills. *Sedimentology*, 49(3), pp.441-449.
- Barker, R. D. (1997). Electrical imaging and its application in engineering investigations. *Geological Society, London, Engineering Geology Special Publication*, 12(1), pp.37-43.
- Barker, R. and Moore, J. (1998). The application of time-lapse electrical tomography in groundwater studies. *The Leading Edge*, 17(10), pp.1454-1458.
- Bartington Instruments (1994). *Operation manual for MS2 magnetic susceptibility system*. OMO408.

- Barton, K. and Fenwick, J. (2005). Geophysical investigations at the ancient royal site of Rathcroghan, County Roscommon, Ireland. *Archaeological Prospection*, 12(1), pp.3-18.
- Beresnev, I., Hruby, C. and Davis, C. (2002). The use of multi-electrode resistivity imaging in gravel prospecting. *Journal of Applied Geophysics*, 49(4), pp.245– 254
- Blundell, A., Dearing, J., Boyle, J. and Hannam, J. (2009a). Controlling factors for the spatial variability of soil magnetic susceptibility across England and Wales. *Earth-Science Reviews*, 95(3-4), pp.158–188.
- Blundell, A., Hannam, J., Dearing, J. and Boyle, J. (2009b). Detecting atmospheric pollution in surface soils using magnetic measurements. A reappraisal using an England and Wales database. *Environmental Pollution*, 157(10), pp.2878-2890.
- Booth, C., Fullen, M., Walden, J., Worsley, A., Marcinkonis, S. and Coker, A. (2008). Problems and potential of mineral magnetic measurements as a soil particle size proxy. *Journal of Environmental Engineering and Landscape management*, 16(3), pp.151-158.
- Bonsall, J. P. T. (2014). A reappraisal of archaeological geophysical surveys on Irish road corridor 2001-2010. Unpublished PhD thesis, University of Bradford, UK, 556 pages.
- Borradaile, G. and Geneviciene, I. (2007). Measuring heterogeneous remanence in paleomagnetism. *Geophysical Research Letters*, 34(12), L12302.
- Botsou, F., Karageorgis, A., Dassenakis, E. and Scoullou, M. (2011). Assessment of heavy metal contamination and mineral magnetic characterization of the Asopos River sediments (Central Greece). *Marine Pollution Bulletin*, 62(3), pp.547-563.
- Bourne, J. H. (1993). Use of magnetic susceptibility, density and modal mineral data as a guide to the composition of granitic plutons. *Mathematical Geology*, 35 (3), pp.357-375.
- Boyko, T., Scholger, R. and Stanjek, H. (2004). Topsoil magnetic susceptibility mapping for pollution monitoring: repeatability of in situ measurements. *Journal of Applied Geophysics*, 55(3-4), pp.249-259.
- Breen, R. (2003). A geophysical investigation of glacial sediments in the Galtrim region of County Meath. Unpublished M.Sc. Thesis, National University of Ireland, Maynooth.

Brunet, P., Clément, R. and Bouvier, C. (2010). Monitoring soil water content and deficit using Electrical Resistivity Tomography (ERT) – A case study in the Cevennes area, France. *Journal of Hydrology*, 380(1-2), pp.146–153.

Busby, J. P. (2000). The effectiveness of azimuthal apparent measurements as a method for determining fracture strike orientations. *Geophysical Prospecting*, 48(4), pp.677-695.

Byrne, M. (1995). An introduction to the methods of archaeological prospection and a study of the theory and techniques of electrical resistivity. Unpublished M. A. Thesis, University College, Cork.

Byrne, M. (2005). An archaeo-geophysical investigation of the ecclesiastical site at the Taghadoe round tower. Unpublished M.Sc. thesis, National University of Ireland, Maynooth.

Calaco-Casado, S. (2006). Geophysical investigation of Quaternary glacial sediments in south Co. Westmeath and north Co. Offaly. Unpublished M.Sc. thesis, National University of Ireland, Maynooth.

Callaghan, L. (2002). The geophysical characteristics of glacial deposits in County Meath. Unpublished M.Sc. thesis, National University of Ireland, Maynooth.

Celano, G., Palese, A., Ciucci, A., Martorella, E., Vignozzi, N. and Xiloyannis, C. (2011). Evaluation of soil water content in tilled and cover-cropped olive orchards by the geoelectrical technique. *Geoderma*, 163(3-4), pp.163-170

Chadima, M. (2016). Magnetic susceptibility and its variations with temperature, measuring field and operating frequency. Examples from various rock types. Czech Republic: institute of geology academy of sciences. Available at: http://www.geolsed.ulg.ac.be/IGCP_652/Chadima-training.pdf.

Chambers, J., Kuras, O., Meldrum, P., Ogilvy, R. and Hollands, J. (2006). Electrical Resistivity Tomography applied to geologic, hydrogeologic and engineering investigations at a former waste-disposal site. *Geophysics*, 71(6), B231-B239.

Conway, J. (1993). A magnetic investigation of the northern units of the Leinster granite. Unpublished M.A. thesis, National University of Ireland, Maynooth.

- Corcoran, A. (2007). An archaeological geophysical investigation of the ancient royal site of Dun Ailinne in Kilcullen, Co. Kildare. Unpublished M.Sc. thesis, National University of Ireland, Maynooth.
- Corwin, D. L., and S. M. Lesch (2005), Apparent soil electrical conductivity measurements in agriculture, *Computers and Electronics in Agriculture*, 46, pp. 11–43.
- Cousin, I., Besson, A., Bourennane, H., Pasquier, C., Nicoullaud, B., King, D. and Richard, G. (2009). From spatial-continuous electrical resistivity measurements to the soil hydraulic functioning at the field scale *C. R. Geoscience*, 341, pp.859-867.
- Coxon, P. (2001). Cenozoic: Tertiary and Quaternary. In: C. Holland, ed. *The Geology of Ireland*. Dunedin Academic Press, pp.387-427.
- Coxon, P., Corcoran, R., Gibson, P. and Mc’Carron, S. (2013). A Holocene pollen diagram from Lough Avullin, Clare Island, Western Ireland. In: D. Synnott, ed., *New Survey of Clare Island*. Royal Irish Academy, Dublin, 7, pp.1-25.
- Creevey A. (2005). An archaeological geophysical investigation of the area surrounding the ecclesiastical remain located at Donaghmore Co Kildare. Unpublished M.Sc. thesis, National University of Ireland, Maynooth.
- Dalan, R. A. (2008). A Review of the Role of Magnetic Susceptibility in Archaeogeophysical Studies in the USA: Recent Developments and Prospects. *Archaeological Prospection*, 15, pp.1-31.
- Dally, K. and Fealy, R. (2005). Digital Soil Information System for Ireland. EPA Report, 2005-S-DS-22-M1.
- De Carlo, L., Perri, M., Caputo, M., Deiana, R., Vurro, M. and Cassiani, G. (2013). Characterization of a dismissed landfill via electrical resistivity tomography and mise-a-la-masse method. *Journal of Applied Geophysics*, 98, 1-10.
- De Jong, E., Pennock, D. and Nestor, P. (2000). Magnetic susceptibility of soils in different slope positions in Saskatchewan, Canada. *Catena*, 40, 291-305.
- Dearing, J. (1994). *Environmental magnetic susceptibility using the Bartington MS2 system*. Chi Publishers. Kenilworth, England. First edition.
- Dearing, J. (1999a) Magnetic Susceptibility. In: *Environmental magnetism: a practical guide* edited by Walden, J., Oldfield, F. and Smith, J. Quaternary Research Association. Technical Guide, No. 6, pp.35-62.

Dearing, J. (1999b). Environmental magnetic susceptibility using the Bartington MS2 system. Chi Publishers. Kenilworth, England. Second edition.

Dearing, J., Bird, P., Dann, R. and Benjamin, S. (1997). Secondary ferromagnetic minerals in Welsh soils: a comparison of mineral magnetic detection methods and implications for mineral formation. *Geophysical Journal International*, 130(3), pp.727-736.

Dearing, J., Dann, R., Hay, K., Lees, A., Loveland, P., Maher, A. and O'Grady, K. (1996a). Frequency dependent susceptibility measurements of environmental materials. *Geophysical Journal International*, 124, pp.228-240.

Dearing, J., Hay, K., Baban, S., Huddleston, A., Wellington, E., and Loveland, P. (1996b). Magnetic susceptibility of soil: an evaluation of conflicting theories using a national data set. *Geophysical Journal International*, 127, 728-734

Deville, I. (1995). A magnetic evaluation of potential landfill sites in the Dublin region. Unpublished M.A. thesis, National University of Ireland, Maynooth.

Dong, C., Zhang, W., Ma, Feng, H., Lu, H., Dong, Y. and Yu, L., (2014). A magnetic record of heavy metal pollution in the Yangtze River subaqueous delta. *Science of Total Environment*, 476-477, 368-377.

Doughan, T. (2004). A geophysical investigation of glacial sediments in the Ballinakill region of County Laois. Unpublished M.A. thesis, National University of Ireland, Maynooth.

Du Noyer, G., O'Kelly, J., Wynne, A. and Wilson, W. (1858). Data and description to accompany quarter sheet 119 of the maps of the Geological Survey of Ireland. Alex Thom and Sons Ltd, Dublin.

Dunlop, D. J. (1995). Magnetism in rocks. *Journal of Geophysical Research*, 100 (B2) 2161-2174.

Dunlop, D. and Ozdemir, O. (1997). *Rock Magnetism. Fundamentals and Frontiers.* Cambridge Studies in Magnetism Series, pp. Xxi + 573.

Egli, R. (2009). Magnetic susceptibility measurements as a function of temperature and frequency I: inversion theory. *Geophysical Journal International*, 177, 395-420.

ElBaghdadi, M., Barakat, A., Sajieddine, M. and Nadem, S. (2012). Heavy metal pollution and soil magnetic susceptibility in urban soil of Beni Mellal City (Morocco). *Environmental Earth Sciences*, 66, 141-155.

- English Heritage (2008). *Geophysical Survey in Archaeological Field Evaluation*. English Heritage Publishing.
- Evans, M. and Heller, F. (2003). *Environmental magnetism: Principles and Applications of Enviromagnetics*. Academic Press.
- Eyre, J.K. (1997). Frequency-dependence of magnetic susceptibility for populations of single domain grains. *Geophysical Journal International*, 129, 209-211.
- Fay, D., Kramers, G., Zhang, C., Mc Grath, D. and Grennan, E. (2007). *Geochemical Atlas of Ireland*. Teagasc and the Environmental Protection Agency.
- Fealy, R.M., Green, S., Loftus, M., Meehan, R., Radford, T., Cronin, C. and Bulfin, M. (2009). *Teagasc EPA soil and Subsoils Mapping Project-Final Report*. Department of Environment, Heritage and Local Government; Environmental Protection Agency; National Development Plan. I (1), pp: 1-140.
- Feely, M. (2002). *IGA Field Guide Mace Head*.
- Fisher, N.I. (1993). *Statistical Analysis of Circular Data*. Cambridge. University Press, pp.277.
- Fisher, N., Lewis, T. and Embleton, B. (1987). *Statistical analysis of spherical data*. Cambridge University Press, pp.329.
- Foster, T., Evans, M. and Heller, F. (1994). The frequency dependence of low frequency, susceptibility in loess sediments. *Geophysical Journal International*, 118, 636-642.
- French, H., Hardbattle, C., Binley, A., Winship, P. and Jakobsen, L. (2002). Monitoring snowmelt induced unsaturated flow and transport using electrical resistivity tomography. *Journal of Hydrology*, 267(3-4), pp.273-284.
- Fialova, H., Maeir, G., Petrovsky, E., Kapicka, A., Boyko, T. and Scholger, R. (2006). Magnetic properties of soils from sites with different geological and environmental settings. *Journal of Applied Geophysics*, 59, 273-283.
- Gaigalas, A., Abrahamsen, N., Kazakauska, V. and Melesyte, M. (2002). Palaeomagnetism of Lithuanian upper Pleistocene sediments. *Geochronometria*, 21, pp.65-72.
- Gautam, P., Blaha, U., Appel, E. and Neupane, G. (2004). Environmental magnetic approach towards the quantification of pollution in Kathmandu urban area, Nepal. *Physics and Chemistry of the Earth*, 29, 973-984.

Geotechdata.info, Soil void ratio, <http://geotechdata.info/parameter/soil-void-ratio.html> (as of November 16, 2013).

George, D. and Gibson, P. (2000). Application of geophysical techniques for groundwater investigations and waste disposal site contamination studies in Co. Monaghan, Republic of Ireland. Environmental Geophysics Unit, National University of Ireland, Maynooth. Report No: EGU01/2000. Interreg 4 programme. 85 pages.

Gibbs-Egar, Z., Jude, B., Dommik, J., Loizeau, J. and Oldfield, F. (1999). Possible evidence for dissimilatory bacterial magnetite dominating the magnetic properties of recent lake sediments. *Earth and Planetary Science Letters*, 168, 1-6.

Gibson, P. J. (1991). An integrated investigation of the Tow Valley Fault System (Ireland) with particular emphasis on remote sensing techniques. Unpublished D. Phil. Thesis, University of Ulster.

Gibson, P. J. (1993). Evaluation of digitally processed geophysical data sets for the analysis of geological features in Northern Ireland. *International Journal of Remote Sensing*, 14(1), pp.161-170.

Gibson, P. J. (2003). Seasonal effects on Two-dimensional time-lapse subsurface resistivity imaging. Proceedings of the Geophysical Association of Ireland Irish Association of Hydrogeologists conference 28/5/03 Geophysical applications in hydrogeological investigations. 1-4.

Gibson, P. J. (2004). Geophysical characteristics of the Tow Valley fault zone in northeast Ireland. *Irish Journal of Earth Sciences*, 22, 1-13.

Gibson, P. J. (2005). Geophysical investigation around the sites of the former monastic settlement, Killeigh, Co. Offaly. Unpublished Report EGU 01/05.

Gibson, P. J. (2007a). *Heritage Landscapes of the Irish Midlands*. Geography Publications. 252 pages.

Gibson, P. J. (2007b). Archaeo-magnetic investigation of the former monastic site at Kilskyre, Co. Meath. *Riocht na Midhe*, XV111. pp.33-38.

Gibson, P. J. (2012). Geophysical Imaging of the Leamonaghan Togher. *Archaeology Ireland*, 26(1), 20-21

Gibson, P., Caloca Casado, S. and Jiménez-Martín, D. (2012). Integrated Coastal Mapping of Dublin Bay Geomorphology based on geophysical data, satellite inferred

bathymetry and 3D integration with INFOMAR datasets. Report: INF-11-07-GIB, 95 pages.

Gibson, P. and George, D. (2006). Geophysical Investigation of the former monastic settlement, Clonard, Co. Meath, Ireland. *Archaeological Prospection*, 13, 45-56.

Gibson, P. and George, D. (2013). *Environmental applications of geophysical surveying techniques* (2nd edition). Nova Science Publishers. 360 pages.

Gibson, P., Lyle, P. and George, D. (2004). Application of resistivity and magnetometry geophysical techniques for near-surface investigations in karstic terranes in Ireland. *Journal of Cave and Karst Studies*, 66(2), pp.35-38.

Gibson, P., Lyle, P. and Thomas, N. (2009). Magnetic characteristics of the Cuilcagh Dyke, Co. Fermanagh Northern Ireland. *Irish Journal of Earth Sciences*, 27, 1-10.

Gibson, P. and Pellicer, X. (2012). Investigation of Quaternary sediments using 2D time-lapse electrical resistivity tomography. *Remote Sensing: Applications in Quaternary Science: Archaeology and Landscape management*. Irish Quaternary Association Annual Symposium. GSI 30th November 2012.

Gibson, P. and Breen, R. (2005). The internal structure of the Galtrim motte, County Meath, as revealed by ground penetrating radar and electrical resistivity geophysical techniques. *Riocht na Midhe*, XXVI, 23-28.

Golden, N., Morrison, L., Gibson, P. and Zhang, C. (2012). High resolution mapping of metal contamination in an urban sports ground (Galway) using ordinary cokriging with magnetic susceptibility data. *Sino-European Symposium on Environment and Health*. Galway, 20-25 August.

Golden, N., Morrison, L., Gibson, P., Potito, A. and Zhang, C. (2015). Spatial patterns of metal contamination and magnetic susceptibility of soils at a bonfire site. *Applied Geochemistry*, 52, 86-96.

Golden, N., Morrison, L., Gibson, P. J., Potito, A. P. and Zhang, C. (2017). Impact of grass cover on magnetic susceptibility measurements for assessing metal contamination of soil. *Environmental Research*, 155:294-306.

Golden Software Inc. (2013). *SURFER 11 User's Guide*.

Graham, J. R. (2001a). Ordovician. In: C.H. Holland, ed., *The Geology of Ireland*. Dunedin Academic Press, pp.82-116.

- Graham, J. R. (2001b). Variscan structures. In: C.H. Holland, ed., *The Geology of Ireland*. Dunedin Academic Press, pp.313-330.
- Greensmith, J. T. (1978). *Petrology of the sedimentary rocks*. George Allen and Unwin.
- Grellier, S., Reddy, K., Gangathulasi, J., Adib, R. and Peters, C. (2007). Correlation between Electrical Resistivity and Moisture Content of Municipal Solid Waste in Bioreactor Landfill. *Geoenvironmental Engineering*, 226(11), pp.1-14.
- Hanesch, M. and Scholger, R. (2005). The influence of soil type on the magnetic susceptibility measured throughout soil profiles. *Geophysical Journal International*, 161, 50–56.
- Hardman, E. and Hull, P. (1883). On the metamorphic rocks of Co, Sligo and Leitrim and the enclosed minerals with the analysis of serpentine. *Scientific Proceedings of the Royal Dublin Society*, 3, 357-370.
- Harvey, A., Foster, G., Hannam, J. and Mather, A. (2003). The Tabernas alluvial fan and lake system, southeast Spain: applications of mineral magnetic and pedogenic iron oxide analyses towards clarifying the Quaternary sediment sequences. *Geomorphology*, 50, 151-171.
- Hatfield, R. and Maher, B. (2009). Fingerprinting upland sediment sources: particle size specific magnetic linkages between soils, lake sediments and suspended sediments. *Earth Surface Processes and Landforms*, 34(10), pp.1359-1373.
- Hirons, K. and Thompson, R. (1986). Palaeomagnetic application of magnetic measurements from inter-drumlin hollow lake sediments near Dungannon, Co. Tyrone, Northern Ireland. *Boreas*, 15, 117-135.
- Hodgson, J. A. and Ture, M. D. (2016). *Tellus A1 Airborne Geophysical Survey Report*. Geological Survey of Ireland.
- Hoffmann, V., Knab, M. and Appel, E. (1999). Magnetic susceptibility mapping of roadside pollution. *Journal of Geochemical Exploration*, 66, pp.313-326.
- Holden, J. (2005). *An introduction to Physical Geography and the Environment* (1st ed). School of Geography, University of Leeds.
- Holden, J. (2008). *An introduction to Physical Geography and the Environment* (2nd ed). School of Geography, University of Leeds.

- Holland, C. H. (2001). Cambrian of Leinster. In: C., Holland, ed., *The Geology of Ireland*. Dunedin Academic Press, 73-81.
- Hopkinson, J. (1889). Magnetic and other physical properties of iron at a high temperature. *Philosophical transactions of the Royal Society of London*, XIV, 443-465.
- Hounslow, M. W. (2006). *Palaeomag-Tools: A tool for analysis of directional data*. lancaster.ac.uk, V.4.2.
- Hounslow, M. and Chepstow-Lusty, A. (2004). A record of soil loss from Butrint, southern Albania, using mineral magnetism indicators and charcoal (AD 450 to 1200). *The Holocene*, 14(3), 321-333.
- Hrouda, F. (2011). Models of frequency-dependent susceptibility of rocks and soils revisited and broadened. *Geophysical Journal International*, 187, 1259-1269.
- Hrouda, F., Muller, P. and Hanak, J. (2003). Repeated progressive heating in susceptibility vs. temperature investigation: a new palaeotemperature indicator?. *Physics and Chemistry of the Earth*, 28(16-19), pp.653-657.
- Huo, J., Reidar, L., Li, B. and Su, P. (2010). Rock magnetism study on the Loess-Paleosol profile at Dali. *Chinese Journal of Geophysics*, 53(3), pp.497-508.
- Huisman, J. A., Hubbard, S. S., Redman, J. D. and Annan, A. P. (2003). *Measuring Soil Water Content with Ground Penetrating Radar: A Review*. *Vadose Zone Journal*, 2, p. 476-491.
- Jennings, J. (2008). *An archaeological geophysical investigation of the ancient monastic site at Kilbenan, Co. Galway*. Unpublished M.Sc. thesis, National University of Ireland, Maynooth.
- Jinmin, M., Saad, R., Saidin, M. and Bery, A. (2013). Electrical Resistivity Survey in Bukit Bunuh, Malaysia for Subsurface Structure of Meteorite Impact Study. *Open Journal of Geology*, 3, 34-37
- Jordanova, D., Petrovsky, E., Jordanova, N., Evlogiev, J. and Butchvarova, V. (1997). Rock magnetic properties of recent soils from northeastern Bulgaria. *Geophysical Journal International*, 128, 474-488.
- Karavul, C., Dedebali, Z., Keskinsezer, A., Beyhan, G. and Demirkol, A. (2010). Magnetic and electrical resistivity image survey in a buried Adramytteion ancient

city in Western Anatolia, Turkey. *International Journal of the Physical Sciences* 5(6), pp.876-883.

Karchegani, P., Ayoubi, S., Lu, S. and Honarju, N. (2011). Use of magnetic measures to assess soil redistribution following deforestation in hilly region. *Journal of Applied Geophysics*, 75, 227-236

Keller, G. and Frischknecht, F. (1966). *Electrical Methods in Geophysical Prospecting*. Pergamon Press, Oxford. 18-184.

Kemna, A., Vanderborghta, J., Kulesab, B. and Vereecken, H. (2002). Imaging and characterisation of subsurface solute transport using electrical resistivity tomography (ERT) and equivalent transport models. *Journal of Hydrology*, 267, pp.125-146

Kibaru, J. (2002). Induced polarization and Resistivity measurements on a suite of near surface soil samples and their empirical relationship to selected measured engineering parameters. Unpublished M. Sc. thesis International Institute for Geo-information Science and Earth Observation Enschede, Netherlands

Kilner, M., Westa, L.J. and Murray, T. (2005) Characterisation of glacial sediments using geophysical methods for groundwater source protection; *Journal of Applied Geophysics*, 57, 4, 293-305.

Koc, A and Pagac, P. (1973). Palaeomagnetism of the Quaternary sediments of the locality Cerveny Kopec (Red Hill). *Studia Geophysica et Geodaetica*, 17, 232-239.

Kovacheva, M., Jordanova, N. and Karloukovski, V. (1998). Geomagnetic field variations as determined from Bulgaria archaeomagnetic data, Part II: the last 8000 years. *Surveys in Geophysics*, 19, pp.431-460.

Landgraf, C. and Royall, D. (2006). Spatial patterns of surface soil magnetism and soil redistribution across a fallow field, northern Alabama. *Southeastern Geographer*, 46(1), pp.1-22.

Laywer, L., Bates, C. and Rice, R. (2001). *Geophysics in the Affairs of Mankind*. Society of Exploration Geophysicists, 507 pages.

Le Borgne E. (1955). Abnormal magnetic susceptibility of the top soil. *Annals of Geophysics*, 11, 399-419

Lecoanet, H, Leveque, F. and Segura, S. (1999). Magnetic susceptibility in environmental applications: comparison of field probes. *Physics of the Earth and Planetary Interiors*, 115, 191-204.

Liu, Q., Deng, C., Yu, Y., Torrent, J., Jackson, M., Banerjee, S. and Zhu, R. (2005). Temperature dependence of magnetic susceptibility in an argon environment: Implications for pedogenesis of Chinese loess/palaeosols. *Geophysical Journal International*, 161(1), pp.102-112.

Lewis, M. A., Cheney, C. S. And Odochartaigh, B. E. (2006). Guide to permeability indices. British Geological Survey Report CR/06/160N.

Liangfu, L. and Binguan, Q. (2012). Research on Influence of Soil Water Content on Soil Resistivity. International Conference on Lightning Protection (ICLP), Vienna, Austria.

Lillie, R. J. (1999). *Whole Earth Geophysics*. 1st ed. Upper Saddle River (NJ): Prentice-Hall Inc.

Loizeau, J., Roze, S., Peytremann, C., Monna, F. and Dominik, J. (2003). Mapping sediment accumulation rate by using volume magnetic susceptibility core correlation in a contaminated Bay (Lake Geneva, Switzerland). *Eclogae Geologicae Helveticae*, 96, S73-S79.

Loke, M. H. (2001). 2-D and 3-D electrical imaging surveys. 127 pages. <http://www.geotomosoft.com/>.

Loke, M. H. (2002). RES2DMOD version 3.01. Rapid 2D resistivity forward modeling using the finite-difference and finite-element methods. 15 pages pdf help booklet.

Loke, M. H. (2014). RES2DINVx32 installation and getting started user's guide. Geotomo software.

Loke, M. H. and Barker, R. D. (1995). Least-squares deconvolution of apparent resistivity pseudosections. *Geophysics*, 60(6), pp.1682-1690.

Loke, M. H. and Barker, R. D. (1996). Rapid least squares inversion of apparent resistivity pseudosections by a quasi-Newton method. *Geophysical Prospecting*, 44(1), pp.131-152.

Lowrie, W. (1997). *Fundamentals of Geophysics*. 2nd ed. Cambridge University Press. Cambridge CB2 8RU, UK.

- Lu, S. G. (2000). Lithological factors affecting magnetic susceptibility of subtropical soils, Zhejiang Province, China. *Catena* 40(4), pp.359–373.
- Lu, S. G. and Bai, S. Q. (2006). Study on the correlation of magnetic properties and heavy metals content in urban soils of Hangzhou City, China. *Journal of Applied Geophysics*, 60(1), pp.1-12.
- Lu, S. G. and Bai, S. Q. (2008a). Magnetic characterization and magnetic mineralogy of the Hangzhou urban soils and its environmental implications. *Chinese Journal of Geophysics*, 51(3), pp.549-557.
- Lu, S. G., Xue, Q., Zhu, L. and Yu, J. (2008b). Mineral magnetic properties of a weathering sequence of soils derived from basalt in Eastern China. *Catena*, 73(1), pp.23-33.
- Lu, S., Chen, Y., Shana, H. and Bai, S. (2009). Mineralogy and heavy metal leachability of magnetic fractions separated from some Chinese coal fly ashes. *Journal of Hazardous Materials*, 169(1-3), pp.246-255.
- Madden, J. (19992). Geophysical signatures of various archeological sites/monuments at Mayo Abbey, Co. Mayo. Unpublished M.Sc. Thesis. National University Ireland, Galway.
- Magiera, T., Strzyszcza, T., Kapickab, A. and Petrovsky, E. (2006). Discrimination of lithogenic and anthropogenic influences on topsoil magnetic susceptibility in Central Europe. *Geoderma*, 130(3-4), pp.299-311.
- Mahmood, S. and Bsoul, I. (2012). Hopkinson peak and superparamagnetic effects in $\text{BaFe}_{12-x}\text{Ga}_x\text{O}_{19}$ nanoparticles. *Proceedings of First European Mediterranean Meeting on Functional Materials*, 29, 8pages.
- Maher, B.A. (1988). Magnetic properties of some synthetic sub-micron magnetites. *Geophysical Journal International*, 94(1), pp.83-96.
- Maher, B. A. and Taylor, R. M. (1988). Formation of ultrafine-grained magnetite in soils. *Nature*, 336, pp.368-370.
- Maher, B. A., (2007). Environmental magnetism and Climate Change. *Contemporary Physics*, 48(5), pp.247-274.
- Maher, B. B. (2009). Rain and dust: magnetic records of climate and pollution. *Elements*, 5, pp.229-234

- Maher, B., Alekseev, A. and Alekseeva, T. (2002). Variation of soil magnetism across the Russian steppe: its significance for use of soil magnetism as a palaeorainfall proxy. *Quaternary Science Reviews*, 21, pp.1571-1576.
- Maher, B. A. (1986). Characterisation of soils by mineral magnetic measurements. *Physics of the earth and planetary interiors*, 42(1-2), pp.76-92.
- Maher, B. A. (1998). Magnetic properties of modern soils and Quaternary loessic paleosols: paleoclimatic implications. *Palaeogeography, Palaeoclimatology, Palaeoecology*, 137(1-2), pp.25-54.
- Malin, S. and Bullard, E. (1981). The Direction of the Earth's Magnetic Field at London, 1570-1975. *Philosophical Transactions the Royal Society*, 299(1450), pp.357-423.
- Mardia, K.V. and Jupp, P. E. (1999). *Directional statistics*. Wiley Series in Probability and Statistics.
- McCabe, M. (2008). *Glacial Geology and Glacial Geomorphology. The landscapes of Ireland*. Dunedin Press, Edinburgh.
- McCarter, W, J. (1984). The electrical resistivity characteristics of compacted clays. *Geotechnique* 34: 263-267.
- McConnell, B. and Philcox, M. (1994). *Geology of Kildare -Wicklow. A Geological Description to Accompany the Bedrock Geology 1:100,000 Scale Map Sheet 16, Kildare Wicklow*. Geological Survey of Ireland.
- McGillivray, P.R. and Oldenburg, D. W. (1990). Methods for calculating Fréchet derivatives and sensitivities for the non-linear inverse problem: A comparative study. *Geophysical Prospecting*, 38(5), pp.499-524.
- Mileti, F., Langella, G., Prins, M., Vingiani, S. and Terribile, F. (2013). The hidden nature of parent material in soils of Italian mountain ecosystems. *Geoderma*, 207-208, pp.291-309.
- Mitchell, F. and Ryan, M. (2001). *Reading the Irish Landscape*. Townhouse Press.
- Mokhtari, P., Ayoubi, S., Gao Lu, S. and Honarju, N. (2011). Use of magnetic measures to assess soil redistribution following deforestation in hilly region. *Journal of Applied Geophysics*, 75(2), pp.227–236.

- Moreno, E., Sagnotti, L., Dinares-Turell, J., Winkler, A. and Cascella, A. (2003). Biomonitoring of traffic air pollution in Rome using magnetic properties of tree leaves. *Atmospheric Environment*, 37(21), pp.2967-2977.
- Morris, J., Long, C., McConnell, B. and Archer, J. (1995). *Geology of Connemara*. Geological Society of Ireland.
- Morris, P., (1970). Palaeomagnetic studies of the Carboniferous system in Ireland. Unpublished Ph.D. Thesis. Trinity College, Dublin.
- Mulhall, M. (2000). Application of ground-based magnetic techniques in the detection for potential diamondiferous geological structures in Inishowen. Unpublished M.A. Thesis, National University of Ireland, Maynooth.
- Mullins, C. E. (1977). Magnetic susceptibility of the soil and its significance in soil science: a review. *Journal of Soil Science*, 28(2), pp.223-246.
- Murphy, C. (2002). Redundant landfills, a geophysical investigation. Unpublished M.Sc. thesis, National University of Ireland, Maynooth.
- Mussett, A. E. and Khan, M. A. (2000). *Looking into the Earth: An introduction to geological geophysics*. Cambridge University Press, Cambridge.
- O'Connor, R. (2000). A magnetic evaluation of a potential landfill site in Cornafean, Co. Cavan. Unpublished M.A. thesis, National University of Ireland, Maynooth.
- Ogungbe, A., Olowofela, J., Da-Silv, O., Alabi, A. and Onori, E. (2010). Subsurface Characterization using Electrical Resistivity (Dipole-Dipole) method at Lagos State University (LASU) Foundation School, Badagry. *Advances in Applied Science Research*, 1(1), pp.174-181.
- Okpoli, C. C. (2013). Sensitivity and Resolution Capacity of Electrode Configurations. *International Journal of Geophysics*, Article ID 608037, 12 pages.
- Open University (1997). *Sediment Analysis Workbook*. 42pages.
- O'Reilly, L. (2005). An archaeological geophysical investigation of the Augustinian priory at Ballyboggan, Co. Meath. Unpublished M.Sc. thesis, National University of Ireland, Maynooth.

Ormsby, A. (2002). A geophysical investigation of a former landfill site: Tom Ruane town park, Ballina, County Mayo. Unpublished M.A. thesis, National University of Ireland, Maynooth.

O'Rourke, T. (2008). An archaeological geophysical investigation of Rattin Castle and Sragh castle and their environs. Unpublished M.Sc. thesis, National University of Ireland, Maynooth.

O'Rourke, T. and Gibson, P. J. 2009 Geophysical investigation of the environs of Rattin Castle Tower House, County Westmeath, Ireland. *Archaeological Prospection* 16, 65-75.

Pakhotnova, V. (1998). An investigation of the magnetic properties of soils. *Russian Physics Journal*, 41(7), pp.656-661.

Pellicer Xavier (2010). Geophysical characterisation and Evolutionary Model of the Quaternary sediments in the North Offaly region of Central Ireland. Unpublished Ph.D. thesis. National University Ireland, Maynooth.

Pellicer, X., Warren, W., Gibson, P. and Linares, R. (2012a). Construction of an evolutionary deglaciation model for the Irish midlands based on the integration of morphostratigraphic and geophysical data analyses. *Journal of Quaternary Science*, 27(8), pp.807-818.

Pellicer, X. and Gibson, P. (2011). 'Electrical resistivity and ground penetrating radar for the characterization of the internal architecture of Quaternary sediments in the midlands of Ireland'. *Journal of Applied Geophysics*, 75, pp.638-647.

Pellicer, X., Zarroca, M. and Gibson, P. (2012b). 'Time-lapse resistivity analysis of Quaternary sediments in the midlands of Ireland'. *Journal of Applied Geophysics*, 82, pp.46-58.

Potter, D. K. (2005). Magnetic susceptibility as a rapid non-destructive technique for improved RCAL and SCAL parameter prediction. *International Symposium of the society of core analysis, Toronto, SCA2005-02*, 13pages.

Quijano, L., Gaspar, L., Chaparro, M. A. P. and Navas, A. (2011). Magnetic susceptibility in topsoils and bulk cores of cultivated calcisols. *Latinmag Letters*, 1, pp.1-6.

Ravindran, A. and Prabhu, M. (2012). Groundwater exploration study using Wenner-Schlumberger electrode array through W-4 2D Resistivity Imaging systems at

Mahapallipuram, Chennai, Tamilnadu, India. *Research Journal of Recent Sciences*, 1(11), pp.36-40.

Reilly C. (2003). A geophysical characterisation of the machair area at Murrivaugh, Mulranny, County Mayo. Unpublished M.A. thesis, National University of Ireland, Maynooth.

Reynolds, J. M. (2011). An introduction to applied and environmental geophysics. 2nd edition. John Wiley and Sons Limited. England.

Revil, A., L. M. Cathles, S. Losh, and J. A. Nunn (1998), Electrical conductivity in shaly sands with geophysical applications, *Journal Geophysical Research*, 103(B10), pp: 23925-23936.

Rhoades, J. D., P. A. C. Raats, and R. J. Prather (1976), Effects of Liquid-Phase Electrical Conductivity, Water Content and Surface Conductivity on Bulk Soil Electrical Conductivity, *Soil Science Society of America Journal*, 40, pp. 651-655.

Rinaldi, V. A., and G. A. Cuestas (2002), Ohmic Conductivity of a Compacted Silty Clay, *Journal of Geotechnical and Geoenvironmental Engineering*, ASCE, 128, pp.824-835.

Robinson, E. and Coruh, C. (1988). *Basic Exploration Geophysics*. John Wiley and Sons Limited. New York.

Robinson, D. A., C. S. Campbell, J. W. Hopmans, B. K. Hombuckle, S. B. Jones, R. Knight, F. Ogden, J. Selker, and O. Wendroth (2008), Soil moisture measurement for ecological and hydrological watershed-scale observatories: a review, *Vadose Zone Journal*, 7, doi:10.2136/vzj2007.0143.

Rothwell, J. and Lindsay, J. (2007). Mapping contemporary magnetic mineral concentrations in peat soils using fine-resolution digital terrain data. *Catena*, 70(3), pp.465-474.

Royall, D. (2001). Use of mineral magnetic measurements to investigate soil erosion and sediment delivery in a small agricultural catchment in limestone terrain. *Catena*, 46(1), pp.15-34.

Ruffell, A. and McKinley, J. (2008). *Geoforensics*, Chichester, Wiley-Blackwell.

- Samouelian, A., Cousin, I., Tabbagh, A., Bruand, A. and Richard G. (2005). Electrical resistivity survey in soil science: a review. *Soil and Tillage Research*, 83, pp.173-193.
- Seaby, R., Henderson, P., Prendergast, J. and Somes, R. (2007). QED statistics 1.1 Guide. Pisces Conservation Ltd.
- Segeer, M., Cousin, I., Frison, A., Boizard, H. and Richard, G. (2009). Characterisation of the structural heterogeneity of the soil tilled layer by using in situ 2D and 3D electrical resistivity measurements. *Soil and Tillage Research*, 103(2), pp.387-398.
- Semenov, V. S. and Pakhpnova, P. I. (1998). An investigation of the magnetic properties of soils. *Russian Physics Journal* 41(7), pp.656-661.
- Sevastopulo, G. D. and Wyse Jackson, P. N. (2001). Carboniferous (Dinantian). In: C. H. Holland, ed., *The Geology of Ireland*. Dunedin Academic Press, pp.241-288.
- Shinners, A. (2007). Geophysical investigation of prehistoric standing stones in the Irish Midlands. Unpublished M.Sc. Thesis, National University of Ireland, Maynooth.
- Singer, M. and Fine, P. (1989). Pedogenic factors affecting magnetic susceptibility of Northern California soils. *Soil Science Society of America Journal*, 53(4), pp.1119-1127.
- Singer, M., Verosub, K., Fine, P. and TenPas, J. (1996). A conceptual model for the enhancement of magnetic susceptibility in soils. *Quaternary International*, 34-36, pp.243-248.
- Sleeman, A., Stanely, G., Flegg, A., McConnell, B. (1994). *Geology of Kildare-Wicklow*. Ireland: Geological Survey of Ireland.
- Smith, J. (1999). An introduction to the magnetic properties of natural materials. In: *Environmental magnetism: a practical guide* edited by Walden, J., Oldfield, F. and Smith, J. Quaternary Research Association. Technical Guide No. 6, pp.5-25.
- Smith, P. J. (1973). *Topics in Geophysics*. Open University Press. England.
- Smyth, M. (1994). Quaternary geology and geophysical studies of Clara and Raheenmore bogs, Co. Offaly, Ireland. Unpublished Ph.D. Thesis. National University Ireland, Galway.

- Snowball, I. and Thompson, R. (1990). A mineral magnetic study of Holocene sedimentation in Lough Catherine, Northern Ireland. *Boreas*, 19, pp.127-146.
- Sprowl, D. and Banerjee, S. (1985). High resolution Paleomagnetic record of geomagnetic field fluctuations from the varved sediments of Elk lake, Minnesota. *Geology*, 13, pp.531-533.
- Strzyszez, Z. and Magiera, T. (2001). Record of Industrial Pollution in Polish Ombrotrophic Peat Bogs. *Physics and Chemistry Earth*, 26(11), pp.859-866.
- Tabbagh, A., Dabas, M., Hesse, A. and Panissod, C. (2000). Soil resistivity: a non-invasive tool to map soil structure horizonation. *Geoderma*, 97, pp.393-404.
- Tansley, A. G., 1939. *The British Islands and Their Vegetation*. Cambridge University Press, 930 p.
- Tetegan, M., Pasquier, C., Besson, A., Nichoulland, B., Bouthier, A., Bourennane, H., Desbourdes, C., King, D. and Cousin, I. (2012). Field-scale estimation of the volume percentage of rock fragments in stony soils by electrical resistivity. *Catena*, 92, pp.67-74
- Theakstone, W. and Harrison, C. (1970). *The analysis of geographical data*. Heinemann Education Books Ltd.
- Thompson, R., Batterbee, R., O'Sullivan, P. and Oldfield, F. (1975). Magnetic susceptibility of lake sediments. *Limnology and Oceanography*, 20(5), pp.687-698.
- Thompson, R. and Oldfield, F. (1986). *Environmental magnetism*. Allen and Unwin. London.
- Tichborne, C. E., (1885). An argentiferous Galenetic-blende at Ovoca. *Scientific Proceedings of the Royal Dublin Society*, III, pp.300-301.
- Tonkov, N. (2008). Geophysical survey of the Thracian site at Halka Bunar locality in the area of the Chirpan Heights. *Geoarchaeology and Archaeomineralogy: Proceedings of the International Conference, 29-30 October 2008 Sofia*, pp.329-332.
- Vahle, C. and Kontny, A. (2005). The use of field dependence of AC susceptibility for the interpretation of magnetic mineralogy and magnetic fabrics in the HSDP-2 basalts. *Hawaii Earth and Planetary Science Letters*, 238(1-2), pp.110-129.
- Van Dam, R., Hendrickx, J., Harrison, B., Borchers, B., Norman, D., Ndur, S., Jasper, C., Niemayer, P., Narty, S. and Simms, J. (2004). Spatial variability of magnetic soil

properties. In Defense and Security. International Society for Optics and Photonics, 5415, pp.665-676.

Van Schoor, M. (2002). Detection of sinkholes using 2D and resistivity imaging. *Journal of Applied Geophysics*, 50(2), pp.393-399

Vidic, N., Verosub, K. (1999). Magnetic properties of soils of the Ljubljana Basin chronosequence, Slovenia. *Chinese Science Bulletin*, 44(S1), pp.75–80.

Watson, K. and Barker, R. (1999). Differentiating anisotropy and lateral effects using azimuthal resistivity offset Wenner soundings. *Geophysics*, 64(3), pp.167-189.

Wenner, F. (1915). A method of measuring earth resistivity. US National Bureau of Standards Scientific paper, 12, pp.469-478.

Waxman, M.H. and Smits, L.J.M. (1968) Electrical Conductivities in Oil-Bearing Shaly Sands. *Society of Petroleum Engineers Journal*, 8, 107-122.

Williams, M. and Harper, D. (2003). *The making of Ireland*. Immel Publishing.

Wilson, R., Drury, S. and Chapman, J. (2000). *The Great Ice Age: Climate Change and Life*. London: Routledge The Open University.

Wilson, R. L. (1959). Remanent magnetism of late Secondary and early Tertiary British rocks. *Philosophy Magazine*, 4, pp.750-755.

Wilson, R. L. (1970). Palaeomagnetic stratigraphy of Tertiary lavas from Northern Ireland. *Geophysical Journal of the Royal Astronomical Society*, 20(1), pp.1-9.

Worm, H. (1998). On the superparamagnetic-stable single domain transition for Magnetite and frequency dependence of susceptibility. *Geophysical Journal International*, 133, pp.201-206.

Yang, P., Mao, R. and Shao, H. (2009). An investigation on magnetic susceptibility of hazardous saline-alkaline soils from the contaminated Hai River Basin, China. *Journal of Hazardous Materials*, 172(1), pp.494-497.

Zaidi, F., Kassem, O., Hussein, M. and Al-Bassam, A. (2012). Application of ERT Survey for Addressing the Issues of Urban Rain Storm Water Logging in the Qassim Province of Saudi Arabia. *International Journal of Geosciences*, 3, pp.726-736.

Zhang, C., Liu, Q., Huang, B. and Su, Y. (2010). Magnetic enhancement upon heating of environmentally polluted samples containing haematite and iron. *Geophysical Journal International*, 181(3), 1381-1394.

Zhou, Q., Shimada, J. and Sato, A. (2001). Three-dimensional spatial and temporal monitoring of soil water content using electrical resistivity tomography. *Water Resources Research*, 37(2), pp.273-285.

Zhou, W., Beck, B. and Adams, A. (2002). Effective electrode array in mapping karst hazards in electrical resistivity tomography. *Environmental Geology*, 42(8), pp.922-988.